

**Contribution to the Study of Heterogeneous Catalytic Reactions
in SCFs: Hydrogenation of Sunflower Oil in Pd Catalysts at
Single-Phase Conditions.**

by

Eliana Ramírez Rangel

December 2005

Submitted to the Department of Chemical Engineering in partial fulfillment of

The requirements for the degree of Doctor at the Universitat

Politécnica de Catalunya

Supervised by:

Dr. Francesc Recasens

Dr. M. A. Larrayoz

**Department of Chemical Engineering
Universitat Politècnica de Catalunya**

To my Mom and my Grandmother

To Oscar Mauricio

Summary

Hydrogenation is a major industrial chemical process. A wide variety of chemicals is obtained by catalytic hydrogenation.

One typical heterogeneous catalytic hydrogenation process is the production of margarine and shortenings from vegetable oils. The hydrogenation of double bonds in fats and oils has the purpose of providing products with the desired melting profile and texture, according to their final use. The hydrogenated oil is more stable and less sensitive to oxidation.

The classic process is carried out in batch reactors where the oil, hydrogen, and catalyst nickel powder are mixed intensively at temperatures between 373 K and 423 K. In this case, the compound to be hydrogenated and or the reaction products are liquid at process conditions; the reaction rate is limited by the concentration of hydrogen on the catalyst surface. The low reaction rate is caused by the low solubility of hydrogen and the high mass-transfer resistance in the liquid phase, which leads to a depletion of hydrogen at the catalyst surface. In the presence of double bonds, this lack of hydrogen also gives rise to double-bond migration and *cis-trans*-isomerization.

Despite of the fact that isomerization of *cis-trans* configuration increases the melting point, conflicting conclusions have resulted from studies on *trans* fatty acids. In several studies, these isomers formed during hydrogenation of fatty edible oils have shown to have similar effects as saturated fats increasing serum cholesterol levels in the blood, believed to be a major cause of heart disease. For this reason, apprehension and public awareness have risen regarding the potential health hazards of *trans* fatty acids intake in the human diet.

The aim of this research is to study continuous single-phase hydrogenation of sunflower oil on supported palladium catalysts using supercritical fluids as a reaction solvent. This would be an alternative process for producing a wide variety of end products having different characteristics (iodine value, *trans*-fatty acid content and saturated content mainly) of industrial foodstuffs interest to be used as low cholesterol precursors for margarine and shortening bases in the next few years. In addition, the objective of the study is to show, on a lab-scale, the potential of heterogeneous catalytic reactions under supercritical single-phase conditions.

This thesis is based on the material published in several technical papers and one patent, which can be found at the end of the thesis. The thesis is structured as follows:

Chapter 1 consists of a background, to explain the idea of use supercritical fluids in the hydrogenation of fats and oils, to describe the state of the art and what are the aims of this research.

Chapter 2 presents a theoretical study for modelling the vapor-liquid high pressure equilibrium for sunflower oil/hydrogen/ C_3H_8 system as well as for sunflower oil/hydrogen/DME in order to determine suitable operating conditions (concentrations, temperatures and pressures) which can bring all hydrogenation reactants and products into a homogeneous reactive fluid phase.

Chapter 3 establishes a better understanding of how operating variables affect the rate of reaction, conversion and final product distribution in a continuous recycle reactor as well as the experimental conditions where a potential CSTR process could be operated to obtain end-products with industrial foodstuff of interest. As an extension of these results, the kinetics of the reaction is worked out.

Chapter 4 it is a consequence of the results of the previous chapter and develops the study of the intraparticle diffusion-reaction mechanisms in supercritical sunflower oil hydrogenation on Pd/C catalyst.

The final chapter contains the experimental details of this thesis.

The last part gathers the main conclusions, discusses the prospects for further investigations and presents the bibliography and the appendixes.

Acknowledgements

I want to thank Professor Francesc Recasens and Professor M. Angels Larrayoz for the supervision of this Thesis. I really appreciate your advices and support throughout my research work.

I thank professors José Luis Cortina and Jordi Bou for sharing with me different stages during these years of intensive work. I also thank people of mechanics laboratory for your attention and your help.

I would like to express my appreciation for my lab-mates (Nancy, Fakher, Kamal, Alfredo and Aline) and for the students that have realised final projects or made an intership (Susana, Joan, Rubén, Silvia, Jordi, Mónica, Cristina, Ana Sofía, Sara, Tiff, Thierry, Mathew and Marine) who made all together an enjoyable space for work.

To all the administrative staff my sincere thanks.

I thank Generalitat de Catalunya as well as The Spanish Ministry of Science and Technology for the financial support during my doctoral studies.

I wish to express my gratitude to people of The Clean Technology Research Group in The University of Nottingham especially to professors Martyn Poliakoff and Paul Hamley. I thank Eduardo, Maia, Joan, Lu, Pete, Jason, Silvia, Su, Rodrigo, Gonzalo and Tomás not only for sharing with me your scientific knowlegde but also for having fun.

I also thank all my friends (Lili, Iván, Laura, Dionisio, Humberto, Leonardo, people from Santa Teresita Church, Silvia, Tiff and Aline) for the prayers and for the support that I have received from them.

My eternal gratitude goes to my family for its continued love and support. I also would like to mention the love that every day I receive from Oscar and my puppies Paca and Coco that has supported me all the time.

Contents

Contents

List of Figures **ix**

List of Tables **xv**

List of Schemes **xix**

Chapter One

Introduction. **1**

1.1 Physical and Chemical Process in Heterogeneous Catalyst Reactions. 1

1.2 Hydrogenation. 2

1.2.1 Hydrogenation of Fats and Oils. 3

1.2.2 Fats and Oil Hydrogenation Mechanism. 7

1.2.3 Fats and Oil Conventional Hydrogenation Process. 8

1.3 Supercritical Fluids. 11

1.3.1 Definition and Properties. 11

1.3.2 SCFs in Heterogeneous Catalysis. 12

1.3.3 SCFs in Fats and Oil Hydrogenation. 21

1.4 Objectives and Scope of this Thesis. 27

1.5 Thesis Structure. 28

1.6 Nomenclature. 29

Chapter Two

High-Pressure Equilibria. **31**

2.1 Introduction. 31

2.2 Objectives and Strategy. 40

2.3 Theoretical Determination of L-V High Pressure Equilibria. 41

2.4 Results and Discussion. 45

2.5 Conclusions. 55

2.6 Nomenclature. 56

Chapter Three

Kinetics of the Sunflower Oil Hydrogenation Process over Palladium-Based Catalysts using SC propane or SC DME as Reaction Solvent.	59
3.1 Introduction.	59
3.2 Objectives.	72
3.3 Sunflower Oil Hydrogenation on Pd/C using SC Propane as Reaction Solvent.	73
3.3.1 Study of the Effect of Operating Variables on Hydrogenation Reaction by means of the Experimental Design.	73
3.3.1.1 Creating the Central Composite Experimental Design.	73
3.3.1.2 Results and Discussion.	77
3.3.2 Kinetic Analysis of CSTR Data: Modeling and Results.	84
3.4 Sunflower Oil Hydrogenation over Pd/Al ₂ O ₃ using SC DME as Reaction Solvent.	90
3.4.1 Experimental Considerations.	90
3.4.2 Kinetic Analysis of CSTR Data: Results and Modeling.	92
3.5 Final Discussion.	98
3.6 Conclusions.	99
3.7 Nomenclature.	100

Chapter Four

Intraparticle Diffusion in Porous Catalyst Particles used in Supercritical Sunflower Oil Hydrogenation.	105
4.1 Introduction.	105
4.2 Objectives and Strategy.	113
4.3 Detection of the Internal Mass Transport Resistance.	113
4.4 Determination of Effective Diffusion Coefficients.	114
4.4.1 Experimental Measurements.	114
4.4.2 Steady-State Diffusion and Chemical Reaction in Porous Catalyst Particle Model under Isothermal Conditions.	115
4.4.3 Results and Discussion.	119
4.5 Conclusions.	134
4.6 Nomenclature.	135

Chapter Five

Experimental.	139
5.1 Introduction.	139
5.2 Raw Materials.	139
5.2.1 Sunflower Seed Oil.	139
5.2.2 Hydrogen.	139
5.2.3 Propane.	139
5.2.4 Dimethyl ether (DME).	139
5.2.5 Catalysts.	140
5.2.5.1 Activation Procedure.	140
5.2.5.2 Test of the Stability of Catalyst Activity.	140
5.3 Safety Procedures and Devices.	140
5.4 Supercritical Fluid Continuous Flow Apparatus.	142
5.4.1 Process and Instrumentation Diagram (P&ID).	142
5.4.2 Equipment List.	145
5.4.3 Experimental Apparatus Description.	146
5.4.3.1 The Gradientless Reactor.	146
5.4.4 Modifications Made to the Supercritical Flow Apparatus.	148
5.4.4.1 The Replacement of the Reactor.	148
5.4.5 Standard Operating Procedure for the Supercritical Continuous Flow Apparatus.	150
5.5 Analytical Techniques.	152
5.5.1 Iodine Value.	152
5.5.2 Preparation of Methyl Esters of Fatty Acids.	153
5.5.3 Silver ion High-Performance Liquid Chromatography.	153
5.6 Nomenclature.	159
Chapter Six	
Conclusions and Prospects for Further Investigations.	161
Chapter Seven	
Bibliography.	165
Appendix A	

Survey of Heterogeneous Catalytic Reactions carried out under SC Conditions or in SCF solvents (Baiker, 1999, Ramírez <i>et al.</i> 2002).	187
Appendix B	
Hydrogenation of Aromatic Compounds in High-Temperature Water.	191
Appendix C	
Estimation of Thermodynamic Properties for Sunflower Vegetable Oil.	207
Appendix D	
Calculating Binary, Vapor-Liquid Equilibria Using The Peng Robinson Equation of State.	217
Appendix E	
Calculating Ternary, Vapor-Liquid Equilibria Using The Peng Robinson Equation of State.	231
Appendix F	
Estimation of Transport Effects.	235
Appendix G	
Estimation of Molecular Diffusivities.	239
Appendix H	
Specification Data Sheets and Analytical Procedures.	243
Publications.	263

List of Figures

- Figure 1-1: Sequence of physical and chemical steps occurring in heterogeneous catalytic gas/liquid reaction (e.g. hydrogenation of liquid compound). Part a shows a representative section of the reactor content consisting of a gas bubble and a solid catalyst particle and corresponding mass-transfer boundary layers (resistances). Part b provides a magnified cross section of the catalyst particle (Baiker, 1999). 1
- Figure 1-2: United States capita fats and oils usage (O'Brien, 1998). 3
- Figure 1-3: *cis/trans* geometric isomers (Engelhard, 1992). 5
- Figure 1-4: Dead-end batch hydrogenation process for triglyceride oils (Albright, 1967). 9
- Figure 1-5: Definition of SC state for a pure component. CP critical point, TP triple point, T_c critical temperature, P_c critical pressure (Brunner, 1994). 11
- Figure 1-6: Catalytic heterogeneous reactions carried out in SCFs. 14
- Figure 1-7: Reactant concentration profile for a heterogeneous catalytic reaction under supercritical conditions. Note that under supercritical conditions gas/liquid transfer resistance is eliminated and external fluid film diffusion resistance (step 3) is lowered due to lower viscosity of SCF. 23
- Figure 2-1: General concentration profiles for substrate (- -) and hydrogen (--) in a classic gas-liquid hydrogenation. d_{gl} = gas-liquid interface, d_{lc} = liquid-catalyst interface, C_{gl} = equilibrium concentration of hydrogen in liquid oil (Härröd *et al.*, 2001). 32
- Figure 2-2: General concentration profiles for substrate (- -), hydrogen (--) and solvent (- - -) in supercritical single-phase hydrogenation. d_{fc} = fluid-solid catalyst interface (Härröd *et al.*, 2001). 33
- Figure 2-3: Phase diagram for sunflower oil, CO₂ and hydrogen system at 10 MPa and 373.15K (mol %). The dark means single phase. The dashed line indicates the hydrogen requirement for full conversion of the substrate. 35
- Figure 2-4: Vapor-liquid equilibrium of the rapeseed oil-carbon dioxide systems at 333.15 and 373.15 K (Klein and Schulz, 1989). 36

- Figure 2-5: VLE near the critical region for the binary system carbon dioxide (1) – sunflower oil (2) (vaporization constants calculated with the PR-EOS). 38
- Figure 2-6: VLE in the critical region for the binary system propane (1) - sunflower oil (2) (vaporization constants calculated with PR-EOS) (Ramírez *et al.*, 2002). 47
- Figure 2-7: VLE in the critical region for the binary system DME (1) - sunflower oil (2) (vaporization constants calculated with PR-EOS). 47
- Figure 2-8: K -values for DME in the DME /sunflower oil system and for propane in propane /sunflower oil system at 473.15 K. 48
- Figure 2-9: VLE and LLE of triglycerides with solvents at a reduced temperature of 1.05. Experimental: ● Bharath *et al.* 1992 ; ■ Coorens *et al.* 1988 ; ◇ Florusse *et al.* 2002 ; - Pereda *et al.* predictions (2002). Figure taken from Pereda *et al.* (2003). 49
- Figure 2-10: Dew and bubble curves for Propane/H₂/tripalmitin ternary system predicted with the PR-EOS at 433.15, 473.15 and 673.15 K and pressures of 16 and 20 MPa (mol %). 50
- Figure 2-11: Dew and bubble curves for the ternary systems estimated with the PR-EOS (see Sandler, 1999): a) Propane/H₂/sunflower oil system at 453.15, 473.15 and 673.15 K and pressures of 18 and 20 MPa b) DME/H₂/sunflower oil at 423.15, 453.15 and 473.15 K and 20 MPa. Both in mol %. 51
- Figure 3-1: Reactant concentration gradients in pores of different widths (Coenen, 1976). 66
- Figure 3-2: Contour map based on empirical quadratic model. High fan speed: a) LHSV *vs* %H₂ at 488.15 K; b) LHSV *vs* %H₂ at 428.15 K. 79
- Figure 3-3: Contour map based on empirical quadratic model. High fan speed: a) %H₂ *vs* T at LHSV=70 h⁻¹ b) %H₂ *vs* T at LHSV=30 h⁻¹. 80
- Figure 3-4: Contour maps on the effect of the reactor recycle speed at different temperatures at constant high space velocity and large %H₂. 81
- Figure 3-5: Operating zones in the LHSV-T plane a) in the high H₂ composition range between 1-3 *trans* wt %, for IV = 95-110 and stearic content % = 12-2 b) in the low H₂ composition range. 82

- Figure 3-6: Plot showing *trans* C18:1 formed *vs* reduction in iodine value in the continuous hydrogenation of sunflower oil over Pd. Initial IV = 130. Data by King *et al.* (2001) lie within dashed region. 83
- Figure 3-7: Plot showing stearic ester *vs* reduction in iodine value in the continuous hydrogenation of sunflower oil over Pd, Initial IV = 130. Data by King *et al.* (2001) lie within dashed region. 83
- Figure 3-8: Linearised plot of hydrogen uptake rate: $\ln r_{H_2}$ *vs* $\ln p_{H_2}$, for 448.15 K and 460.15 K. Upper line slope is 0.52, bottom line slope = 0.48. 86
- Figure 3-9: Parity plot of component concentrations in CSTR *vs* those predicted by kinetic model. 88
- Figure 3-10: Iodine value (IV) and *trans* content as a function of temperature and space velocity at 4% H₂ mol content. Solid line= IV, dashed line= *trans* content. 93
- Figure 3-11: Iodine value (IV) and *trans* content as a function of temperature and H₂ mol content at WHSV= 200 h⁻¹. Solid line= IV, dashed line= *trans* content. 94
- Figure 3-12 Effect of hydrogen pressure on the hydrogenation activity of the catalyst. 95
- Figure 3-13: Linearised plot of hydrogen uptake rate: $\ln r_{H_2}$ *vs* $\ln p_{H_2}$, for 483.15 K. 96
- Figure 3-14 Parity plot of component concentrations in CSTR *vs* those predicted by kinetic model. 97
- Figure 4-1: Random-pore model. 106
- Figure 4-2: Concentration profiles of hydrogen and sunflower oil components in 2% Pd/C at 484.15 K, 20 MPa, feed composition (Oil:H₂:C₃H₈): 1:4:95 mol %. a) $d_p = 2$ mm b) $d_p = 0.92$ mm. 119
- Figure 4-2: Intraparticle concentration profiles of hydrogen and oil components in 2% Pd/C at 484.15 K, 20 MPa, feed composition (Oil:H₂:Propane): 1:4:95 mol %. c) $d_p = 0.47$ mm. 120
- Figure 4-3: Intraparticle concentration profiles in oil hydrogenation in SC propane at 457.15 K, feed composition (Oil:H₂:Propane): 1:4:95 mol % and $d_p = 2$ mm. a) P=20 MPa 120

- Figure 4-3: Intraparticle concentration profiles in oil hydrogenation in SC propane at 457.15 K, feed composition (Oil:H₂:Propane): 1:4:95 mol % and $d_p = 2$ mm. b) $P = 27.5$ MPa. 121
- Figure 4-4: Intraparticle concentration profiles in oil hydrogenation in SC propane at 484.15 K, $P = 27.51$ MPa. Feed composition (Oil:H₂:Propane): 1:4:95 mol %, $d_p = 2$ mm. 121
- Figure 4-5 Sensitivity of the proposed model with H₂ effective diffusivity values at 484.15 K, 20 MPa. Feed composition (Oil:H₂:Propane) of 1:4:95 mol %. 122
- Figure 4-6: Effectiveness factor with respect to hydrogen for several slab catalyst particles thickness. 123
- Figure 4-7: Estimated molecular diffusivity of hydrogen and triglycerides in SC C₃H₈. 129
- Figure 4-8 Relative sizes of reactants taking place in the pores of 2% Pd/C catalyst during the hydrogenation. 130
- Figure 4-9: Influence of temperature and pressure on (D_e/D) ratio. 130
- Figure 4-10: Variation of $(\rho_p K_A D_s)/D$ with temperature. 132
- Figure 4-11: General correlation of surface diffusivities from Sladek *et al.* (1974). 133
- Figure 5-1: Change in product distribution and iodine value (IV) during short term operation ($P = 20$ MPa $T = 444.15$ K, feed mol composition.: sunflower oil = 1%, H₂ = 8%, C₃H₈ = 91%). 141
- Figure 5-2: Explosion-proof compartment for gases. 141
- Figure 5-3: Simplified process diagram. 143
- Figure 5-4: Schematic of the supercritical fluid continuous flow apparatus. 144
- Figure 5-5: Robinson-Mahoney “micro” stationary catalyst basket reactor (Robinson, 1986). 147
- Figure 5-6: Operating limits for steels in hydrogen service. Each steel is suitable for use under hydrogen-partial-pressure-temperature conditions below and to the left of its respective curve (Perry, 1984). 149

Figure 5-7: Separation of fatty acid methyl esters standards of known concentrations.	154
Figure 5-8: Calibration curves for main components of sunflower oil using HPLC (210 nm). a) Methyl linoleate and b) Methyl oleate.	155
Figure 5-8: Calibration curves for main components of sunflower oil using HPLC (210 nm). c) Methyl elaidate and d) Methyl stearate.	156
Figure 5-9: Separation of fatty acid methyl esters of sunflower oil before hydrogenating.	158
Figure B-1: Experimental setup for hydrogenation reactions.	193
Figure B-2: GC calibration of a) Cyclohexanone and b) Cyclohexanol.	196
Figure B-3: GC calibration of a) Acetophenone and b) Phenylethanol.	198
Figure B-4: Effect of mol organic-H ₂ ratio on yield (523.15 K, 16 MPa and 19 s.).	199
Figure B-5a: GC calibration of Styrene.	200
Figure B-5b: GC calibration of Ethylbenzene.	201
Figure B-6: GC calibration of a) Benzaldehyde and b) Benzyl Alcohol.	202
Figure B-7: Effect of pH of HCO ₂ NH ₄ solution on reaction yield.	204
Figure E-1: Dew and bubble curves for the ternary systems estimated with the PR-EOS (see Sandler, 1999): Dimethyl ether (DME)/Hydrogen (H ₂)/sunflower oil system at 473.15 K and 20 MPa. In mol %.	233

List of Tables

Table 1-1: Typical acid compositions of some edible plant fats and oils (Engelhard, 1992).	5
Table 1-2: Properties of C-18 Fatty Acids (Engelhard, 1992).	6
Table 1-3: Comparison of the physical properties of gases, liquids and SCFs (McCoy, 1999).	12
Table 2-1: Critical properties of several solvents for chemical reactions (Yaws, 1999).	34
Table 2-2: Solubility of triglycerides in different reaction media (Brunner, 1986).	38
Table 2-3: Physical property data for hydrogenation species (Yaws, 1999).	46
Table 2-4: Scope of variables of reaction.	54
Table 3-1: Effects of process variables on rate and selectivity in vegetable oil hydrogenation (Allen, 1982).	67
Table 3-2: Scope of variables of reaction.	75
Table 3-3: Coded 2^4 factorial design matrix.	76
Table 3-4: Coded centre and star points design matrix.	76
Table 3-5: Effects of the increase either in the temperature, the LHSV or the %H ₂ for the mean values of the other variables on the responses.	78
Table 3-6: Partially hydrogenated vegetable oils <i>vs.</i> commercial margarine feed stocks (DP. 305.15-312.15 K). Data on Iodine Value, <i>trans</i> content and stearic production.	84
Table 3-7: Fitted parameters values for the kinetic model.	87
Table 3-8: Kinetic parameters, according to equation (3.40), for the hydrogenation of sunflower oil over Pd/C as catalyst and propane as solvent.	89
Table 3-9: Operating experimental conditions used in the sunflower oil hydrogenation over Pd/Al ₂ O ₃ with DME as reaction solvent.	92

Table 3-10: Effect of reaction conditions on sunflower oil hydrogenation. Oil concentration: 1 mol%; P=20 MPa; catalyst: 0.5% Pd/Al ₂ O ₃ ; solvent: DME.	92
Table 3-11: Fitted kinetic parameters values for Pd/Al ₂ O ₃ – DME reaction system.	96
Table 3-12: Kinetic parameters, according to equation (3.40), for hydrogenation of sunflower oil using Pd/Al ₂ O ₃ as catalyst and DME as solvent.	97
Table 3-13: Activation energies reported in the available literature.	98
Table 4-1: Tortuosity factors for diffusion in catalysts at 6.5 MPa (Butt,1999).	108
Table 4-2: Tortuosity factors for high-pressure extraction of porous solids (Stüber <i>et al.</i> , 1997).	110
Table 4-3: Effect of particle diameter on the conversion at constant apparent residence time (4.2 s). Experimental conditions: 0.25 g of 2% Pd/C at 20 MPa, feed composition (Oil:H ₂ :Propane):1:4:95 mol %.	113
Table 4-4: Experimental reaction runs on 2% Pd/C for determination of intraparticle diffusion at constant final IV (80-100). Feed composition (Oil:H ₂ :Propane): 1:4:95 mol %.	114
Table 4-5 Model sensitivity with fitted parameters at 484.15 K, 20 MPa and feed composition (Oil:H ₂ :Propane) of 1:4:95 mol %.	123
Table 4-6: Intrinsic kinetic parameters for the SC sunflower oil hydrogenation on Pd/C.	124
Table 4-7: Constrains of Levenberg-Marquardt algorithm.	125
Table 4-8: Fitted effective diffusion coefficients for hydrogenation species on 2% Pd/C catalyst (d _p range=0.47-2 mm).	125
Table 4-9: Estimated selectivities for SC sunflower oil hydrogenation on 2% Pd/C at 487.15K, 200 MPa and a feed composition (Oil:H ₂ :Propane) of 1:4:95 mol %.	127
Table 4-10: Molecular diffusivities for C ₃ H ₈ -Triglycerides and C ₃ H ₈ -H ₂ under several operating conditions.	128
Table 4-11: D _e /D ratio for triglycerides and hydrogen in SC propane on 2% Pd/C.	129

Table 4-12: $(\rho_p K_A D_s)/D$ ratio for triglycerides in SC propane on 2% Pd/C.	132
Table 5-1: Equipment list of the supercritical experimental apparatus.	145
Table 5-2: F-126 steel characterization.	150
Table 5-3: Chromatographic analysis of sunflower oil raw material.	157
Table A-1: General overview of catalytic heterogeneous reaction in SCFs.	187
Table B-1: Screening hydrogenation reactions.	192
Table B-2: Effect of operating variables on cyclohexanol yield.	196
Table B-3: Effect of operating variables on 1-phenylethanol yield.	199
Table B-4: Effect of operating variables on ethylbenzene yield.	201
Table B-5: Effect of operating variables on benzyl alcohol yield.	203
Table B-6: Research results in comparison with those of Bryson <i>et al.</i> (2004).	204
Table C-1: Sunflower oil triacylglycerol composition by reversed-phase high performance liquid chromatography with flame ionization detection (Neff <i>et al.</i> (1994).	207
Table C-2: Ambrose group contributions for critical constants (Reid <i>et al.</i> , 1987).	209
Table C-3: Estimated critical properties for pure components of sunflower oil.	210
Table C-4: Coefficients for equation C.10 (Reid <i>et al.</i> , 1987).	211
Table C-5: Coefficients for equation C.14.	212
Table C-6: Estimated sunflower oil critical constants.	214
Table E-1: Dew and bubble curves data for the ternary system Dimethyl ether (1)/Hydrogen (2)/Sunflower Oil (3) system at 453.15 K and 20 MPa, x denotes either liquid or vapor phase mole fraction.	232
Table F-1: Evaluation of intraparticle mass transport limitation.	236
Table G-1: Molecular diffusivities for C ₃ H ₈ -Triglycerides and C ₃ H ₈ -H ₂ under several operating conditions.	241

List of Schemes

Scheme 1-1: Chemistry of triglycerides (Engelhard, 1992).	4
Scheme 1-2: Unsaturated carbon-carbon double bond hydrogenation.	7
Scheme 3-1: Kinetic model for oil hydrogenation developed by Bailey (1949).	59
Scheme 3-2: Kinetic model for cottonseed oil hydrogenation by Elbid and Albright (1957).	60
Scheme 3-3: Kinetic reaction sequence for oil hydrogenation by Albright (1965).	61
Scheme 3-4: Kinetic model for cottonseed oil hydrogenation by Albright (1967).	62
Scheme 4-1: Flow chart for the parameter fitting procedure for the smallest particle diameter catalyst ($d_p = 0.47$ mm, 2% Pd/C).	117
Scheme 4-2: Flow chart for the parameter fitting procedure for the largest particle diameter catalyst ($d_p = 2$ mm, 2% Pd/C).	118
Scheme B-1: Hydrogenation of cyclohexanone.	195
Scheme B-2: Hydrogenation of acetophenone.	197
Scheme B-3: Hydrogenation of styrene.	200
Scheme B-4: Reactivity of organic groups.	201
Scheme B-5: Hydrogenation of benzaldehyde.	202
Scheme C-1: Pseudo-component which represents a vegetable oil (Pereda <i>et al.</i> , 2002).	207

Chapter One

Introduction.

1.1 Physical and Chemical Process in Heterogeneous Catalyst Reactions.

By definition, in homogeneous catalysis, reactants and catalyst form a single fluid phase, whereas in heterogeneous catalysis reactants and catalyst are present in different phases (See Figure 1-1), rendering mass and heat transfer through interphases a necessary prerequisite for reaction.

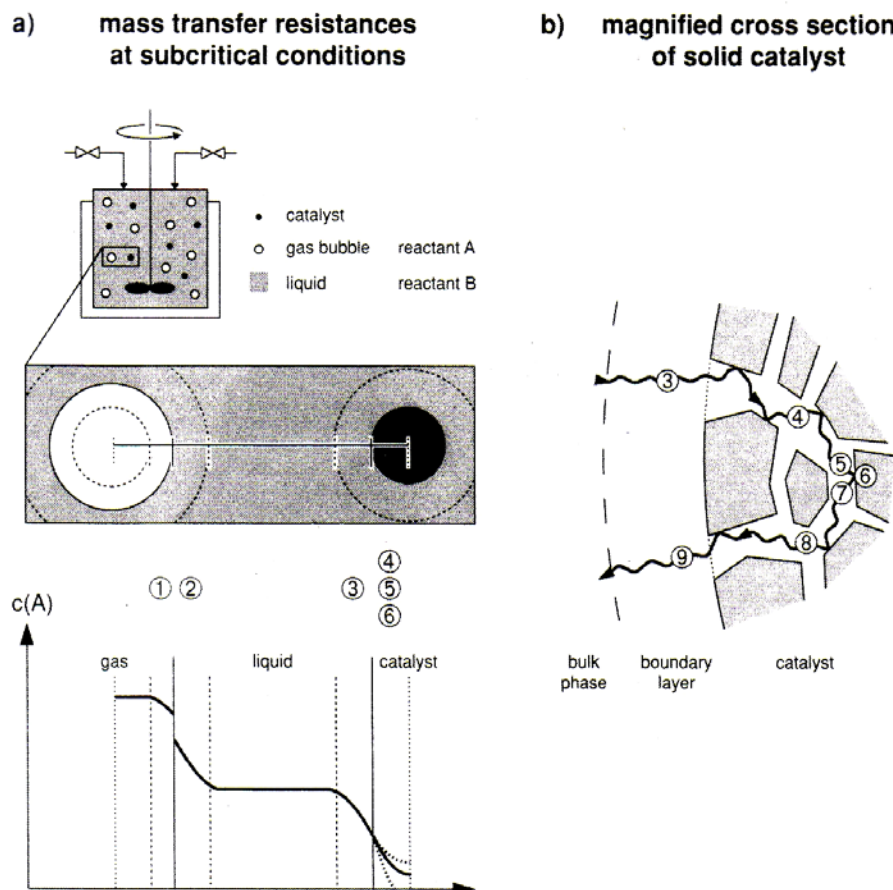


Figure 1-1: Sequence of physical and chemical steps occurring in heterogeneous catalytic gas/liquid reaction (e.g. hydrogenation of liquid compound). Part a shows a representative section of the reactor content consisting of a gas bubble and a solid catalyst particle and corresponding mass-transfer boundary layers (resistances). Part b provides a magnified cross section of the catalyst particle (Baiker, 1999).

When a heterogeneous catalytic reaction occurs, several physical and chemical processes must take place in proper sequence. This sequence of physical and chemical steps is schematically illustrated in Figure 1-1., parts a and b, for a solid-catalyzed gas/liquid reaction such as a hydrogenation of a liquid substrate.

No matter how active a catalyst particle is, it can be effective only if the reactants (hydrogen and substrate) reach the external and internal catalytic surface. The catalytic process can be broken down into several steps: (1) transfer of gaseous reactant from bulk phase to gas/liquid interface (diffusion) and (2) from there to bulk liquid phase (adsorption and diffusion); (3) transfer of both reactants (gas and liquid) from bulk liquid to external surface of the catalyst particle (diffusion through stagnant external film surrounding catalyst particle) ; (4) transfer of reactants into porous catalyst (internal diffusion); (5) adsorption of reactants following either step 3 or 4; (6) surface reaction; (7) desorption and transfer of product(s) by (8) internal and (9) external diffusion to bulk liquid or gas phase.

1.2 Hydrogenation.

Hydrogenation is defined as the chemical reaction between molecular hydrogen and an element or compound, ordinarily in the presence of a catalyst. The reaction may be one in which hydrogen simply adds to a double or triple bond connecting two atoms in the structure of the molecule or one in which the addition of hydrogen results in dissociation (breaking up) of the molecule (called hydrogenolysis, or destructive hydrogenation).

One of the oldest and most diverse catalytic processes is the selective hydrogenation of functional groups contained in organic molecules to produce (1) fine chemicals, (2) intermediates used in the pharmaceutical industry, (3) monomers for the production of various polymers, and (4) fats and oils for producing edible and nonedible products. With the exception of a few large scales, continuous hydrogenation processes in petroleum refining, hydrogenation products are often made on a small scale in batch reactors. Batch processes are usually most cost effective since the equipment need not be dedicated to a single reaction as it almost always is for large scale, fixed bed product of chemicals. The catalyst is generally powdered and slurried with the reactants; a solvent is usually present to influence product selectivity and to absorb the reaction heat liberated by the reaction. Since most hydrogenations are highly exothermic, careful temperature control is required to achieve the desired selectivity and prevent temperature runaway (Farrauto, 1997).

1.2.1 Hydrogenation of Fats and Oils.

Hydrogenation of fats and oils is one of the first commercial hydrogenation processes. Not many years after Sabatier demonstrated that double bonds in light hydrocarbons could be hydrogenated in the vapour phase using nickel or noble metal catalysts, W. Normann patented (1902) a liquid phase hydrogenation process for fats and oils. A plant was built in England in 1907, and Procter and Gamble obtained rights to the Normann patent in 1911 (Rase, 2000).

Over the years, the production of edible oil fats and oils has soared, with vegetable sources now dominating the field formally held by butter and lard as shows Figure 1-2. In 1950 the food fat marked in United States was split approximately equally between animal fats (lard, tallow and butter) and edible vegetable oils. Twenty years later in 1970, edible vegetable oils accounted for three-fourths of the total and animal facts only one-fourth. Vegetable oils became dominate mainly because of competitive pricing for vegetable oil, increased hydrogenation capacity, consumer preference shifts from butter to margarines, and nutritional concerns regarding cholesterol and saturated fats (O'Brien, 1998).

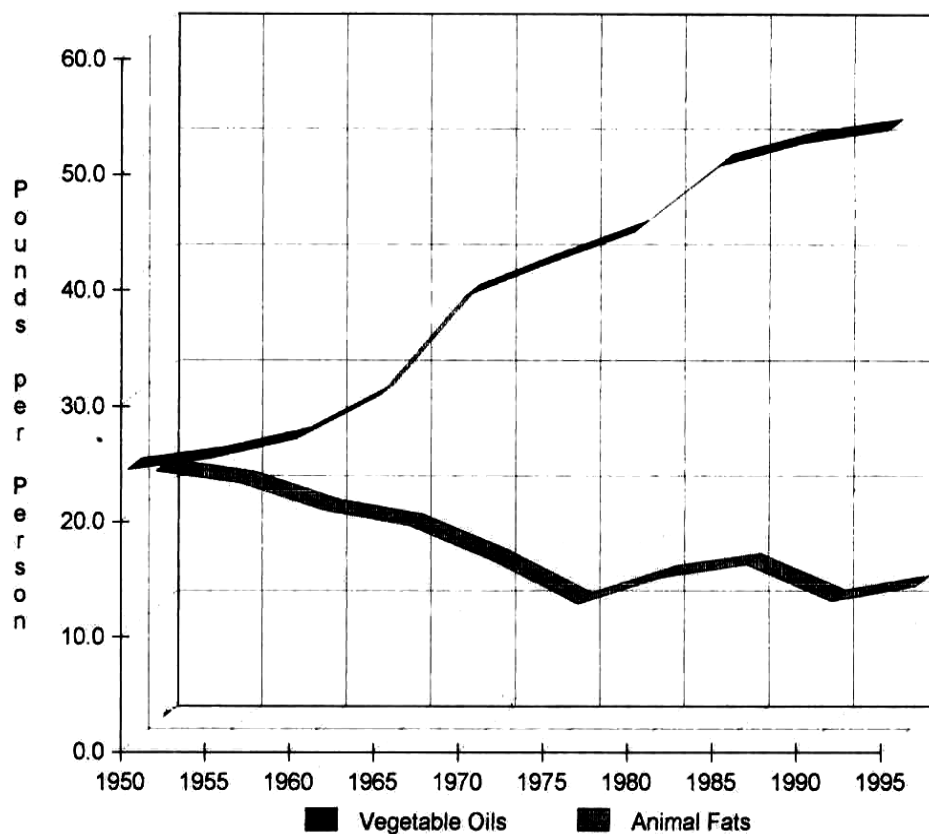
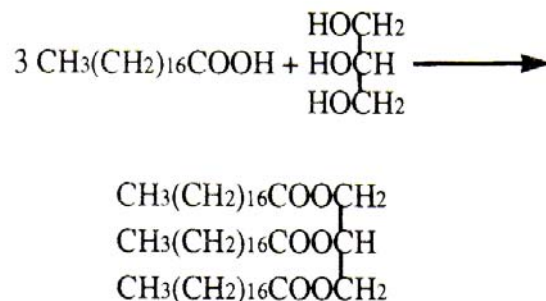


Figure 1-2: United States capita fats and oils usage (O'Brien, 1998).

Chemically, fats and oils are a combination of glycerine and fatty acids (see Scheme 1-1). The glycerine molecule has three separate points where a fatty acid molecule can be attached, thus the common reference to fats and oils as triglycerides.



Scheme 1-1: Chemistry of triglycerides (Engelhard, 1992).

Physically, fats and oils are liquids at room temperatures and oils are liquids at room temperature. The different properties are to a large extent determined by the fatty acid composition and the extent of saturation or unsaturation present. These aspects are identified by the carbon chain length and the number and position of the double bonds for individual fatty acids, and their position on the glycerine. Generally, solid fats are indicated by a dominance of saturated fatty acids and liquid oils are evidence of a high level of unsaturated fatty acids.

Edible fats and oils carbon chain lengths vary between 4 and 24 carbon atoms with up to three double bonds. The length of carbon chain of 16 and 18 is the most common. Table 1-1 provides a summary of fatty acid composition of various vegetable fats and oils.

There are two reasons to hydrogenate oils. One is to change naturally occurring fats and oils into physical forms with consistency and handling characteristics required for functionality. With hydrogenation, edible fat and oil products can be prepared with creaming capabilities, frying stability, sharp melting properties, and the other functional characteristics desired for specific applications. Another reason for hydrogenation is to increase oxidative stability. Flavour stability is necessary to maintain product acceptability for prolonged periods after processing, packaging, and use as an ingredient in a finished product. A wide range of fats and oils products can be produced with the hydrogenation process, depending upon the conditions used, the starting oils and the degree of saturation or isomerization.

Table 1-1: Typical acid compositions of some edible plant fats and oils (Engelhard, 1992).

Fatty Acid	Coco-nut	Palm Kernel	Palm	Cotton-seed	Sun-flower	Corn	Soy-bean	Canola	Rape-seed	
6-0	1									Saturates
8-0	8	3								
10-0	6	4								
12-0	47	48								
14-0	18	16	1	1						
16-0	9	8	45	21	7	11	11	4	3	
18-0	3	3	4	3	5	2	4	2	1	
20-0										
16-1				1						MU
18-1	6	16	40	19	19	28	24	61	13	
20-1									7	
22-1								1	52	PU
18-2	2	2	10	54	68	58	54	22	14	
18-3				1	1	1	7	10	10	

*Monounsaturates **Polyunsaturates

Fatty acids of natural triglycerides with unsaturation all occur in the *cis* isomeric form and multiple double bonds are isolated on either of side of a methylene group. However, hydrogenation can cause isomerization to a *trans* configuration and also conjugated double bonds as shows Figure 1-3.

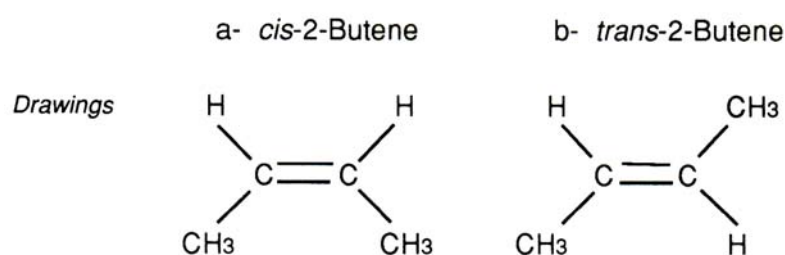
**Figure 1-3: *cis/trans* geometric isomers (Engelhard, 1992).**

Table 1-2 illustrates the effect of saturation on iodine value (IV) and melting point. Since iodine value is the gram of iodine that react with one gram of fat so as to saturate all existing double bonds, it is direct measure of unsaturation at any point in the hydrogenation process. It is clear from Table 1-2 that the melting point increases with increased saturation (lower IV) and also with isomerization of *cis* to *trans* configuration (oleic to elaidic). Thus, by proper choice of catalyst and operating conditions, it is possible to arrive at the desired properties for the production of a given product.

Table 1-2: Properties of C-18 Fatty Acids (Engelhard, 1992).

ACID	C=C	Free Acids		Triglycerides	
		IV	Melting point (K)	IV	Melting point (K)
Linolenic (C18:3)	3	273	262.15	261.6	249.15
Linoleic (C18:2)	2	181	268.15	173.2	260.15
Oleic (<i>cis</i> C18:1)	1	90	289.15	86.0	278.15
Elaidic (<i>trans</i> C18:1)	1	90	317.15	86.0	315.15
Stearic (C18:0)	0	0	343.15	0	346.15

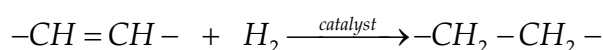
Despite of the fact that with the isomerization of *cis* to *trans* configuration increases the melting point, conflicting conclusions have resulted from studies on *trans* fatty acids. These isomers formed in hydrogenation of fatty oils have in some studies been shown to have similar effects as saturated fats (Oomen and Ocke, 2001). Other studies suggest that the *trans* acids increase both low-density lipoproteins (LDL) and high-density lipoproteins (HDL) levels. Some health organizations are recommending reduction in *trans* fatty acids in the diet, which might suggest using more liquid margarine and oils that have been hydrogenated only lightly (Rase, 2000) because polyunsaturated fats have been recommended in the diet as a means for reducing serum cholesterol levels in the blood, believed to be a major cause of heart disease. More recently, cholesterol associated with (HDLs) has been determined to be a favourable form of cholesterol, but the (LDLs) have been targeted as the ones that can cause heart disease and thrombosis. Ingestion of saturated fats has been implicated as a major contributor to a higher proportion of LDL in the blood, although saturated fats vary in this effect with the diary products (high), beef fat (less), and cocoa butter (slightly).

Apprehension and public awareness have risen regarding the potential health hazards of *trans* fatty acids intake in the human diet. To present, Denmark has been the only country in the world where the Ministry of Health has limited by law the % *trans* content to less than 2% on fatty acid components for human ingestion since May 2003. The committee of experts Codex Alimentarius of the FAO is on a debate regarding the inclusion of *trans* fatty acids content on food labels. On the other hand, the EU is favourable to include this on the label, but legal action is yet to be taken. In the US, the government (through the FDA) has put forward a campaign (announced by the Surgeon General in 2003) to label by law the % *trans* content and (or together with) the

% saturated fat, before 2006. The efforts of King and co-workers (2001) to develop a low *trans* process at the FDA, are in this direction.

1.2.2 Fats and Oil Hydrogenation Mechanism.

The basic hydrogenation of an unsaturated carbon-carbon double bond appears to be very simple but is extremely complex:



Scheme 1-2: Unsaturated carbon-carbon double bond hydrogenation.

As this reaction shows, hydrogenation can take place only when the three reactants have been brought together- the unsaturated oil, a liquid, the catalyst (which is a solid), and hydrogen gas. Thus the physical mechanism of bringing the reactants together has been devised without understanding what happened when the reactants were together in the correct structure to cause reaction.

The three phases of the system-gas, liquid and solid-are brought together in a heated stirred reactor with hydrogen available under pressure. The hydrogen must be dissolved in the liquid-solid phase before reaction can occur since the dissolved hydrogen is the only hydrogen available for reaction. The hydrogen may then diffuse through the liquid to the solid catalytic surface. In general, at least one of the reactants must be chemisorbed on the surface of the catalyst. However, the reaction between unsaturated hydrocarbons and hydrogen proceeds by way of surface organometallic intermediates.

Edible oil hydrogenation is a heterogeneous reaction which involves several steps as has been explained at the beginning of this chapter (See Figure 1-1). Each unsaturated group of the fatty acid chain can transfer back and forth between the main body of the oil and the bulk of surface of the catalyst. These unsaturated groups can be adsorbed on the catalyst surface. Each adsorbed unsaturated group can react with a hydrogen atom to form an unstable complex that is a partially hydrogenated double bond. Some of the complexes may react with another hydrogen atom to complete the saturation of the double bond. If the complex does not react with another atom of hydrogen, a hydrogen is removed from the adsorbed molecule and the "new" unsaturated bond is desorbed. Both the saturated and the unsaturated bonds are desorbed from catalyst surface and diffused into the main body of the oil. Thus not only are some of the bonds saturated, but some may also be isomerized to new position or new geometric forms.

A similar series of steps occurs when one of the double bond of a polyunsaturated fatty acid chain is hydrogenated. Isomerization reactions also occur in these cases, and at least part of the double bonds is isomerized to new positions. If a methylene-interrupted diene is reacted on the catalyst surface, the double bonds may be conjugated before saturation of one of the bonds. Also, the conjugated diene may be desorbed from the catalyst surface into the main body of oil before being readsorbed and partially saturated.

If the mixture to be hydrogenated contains both monoenes and dienes and polyenes, there may be competition between the different unsaturated systems for the catalyst surface. Thus the dienes may be preferentially adsorbed from the oil to the catalyst surface and partially isomerized and/or hydrogenated to a monoene and then desorbed to diffuse to the main body of the oil: The di- and polyenes are preferentially adsorbed until their concentration in the oil is very low, and the monoenes then may be adsorbed and reacted.

Since the oils that are hydrogenated are composed of a mixture of fatty acids, the selectivity of the reaction is very important.

1.2.3 Fats and Oil Conventional Hydrogenation Process.

The total annual production of hydrogenated oils is about 25 million tons (Mielke, 1992 and Fitch, 1994). The upgrading of oils by hydrogenation and isomerization is usually carried out in either batch or continuous processes (mostly batch) with a stirred slurry phase reactor (Sourelis, 1956). The industry is dominated by dead-end batch hydrogenators with a 2:1 or 3:1 liquid level to diameter and a top "dead" space for hydrogen accumulation. A typical industrial batch dead-end process is shown in Figure 1-4. A portion of the oil charge which is weighed into the supply tank is used to mix with the catalyst (usually based on nickel, load ranging from 0.01 to 0.2 wt% per batch) in the mix tank (made of carbon steel and with a capacity of 5 to 20 m³) under vacuum and the agitator and heating are started. When a temperature about 323.15 K below the reaction temperature is reached, vacuum turned off, and hydrogen is added. Agitation of the catalyst-oil mixture serves the double purpose of promoting solution of hydrogen in the oil and continuously renewing the oil at the catalyst surface. Cooling water is turned on, and the heat of reaction increases the system temperature to the desired reaction temperature. When the reaction pressure had been reached, only enough hydrogen is added to maintain pressure. Finally, when the reaction has been completed, hydrogen flow is discontinued and the hot product is then passed through a heat

exchanger where it is used to preheat the incoming feed. The product is cooled to about 373.15 K and filtered to remove the powdered catalyst which is reused in subsequent cycles.

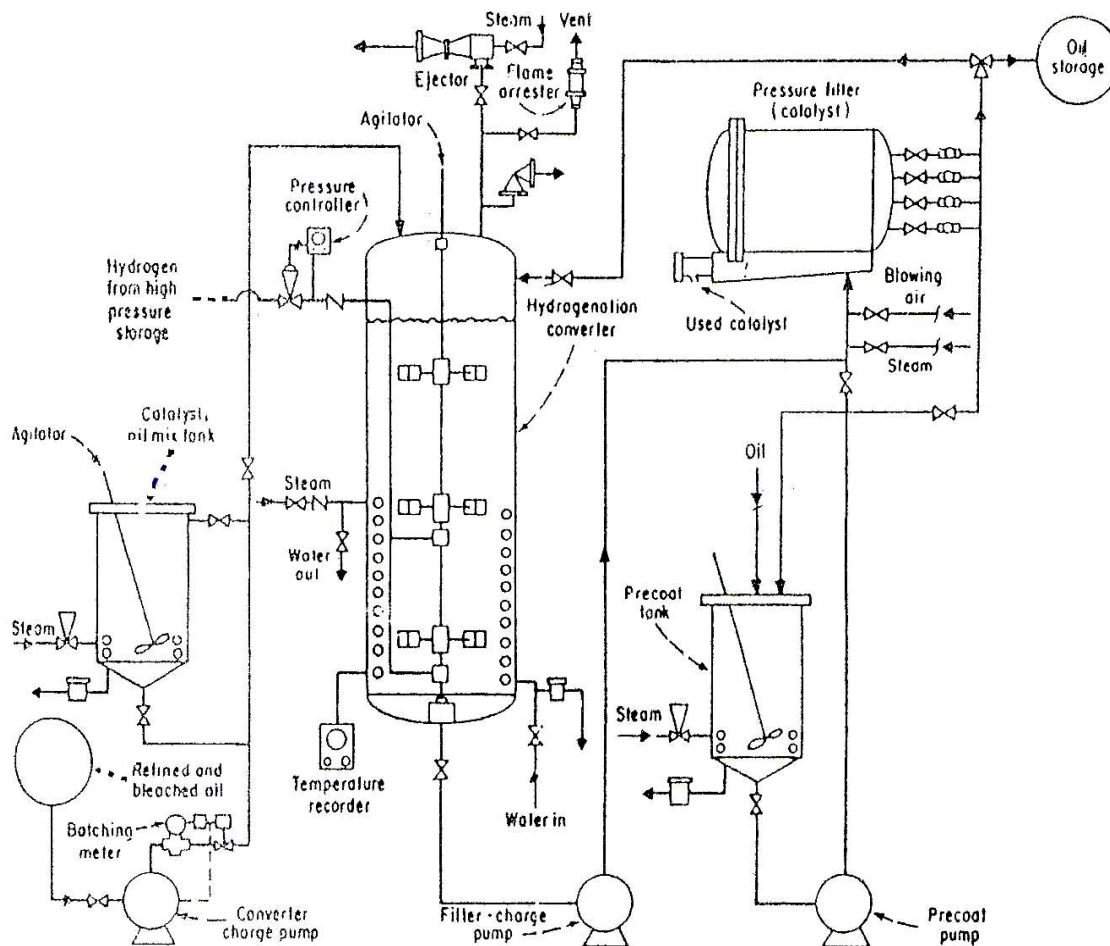


Figure 1-4: Dead-end batch hydrogenation process for triglyceride oils (Albright, 1967).

Although the dead-end hydrogenator just described dominates the industry, other reactors are offered as licensed processes. These include loop reactors, which employ a mixing jet that uses hydrogen to propel the oil into the reactor while mixing the liquid and circulating it through external heat exchangers. Although, the loop reactors are better mixed and provide better heat transfer, they are more difficult to start up and are more likely to produce catalyst fines if not properly operated (Rase, 2000).

Operating conditions vary depending on feed and desired product. Normal ranges are 393.15-473.15 K and 0.1-0.5 MPa. The reaction time is about 2 hours. The reactor operates initially in the semibatch mode as hydrogen is added at relatively high rates until the pressure builds up to the desired value. After this time, only a small amount of hydrogen is added to maintain the pressure, a decline of which is caused by hydrogen consumption and a bleed gas stream operated to expel impurities. In the second mode

hydrogen continues to bubble but at a low rate. The impeller near the surface will also draw some hydrogen from the vapour space and cause further contacting. The end point can be detected approximately by refractive index, which correlates with iodine value or by noting hydrogen consumption. If the end point is critical, the agitator can be stopped to allow time for more thorough laboratory work such as iodine value and isomer analysis. This procedure is time consuming. Alternatively, batches of differing end points can be blended to produce the desired product. Final good products can also be produced by mixing a higher melting more saturated product with a liquid oil containing high amounts of acid groups with two and three pairs of double bonds such as safflower, soybean and corn oils. (Rase, 1977).

As a rule, liquid-phase hydrogenations are strongly exothermic reactions (heats of reactions between 65-550 KJ/mol). For this reason, reactors have to be fitted with large heat-exchange areas, either internally or on an external circulation loop. The external exchanger offers the advantage of having almost unlimited space available for its layout. However, temperature distribution in the reactor is not uniform because the heat is generated and removed in two different locations. A dynamic temperature regulation system is needed because the system requires rapid switching from heating (to start the reaction) to full cooling. Runaway conditions are possible because the reaction is exothermic and it is operated in the batch mode. Fortunately, the reaction can be stopped almost instantaneously by suppressing the mass transfer of hydrogen (by stopping the agitator, for example). Nevertheless the safety system has to be designed carefully for failsafe operation and the quickest possible response (Landert and Scubla, 1995).

The low solubility of H₂ in the oil and the high mass transfer resistance for the hydrogen from the gas phase to the catalyst surface (See Figure 1-1) leads to a depletion on H₂ at the catalyst surface, which in turn, slows down the reaction rate and gives rise to double bond migration and *cis-trans* isomerization (Rylander, 1985 and Grau *et al.*, 1988). On the other hand, internal transport limitations on hydrogen and triglycerides to the active sites of the catalyst have a strong influence on both selectivity and *trans* production. For partially hydrogenated oil, a *trans* content of 30 to 50% is normal to a iodine value (IV) of 70.

The current commercial batch process using nickel catalyst, either supported on kieselguhr or silica, has some disadvantages: (1) Discontinuous operation, (2) Low space-time-yields, (3) Undesirable by-products as a result of strong hydrogen mass-transfer and (4) High variable costs (e.g. man-power, energy and filtration). On the

other hand, the use of the supported nickel catalyst also leads to additional problems including undesirable by-products (*trans* fatty acids) with an impact on health (high cholesterol and lipid level in blood), catalyst deactivation through formation on nickel soaps in free fatty acid hydrogenation, nickel residues which could be toxic (Niboer *et al.*, 1993).

A way to increase the concentration of hydrogen at the catalyst surface is to introduce a supercritical solvent into the reaction mixture. The role of supercritical fluid is minimized the transport resistance for hydrogen. As a consequence, the effective hydrogen concentration at the catalyst surface is significantly enhanced, leading to extremely high reaction rates compared to the traditional two-phase gas-liquid approach (Baiker, 1999 and Fan, 1999).

1.3 Supercritical Fluids.

1.3.1 Definition and Properties.

A supercritical fluid (SCF) is defined as the state of a compound, mixture or element above its critical pressure (p_c) and critical temperature (T_c) but below the pressure required to condense it into a solid (Jessop and Leitner, 1998). However, the last term of this definition (“but below the pressure required to condense it into a solid”) is generally omitted because the pressure required to condense a SCF into a solid is generally impracticably high (Clifford, 1998). The critical point corresponds to the highest T and P at which the substance can exist as a vapour and liquid in equilibrium.

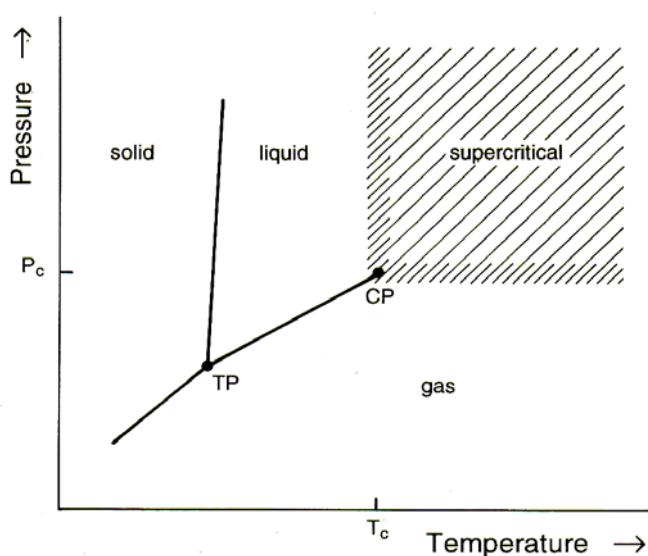


Figure 1-5: Definition of SC state for a pure component. CP critical point, TP triple point, T_c critical temperature, P_c critical pressure (Brunner, 1994).

The properties of an SCF vary over a wide range depending on the temperature and pressure, but are generally intermediate between those of liquids and gases (Table 1-3). However, these properties, especially density, are highly sensitive to small changes in T and P near the critical point.

Table 1-3: Comparison of the physical properties of gases, liquids and SCFs (McCoy, 1999).

Property	Gas	SCF	Liquid
Density (g/cm ³)	10 ⁻³	0.4	1
Viscosity (Pa s)	10 ⁻⁵	10 ⁻⁴	10 ⁻³
Diffusivity (cm ² /s)	0.1	10 ⁻³	10 ⁻⁵ -10 ⁻⁶

As can be seen from Table 1-3, the density of SCFs is approximately, two orders of magnitude higher than that of a gas but it is also less than half of that of a liquid. Viscosity and diffusivity are highly dependent on T and P changes. Both properties are, in general, at least an order of magnitude lower and higher, respectively, compared to liquids.

The liquid-like density of an SCF, enables many materials to be dissolved to a level which is orders of magnitude higher than that expected from ideal gas considerations. Temperature and pressure can therefore be used as variables to control the solubility and separation of a solute. In contrast, diffusivity and viscosity represent transport properties, meaning that the diffusion of a species in a SCF will occur faster than that in a liquid. Also, SCFs will be more efficient at penetrating into microporous solid structures (Jessop and Leitner, 1998). The most important feature of SCFs that really differentiate them from liquid solvents is their tunability: simple alterations in temperature and pressure modify the physical properties from gas-like to liquid-like.

SCFs have been considered very useful as reaction media because of the high solubility of liquid and solids, especially when compressed to liquid-like densities, but also their tunability, which allows one to control the solubility of organic solutes. In addition, SCFs have the ability to dissolve gases such as H₂, O₂ and CO (Baiker, 1999).

1.3.2 SCFs in Heterogeneous Catalysis.

Catalytic heterogeneous reactions are generally controlled by the rate of diffusion of the reactants to and into the catalyst surface (see Figure 1-1). SCF have a great deal of potential for heterogeneous catalysis, where the reactants and the catalyst are in different phases. Normally, the catalyst is a solid, and the SCF is used as a solvent for

organic substrates. The use of SCFs as reaction media can be a real advantage when using heterogeneous catalysts, since the diffusion rates are enhanced compared to reactions in the liquid phase. Diffusion is not only enhanced in the bulk fluid, but also within the pores of the catalyst particles (Jessop and Leitner, 1998).

SCFs, either used as solvents or reactants, provide several opportunities to enhance and control heterogeneous catalytic reactions. Important possibilities include (i) control of phase behaviour, elimination of gas/liquid and liquid/liquid mass transfer resistances, (ii) enhanced diffusion rate in reactions controlled by external (fluid/particle) diffusion, (iii) enhanced heat transfer (iv) easier product separation, (v) improved catalyst lifetime by dissolution of deactivating deposits, (vi) tunability of solvent properties by pressure and cosolvents, (vii) enhancement of the reaction rate, (viii) control of selectivity by solvent-reactant (solute) interaction and (ix) process intensification (Baiker, 1999).

More important is that due to the higher reaction rates and easy product separation, the combination of heterogeneous catalysts with SCFs allows the use of continuous flow reactors (Baiker, 1999). Compared to liquid-phase reactions, reactions in SCF are characterized by reduced viscosity and enhanced mass transfer. In addition, the good thermal transport properties of supercritical fluids are an advantage because hydrogenation is usually a highly exothermic reaction. The benefits of using fixed-bed continuous reactors include better process control, increased productivity, easy separation of products from the catalyst and enhanced margins of safety (Anderson, 2001). Furthermore, continuous reactors for SCFs present many advantages over batch reactors. For example, they do not need to be depressurised to load the reactants or to recover the products. The product recovery is accomplished by a depressurisation step once the reaction is finished (Hyde *et al.*, 2001). Industry in particular, favours continuous processes because they are more cost efficient and the reactors can be kept smaller in size (Tundo, 1991). This reduction in size reduces both costs and safety problems of the high-pressure equipment needed for supercritical reactions.

A wide range of catalytic reactions can be carried out in supercritical fluids, such as Fisher-Tropsch synthesis, isomerization, hydroformylation, fats and oils hydrogenation, synthesis of chemicals, biocatalysis and polymerization (See Figure 1-6).

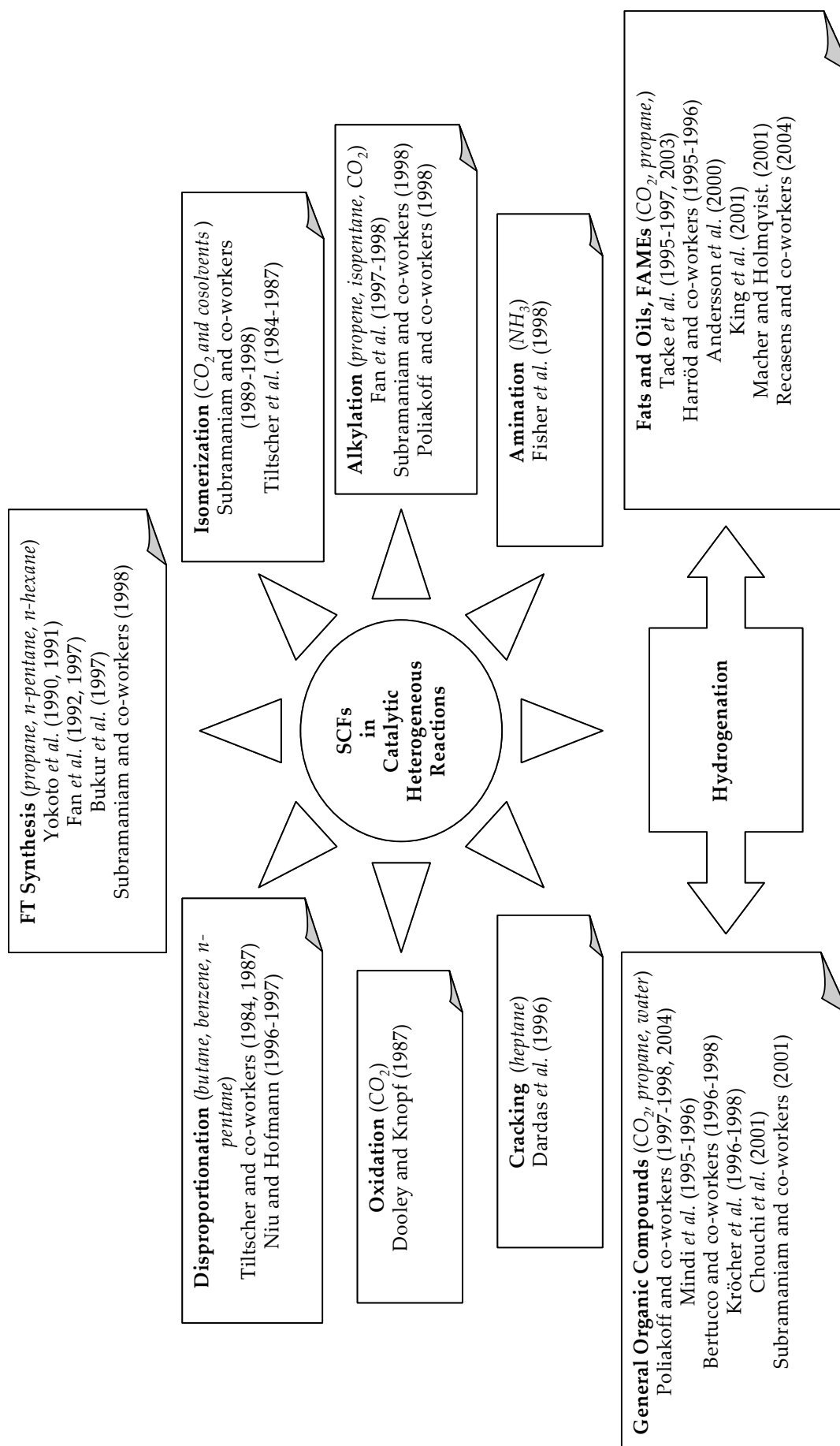


Figure 1-6: Catalytic heterogeneous reactions carried out in SCFs.

The majority of the studies which have been conducted on SCFs, have focused on four fluids, CO₂, ethane, ethene and water. However, CO₂ is by far, the most widely used SCF (Jessop and Leitner, 1999). This is because SC CO₂ is non-toxic, non-flammable, relatively cheap and inert. Appendix A provides an overview of these studies, indicating the conditions and main features of the various investigations.

In the case of alkylation reaction, Fan *et al.* (1997-1998) found from the experimental results that the supercritical operation mode resulted in significantly slower catalyst deactivation, higher catalyst activity as well as an improved selectivity of the substrates. The increase in the catalyst life-time has been attributed to the higher solubility of heavy organic residues ("coke") in SCFs than in the correspondent gases. The coke formed, might block the catalyst active sites; therefore, deactivating the catalyst. Due to the enhanced diffusivity in SCFs, the transfer of coke precursors from the internal and the external catalyst surface is accelerated, increasing the catalyst life-time (Poliakoff and co-workers, 1998, Subramaniam, 2001 and Subramaniam *et al.*, 2002).

Fischer *et al.* (1998) investigated the influence of pressure on conversion and product selectivity of the influence of pressure on conversion and product selectivity o the amination of amino-1-propanol with ammonia over a Co-Fe catalyst. The experiments, which were conducted in a continuous tubular reactor at 468.15 K and a molar feed ratio of reactants R-OH/NH₃= 1:20 in the total pressure range 5.0-13.5 MPa, indicated a striking change of the selectivity to the desired product, 1,3-diaminopropane from 4% to 40% in the near critical region of ammonia (T_c=405.15 K, P_c=11.4 MPa). Comparing to selectivity, corresponding changes in conversion were small.

Dardas *et al.* (1996) used an in situ cylindrical reflectance infrared technique (CIR-IR) to study supercritical *n*-heptane cracking. Their results showed that a significant number of Brønsted acid sites and terminal silanols are consumed during catalytic cracking, new spectral bands appear and acid sites regained a significant percentage of their initial concentrations of their initial concentrations during supercritical cracking, indicating that the catalyst starts recovering its activity under there process conditions.

Tiltscher and co-workers (1984, 1987) studied the disproportionation of 1,4-diisopropylbenzene under gaseous and supercritical conditions using a zeolite 13NaHX catalyst in an internal differential reactor. The authors concluded that raising the pressure in the supercritical region enhances desorption of the adsorbed products due to increased dissolution power of SCF and suggested that this effect can be used to prolong catalyst lifetime and to direct the product distribution of multiple reactions.

Niu and Hoffman (1996, 1997) reached the same conclusion for the catalyst lifetime in the disproportionation of ethylbenzene over HY-zeolite under supercritical conditions.

Vieville *et al.* (1993-1994) investigated the esterifications of oleic acid by methanol catalyzed by sulfonic acid resins in supercritical CO₂. The esterification of carboxylic acids with alcohols is an example of a reversible reaction, which has been studied at supercritical conditions. The authors found similar parametric sensitivity of the reaction rate in supercritical carbon dioxide as in *n*-hexane. However the reaction was faster in supercritical carbon dioxide. This fact was attributed to increased solubilization of methyl oleate and higher diffusivity.

Considerable effort has been expended in exploring the application of supercritical fluids in Fisher-Tropsch (FT) synthesis (Baiker, 1999), which provides a means to synthesize higher hydrocarbons in the liquid fuel range from synthesis gas (CO and H₂). The classical synthesis route involves an exothermic gas-phase reaction, and consequently efficient heat removal is essential. Another problem arises from condensation of higher hydrocarbons formed during reaction within the catalyst pores, which can cause catalyst deactivation. In a liquid-phase process, the lower diffusivity leads to mass-transfer limitations and consequently to lower overall reaction rate. In some early studies, Yokota and co-workers (1990, 1991) demonstrate that the supercritical FT reaction shows unique characteristics such as high diffusivity of reactant gases, effective removal of reaction heat as well as in situ extraction of high molecular weight hydrocarbons (wax). These authors concluded that in the supercritical phase reaction, both the desorption and the diffusion of the product were so well-balanced that the overall mass transfer of the products was most effective in the supercritical phase and thus the hydrogenation of primary olefins was effectively suppressed.

Bukur *et al.* (1997) studied the effect of process conditions on olefin selectivity during FT synthesis in supercritical propane. They found that the total olefin and 2-olefin selectivity were essentially independent of reaction temperature but under supercritical conditions the total olefin content was greater while the 2-olefin content decreased. The authors concluded that undesired secondary reactions (isomerization, hydrogenation and readsorption) of high molecular weight α -olefins occur to a smaller extent during supercritical operation, due to higher diffusivities and desorption rates of α -olefins in the supercritical propane than in the liquid-filled catalysts pores.

On the first reaction investigated under supercritical conditions was the *cis/trans* isomerization of α -olefins (Tiltscher and co-workers, 1984-1987). Particularly, the isomerization of 1-hexene turned out to be a suitable model system for investigation. Interesting features of this reaction are the product formation via a system of complex parallel and consecutive reactions and the fact that *trans* isomers are thermodynamically more stable than *cis* isomers. These authors found that the initial *cis/trans* ratio increases with pressure in the supercritical region. This behaviour is attributed to the kinetic favouring of *cis*-hexane-2 formation due to its enhanced desorption in the supercritical phase.

Subramaniam and co-workers (1989-1998) have focused their attention on the isomerization of 1-hexene catalyzed by Pt/alumina. Continuous fixed-bed reactor experiments were used to investigate catalyst deactivation in hexane/CO₂ mixtures. The activity of the catalyst decreased at a subcritical pressure, whereas at a nearly identical temperature but supercritical pressure no catalyst deactivation was observed. The stable activity of the catalyst under supercritical conditions was explained by the solvent power of the SCF which presumably prevented deposition of higher molecular weight oligomers in the catalyst pores. In subsequent works (Subramaniam and co-workers, 1990, 1992 and 1994) these authors concluded that near-critical reaction mixtures provide an optimum combination of solvent and transport properties that is better than either subcritical (gas-like) or dense supercritical (liquid-like) mixtures for maximizing the isomerization rates and minimizing catalyst deactivation rates.

Dooley and Knopf (1987) studied the partial oxidation of toluene to benzaldehyde with air in supercritical CO₂ in the presence of redox or acid catalysts. The high-pressure process affords much better selectivity to partial oxidation products. A similar improvement was noticed by Gaffney and Sofranko (1993 and 1993) for the oxidation of propene to propylene glycol under supercritical conditions and by Fan *et al.* (1997) for the oxidation of isobutane to *tert*-2-butyl alcohol.

Most of the work in supercritical water has focused on supercritical water oxidation, which is an effective means for complete oxidation of many organic wastes. Advantages to conducting this reaction above the critical point include faster reaction rates, single fluid phase, and complete miscibility of nonpolar organics with supercritical water (Baiker *et al.*, 1999).

Hydrogenation of organic compounds is a process of major chemical importance (Poliakoff *et al.*, 1999). Gaseous H₂ is an expensive and versatile reagent for

hydrogenation but it can often be difficult to use in practice. Laboratory-scale hydrogenation is usually slow because H_2 is sparingly soluble in common solvents, while high-pressure industrial-scale reactions can be difficult to control because they are highly exothermic. The mass-transfer resistances involved in the reaction were illustrated early in Figure 1-1.

SCFs are becoming increasingly attractive as solvents for environmentally more acceptable chemical processes. Their densities are comparable to those of organic liquids, and the gas-like nature of the fluids renders them completely miscible with permanent gases such as H_2 . By constant, the solubility of gaseous H_2 in conventional organic solvents is relatively low. Thus, SCFs are potentially attractive solvents for hydrogenation reactions which significant advantages over conventional methods, particularly because gas-phase reactions often generate significant amounts of by-products and conversion can be poor in liquid-phase reactions.

On the other hand, their reduced viscosity and enhanced mass transfer make SCFs highly suitable as solvent for continuous flow reactors. In addition, their good thermal transport properties are on advantage because hydrogenation is usually a highly exothermic reaction. Until 1996, relative few articles have been published on hydrogenation in SCFs (Howdle *et al.*, 1990; Rathke, *et al.*, 1991; Jessop and co-workers (1994-1996); Burk *et al.*, 1995; Minder *et al.*, 1995; Kröcher *et al.*, 1996) and most of those have involved hydrogenation as a batch process, carried out in sealed autoclaves. Reports on supercritical hydrogenation as a continuous process were even rarer.

Supercritical fluids (carbon dioxide, propane, ethane) have been applied advantageously as solvents in several hydrogenations reactions, including hydrogenation of fats and oils as well as a great range of organics compounds.

Bertucco and co-workers (1996, 1997) studied hydrogenation kinetics of organics on Pd/ Al_2O_3 in a Berty-type of reactor with SC CO_2 as a solvent. The system was clearly subject to liquid condensation during operation, as noted by the authors. Devetta *et al.* (1999) carried out the three-phase catalytic hydrogenation of an unsaturated ketone using SC CO_2 as a solvent in order to simulate the performance of a semi-industrial trickle-bed reactor. An industrial Pd on alumina supported catalyst was used, in form of egg-shell pellets. Experiments were carried out at 20 MPa and temperatures ranging from 323.15 to 453.15 K and data were collected over the whole conversion range, allowing for a thorough inspection of the reaction rate composition dependencies. The results proved the positive effect of supercritical CO_2 : the reaction rate was increased

and product conversion was double with respect to the absence of supercritical solvent. Despite of the fact that these authors observed large increases in the reaction rate, they are not as high as those observed in the work of Härröd *et al.* (1997, 1999). The later authors attribute this difference to the fact that the SCF, H₂ and the substrate form a unique reactive single phase. A quite different explanation for the effectiveness of hydrogenation has been put forward by Bertucco (1996, 1997) who suggests that, for the hydrogenation of higher molecular weight organic substrates, SC CO₂ dissolves in the organic substrate to form an “expanded liquid”, which may contain up to 80% CO₂. The high rates of hydrogenation arise because H₂ is much more soluble in this expanded liquid than in the normal liquid substrate (Freemantle, 2001). The practical conclusion from these contradictory facts is that one-phase and two-phase systems exhibit very different hydrogenation rates. This is interesting to know since phase behaviour during reaction should dictate the type of reactor to be used in the process.

A wide range of substrates including alkenes, alkynes, ketones and aldehydes, epoxides, phenols, nitriles, etc., was hydrogenated using SC CO₂ or supercritical propane as solvents by Hitzler *et al.* (1997, 1998). One important finding is that the operating conditions (temperature, pressure and hydrogen/substrate mole ratio) can be tuned to drive the multiple reaction system to the desired product distribution. Conversion of starting materials, product selectivity and space-time yields of the catalyst were high, and the reactors themselves were very small (5- and 10 cm³). The authors claim that even with a 5 cm³ reactor throughputs can be reached with are larger than those needed by most synthetic organic laboratories. However, for judging the economical value of this approach a comparison with corresponding continuous hydrogenations in conventional solvents and the extra costs imposed by the supercritical fluid application need to be considered.

Chouchi *et al.* (2001) presented preliminary data on the hydrogenation of α -pinene on Pd/C in SC CO₂ in a stirred tank batch reactor. Again it was found that larger rates developed as soon as a two-phase system formed but the rate enhancement was less than that observed by Härröd *et al.* (1996, 1997). These authors attributed this phenomenon to the fact that SC CO₂ can dissolve extensively in the liquid reactant, leading to the formation of an “expanded liquid” as suggested early Bertucco and co-workers (1997).

Arunajatesan *et al.* (2001) carried out hydrogenations of cyclohexene in SC CO₂, studying reactor temperature, pressure, and the effect of these variables on catalyst deactivation. They checked visually for liquid formation by means of a view cell. They

obtained excellent temperature control and catalyst stability with the use of a near-critical solvent. This provided an effective heat removal capacity and avoided oligomer formation that adsorbs strongly on the catalyst, causing deactivation. Liquid-like heat capacities were key factors in controlling the adiabatic temperature rise for the reaction in a potential runaway. Some of these authors' findings are consistent with previous results on coke deposition control in an SCF solvent (Subramaniam *et al.*, 1999).

By generating simultaneous both hydrogen and supercritical carbon dioxide, a new continuous hydrogenation process avoids the problems of handling gases under pressure, developed by chemist at the University of Nottingham (England), the gasless laboratory technology relies on the decomposition of liquid formic acid, HCO_2H , over a heated platinum or palladium catalyst at 723.15 K in a miniature reactor. The resulting H_2 and supercritical CO_2 are mixed with the material to be hydrogenated (Cyclohexene and Oct-1-ene), and then passed over a noble-metal catalyst in a second reactor. Decomposition of HCO_2H yields H_2 and CO_2 in a 1:1 ratio. Decomposition of $\text{HCO}_2\text{C}_2\text{H}_5$ in the absence of HCO_2H opens up possibilities for carrying out other supercritical fluid reactions. Hyde and Poliakoff (2004) have demonstrated, for example, that the equipment can be used for acid-catalyzed Friedel-Craft alkylations too.

Garcia *et al.* (2004) and Ramírez (2004) continued working on “gasless” reactions technology in association with researchers from University of Nottingham but evaluating the potential of near-critical water and SC water to develop more environmental friendly process. Two of the most important processes on industrial scale are hydrogenation and oxidation reactions. High temperature pressurised water provides an advantage for such reactions. Water can act as a solvent for both gases and organic substrates providing a single phase reaction which overcomes mass transfer limitations providing rapid reaction rates. However, both processes require the use of gases such as hydrogen and oxygen. It was have found that compresses hydrogen and oxygen, although possible, is expensive, required safety precautions and it is difficult to control on the small scale required for bench-work. One practical solution to this problem is to generate oxygen or hydrogen by thermal decomposition of the right precursors. Thus, hydrogen peroxide can be used as source of oxygen and formic acid or related formates to generate hydrogen. The “gasless” hydrogenation of aromatic compounds in near-critical water was carried out using the formic acid (HCO_2H), sodium formate (NaCO_2H) or ammonium formate ($\text{NH}_4\text{CO}_2\text{H}$) aqueous solutions as a hydrogen source by thermal decomposition. No catalyst has been required. The reduction of different cyclic and aromatic ketones, olefins and aldehydes was done

using a green process achievable with very simple equipment (See Appendix B for more details) under pressures between 15 and 20 MPa, temperatures between 413.15 and 563.15 K and residence times between 6 and 30 s in a continuous flow reactor. Conversions up to 80% combined with mass recoveries around 99% obtained so far show an interesting way for this type of reaction. The real challenge was to develop easier, safer and greener reactions. In addition, an exciting possibility was that the same apparatus could be used either for oxidation, *via* aqueous H₂O₂ as source of oxygen, or hydrogenation purposes, *via* HCOOH, NH₄CO₂H or NaCO₂H as source of hydrogen without significant change to the apparatus.

The effect of SCFs on fats and oil hydrogenation will be discussed as follows:

1.3.3 SCFs in Fats and Oil Hydrogenation.

The fluid most considered for supercritical hydrogenation is carbon dioxide (CO₂) as can be seen from Figure 1-6. However, CO₂ is not a good solvent for heavy compounds. For methyl palmitate and components with similar chain lengths attached to it (i.e., alkanes, fatty acids, fatty acids ethyl esters, etc.), CO₂ gives a phase split up to very high pressures, whereas propane shows complete miscibility, even for heavier compounds like triglycerides, under similar conditions. Propane has the advantage of lower critical pressure than CO₂, but this is offset by its flammability.

The mass transfer of H₂ and triglycerides to the catalyst surface can be improved not only by the optimization of the process parameters (temperature, H₂ pressure, catalyst concentration, etc.) in combination with a supercritical fluid as a reaction medium but also by the architecture of the catalyst comprising suitable pore geometries with a mean pore size appropriate for effective diffusion of triglycerides (Coenen, 1986). As an unavoidable side reaction occurring during the catalytic edible oil hydrogenation, the geometric isomerization leading to the formation of *trans* fatty acids can be influenced by the type of the dispersed metal on the solid support (Schmidt, 2000) and the surface characteristics of the support. Noble metals supported on various solids including alumina, silica and activated carbon have been studied for their activity, selectivity and *trans* fatty acids formation. These studies have shown that noble-metal catalysts are sensitive to intraparticle diffusion gradients attributable to the high activity of such metals. Although they may appear to be cost-prohibitive, their extremely high activities and the possibility of reuse may offset the cost limitation and they could be viable alternative to Ni (Cecchi *et al.*, 1979 and Hsu *et al.*, 1986), which is usually the catalyst employed in conventional edible oil hydrogenation. As a possible candidate, Pd was

shown to exhibit an activity of 80-100 times that of Ni (Gray and Russell, 1979 and Ray, 1985). Thus, the catalyst formulation is an important factor contributing to the *trans* fatty acids and saturated fatty acids production during hydrogenation, besides the process conditions (Coenen, 1986). It is desirable to design catalysts with tailored surface characteristics, having higher selectivity for the formation of monoene fatty acids with a *cis* configuration and lower selectivity for production of saturated fatty acids. Therefore, most of recent studies on supercritical fats and oils hydrogenation reported in Table A-1 are based on supported palladium instead of nickel catalysts.

Tacke *et al.* (1996, 1997 and 2003) reported full or partial hydrogenation of fats and oils, fatty acids, and fatty acid esters using near-critical and supercritical CO₂ and/or propane as solvent at temperatures between 333.15 and 393.15 K with a total pressure up to 10 MPa. The reactions were conducted in a continuous fixed bed reactor with palladium (Pd) on Deloxan as proprietary catalyst. The authors observed significantly improved space-time yields compared to those of hydrogenation in other types of reactors (such as conventional trickle bed and slurry), a longer catalyst life, and a higher selectivity.

Härrod and co-workers (1996, 1997, 1999) succeeded in overcoming the solubility problem and the transport resistance for hydrogen. They used near-critical or supercritical propane, which is miscible with both, oil and hydrogen thus forming an essentially homogeneous phase, and fed it into a continuous fixed-bed reactor packed with a commercial palladium catalyst. Under these conditions they achieved extremely high reaction rates, according to the authors about 400 times higher, for the partial hydrogenation of fatty acid methyl esters compared to the traditional technique. The tremendous rate enhancement was attributed to the elimination of gas/liquid mass transfer (See Figure 1-7) as a consequence of the essentially homogeneous phase under supercritical conditions, which facilitated the increase in the hydrogen concentration at the catalyst surface. Thus in this situation, the reactants can go directly to catalyst surface, and the products can come off without resistance. Another benefit of supercritical conditions was that the concentration of *trans*-fatty acids was considerably reduced compared to conventional processes using the same catalyst and the same degree of hydrogenation. On the other hand, propane is allowed for unlimited use in the production of foodstuffs (EC directive 88/344, 1984).

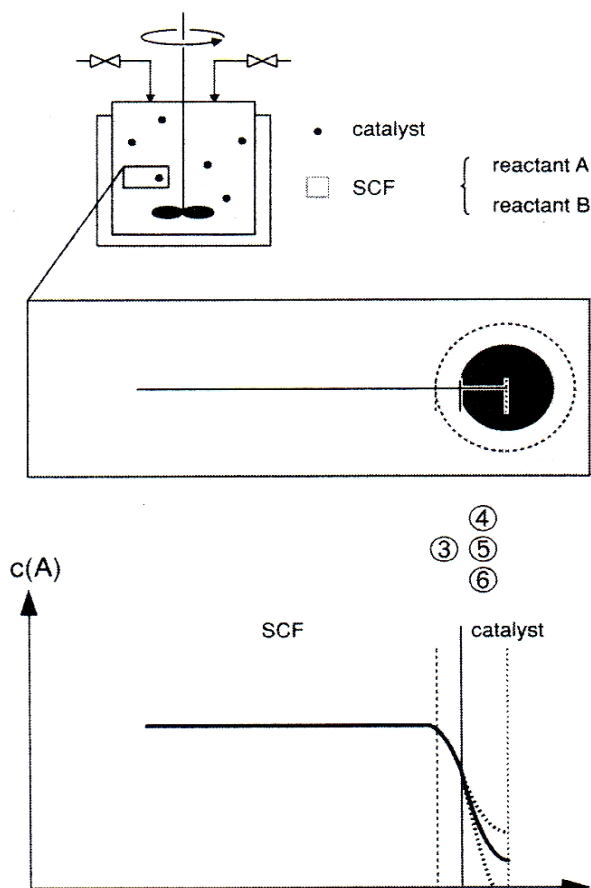


Figure 1-7: Reactant concentration profile for a heterogeneous catalytic reaction under supercritical conditions. Note that under supercritical conditions gas/liquid transfer resistance is eliminated and external fluid film diffusion resistance (step 3) is lowered due to lower viscosity of SCF.

Andersson *et al.* (2000) also studied the hydrogenation of FAMES in different supercritical gaseous mixtures ($H_2/SC\ CO_2$, $H_2/SC\ C_3H_8$) using defined reaction conditions (15-25 MPa, 483-523.15 K) and conventional catalysts (chromium free and copper chromite) in order to determine the advantages and disadvantages of each reactant system. One important feature of their work is that by coupling the lipase-catalyzed transesterification based on SC CO_2 with the SC hydrogenation, a new green process emerges for the sustainable production of mixtures of fatty acid alcohols directly from the vegetable oil.

King *et al.* (2001) studied the hydrogenation of soybean oil at 14 MPa and 393.15–413.15 K with conventional nickel catalyst in a dead-end reactor with a headspace consisting of either a binary fluid phase consisting of varying amounts of carbon dioxide mixed with hydrogen or neat hydrogen for comparison purposes. These authors found that depending on the chosen reaction conditions, a wide variety of end products can be

produced having different iodine values, percentage *trans* fatty acid content, and dropping points or solid fat indices. Although addition of carbon dioxide to the fluid phase containing hydrogen retards the overall reaction rate in most of the studied cases, the majority of products have low *trans* fatty acid content, consistent with a nonselective mode of hydrogenation.

Macher and Holmqvist (2001) carried out the hydrogenation of palm oil in near-critical and supercritical propane using a small (0.5 cm³) continuous fixed reactor and 1% Pd/C as catalyst, temperature (338.15–408.15 K), H₂/triglyceride mol ratio (4–50), and residence time (0.2–2 s) to assess the iodine value (IV) as a function of the operating variables. The authors observed high reaction rates (a residence time of 2 s is sufficient at 393.15 K), which indicates that the reaction could also be run successfully at lower temperatures.

Ramírez and Larrayoz (2002) presented preliminary experimental data from a continuous, single-phase hydrogenation of sunflower oil on Pd/C carried out in a Robinson- Mahoney-type of reactor, with a fixed bed catalyst using propane as SC solvent. A wide range of hydrogenation products were obtained with certain plastic characteristics for further food application by tuning the operating conditions.

In a later work, Ramírez *et al.* (2004) reported the fluid-phase hydrogenation on sunflower oil in dense propane with 1 mol % vegetable oil, 9% H₂, and 90% propane at 428.15–488.15 K and 20 MPa. The reaction was run continuously in a single-fluid phase, using a laboratory setup. The catalyst was 2% Pd supported on C. The authors used the design of experiments and response surface methodology to achieve optimum hydrogenation conditions for Pd catalyst in SC propane in a continuous stirred reactor as well to show that it was possible to obtain a hydrogenated fat with 2–3 wt % *trans* content in a single pass through the reactor in a continuous process, with a final iodine value around 70. The experimental results showed that one principal advantage of using propane as a supercritical fluid is the low *trans* acid content, as well as low stearic acid, compared with that of the conventional process. No deactivation of the catalyst was observed. Furthermore, kinetics of the reaction using the Hashimoto *et al.* (1971) scheme was determined.

From the facts mentioned previously, the combination of supported precious metal fixed-bed catalysts together with near critical or supercritical solvent creates new possibilities for continuous fixed-bed hydrogenations with significantly improved space-time-yields and catalyst life-times. Short residence times and well-balanced

diffusion and desorption of products and reactants results in a decrease in undesirable by-products and therefore higher selectivity. The main advantages of supercritical single-phase fat and oil hydrogenation on supported metal catalysts can be summarized as follows (Härrod *et al.*, 2001):

- Extremely high reaction rates have been achieved even for very large molecules. The reaction time is in the range of seconds compared to hours in the traditional process; therefore only continuous reactors are suitable for this type of reactions.
- Controlled reaction selectivity. The concentration at the catalyst surface (both substrate and hydrogen) can be controlled independently of the process conditions. The unique feature is that very high concentrations of hydrogen can be achieved leading to much for example to the suppression or decrease of *trans*-fatty acids in partial hydrogenation.
- The product quality can be improved. Depending on the chosen reaction conditions, a wide variety of end products can be produced having different iodine values, dropping points or solid fat indices with low percentage *trans* fatty acid contents.
- Extremely high degrees of conversion can be achieved by increased the reaction time greatly. However, the reactor volume will still be very small because of the extremely high reaction rate.
- The short residence times in the reactor give less subject to time-thermal degradation of heat-sensitive products and/or substrates.
- The addition of the solvent makes possible to control the temperature in the reactor despite the exothermic reactions and high reaction rates. The reactor operates nearly adiabatically, but the temperature rise in the reactor can be controlled, because the solvent acts an internal cooling medium. The concentration of the substrate determines the maximal temperature rise and therefore, by controlling the concentration, the maximal temperature rise is controlled. In this way, the amount of unwanted side-products can be reduced.
- The catalyst life might be improved. Several studies on isomerization and polymerization process indicate that indicate supercritical solvents can dissolve coke precursors on the catalyst surface, and remove them before they can form coke and this improves the catalyst life (Tiltscher, 1986 and Subramaniam, 2000).

Since coke formation also occurs in hydrogenation process, it is reasonable to believe that catalyst life can be improved also for supercritical-phase hydrogenation. This means reduced consumption of catalyst and reduced production costs.

- Easy separation of the product from the supercritical fluid just by reducing the pressure in the reactor effluent stream.
- Scaling up is facilitated because of the single-phase conditions. Hotspots and channelling can be avoided and this leads to a better selectivity.

The economy of the whole process seems to be favourable. Extremely high volumetric reaction rates can be achieved lead to much smaller and cheaper plants. The concentration of the substrate in the solvent (i.e. loading) is crucial, as in any other solvent-based process. The recovery of the solvent represents a con for the process. It is important that the amount of solvent is as low as possible. By increasing the pressure in the reactor it is possible to increase the concentration of substrate and in this way reduces the amount of solvent that has to be recovered (Härröd *et al.*, 2001). Recently several plants have been taking in operation during 2002: one pilot-plant in Göteborg, Sweden (Härröd Research AB) and one industrial-plant in Consett Co. Durham, United Kingdom (Thomas Swan & Co Ltd). The former hydrogenates fatty acid methyl esters to fatty alcohols (10 kg_{alcohols}/h, 40 kg_{propane}/h, maximum pressure 30 MPa, and maximum temperature 573.15 K) and the latter, its first product was isophorone using CO₂ as solvent and Pd as catalyst. The designed capacity of their plant is 1000 ton/year, i.e. about 125 kg_{product}/h.

Another con is to maintain single-phase conditions in a system of solvent and substrate, the pressure has to be increased when hydrogen is added. Typical pressures are 15 to 30 MPa. 30 MPa is considered as a technical/economical maximum pressure today. This means that for some processes the pressure in the reactor has to be increased compared to the traditional process (Härröd *et al.*, 2001). On the other hand, 30 MPa is used in some traditional processes today i.e. production of fatty alcohol, and for these processes the pressure might be reduced (van den Hark and Harrod, 2001).

Regarding safety, there is no big *additional* risk in using high pressures and possibly flammable solvents. The risk of using high pressures is compensated by the smaller volume of the plant (risk = pressure x volume), and the explosion-risk is already present

in all plants using hydrogen. The technology for handling these solvents and risk is well known in the petrochemical industry.

1.4 Objectives and Scope of this Thesis.

The aim of this research is to study continuous single-phase hydrogenation of sunflower oil on supported palladium catalysts using supercritical fluids as a reaction solvent. This would be an alternative process for producing a wide variety of end products having different characteristics (iodine value, *trans*-fatty acid content and saturated content mainly) of industrial foodstuffs interest to be used as low cholesterol precursors for margarine and shortening bases in the next few years. In addition, the objective of the study is to show, on a lab-scale, the potential of heterogeneous catalytic reactions under supercritical single-phase conditions.

The specific aims are to:

- Design, build and put into operation a lab-scale supercritical hydrogenation plant for carrying out the reaction in continuous mode at high pressure.
- Determination of conditions for the hydrogenation process under a single phase is really present. Therefore, it is essential to know the phase behaviour of the reactive system in the region of interest in terms of pressure, temperature and composition.
- Study how the operational variables that affect the sunflower hydrogenation process with regards to both the reduction in iodine value and the formation of *trans* C18:1 isomer, parameters that are necessary for further industrial food application by means an statistical response-surface methodology based on experimental design. The study should show the regions where a potential CSTR process could be operated to obtain a certain iodine value and a minimum *trans* C18:1 content.
- Demonstrate the feasibility of improving the reaction rate as well as the selectivity for the fats and oil hydrogenation with commercial Pd catalyst by reducing the number of reactive phases using a supercritical fluid such as propane or dimethylether (DME) as a reaction solvent.
- Analysis of the steady-state CSTR reaction rate data in order to determine of the kinetic constants, and their temperature dependency, for the multiple reactions

of hydrogenation–isomerization network involving triglyceride species. The kinetic formalism, proposed earlier for vegetable oil hydrogenations by Albright (1967) and Hashimoto *et al.* (1971), is used.

- Study the intraparticle diffusivity of triglycerides and hydrogen in supported Pd under supercritical hydrogenation reaction conditions in order to determine the effective diffusion coefficients in the porous catalyst particle. The aim is to have an insight about the mass transport mechanisms in pellets filled with SC fluid.

The scope of the work presented here is the single-phase hydrogenation of sunflower oil on Pd/C in SC propane in a continuous recycle reactor. Further work would involve the development of a pilot-scale integral packed bed reactor for operation under industrial conditions. However, this falls outside the scope of the present thesis.

1.5 Thesis Structure.

This thesis is based on the material published in several technical papers and one patent, which can be found at the end of the thesis.

Chapter 1 consists of a background introduction aimed to explain the idea of use supercritical fluids in the hydrogenation of fats and oils and to describe the state of the art and what are the aims of this research.

Chapter 2 presents a theoretical study for modelling the vapor-liquid high pressure equilibrium for sunflower oil/hydrogen/C₃H₈ system as well as for sunflower oil/hydrogen/DME in order to determine suitable operating conditions (concentrations, temperatures and pressures) necessary to bring all hydrogenation reactants and products into a homogeneous reactive fluid phase.

Chapter 3 establishes a better understanding of how operating variables affect the rate of reaction, conversion and final product distribution in a continuous recycle reactor as well as the experimental conditions where a potential CSTR process could be operated to obtain end-products with industrial foodstuff of interest. As an extension of these results, the kinetics of the reaction is worked out.

Chapter 4 it is a consequence of the results of the previous chapter and develops the study of the intraparticle diffusion-reaction mechanisms in supercritical sunflower oil hydrogenation on Pd/C catalyst.

The final chapter contains the experimental details of this thesis.

The last part gathers the main conclusions, discussion of prospects for further investigations and presents the bibliography and the appendixes.

1.6 Nomenclature.

IV	iodine value [g I ₂ /100 g oil]: 1 IV =36 mol H ₂ /m ³ oil
P	pressure [MPa]
P _c	critical pressure [MPa]
T	temperature [K]
T _c	critical temperature [K]

Acronyms

C18:0	stearic fatty acid
C18:2	linoleic fatty acid
C18:3	linolenic fatty acid
<i>cis</i> C18:1	oleic fatty acid
CSTR	continuous stirred-tank reactor
CO	carbon monoxide
CO ₂	dioxide carbon
C ₃ H ₈	propane
CP	critical point
DME	dimethyl ether
EC	European Community
EU	European Union
FAME	fatty acid methyl ester

FAO	Food and Agriculture Organization of the United Nations
FDA	Food and Drug Administration
FT	Fisher-Tropsch
H ₂	hydrogen
HDL	high-density lipoprotein
IV	iodine value
LDL	low-density lipoprotein
Ni	nickel
Pd	palladium
SC	supercritical
SCF	supercritical fluid
<i>trans</i> C18:1	elaidic fatty acid
TP	triple point
US	United States

Chapter Two

High-Pressure Equilibria.

2.1 Introduction.

Hydrogenation is one of the most important chemical processes. A wide variety of chemicals is obtained by heterogeneous catalytic hydrogenation. The hydrogenation of double bonds in fats and oils has the purpose of providing products with the desired melting profile and texture, according to their final use. The hydrogenated oil is more stable and less sensitive to oxidation. The classic process is carried out in batch reactors (5 – 20 m³), where the oil, hydrogen, and catalyst nickel powder are mixed intensively at temperatures between 373.15 K and 423.15 K and low pressures (0.1-0.3 MPa) (Farrauto and Bartholomew, 1997).

The conventional oil hydrogenation is carried out in gas-liquid phase. At the surface of the liquid oil, the hydrogen gas is in equilibrium with the liquid phase (see Cgl in Figure 2-1). Most hydrogenation catalysts are very active. In combination with the poor mass transport properties in the liquid, large concentration gradients occur at the gas-liquid and liquid-catalyst interfaces. There is also another concentration gradient, from the catalyst surface into the pores. Thus, The low solubility of hydrogen in oil at these conditions, together with the transport resistances, lead to low concentration of hydrogen at the catalyst surface and very low reaction rates. Commercial oils, which are partially hydrogenated, contain normally 30-40 % *trans*-fatty acids (King *et al.*, 2000). According to the half-hydrogenation theory (Horiuti and Polanyi, 1934), the *trans*-fatty acid formation increases when the hydrogen concentration at the catalyst surface decreases.

The favourable solvent and transport properties of supercritical fluids SCF make them an adequate medium for chemical reactions and offer great opportunities for process improvement (Savage *et al.*, 1995; Baiker *et al.*, 1999). The application of a suitable supercritical fluid to a gas-liquid hydrogenation process can bring all reactants and products into a homogeneous fluid phase in contact with the solid catalyst at the required molar ratio of the reactants by choosing suitable solvent and suitable conditions (concentrations, temperatures and pressures).

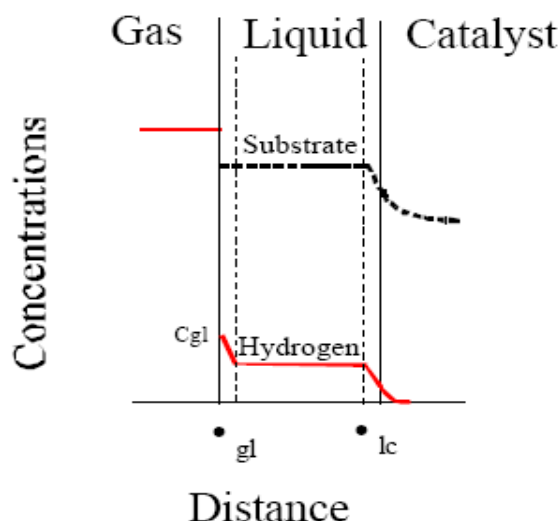


Figure 2-1: General concentration profiles for substrate (- -) and hydrogen (--) in a classic gas-liquid hydrogenation. d_{gl} = gas-liquid interface, d_{lc} = liquid-catalyst interface, C_{gl} = equilibrium concentration of hydrogen in liquid oil (Härröd *et al.*, 2001).

The single-phase condition eliminates the transport resistance at the gas-liquid interface (See Fig. 2-2). This resistance is the restricting factor in the traditional fixed bed reactors. Compared to the gas-liquid conventional process, the mass transport resistances are strongly reduced or completely removed. The reasons are the reduced viscosity and the increased diffusivity in the supercritical fluid. The single-phase condition makes it possible to feed the catalyst with hydrogen in excess. Compared to the gas-liquid reaction, much higher hydrogen concentrations at the catalyst surface are possible within a single-phase reaction. This fact leads to very high reaction rates (Härröd and Møller, 1999, Van den Hark *et al.*, 1999, 2001, 2001a and Macher *et al.*, 1999).

The concentration profiles for the supercritical single-phase reaction are similar to those in gas-phase reactions. The main differences are that large molecules can be processed under reasonable concentrations, pressures and temperatures and an adequate temperature control for exothermic hydrogenation reactions is possible due to the good heat transport properties of the supercritical solvent.

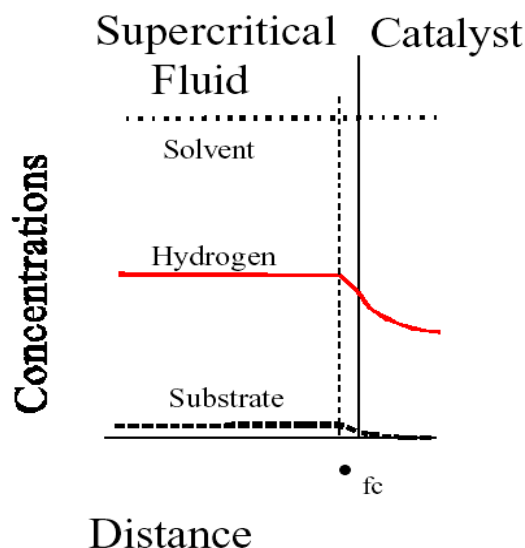


Figure 2-2: General concentration profiles for substrate (- -), hydrogen (--) and solvent (- - -) in supercritical single-phase hydrogenation. d_{fc} = fluid-solid catalyst interface (Härröd *et al.*, 2001).

The phase behaviour, viscosity, and density at different operating conditions can explain many of the effects of the solvent on the reaction. The main benefits of supercritical hydrogenation are process intensification, smaller reactors and improved selectivity due to the independent control of temperature, pressure, and composition of the reactants at the catalyst surface (Hitzler *et al.*, 1998). On the other hand, due to the superior heat and mass-transport properties of supercritical fluids, the use of continuous reactors instead of traditional batch units is allowed. The low viscosity of the reaction medium improves the operation of the reactor and reduces the pressure drop; the low surface tension also assures a better wetting of the catalyst surface within the reaction mixture. The unique solvent properties of supercritical fluids guarantee, in principle, an easy separation of the products from the reaction system.

The choice of the solvent is not trivial. The aim of adding a supercritical solvent as a reaction medium may be diverse, e.g. to dissolve a heavy substrate, to limit catalyst deactivation, to improve selectivity, or to enhance mass transport. The final decision about solvent selection will also take into account other properties, such as solvent inertness at the reaction conditions and also environmental and economical considerations. On the other hand, the phase behaviour of supercritical hydrogenation mixtures can be quite complex. Drastic changes in density and solubility with temperature, pressure, and composition can be expected due to the presence of a near-critical or supercritical solvent in a mixture with permanent gas hydrogen and heavy liquid components. The large difference in molecular size and volatility between these

components is likely to give rise to liquid-phase split and multiphase behaviour (Peter and co-workers, 1993). The solubility of most gases falls with increasing temperature, while it rises for highly supercritical gases like hydrogen. It is then expected that the slope of a pressure-temperature phase diagram will change sign according to the relative amount of hydrogen/supercritical fluid present in the reactive mixture.

In order to find an adequate solvent and operating conditions, it is necessary to determine the phase boundaries of a multicomponent reactive system containing hydrogen, solvent, substrate, and hydrogenation products. The critical temperature of the solvent is a key property for solvent selection. The solvent should have a critical temperature lower than the reaction temperature. In this way the complete miscibility of the pair solvent/hydrogen is assured. On the other hand, the critical temperature of the solvent should not be too low, compared to the reaction temperature, to achieve liquid-like densities and hence higher solvent capacity. Table 2-1 shows the critical temperature and pressure of solvents that have been reported in the literature as supercritical reaction media.

Table 2-1: Critical properties of several solvents for chemical reactions (Yaws, 1999).

Solvent	T _c (K)	P _c (MPa)
Ethylene	283.1	5.11
Xenon	289.8	5.87
Carbon dioxide	304.2	7.38
Acetone	508.1	4.70
Ethane	305.5	4.88
Nitrous oxide	309.7	7.26
Sulfur hexafluoride	318.7	3.72
Propane	370.3	4.24
Hydrogen sulfide	373.5	9.0
Dimethyl ether	400.1	5.37
Ammonia	405.6	11.4
Pentane	470.2	3.37
1-Propanol	508.5	4.76
Methanol	513.7	7.99
Ethanol	516.6	6.38
1-Butanol	548.2	4.29
Benzene	562.1	4.89
Ethylendiamine	593.0	6.27
Water	647.3	22.11

According to Table 2-1, there are only a few solvents allowed for unlimited use for processing of foods in the European Community (EU): Nitrous oxide, carbon dioxide, propane, acetone and ethanol (EC directive 88/344, 1984). The former is not stable at high temperatures and the two latest have a high critical temperature value.

For vegetable oil hydrogenation processes, carbon dioxide has been investigated as a solvent. The first one to use it as a solvent in a hydrogenation process was Zosel (1976). The substrate was triglycerides. A phase diagram for this system is presented in Figure 2-3.

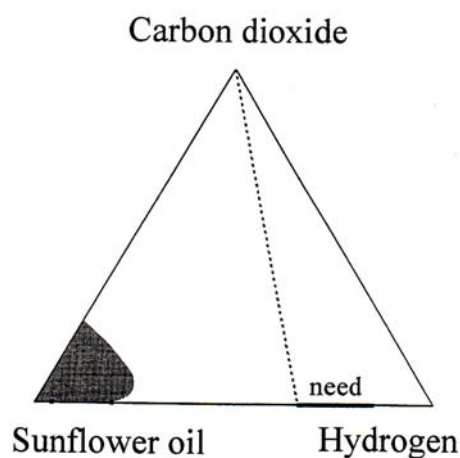


Figure 2-3: Phase diagram for sunflower oil, CO₂ and hydrogen system at 10 MPa and 373.15K (mol %). The dark means single phase. The dashed line indicates the hydrogen requirement for full conversion of the substrate.

The solubility of triglycerides in carbon dioxide is below 1 wt. % (0.05 mol %) at 353.15 K and 30 MPa (McHugh and Krukoniš, 1994). Supercritical CO₂ is miscible with H₂. Therefore the single-phase area with CO₂/triglyceride/H₂ is too small in Fig. 2-3 and a very large mixing gap occurs between the CO₂/H₂ phase and the CO₂/triglyceride/H₂ phase (see Figure 2-3). The solubility of H₂ in oil can be seen at the baseline between the oil and the hydrogen in Figure 2-3. The stoichiometric need of hydrogen depends on the reaction, but generally it is above 50 mol %. This means that one gas phase and one liquid phase have to be present in the reactor (see “need” in Figure 2-3). This ratio between oil and H₂ has to be maintained even when a solvent is added. Thus, the composition of the feed to the reactor has to be to the right of the dotted line in Figure 2-3. In practice, the stoichiometric ratio has to be exceeded to some extent for technical reasons.

As can be seen in Figure 2-3, using CO₂ as a solvent does not reduce the number of phases during the hydrogenation. The observed hydrogenation reaction rates for triglycerides in a slurry system (Zosel, 1980) and for fatty acid methyl esters in a fixed-bed system (Tacke, 1995) are similar to the corresponding traditional gas-liquid processes without CO₂. Thus, CO₂ has only a marginal effect on the hydrogenation rate on FAME or TG at technical/economical conditions.

It is known that carbon dioxide is not a good solvent for hydrocarbon substrates; liquid-liquid immiscibility has been reported by Schneider (1991) for hydrocarbons containing more than eight carbon atoms. Therefore, the application of CO₂ as supercritical reaction medium is in principle limited to low molecular-weight substrates.

Solubility, viscosity and density for some triglyceride/hydrogen/CO₂ systems have been measured by Richter (2000). The authors found that slightly increased hydrogen concentrations can be achieved using CO₂ and that at relevant temperatures, pressures and concentrations for hydrogenation processes a two-phase system is always occurring. A similar conclusion was reached by Klein and Schulz (1989) who found that in the mixtures CO₂-rapeseed oil, the partial miscibility persists until very high pressures (See Figure 2-4).

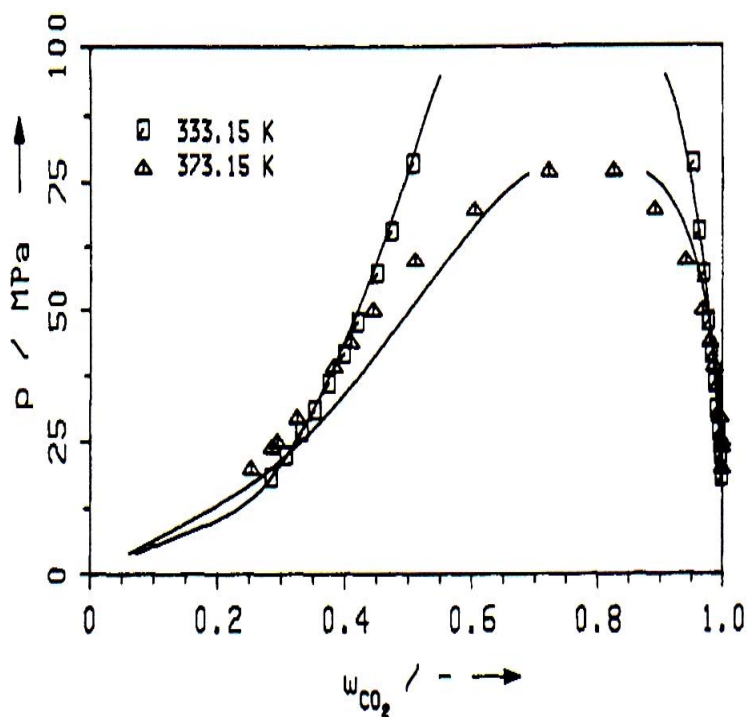


Figure 2-4: Vapor-liquid equilibrium of the rapeseed oil-carbon dioxide systems at 333.15 and 373.15 K (Klein and Schulz, 1989).

The phase behaviour of (pseudo-) binary and pseudo ternary mixtures of soybean oil, hydrogen and the supercritical fluid carbon dioxide were measured by Weidner *et al.* (2004) at temperatures of 373.15 and 403.15 K in a pressure range between 0.1 and 18 MPa. They found that carbon dioxide and hydrogen are completely miscible at the investigated conditions, which are supercritical with respect to the critical data of carbon dioxide whereas the solubility of oil in the carbon dioxide is very low. This solubility is only increased with increased pressure and/or decreasing temperature. The binary system hydrogen and soybean oil shows a different temperature dependency: with increasing temperature, the solubility of hydrogen increases. Additionally the solubility of hydrogen in oil is much lower than that of carbon dioxide. On the other hand, addition of CO₂ to a mixture of soybean oil and hydrogen lead to a slightly rise of the mixture density with increasing solvent concentration. A similar behaviour was observed with the viscosity: adding more carbon dioxide results in a viscosity increase. Therefore, CO₂ is not acting as a diluent which reduces the viscosity of the oil.

In commercial processes for edible oils, solvents are not used because the improvement of productivity is not enough to compensate for the extra costs of adding a solvent (Veldsink *et al.*, 1997) as well as the environmental penalties involved with the toxicity of the product and solvent loss. CO₂ has been also used for hydrogenation of other substrates by Hitzler *et al.* (1998) and Bertuccio *et al.* (1995). The later researchers concluded that their system was operated at two-phase conditions because, from an industrial point of view, the pressure required to form a single-phase system becomes too expensive.

This fact is in agreement with that found by Ramírez *et al.*, 2002. They studied the binary vapor-liquid equilibrium (VLE) for sunflower oil in CO₂ in terms of the VLE constants as a function of pressure at constant temperature as shown Figure 2-5. The equilibria calculations were performed in terms of the convergence pressure and even these were only approximated ($k_{12}=0$, $\eta_{12}=0$, were assumed), the CO₂-oil binary mixture has a convergence pressure of around 33 MPa, which is significantly high from an operating point of view. The benefits of enhanced reaction rate and improved selectivity are related to the costs of working at higher pressure. The technical/economical limit for standard materials is somewhere around 300 bar.

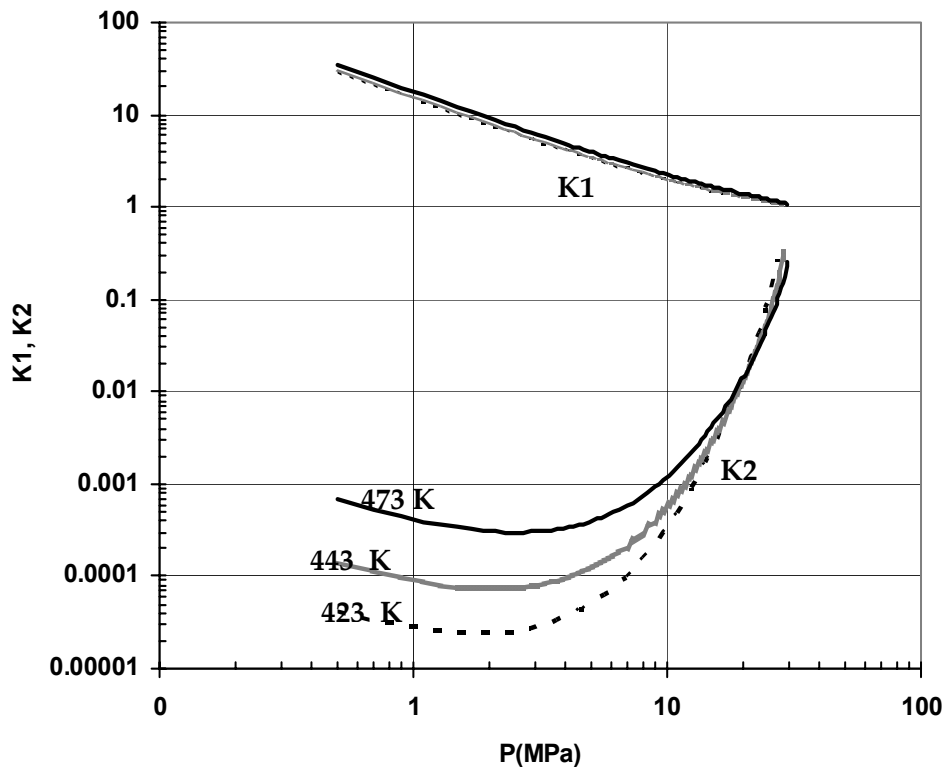


Figure 2-5: VLE near the critical region for the binary system carbon dioxide (1) – sunflower oil (2) (vaporization constants calculated with the PR-EOS).

The solubility data of triglycerides in different media is presented in Table 2-2.

Table 2-2: Solubility of triglycerides in different reaction media (Brunner, 1986).

Media	T (K)	P (MPa)	Triglycerides wt %
CO ₂	353.15	30	1.1
CO ₂	353.15	70	8.1
CO ₂ + 12% Ethanol	323.15	18	8.3
CO ₂ + 20% Ethanol	323.15	18	∞
Propane	384.15	9.6	12
Propane	384.15	11	∞

Although CO₂ is an attractive supercritical solvent because it is environmentally benign, cheap, non-toxic and non-flammable, propane draws special attention as solvent as being reflected in Table 2-2. The hydrocarbon nature of fatty oils makes C₃H₈ a better solvent than CO₂. Mixtures of CO₂ and n-paraffins with carbon number greater than 7 display liquid-liquid phase splits at very high pressures (Fall *et al.*, 1985), whereas C₃H₈

and n-paraffins of up to 30 carbon atoms are completely miscible in the liquid state (Peters *et al.*, 1989). Therefore, investigations for substitutes of CO₂, with emphasis on lower alkanes (ethane to hexane) are currently underway (Hizler and Poliakoff, 1997 and De Jong *et al.*, 2001).

Propane was identified as a potential near-critical or supercritical solvent for hydrogenation of edible oils by Coorens *et al.* (1988), Schieman (1993), Straver *et al.* (1998), Fornari *et al.* (2001) and Richter *et al.* (1999). These authors consider propane attractive because it is a better solvent for vegetable oil due to its structure mainly as hydrocarbons. Their works are based on modelling the phase behaviour of systems with vegetable oils and fats in near-critical or supercritical conditions.

Rovetto *et al.* (2004) reports the experimental phase equilibrium data on binary and ternary mixtures of methyl palmitate, hydrogen and propane covering a temperature region between 360.15 and 450.15 K, and pressures up to 15 MPa. In general, they concluded that increasing propane concentration causes the increase of solubilities of the reaction mixture hydrogen + methyl palmitate, which suggests that propane could be an adequate solvent for the homogeneous hydrogenation of fatty methyl esters.

Härröd and Møller (1999), Van den Hark *et al.* (2000) and Macher *et al.* (2001) report increments in the supercritical hydrogenation rates of oils and derivatives of up to 1,000 times, compared to the traditional gas-liquid process as well as a lower degree of *cis-trans* isomerization in a continuous fixed-bed reactor, using commercial catalysts. Similar to the hydrogenation of triglycerides (Härröd *et al.*, 1996; Richter *et al.*, 1999) a single-phase system can be achieved by adding a supercritical fluid such as propane. At single-phase conditions, the reaction rates are significantly higher and less by-products are formed (van den Hark *et al.*, 2000). Additionally, the required pressure and hydrogen excess are lower than in conventional processes.

The regions of homogeneous phase behaviour for the system H₂-C₃H₈-triglyceride have been predicted by means of group of contribution equation of state (Pereda *et al.*, 2000). The conceptual design of process conditions as well as procedures to determine the range of feasible operating conditions for sunflower oil hydrogenation in supercritical propane were studied by Pereda *et al.* (2003). These authors applied a group of contribution equation of state to predict the required phase equilibrium scenarios for solvent containing reactive mixtures.

It is worth investigating the possibility to apply alternative solvents for near-critical or supercritical hydrogenation process of edible oils. Another potential candidate solvent is dimethyl ether ((CH₃)₂O) (DME). Despite the fact that DME is not allowed as a food processing solvent, its properties in ternary systems as in near-critical or supercritical solvent are currently investigated. DME may have a future as a replacement for engine fuel obtained from fossil reserves. Nowadays, it is used primarily as a propellant for spray cans due to its high solubility in both polar and nonpolar solvents, as a fuel in engines and as a raw material in the synthesis of light olefins, such as ethylene and propylene (Sardesai, 1997). The thermodynamic studies are scarce and most of them are related to the production of DME from methanol by dehydration (Hansen *et al.*, 1995) and its application as propellant in the aerosol industry (Bohnen, 1981 and 1986). Experimental data on the phase behaviour of the binary system DME/tripalmitin and DME/fatty acid esters were reported by Florusse *et al.* (1999) and Brake *et al.* (2002) respectively. Thermo- and fluid dynamic aspects of the hydrogenation of triglycerides and esters in presence of DME were studied by Weidner *et al.* (2004).

As mentioned above, supercritical hydrogenation is demonstrably effective and is potentially attractive because reaction rates can be greatly increased by using a supercritical solvent to bring the reactive hydrogenation mixture into a single homogeneous phase. This fact provides a significant advantage of the supercritical process over conventional methods. However, a major question is whether a single phase is really present at the operating conditions. When dealing with a reaction mixture, attention must be paid not only to the critical points of the single components but also to the phase behaviour of the complete mixture. On the other hand, there is not enough data available for propane or DME/hydrogen/sunflower oil systems for the purpose of the reactions. Therefore, the aim of this chapter is to explore the properties of propane and DME as promising supercritical solvents for single-phase sunflower oil hydrogenation by means of the study of the corresponding high-pressure phase equilibrium.

2.2 Objectives and Strategy.

To study theoretically the vapor-liquid high pressure equilibrium for sunflower oil/hydrogen/C₃H₈ system as well as for sunflower oil/hydrogen/DME system in order to determine suitable operating conditions (concentrations, temperatures and pressures) which can bring all reactants and products into a homogeneous reactive fluid phase.

The phase envelopes have been modelled using the Peng-Robinson equation of state (PR-EOS) along with the one-fluid Van der Waals-1 mixing rules with two interaction parameters: k_{ij} nor η_{ij} .

2.3 Theoretical Determination of L-V High Pressure Equilibria.

The thermodynamics of high-pressure vapor-liquid equilibria is, in principle, similar to that of the solubility of gases in liquids. However, the general concepts are not completely useful to determine the equilibria because the treatment concerns a wide range of liquid-phase concentrations, not only dilute solutions.

It is possible to analytically represent high-pressure equilibria using for the liquid phase the common thermodynamic functions: Henry's constant, activity coefficient and partial molar volume. However, experience has shown that in typical cases, these functions are not useful, especially for multicomponent mixtures. A more successful route to quantify high-pressure vapor-liquid equilibria is provided by the fugacity coefficient applied to both phases.

Considering a binary liquid mixture with mole fractions x_1 and x_2 at temperature T and pressure P ; in equilibrium with the liquid mixture and a vapor mol fractions y_1 and y_2 , the equations of equilibrium are:

$$f_1^V = f_1^L \quad \text{or} \quad \phi_1^V y_1 = \phi_1^L x_1 \quad (2.1)$$

and

$$f_2^V = f_2^L \quad \text{or} \quad \phi_2^V y_2 = \phi_2^L x_2 \quad (2.2)$$

where f is the fugacity and ϕ is the fugacity coefficient. This introduces the compositions x_i and y_i into the equilibrium equations, but none is explicit, because the ϕ_i are functions, not only of T and P , but of the composition. Thus, equations 2.1 and 2.2 represent N complex relationships connecting T , P , the x_i and the y_i suitable for computer solution.

To calculate fugacity coefficients, it can be used an equation of state that is valid for both the vapor-phase mixture and liquid-phase mixture. For each component i in the vapor-phase, we have:

$$\ln \phi_i^V = \frac{1}{RT} \int_{V^V}^{\infty} \left[\left(\frac{\partial P}{\partial n_i} \right)_{T,V,n_j} - \frac{RT}{V} \right] dV - \ln \frac{PV^V}{n_T RT} \quad (2.3)$$

Here n_i is the number of moles of component i and n_T is the total number of moles in the vapor phase. Similarly, for each component i in the liquid phase, we have:

$$\ln \phi_i^L = \frac{1}{RT} \int_{V^L}^{\infty} \left[\left(\frac{\partial P}{\partial n_i} \right)_{T,V,n_j} - \frac{RT}{V} \right] dV - \ln \frac{PV^L}{n_T RT} \quad (2.4)$$

where n_i and n_T now refer to the liquid phase.

To use equations 2.3 and 2.4, a suitable equation of state is required which holds for the entire range of possible mole fractions x and y at system temperature T and for a density range between 0 and $(n_T/V)^L$. This last condition is necessary because the integrals go from the ideal-gas state (infinite volume) to the saturated-vapor and saturated-liquid densities. At present, there are no satisfactory equations of state that meet these requirements with generality. However, for many mixtures, there are reasonable, approximate equations of state that provide useful results.

The simplest procedure for using equations 2.3 and 2.4 is to choose an equation of state that holds for pure fluid 1 and for pure fluid 2 and to assume that this same equation of state holds for all mixtures of 1 and 2 by interpolation.

The most commonly used cubic EOSs are the Peng Robinson (Peng and Robinson, 1976) and the Soave-Redlich-Kwong (Soave, 1972) equations. They produce essentially equivalent results since both equations are cubic in volume. The PR equation is:

$$P = \frac{RT}{v-b} - \frac{a(T)}{v(v+b)+b(v-b)} \quad (2.5)$$

where v is the molar volume, a accounts for intermolecular interactions between the species in the mixture, and b accounts for size differences between the species of the mixture. Peng and Robinson give the following prescriptions for a and b :

$$b = 0.07780 \left(\frac{RT_C}{P_C} \right) \quad (2.6)$$

$$a(T) = a(T_C) \alpha(T_R, w) \quad (2.7)$$

$$a(T_C) = 0.45724 \frac{R^2 T_C^2}{P_C} \quad (2.8)$$

$$\alpha = \sqrt{1 + (m(1 - T^{1/2}))} \quad (2.9)$$

$$m = 0.37464 + 1.54226w - 0.26992w^2 \quad (2.10)$$

$$w = 1.000 - \log_{10} \left(\frac{P^{sat}}{P_C} \right)_{T_R=0.7} \quad (2.11)$$

where T_c is the critical temperature, P_c is the critical pressure, T_R is the reduced temperature ($T_R=T/T_c$), and w is the acentric factor for component i . Each of these pure component properties, including the acentric factor, can usually be found in the literature for most of the common low-to-moderate molecular weight hydrocarbons (Reid, Prausnitz and Polling, 1987).

When dealing with gas and liquid mixtures, it is necessary to define combining rules for a_{mix} and b_{mix} to use the equation of state in order to calculate mixture properties. In this development it will use the so-called van der Waals-1 mixing rules that assume random mixing of the components. These equations are used once for the gas phase mixture and once for the liquid phase mixture.

$$a_{mix} = \sum_i \sum_j x_i x_j a_{ij} \quad (2.12)$$

$$a_{ij} = (a_{ii} a_{jj})^{0.5} (1 - k_{ij}) \quad (2.13)$$

$$b_{mix} = \sum_i \sum_j x_i x_j b_{ij} \quad (2.14)$$

$$b_{ij} = \frac{(b_{ii} + b_{jj})}{2} (1 - \eta_{ij}) \quad (2.15)$$

where k_{ij} and η_{ij} are mixture parameters, usually determined by fitting pressure-composition data, and x denotes either liquid or gas phase mole fraction. With these mixing rules, the analytical expression obtained for the vapor phase fugacity coefficient of component i is:

$$\ln \phi_i^V = \frac{b_i^*}{b_{mix}} \left(\frac{Pv^V}{RT} - 1 \right) - \ln \left(\frac{Pv^V}{RT} - B \right) - \frac{A}{2.828B} \left(\frac{2 \sum_j x_j a_{ij}}{a_{mix}} - \frac{b_i^*}{b_{mix}} \right) \ln \left(\frac{\frac{Pv^V}{RT} + 2.414B}{\frac{Pv^V}{RT} - 0.414B} \right) \quad (2.16)$$

where a_{mix} and b_{mix} are determined using 2.12 through 2.15 with the gas phase mole fractions, and A and B are:

$$A = \frac{a_{mix} R^2 T^2}{P} \quad (2.17)$$

$$B = \frac{b_{mix} RT}{P} \quad (2.18)$$

The term b_i^* is defined as:

$$b_i^* = \left[\frac{\partial (b_{mix} N)}{\partial N_i} \right]_{T, V, n_{j \neq i}} = 2 \sum_k x_k b_{ik} - b_{mix} \quad (2.19)$$

where N is the total number of moles in the mixture and x denotes either liquid or gas phase mole fractions. The analytical expression obtained for the liquid phase fugacity coefficient of component i is similar to equation 2.16:

$$\ln \phi_i^L = \frac{b_i^*}{b_{mix}} \left(\frac{Pv^L}{RT} - 1 \right) - \ln \left(\frac{Pv^L}{RT} - B \right) - \frac{A}{2.828B} \left(\frac{2 \sum_j x_j a_{ij}}{a_{mix}} - \frac{b_i^*}{b_{mix}} \right) \ln \left(\frac{\frac{Pv^L}{RT} + 2.414B}{\frac{Pv^L}{RT} - 0.414B} \right) \quad (2.20)$$

Neither k_{ij} nor η_{ij} are expected to be functions of temperature, pressure, or composition. Normally, both are expected to have absolute value much less than 1.0. The parameter k_{ij} is a binary mixture parameter associated with the intermolecular interactions between a pair of unlike species. The value of this parameter usually ranges between -0.1 and 0.15. It can also be negative, although a negative value usually indicates the presence of specific chemical interactions, such as hydrogen bonding. It is questionable whether an EOS approach should be used when calculating the properties of a mixture that has components that hydrogen bond, because a cubic EOS accounts only for dispersion forces between the mixture components and not for chemical forces. Also, a different set of mixing rules is needed for a_{mix} and b_{mix} since the components are not expected to distribute randomly in solution if they can hydrogenate bonds.

The binary mixture parameter η_{ij} , typically a small negative number, is associated with the packing of unlike components. Many times it is more expedient to set η_{ij} equal to zero especially if only a limited amount of data is available. If η_{ij} is set equal to zero, the

mixing rule for b_{mix} reduces to a single summation in mole fraction, b_i^* becomes equal to b_i , and the equation for the fugacity coefficient of component i reduces to the original expression given by Peng and Robinson (1976). However, Deiters and Schneider (1976) have recommended to use the Redlich-Kwong equation. They have calculated P - x isotherms and critical mixture curves for systems that have critical mixture pressures (McHugh and Krukonic, 1994).

For typical calculations it is convenient to express phase-equilibrium relations in terms of K values or equilibrium ratios. The definition of K has no thermodynamic significance but K is commonly used in chemical engineering calculations where it is convenient for writing materials balances. A K value is simply the equilibrium ratio of the vapour to liquid composition. Therefore, the equilibrium ratios (K factors) are given by

$$K_1 = \frac{y_1}{x_1} = \frac{\phi_1^L}{\phi_1^V} \quad (2.21)$$

$$K_2 = \frac{y_2}{x_2} = \frac{\phi_2^L}{\phi_2^V} \quad (2.22)$$

To calculate the equation of state of high-pressure vapour-liquid equilibria, the computational procedure is not trivial. In a typical case, the given quantities for a binary mixture may be P and x_1 (and x_2). Equations 2.1, 2.2, 2.3 and 2.4 must then be used to find T , y_1 (and y_2). However, to use 2.3 and 2.4 the molar volumes v^V and v^L must be known. In order to determine these parameters, the equation of state for the mixture (say, equation 2.5) is applied twice, once for the vapour mixture and once for the liquid mixture.

As far as the binary system is concerned here, there are four unknowns: y , T , v^V and v^L . To find these, it is necessary to solve simultaneously four independent equations. Equations 2.1 and 2.2 [with equations 2.3 and 2.4 substituted for the fugacity coefficients] and 2.5 twice (once for each phase) can be employed. A similar procedure is used for multicomponent mixtures (Prausnitz *et al.*, 1986).

2.4 Results and Discussion.

The application of a thermodynamic model in phase equilibrium calculations requires the knowledge of pure components properties and the interaction parameters between

components. Since vegetable oils are complex mixtures of triglycerides with fatty acids containing different chain length and degree of saturation, its physical properties such as vapor pressures, critical properties, acentric factor, etc. are not always available. Thus, it was necessary to make a rough estimation of them according to the Chueh–Prausnitz approximation (Reid *et al.*, 1987) (see Appendix C). For the other components, hydrogen, propane and DME, the physical properties are presented in Table 2-3.

Table 2-3: Physical property data for hydrogenation species (Yaws, 1999).

Compound	Molecular Weight (g/mol)	T _c (K)	P _c (MPa)	V _c (cm ³ /mol)	w
Sunflower* Oil	875	859	2	3261	1.730
Propane (C ₃ H ₈)	44.01	370.3	4.24	202.9	0.153
Hydrogen (H ₂)	2.02	33,18	1.31	64.2	-0.22
DME (C ₂ H ₆ O)	46.07	400.1	5.37	168.8	0.204

*The physical property data for sunflower oil was estimated in Appendix C.

The binary vapor-liquid equilibria (VLE) for the systems sunflower oil in C₃H₈ and DME were modelled in terms of VLE constants as a function of pressure at constant temperature (Ramírez *et al.*, 2002). The VLE constants were calculated for both systems, estimating the equilibrium ratios (K_i) values from the fugacity coefficients calculated with the PR-EOS (McHugh and Krukoni, 1994; Sandler, 1999). For more details see Appendix D. The calculations were performed in terms of the convergence pressure (Hougen *et al.*, 1954). The binary parameters k_{ij} and η_{ij} were set to zero as suggested by Brunner (1994) when experimental phase equilibrium data on natural product-SCF mixture is scarce. There is no experimental information in the concentration region of interest for homogeneous hydrogenation.

The vapor-liquid equilibrium was predicted for C₃H₈ /sunflower oil system at 400, 450 and 473 K as shown in Figure 2-6.

Figure 2-7 presents the vapor-liquid equilibrium predicted for DME/sunflower oil at 453, 474, 523.15 and 573.15 K respectively.

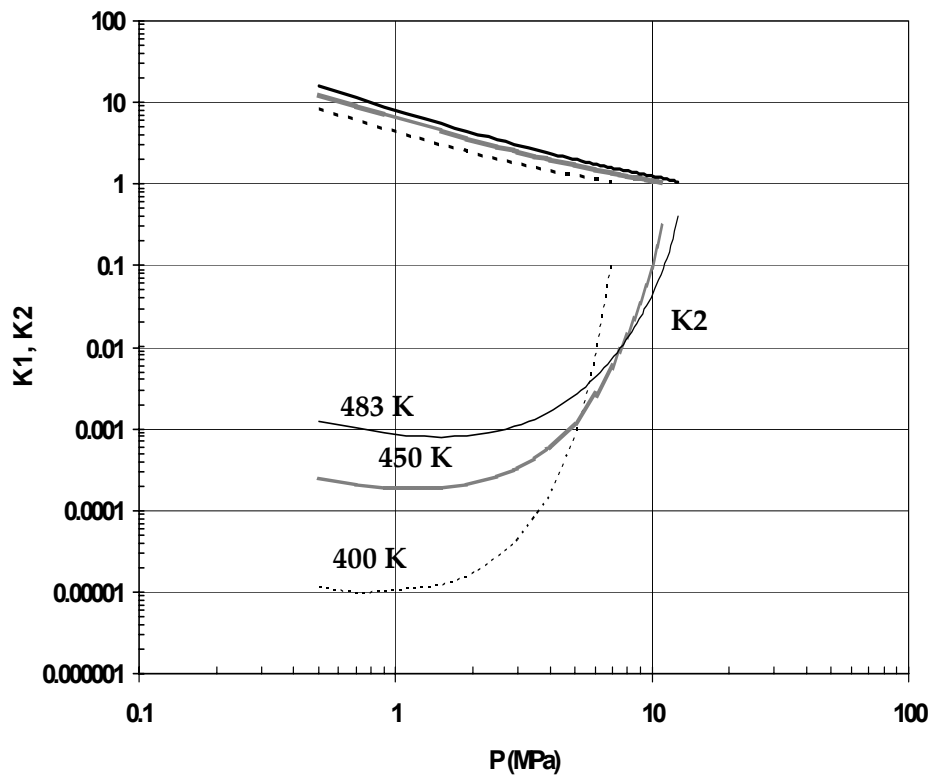


Figure 2-6: VLE in the critical region for the binary system propane (1) - sunflower oil (2) (vaporization constants calculated with PR-EOS) (Ramírez *et al.*, 2002).

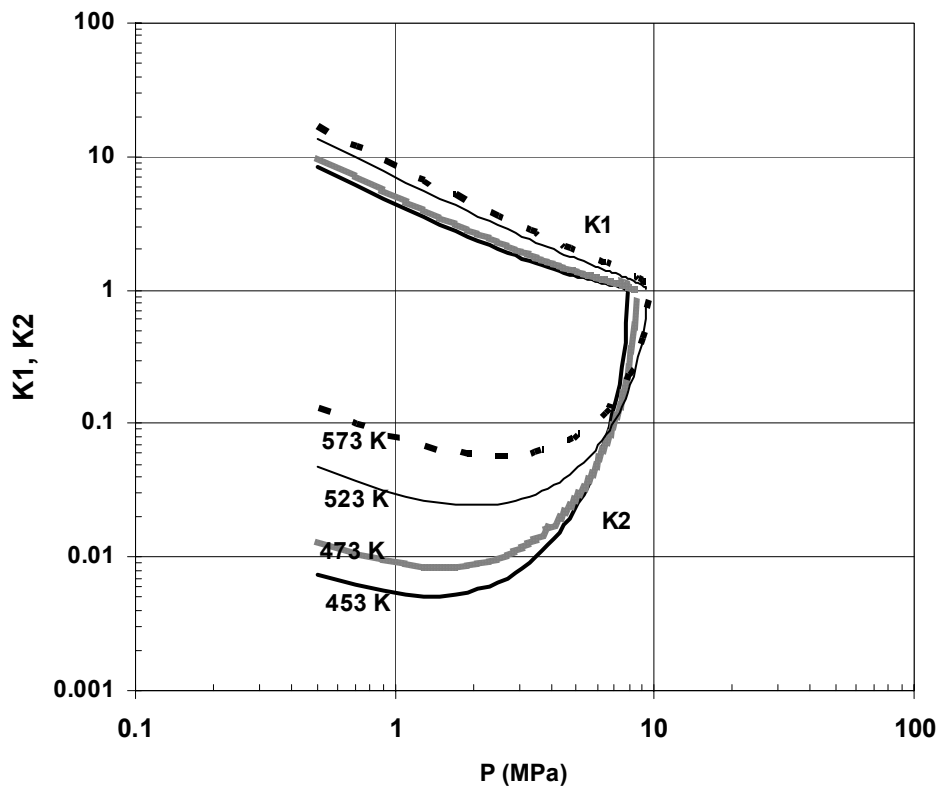


Figure 2-7: VLE in the critical region for the binary system DME (1) - sunflower oil (2) (vaporization constants calculated with PR-EOS).

Despite of the fact that this is an approximate estimation, the propane– oil binary mixture exhibits a convergence pressure at around 14 MPa, whereas the system with DME instead of C_3H_8 has a convergence pressure at around 10 MPa. Therefore, with respect to the reactor operating pressure, it would be less expensive to use DME rather than propane.

A comparison of the K values for dimethyl ether with the predicted data for propane for the isotherm 473.15 K was established in Figure 2-8.

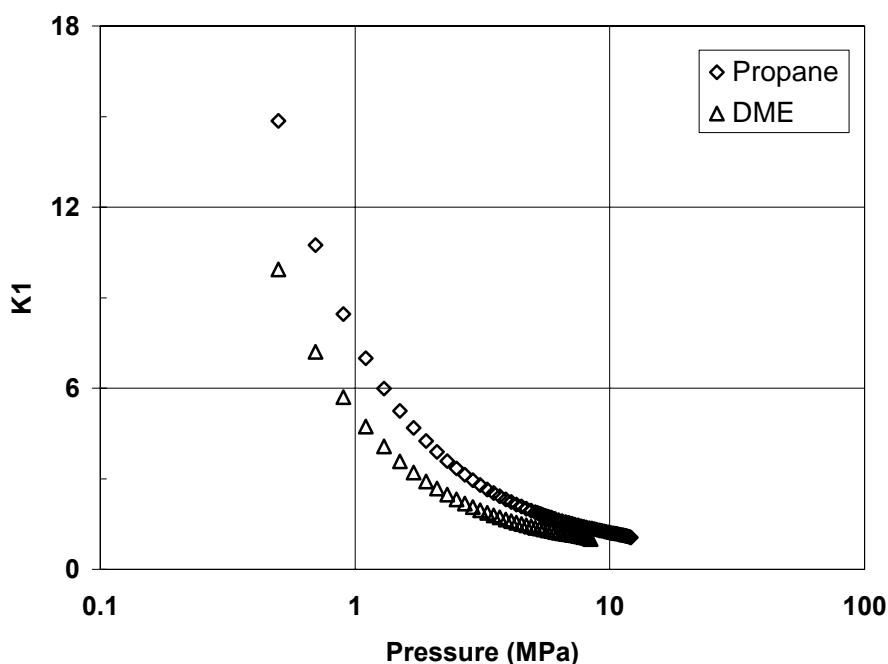


Figure 2-8: K -values for DME in the DME /sunflower oil system and for propane in propane /sunflower oil system at 473.15 K.

In Figure 2.8, the K values for dimethyl ether are lower than those for propane because propane has a higher vapor pressure than DME. The polar nature of dimethyl ether seems to be more compatible with sunflower oil than propane owing to the fact that vegetable oils which mainly consist of mixtures of triglycerides with long-fatty acid chains are considered slightly polar molecules (Fornari *et al.*, 2001). Besides, polarity plays a major role in making the more polar solvent more soluble in the hydrogenation substrate as shows the Figure 2-9 reported by Pereda *et al.* (2003).

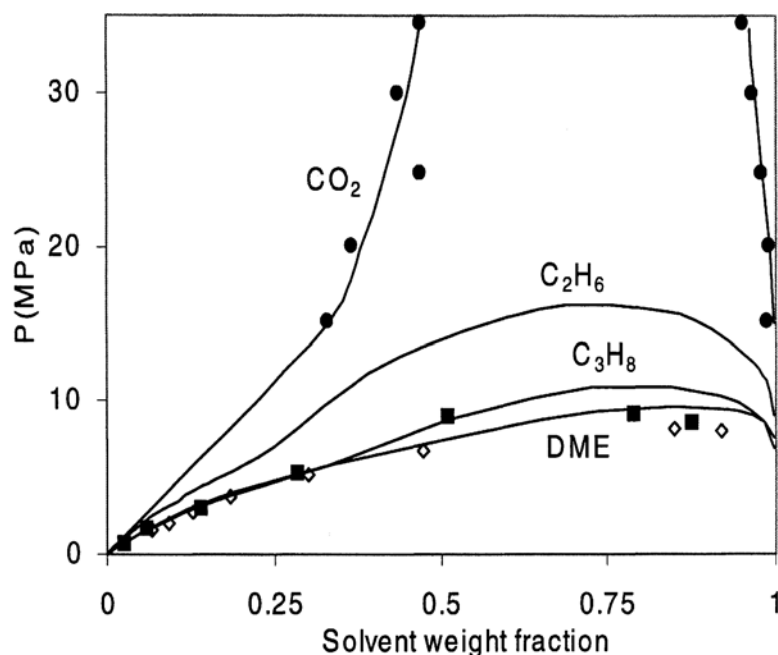


Figure 2-9: VLE and LLE of triglycerides with solvents at a reduced temperature of 1.05. Experimental: ● Bharath *et al.* 1992 ; ■ Coorens *et al.* 1988 ; ◇ Florusse *et al.* 2002 ; - Pereda *et al.* predictions (2002). Figure taken from Pereda *et al.* (2003).

It becomes clear from the figure presented above that carbon dioxide is not a good solvent for the supercritical hydrogenation of fats and oils, because the region of partial miscibility extends to very high pressures. However, other solvents, such as dimethyl ether and propane, achieve complete miscibility at moderate pressures.

The vapor-liquid equilibrium for propane/hydrogen/sunflower oil and DME/hydrogen/sunflower oil ternary systems has been modelled with the PR-EOS using HYSYS 2.4.1 Build 3870 (Hyprotech, USA). The software provides the composition for each component in the liquid and vapor phases respectively, as well as the total vapor fraction. The curve of bubble points is reached when the fraction of vapor is null and the curve of dew points when it is 1. To find these points, the pressure and temperature were set constant and the composition of the ternary mixture was varied. For each point, solvent composition was set constant and the rest of the composition was varied until the total vapor fraction reached either 0 or 1 value. After that, the procedure was repeated with other propane compositions in order to build bubble and dew curves (For more details see Appendix E).

First of all, the VLE estimation method was proved with H₂-cyclododecatriene (CDT)-CO₂ system using the experimental data from Eftaxias *et al.* (2001) at 423.15 K and 20 MPa and with the ternary hydrogen-propane-tripalmitin mixture at pressure of 439.15 K and 12 MPa reported by Rovetto *et al.* (2001) (see Figure 2-10). For both systems under

study, the quality of PR-EOS predictions was reasonably good with a relative error of 8% in the worst case (Zgarni, 2000).

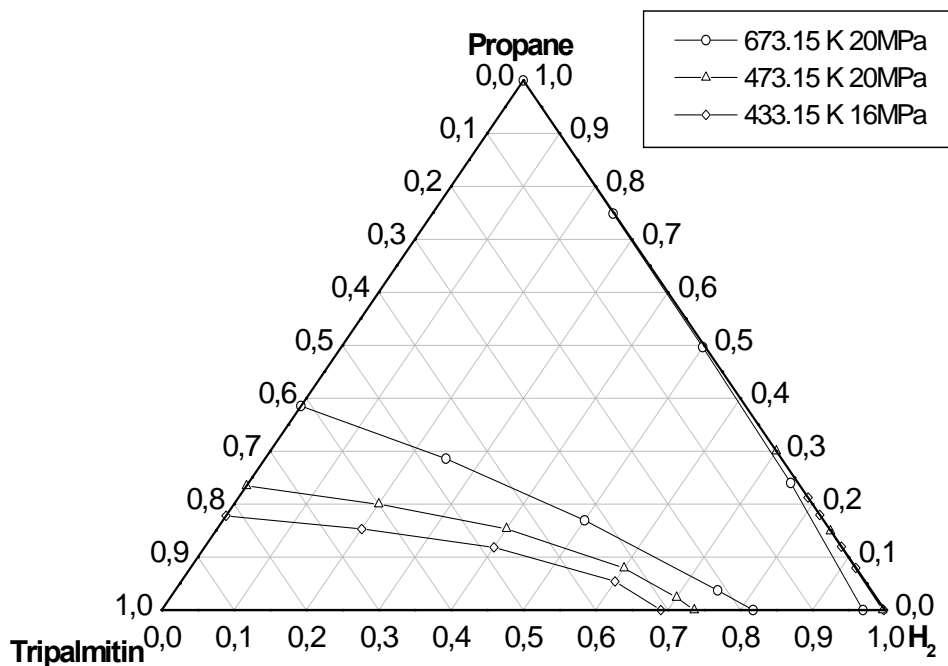


Figure 2-10: Dew and bubble curves for Propane/H₂/tripalmitin ternary system predicted with the PR-EOS at 433.15, 473.15 and 673.15 K and pressures of 16 and 20 MPa (mol %).

Vapor-liquid equilibrium for propane/hydrogen/sunflower oil at 453, 473 and 673 and pressures of 18 and 20 MPa are presented in Figure 2-11a along with that for DME/hydrogen /sunflower oil at 423.15, 453.15 and 473.15 K and 20 MPa (see Figure 2-11b). The binary parameters k_{ij} for oil-H₂, H₂-solvent and oil-solvent pairs were set to zero.

Both ternary fluid-phase diagrams are of type I, because there are two complete miscible binary pairs: H₂/solvent and sunflower oil/solvent (see Figure 2-11). The limitation of partial miscibility of triglycerides with CO₂ is not found when either propane or DME is used as solvent. The PR-EOS predictions are in good agreement with those reported on hydrogen/propane/sunflower oil mixtures by Pereda *et al.* (2003). From Figure 2-11, it can be noticed that by increasing the temperature the region of complete system miscibility becomes greater. This fact is in agreement with the results reported by Hitzler *et al.* (1998) for the cyclohexane/ CO₂ /H₂ reactive system.

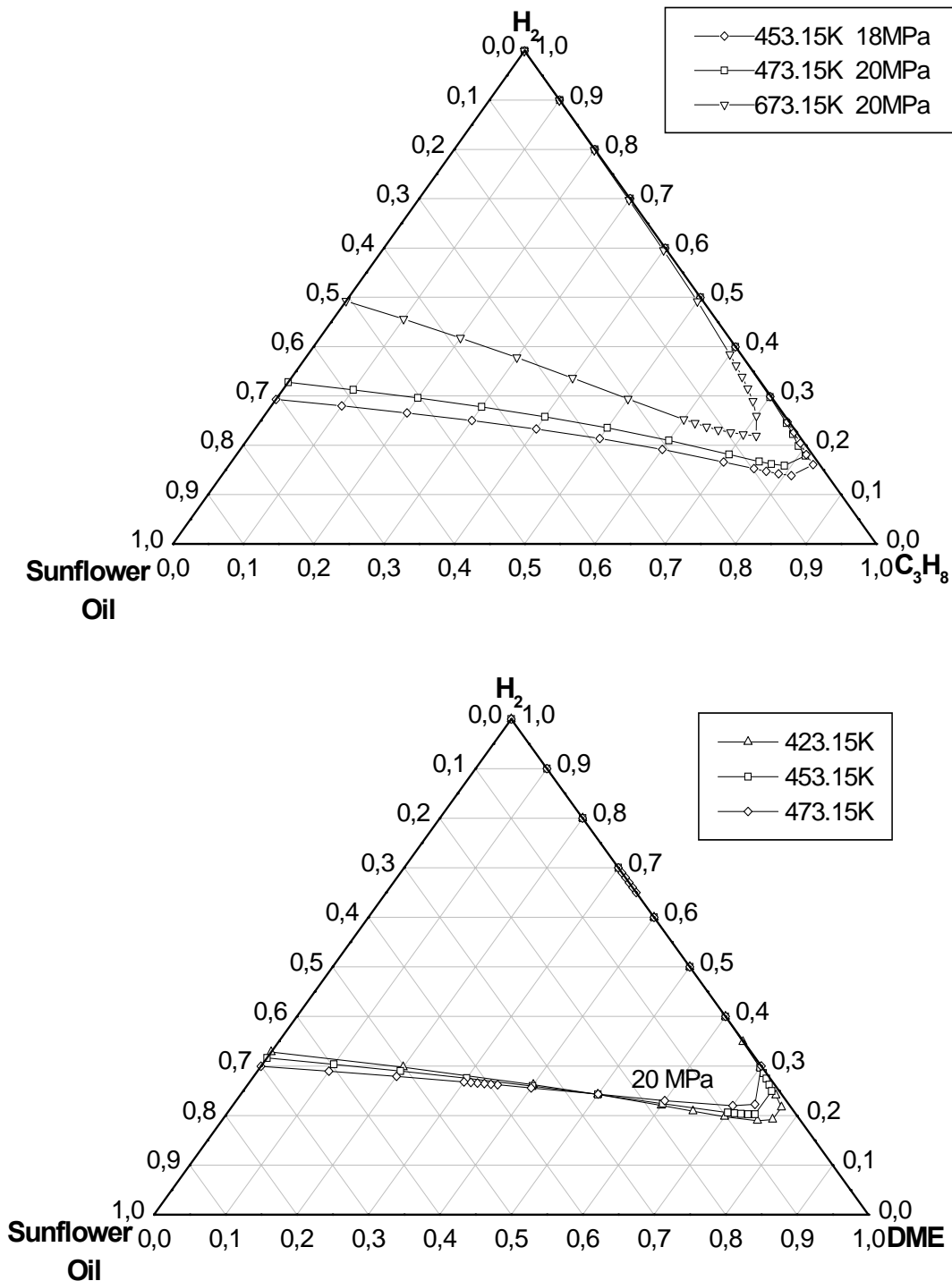


Figure 2-11: Dew and bubble curves for the ternary systems estimated with the PR-EOS (see Sandler, 1999): a) Propane/ H_2 /sunflower oil system at 453.15, 473.15 and 673.15 K and pressures of 18 and 20 MPa b) DME/ H_2 /sunflower oil at 423.15, 453.15 and 473.15 K and 20 MPa. Both in mol %.

The solubility of H_2 in liquid propane is low even at high pressures; however at supercritical temperatures of propane, both gases are completely miscible at the pressures of interest (Pereda *et al.*, 2000 and Weidner *et al.*, 2004). Schiemann (1993)

studied the phase equilibrium hydrogen/propane/sunflower oil system at 373.15 K and 12 MPa for mixtures with propane concentrations up to 50 molar %. According to these experimental data, the addition of propane to a hydrogen/oil mixture produces a large increment in the solubility of hydrogen in the liquid phase. Even though propane/triglyceride mixtures exhibit a region of partial liquid miscibility at high solvent concentrations and temperatures close to the critical temperature of C₃H₈, complete miscibility is achieved by increasing the pressure (Straver *et al.*, 1998; de la Fuente *et al.*, 1994; Weidner *et al.*, 2004). Therefore it is possible to find conditions where propane exhibits a complete miscibility with both hydrogenation reactants (H₂ and the fatty oil) using temperatures above the critical temperature as well as increasing the system pressure.

From a hydrogenation point of view, it is interesting to study the conditions of complete miscibility keeping a given molar ratio between H₂ and oil. The optimum conditions for supercritical propane hydrogenation of fatty oils require complete miscibility of the ternary mixture at the stoichiometric ratio of H₂ and oil. This ratio is generally above one (Pereda *et al.*, 2000).

Previous research by Macher *et al.* (1999) and Van den Hark and Härrod (2001), along with predictions by Pereda *et al.* (2002) suggests that high propane concentration (≥ 75 mol %) is needed in the supercritical hydrogenation process to achieve single-phase conditions at the required ratio of the reaction components. As shown in Figure 2-11, the homogeneous region is reached at high solvent molar compositions for both reactive systems under study. However, a slightly lower solvent concentration (approximately 75 mol %) is needed for the system with DME than for propane system at 473.15 K and 20 MPa, which allows even higher ratios between hydrogen and sunflower oil.

It is of high interest to understand why a solvent, which does not take part in the chemical reaction itself, has such a pronounced effect on the overall conversion rate and why different solvents have such different effects. Depending of the reaction temperature, either DME or propane is the better solvent. This fact was studied by Brake *et al.* (2002) for methyl oleate/hydrogen/propane and methyl oleate/hydrogen/DME systems. These authors found that DME is the better solvent up to temperatures of about 460.15 K for a feed molar oil:H₂:solvent composition of 1:10:89%. Above this temperature, single-phase conditions are achieved at lower pressures in the presence of propane. This is also true for higher hydrogen excess or

lower SCF-concentration. At these compositions the required pressures to reach single-phase conditions are significantly higher and may reach 20 to 30 MPa.

Despite the fact that the principle phase behaviour of DME is similar to that in the propane system (Weidner *et al.*, 2004), the region of complete miscibility between sunflower oil, hydrogen and DME is larger than in the propane system (see Figure 2-11). This indicates that DME is a slightly better solvent for vegetable oil hydrogenation than propane because of its better solubility with the triglycerides. This fact is directly related to that reported by Weidner *et al.* (2004). Their research is focused on the effect of adding a supercritical fluid as a hydrogenation solvent on the phase behaviour. Contrary to the systems with carbon dioxide, gradual increasing of propane or DME concentration related to saturated vegetable oil leads to a reduction of the density as well of the viscosity of the mixture. The effect of DME is slightly larger than that of propane.

As in any solvent-based process, the amount of solvent in relation to the amount of reactants used is an important parameter for process economics. For this reason, low substrate concentrations should not be used because with a “diluted” reaction mixture, large solvent volumes have to be circulated through the system to produce a given amount of product. Thus, it is important to optimise the substrate concentration in the mixture but this amount is limited if single-phase conditions have to be secured in the reactor due to the fact that the viscosity of the reaction mixture increases fast as more substrate is dissolved in propane (Richter, 2000). In addition, when the hydrogen concentration in the ternary mixture is increased, it acts as an anti-solvent, raising the equilibrium pressures of the entire system. This phenomenon may reduce the solubility of the substrate in the supercritical medium (Rovetto *et al.*, 2004; Hitzler *et al.* 1998). Thus, the hydrogen concentration has to be kept as low as possible.

Van den Hark and Härrod (2001) studied the supercritical hydrogenation of fatty acid methyl esters (FAMES) at 15 MPa and 553.15 K using propane as reaction solvent. These authors found that at high substrate concentrations (2 mol % of oil and 20 mol % of hydrogen), a rapid fall of the reaction rate was observed due to the split of the supercritical homogeneous reaction mixture into two phases. In this case, the large excess of hydrogen available to the catalyst, if the reaction mixture forms a single-phase, turns the substrate, not hydrogen, into the limiting factor. It is suggested that hydrogen ratios around 10 or lower are of interest and the minimum required propane feed is five to six times the product weight in order to create the necessary single-phase conditions.

A similar conclusion was reached by Pereda *et al.* (2003) who have been studying the phase equilibrium hydrogen/propane/sunflower oil system at 373.15 K and 12 MPa. It is concluded that the limits of the one-phase region change with the value of the stoichiometric ratio H₂/oil in the mixture. They derived a general expression relating the required propane fraction, to have the vegetable oils in a single vapor phase in terms of the mol oil/mol H₂ stoichiometric ratio in the reactor feed:

$$R = \frac{\text{Weight}_{C_3H_8}}{\text{Weight}_{oil}} = (1 + MR) \frac{x_{C_3H_8}^{\max}}{(1 - x_{C_3H_8}^{\max})} \left(\frac{MW_{C_3H_8}}{MW_{oil}} \right) \quad (2.23)$$

This equation was derived from the condition where total molar mixture composition is equal to 1. *MR* represents the molar ratio H₂/oil in the reactive mixture and *MW*_{C₃H₈} and *MW*_{oil} are the molecular weight of propane and oil, respectively.

Based on the facts already cited, as well as on phase equilibrium predictions, suitable operating conditions (concentrations, temperatures and pressures) which can bring all hydrogenation reactants and products into a homogeneous reactive fluid phase can be determined as follows:

Table 2-4: Scope of variables of reaction.

Variables		Operating Range
Temperature (K)		423.15-573.15
Pressure (MPa)		15-30
Feed Composition (mol %)	Sunflower Oil	≤2
	Hydrogen	2-10
	Solvent (C ₃ H ₈ or DME)	≥80

The temperature operating range was chosen above the critical temperature values for the solvents (see Table 2-1) but not too high in order to avoid by-products formation e.g. over-hydrogenation of the reaction products or product decomposition.

The pressure operating range was set enough higher than the critical pressure value for both solvents whereas limit pressure value was chosen in agreement with the technical/economical limit for the standard materials which is somewhere around 30 MPa.

In general, the phase equilibrium for systems of nonpolar or weakly polar compounds is correlated surprisingly well by any of the Van der Waals-type of equations of state, over a wide range of temperatures and pressures. Only in the critical region there are greater deviations from experimental values. However, experimental errors in this region are also larger and the deviation calculated with the equations of state tends to be greater than experimental errors (Brunner, 1994). Therefore, the ternary phase equilibrium calculations should be used in a predictive way. Even in equilibria calculations, substantial errors can be tolerated since operating conditions will be well-chosen away from critical and limited conditions in order to ensure homogeneous single-phase operation.

Van den Hark and Härrod (2001) noticed the hydrogenation phase transition because the fall in the reaction rate followed by a sudden change in the pressure drop due to the increase of the mixture viscosity. The possible explanation of these facts would be the pore condensation of the substrate. In this situation, the process is operated under conditions comparable to those of the conventional processes and the advantages of the propane addition are lost. These authors suggest that one of the most simple methods of determining single-phase conditions is to observe the reaction rate. The difference in reaction rate between two-phase and single-phase conditions is dramatic. For a given system the reaction rate is a proof of the presence or absence of a liquid phase.

Preliminary runs with C_3H_8 as solvent, were carried out in order to check out if the reaction mixture was in a homogeneous single-phase. For a molar feed composition consisting of 1:4:95 % at 423.15 K and 20 MPa, the condensation into the reactor seemed to occur because the material balance (which assures the conservation of mass) for the oil in the well-mixed stirred-tank reactor (CSRT) was not accurate. This suggests that the catalyst was saturated with oil. This behaviour was expected because these operating values were close to those corresponding to the critical mixture values estimated with the Chueh–Prausnitz (Reid *et al.*, 1987) approximation: 420.15 K and 8.8 MPa. A later run was performed, increasing the temperature to 433.15 K. In that run, non-condensing conditions were monitored by watching the rate of reaction as suggested by Van den Hark and Härrod (2001).

2.5 Conclusions.

The Peng-Robinson (PR) (Peng and Robinson, 1976) equation of state was used to predict high-pressure vapor-liquid equilibrium (VLE) for sunflower oil/ H_2 / C_3H_8 and sunflower oil/ H_2 /DME reactive systems. VLE representations were obtained by using

the one-fluid van der Waals mixing rules with k_{ij} and η_{ij} as binary interaction parameters.

The capability of PR-EOS to represent the phase-equilibrium conditions in several mixtures was previously studied, based on experimental data from the literature (Eftaxias *et al.*, 2001 and Rovetto *et al.*, 2001). A good representation of these experimental data was obtained (a relative error of 8% in the worst case).

The VLE predictions for sunflower oil/H₂/C₃H₈ and sunflower oil/H₂/DME ternary systems along with experimental VLE considerations from other researchers, who have worked on similar reactive systems, were employed for determining suitable operating conditions (concentrations, temperatures and pressures) that could assure all hydrogenation reactants and products were into a homogenous reactive fluid phase. Later experimental runs allowed to confirm that a unique supercritical single-phase was presented into the reactor under chosen operating conditions by means of checking oil material balance as well as monitoring the rate of reaction.

2.6 Nomenclature.

a	Van der Waals parameter that accounts for intermolecular interactions between species in the mixture [(Pa m ⁶ /mol ²)]
b	Van der Waals parameter that accounts for size differences between the species of the mixture [m ³ /mol]
C _{gl}	equilibrium concentration of hydrogen in liquid oil [cm ³ /mol]
dfc	fluid-solid catalyst interface
dgl	gas-liquid interface
dlc	liquid-catalyst interface
f	fugacity [MPa]
k ₁₂	parameter of binary mixture
K _i	VLE constant. $K_i = y_i/x_i$, where $i = 1$ for SCF and $i = 2$ for sunflower oil
MR	molar ratio hydrogen/substrate in the reactive mixture
MW	molecular weight [kg/mol]

N	total number of moles in the mixture
n_i	number of moles of component i
n_T	total number of moles in the vapor phase
P	pressure [MPa]
P_c	critical pressure [MPa]
P_R	reduced pressure. $P_R=P/P_c$
P^{sat}	saturation pressure [MPa]
R	gas-law constant [8.314 J/(mol K)]
T	temperature [K]
T_c	critical temperature [K]
T_R	reduced temperature. $T_R=T/T_c$
v	molar volume [m ³ /mol]
V	volume of the mixture [m ³]
w	acentric factor
x	liquid mol fraction, where $i=1$ for SCF and $i=2$ for solute
y	vapor mol fraction, where $i=1$ for SCF and $i=2$ for solute

Greek letters

η_{12}	parameter of binary mixture
ϕ	fugacity coefficient
∞	infinite dilution

Acronyms

CO ₂	dioxide carbon
C ₃ H ₈	propane
DME	dimethyl ether
EOS	equation of state
FAME	fatty acid methyl ester
H ₂	hydrogen
PR	Peng-Robinson
VLE	vapour-liquid equilibrium

Sub- and Superscripts

1	volatile component (light)
2	non-volatile component (heavy)
c	critical
i	component
L	liquid phase
mix	mixture
R	reduced
sat	saturation
V	vapor phase

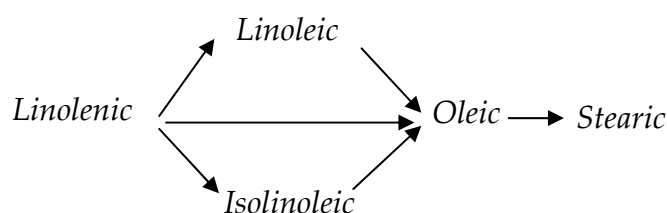
Chapter Three

Kinetics of the Sunflower Oil Hydrogenation Process over Palladium-Based Catalysts using SC propane or SC DME as Reaction Solvent.

3.1 Introduction.

The chemistry of hydrogenation reactions is complex as both the mono- and poly-unsaturated acid groups in the oil hydrogenate at different rates, depending on the operating conditions. Furthermore, geometrical and structural isomerization of double bounds can occur, and this has an important effect on the physical properties of the final products (Patterson, 1983).

The first mechanistic kinetic model for vegetable oil hydrogenation was developed by Bailey (1949) who proposed the following scheme of reactions of the unsaturated triglycerides for the batch hydrogenation of linseed, soybean and cottonseed oil.



Scheme 3-1: Kinetic model for oil hydrogenation developed by Bailey (1949).

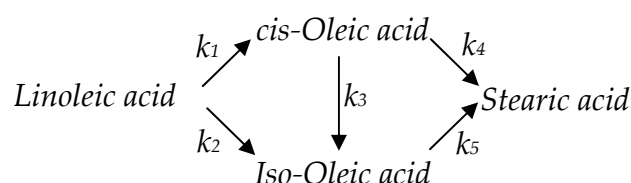
Using this model, Bailey considered each reaction to be first order and irreversible and thus developed the kinetics equations to represent the concentration of each acid group as a function of time as well as determined the effect of operating variables on process selectivity, *iso*-oleic acid formation and hydrogenation rate. The increase of temperature, hydrogen pressure, nickel catalyst concentration and agitation increase the reaction rate whereas selectivity and isomerization is favoured at higher temperature and catalyst concentration as well as at lower pressure and agitation.

The term “selectivity” applied to hydrogenation reaction had two meanings in the industry. Originally, the term was defined by Richardson *et al.* (1924) as the conversion of linoleic acid to a monoene, compared to the conversion of the monoene to stearic acid. This was also known as *chemical selectivity* since it compared the rates of chemical reactions. Another type of “selectivity” was applied to the catalyst. If a catalyst was

“selective”, it produced an oil of softer consistency or lower melting point at a given Iodine Value (IV).

From relative reaction rate constants calculated for several runs by Bailey, the selectivity (ratio) of the reaction was defined as the ratio of the reaction rate constant for linoleic to oleic, divided by the reaction rate constant for oleic to stearic. If the ratio was 31 or above, the hydrogenation was selective and below 7.5, non-selective. Ideally, selectivity ratio (SR) should be large, since production of oleic acid is desired, while its further reaction to saturated stearic acid is undesirable.

Elbid and Albright (1957) proposed a network of chemical reactions (see the scheme as follows) for cottonseed oil hydrogenation taking into account the presence of *trans* configurations of the double bonds because of their strong influence on the softening point and consistency of the final product.



Scheme 3-2: Kinetic model for cottonseed oil hydrogenation by Elbid and Albright (1957).

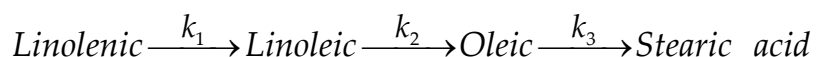
It was assumed that each of the reactions was irreversible and pseudo-first order. They proposed a mechanism for selectivity based on preferential physical adsorption of linoleic instead of oleic acid on the catalyst surface as well as on the assumption that the rate-controlling step is the surface reaction between atomically chemisorbed hydrogen and physically absorbed unsaturated as suggested before Boelhouwer *et al.* (1950), Krane (1953) and Allen and Kiess (1956).

Elbid and Albright’s research focussed on the effect of the operating variables as temperature, pressure and concentration of the nickel catalyst on the hydrogenation rate and selectivity over a wide range of experimental conditions but they applied a vigorous agitation in order to minimize/eliminate mass transfer resistances. For that reason, their experimental results were quite different that those obtained by other researchers (e.g. Moore (1917), Richarson *et al.* (1929) and Bailey (1949)) who used relatively low degrees of agitation. The overall rate of hydrogenation was directly proportional to temperature, pressure and catalyst concentration. A little change in selectivity was found with temperature while slightly more *iso*-oleic acid was formed at

high temperature. Both selectivity and isomerization decreased with increased pressure whereas catalyst concentration had no significant influence on them.

Because most of the former hydrogenation studies of triglycerides had been at relatively low pressure (up to about 1 MPa), Wisniak and Albright (1961) carried on the hydrogenation of cottonseed oil applying moderate hydrogen pressures in order to clarify the reaction mechanism. They made the same assumptions explained above. Similar results as those reported by Elbid and Albright (1957) were obtained but they discovered that the overall rate of hydrogenation was proportional to the system pressure to the power of 0.6.

A simpler reaction sequence was proposed by Albright (1965). Since the linolenic acid produces several different dienes (isolinoic acids) when one double bond is hydrogenated and since there would be little difference in the rates of hydrogenation of the mixture of dienes, these were included in one term. Also, since the addition of two moles of hydrogen to linolenic acid to produce oleic acid directly has not been shown to occur, the shunt was eliminated from the model, and since geometric and positional isomers that are formed were believed to have almost the same reactivity, these were not included in the model. Thus the model is simplified to:



Scheme 3-3: Kinetic reaction sequence for oil hydrogenation by Albright (1965).

k_1 , k_2 and k_3 are the reaction rate constants and the model assumptions were a chemical reaction sequence of first order (the reaction rate depends on the concentration of unsaturated acids), irreversible “elementary” steps and that H_2 is present in large excess. Various selectivity ratios have been derived from this kinetic scheme:

$$\text{Linoleic Selectivity } (S_I) = \frac{k_2}{k_3} \quad (3.1)$$

$$\text{Linolenic Selectivity } (S_{II}) = \frac{k_1}{k_2} \quad (3.2)$$

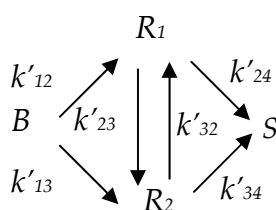
Here S_I and S_{II} express the preferred saturation of double bonds in dienes over monoenes and trienes over dienes, respectively. Most commercial nickel catalysts under the conditions used for nickel commercial hydrogenations (0.3 MPa, 423.15-498.15 K) have an S_I of 30-90. In general, a hydrogenation catalyst is thought to be selective if S_I is higher than 10.

The reaction rates for the mechanism presented above were found to be pseudo-first order with respect to the oil triglycerides by Bern *et al.* (1975), Snyder *et al.* (1978), Chen *et al.* (1981) and Allen (1981). On the other hand, several authors found a first-order reaction rate with respect to the hydrogen concentration (e.g. Elbid and Albright (1957), Wisniak and Albright (1961), Marangozis *et al.* (1977))

Using a similar simplified kinetic scheme by Albright (1965), Cordova and Harriot (1975) have studied the hydrogenation of methyl linoleate using 1% Pd on carbon as a catalyst. The reaction kinetics of the first step (i.e. linoleate to oleate) was studied using the initial rate data where no stearate is formed. Similarly, the kinetics of the second step (i.e. oleate to stearate) was studied using the data in the region where the linoleate is completely reacted. They found the first reaction to be first-order and the second reaction to be half-order with respect to hydrogen.

The hydrogenation of methyl linoleate to methyl oleate and methyl stearate was studied in a stirred batch reactor using several particle size fractions of 1% Pd/C catalyst by Tsuto *et al.* (1978). Using the “conventional” reaction scheme (see Scheme 3.3), they found that the hydrogenations of both substrates were first order with respect to hydrogen, which did not completely agree with Cordova and Harriott (1975), but some of the linoleate appeared to react directly to stearate (shunt reaction) perhaps because of nonequilibrium adsorption of reactants.

The model used by Albright (1967) (see chemical scheme presented as follow) was found to be applicable for the hydrogenation of cottonseed oil by Hashimoto *et al.* (1971) using the experimental data from Eldib and Albright at low pressure (1957) and that from Wisniak and Albright (1961) at high pressure in which the mass transfer effects were essentially eliminated.



Scheme 3-4: Kinetic model for cottonseed oil hydrogenation by Albright (1967).

Hashimoto *et al.* (1971) proposed first-order rate equations with respect to the compositions of the various liquid components in the liquid phase. *B*, *R*₁, *R*₂ and *S* represent di-unsaturated, *cis*-mono-unsaturated, *trans*-mono-unsaturated and saturated

fatty acid groups, respectively. The $(k_{i,j})$'s are the respective pseudo first-order reaction rate constants in which the effect of hydrogen pressure is included:

$$k'_{12} = k_{12} C_{H_2}^{1/2} \quad (3.3)$$

$$k'_{13} = k_{13} C_{H_2}^{1/2} \quad (3.4)$$

$$k'_{23} = k_{23} C_{H_2}^{1/2} \quad (3.5)$$

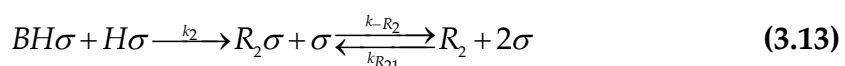
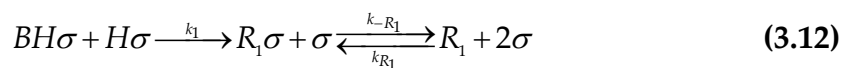
$$k'_{32} = (k_{23} / 3) C_{H_2}^{1/2} \quad (3.6)$$

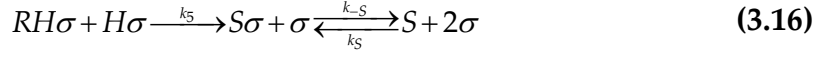
$$k'_{24} = k_{24} C_{H_2} \quad (3.7)$$

$$k'_{34} = k_{34} C_{H_2} \quad (3.8)$$

In order to decrease the number of parameters to solve in this reaction scheme, it was assumed that $k'_{32} = k'_{23}/3$, based on equilibrium ratio of the *cis/trans* of mono-unsaturates reported by several authors e.g. Litchfield *et al.* (1963) and Albright (1967), and $k'_{24} = k'_{34}$ suggesting that the rates of hydrogenation for the mono-unsaturated fatty acid groups are almost equal.

The detailed reaction mechanism, which explained this kinetic behaviour, suggests that hydrogen atoms were formed by the dissociation of hydrogen molecules on the catalyst surface. Based on the basic concepts of Allen and Kiess (1956), the researchers have assumed that a single activated hydrogen atom attack the double bond to yield an unstable partially unsaturated complex. If the concentration of hydrogen atom is high on the catalyst surface, the complex will probably react with another hydrogen atom to complete the saturation and thus the hydrogenation occurs. On the other hand, in the opposite case, the complex will decompose to reform a double bond. However this double bond may be in the original position or in the adjacent position because either of the hydrogen adjacent to the free radical centre may be removed. Since the complex may obtain free rotation, the subsequent removal of a hydrogen atom results in the production of a *cis* or *trans* double bond. The completed mechanism is presented as follows:





σ represents an unoccupied active centre on the catalyst surface. $H\sigma$, $B\sigma$, $R_1\sigma$, $R_2\sigma$ and $S\sigma$ refer to the adsorbed forms of hydrogen, di-unsaturated, *cis*-mono-unsaturated, *trans*-mono-unsaturated and saturated acid groups respectively. $BH\sigma$ is an adsorbed complex that is formed by attack of a hydrogen atom to one of the two double bonds of di-unsaturated fatty acid groups B, and $RH\sigma$ is an adsorbed complex formed from mono-unsaturated acid groups containing both of the *cis* and *trans* configurations.

In the above model, all positional isomerizations and geometrical isomerization steps are not taken into account because of their complexities. They assumed that adsorption and desorption steps at equilibrium, the catalyst surface is sparsely covered by adsorbed components and thus the concentration of unoccupied sites is essentially independent of the concentration in the liquid phase and the rate equations apply to the time elapsed after the induction and also that intraparticle diffusional gradients are negligible. The following restrictions among the rate constants were held:

$$k_{-0} \ll (k_1 + k_2)\sqrt{K_A}\sqrt{C_{H_2}} \quad (3.17)$$

$$k_{-3} + k_{-4} \gg (k_5)\sqrt{K_A}\sqrt{C_{H_2}} \quad (3.18)$$

Under the assumptions mentioned above, the rate constants for the stoichiometric constants k_{ij} were defined as:

$$k_{12} = k_1 k_0 [\sigma_2]^2 K_B \sqrt{K_A} / (k_1 + k_2) \quad (3.19)$$

$$k_{13} = k_2 k_0 [\sigma_2]^2 K_B \sqrt{K_A} / (k_1 + k_2) \quad (3.20)$$

$$k_{23} = k_3 k_{-4} [\sigma_2]^2 K_{R_1} \sqrt{K_A} / (k_{-3} + k_{-4}) \quad (3.21)$$

$$k_{32} = k_4 k_{-3} [\sigma_2]^2 K_{R_2} \sqrt{K_A} / (k_{-3} + k_{-4}) \quad (3.22)$$

$$k_{24} = k_5 k_3 [\sigma_2]^2 K_{R_1} K_A / (k_{-3} + k_{-4}) \quad (3.23)$$

$$k_{34} = k_5 k_4 [\sigma_2]^2 K_{R_2} K_A / (k_{-3} + k_{-4}) \quad (3.24)$$

$$K_A = \frac{k_A}{k_{-A}} \quad (3.25)$$

$$K_B = \frac{k_B}{k_{-B}} \quad (3.26)$$

$$K_{R_1} = \frac{k_{R_1}}{k_{-R_1}} \quad (3.27)$$

$$K_{R_2} = \frac{k_{R_2}}{k_{-R_2}} \quad (3.28)$$

$$K_S = \frac{k_S}{k_{-S}} \quad (3.29)$$

K represents the adsorption equilibrium constants, k_i the rate for respective elementary reaction and $[\sigma^2]$ is the concentration of active sites on the catalyst surface.

These authors concluded from the analysis of their hydrogenation results that the rate of hydrogenation for di-unsaturated fatty groups to mono-unsaturated and the rate of the geometrical isomerizations between mono-unsaturated were half order with respect to hydrogen concentration, whereas the hydrogenation rate of mono-unsaturated to saturated groups was the first order.

Owing to the distinct physico-chemical properties of the *cis* and *trans* isomers also, another type of selectivity was defined by Coenen (1976). The *Specific Isomerization* (S_i), gives the number of *trans* double bond formed per double bond hydrogenated. As well as most of the hydrogenation researchers, he studied the influence of process conditions on dissolved hydrogen concentration near catalyst surface and on selectivities S_i and S_i and found similar results to those reported at relatively low degrees of agitation. Meanwhile, Coenen determined the effect of pore width on selectivity as shows in Figure 3-1.

According to the zone A, the pore width is much bigger than the size of triglyceride molecules. Therefore, oil and hydrogen can go more freely in and out without much hindrance. In this situation, hydrogenation favours the most unsaturated fatty acids. In pores of medium width, a point will be reached where the poly-unsaturated will be almost fully hydrogenated. In this zone (zone B), the hydrogenation of mono-unsaturates starts to occur. Finally, in pores where the access is highly restricted (zone C), it exists a semi-stagnant population of fully hydrogenated material.

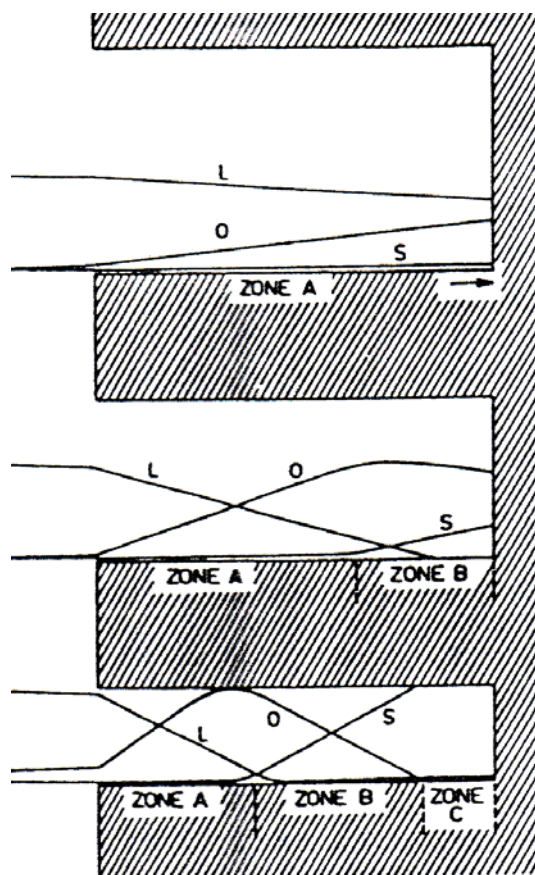


Figure 3-1: Reactant concentration gradients in pores of different widths (Coenen, 1976).

From the obtained experimental results, it was found that the relative hydrogen concentration on the catalyst surface increases with conversion. This may be explained by the fact that the concentration gradient of hydrogen decreases as the reaction progresses because of the decrease in the reaction rate. It is evident that high concentration of hydrogen on the catalyst surface brings low overall yields, that is, low selectivity. This fact is also understood by noting that the order of reaction with respect to hydrogen concentration in the mono-unsaturated acid groups is higher than those of other reactions. Therefore, it may be concluded that operating variables, which cause a decrease in hydrogen concentration at the catalyst surface, favours the selectivity.

Rise (1977) studied the hydrogenation of cottonseed oil using a nickel catalyst and based on the model and the mechanism proposed by Hashimoto *et al.* (1971). It was found that both selectivity (relative reactivity of poly-unsaturates compared to mono-unsaturates) and isomerization of mono-saturates are favoured by low hydrogen concentration at the catalyst surface, which is in turn encouraged by low agitation, high temperature and low pressure. On the other hand, he found a better model fit using $k'_{24}/k'_{34}=9.29$ instead of that value suggested by Hashimoto (1971). The possible

explanation is that the model is not very sensitive to these values as measured by overall performance such as iodine value and reaction time.

Marangozis *et al.* (1977), studied the hydrogenation of cottonseed oil experimentally in an agitated slurry reactor. Their data have been compared and discussed with most of the literature data on the subject using the kinetic scheme proposed by Albright (1967). The results suggest that chemisorption of hydrogen is significant only at pressure higher than about 10 bar, as observed in the work of Wisniak and Albright (1961). At lower pressures, the reaction was pseudo-second order i.e., first order with respect to hydrogen and first order with respect to the unsaturated oil concentration at a given catalyst concentration.

Gut *et al.* (1979) have investigated the kinetics of the hydrogenation of sunflower oil using a nickel catalyst supported by silica. They proposed two models. One of them, it is a simplified scheme proposed by Albright (1965), which mechanism assumes that hydrogen and the reactants are adsorbed on different sites of the catalyst. This model does not distinguish between the *cis*- and *trans*-isomers. The other model is similar to that used by Hashimoto (1971) but with the simplifying assumption that the mono-unsaturated *cis*- and *trans*-fatty acids are identically adsorbed onto the catalyst's surface by forming a half-hydrogenated adsorbate.

The kinetics of soybean oil hydrogenation was studied by Allen (1981) using a first order model with irreversible "elementary" steps similar to that proposed by Albright (1965). Their results suggested that concentrations of linolenic and linoleic acid decrease exponentially with the time, whereas the concentration of oleic acid goes through a maximum and that of stearic acid increases steadily with the time. The effect of the operating variables on hydrogenation rate and selectivity is summarized in Table 3-1.

Table 3-1: Effects of process variables on rate and selectivity in vegetable oil hydrogenation (Allen, 1982).

Increase in	Results		
	Reaction Rate	SI	Isomerization
Temperature	++++	++++	++++
Pressure	+++	---	---
Agitation	++++	----	----
Catalyst Concentration	++	+	-

The above summary shows that hydrogenation rate increases very significantly with increasing total pressure and temperature. Increasing the temperature increases rate of surface reaction as well as H₂ solubility, whereas decreases the oil viscosity. Increasing the pressure increases the concentration of H₂ at the catalyst surface, thereby positively influencing the surface reaction rate. The rise of agitation rate also increases the overall rate by increasing area of the gas-liquid interface and decreasing the thickness of the liquid-solid interface, thereby increasing the effective rate of H₂ mass transfer to the catalyst surface.

Increasing temperature also increases the selectivity ratio and the *trans:cis* isomerization ratio. However, the effect of increasing total pressure is to lower S_i and the *trans:cis* ratio, since selectivity and *trans* isomerization ratios are higher at lower surface H₂ concentration, i.e. a higher surface concentration leads to faster product saturation; increasing agitation rate has the same kind of effect on selectivity as increasing pressure.

Santacesaria *et al.* (1994) developed a comprehensive kinetic model for rapeseed oil hydrogenation over a palladium catalyst in which all possible isomerization reactions were involved. In this model, however, each reaction rate was obtained from those calculated using the simplest mechanistic model (see Scheme 3.3), assuming a 3:2:1 ratio between the equilibrium adsorption constants of the mono-unsaturated triglycerides, corresponding to the probability of a double bond to react at the catalyst surface and considered that the reaction is zero order with respect to hydrogen. The kinetic constants obtained by fitting experimental data gave quite similar results for the poly-unsaturated fatty acids. However, very different results were obtained for the mono-unsaturated ones. In the case of the poly-unsaturated fatty acids, double bond migration with the formation of conjugated dienes would occur before hydrogenation. Conjugated dienes are more quickly hydrogenated than isolated or single double bonds.

González-Marcos *et al.* (1998) have incorporated the *cis-trans* isomerization of monoenes to the Scheme 3.3. A series of prepared nickel catalyst supported on silica and a commercial catalyst have been tested in the sunflower hydrogenation. As a result of this study, in the case of absence of diffusion, it was found that the pressure had a very little effect on the distribution of components in the hydrogenated product whereas increasing temperature produced an important increase in S_i while S_i remained nearly unchanged. However, for normal industrial operations including catalysts with high nickel content, the presence of diffusion controls is certain to occur. The apparent

activation energies were found to be lower than those of the kinetic operation and the hydrogen reaction order increased up to the unity. With respect of selectivities, the presence of mass transfer limitations produced higher values of S_I and S_i . Both of them increased with temperature; S_I also increased with pressure, while S_i decreased with it.

Jonker *et al.* (1999) studied the intrinsic kinetics of the monoenic fatty acid methyl ester hydrogenation over nickel. On the basis of the Horiuti-Polanyi mechanism, involving a half-hydrogenated surface intermediate, kinetic rate equations were derived following the Langmuir-Hinshelwood-Hougen-Watson approach. Kinetic experiments in the absence of diffusion limitation were carried out for $333.15 \leq T \leq 443.15$ K, $0.02 \leq P \leq 0.5$ MPa, and several compositions of oleate, elaidate and stearate. The statistically most significant model assumes the formation of the half-hydrogenated surface intermediate as the rate-determining step and an equilibrium associative hydrogen adsorption.

The kinetics for soybean oil hydrogenation using a commercial Ni/Al₂O₃ catalyst were investigated by Fillion *et al.* (2001) operating under a wide range of temperatures (383.15-443.15 K), pressures (0.12-0.68 MPa), and catalyst loadings (0.02-0.16 Ni wt %). A simple kinetic model (Scheme 3.3) where both *cis*- and *trans*-monoenes were combined and a novel comprehensive model similar to that reported by Gut *et al.* (1979) were developed to describe the hydrogenation process based on Langmuir-Hinshelwood kinetic expressions. The catalyst activity and mass-transfer coefficients were incorporated in both models.

Hydrogenations of sunflower oil over novel structured catalysts with pore sizes ranging from 3 to 20 nm and metal concentrations on the support ranging from 0.7 to 5.0% (w/w) were investigated and compared to a commercial Ni catalyst by Plourde *et al.* (2003). Their results showed that catalyst supports with pore diameters between 7 and 8 nm were more active and selective than supports with lower pore diameters. At the same metal loading and mean pore diameter, the activity was also higher with supports having smaller pore volumes and surface areas, suggesting that the pore depth and geometry of the supports may play an important role in the activity of the supported catalysts. A Pd catalyst at a metal loading of 1% (w/w) had as much activity as a Ni catalyst but was more selective toward *cis*-monoenes with similar selectivity toward *trans*-unsaturated acids at equal IV reductions.

The recent interest in the use of supercritical fluids as reaction media is associated with their solvent power under reaction conditions and their performance as solvents for rapid mass and heat transfer (Savage *et al.*, 1995). On the other hand, supercritical

carbon dioxide is already considered a solvent of choice for green chemical processing (Beckman, 2003). In the case of hydrogenation, the SC fluid is employed to dissolve all the reactants (oil triglycerides and H₂) and form a single, homogeneous vapor phase, in which the mass transport resistance problem is alleviated. As regards to the reactants, their concentrations on the catalyst can be varied in a more flexible manner and not dictated by the unfavourable equilibrium solubility as in the case for H₂ in multiphase reacting systems. In this way, higher reaction rates can be reached and the amount of unwanted by-products can be reduced in order to obtain a higher product quality. Poliakoff and co-workers (1998) have reported on the unique ability of SC solvents to change selectivity in a quite large number of organic processes.

Tacke *et al.* (1996, 1997 and 2003) reported full and partial hydrogenation of fats and oils, fatty acids and fatty acid esters using near critical and supercritical CO₂ and/or propane mixtures at temperatures between 333.15 and 393.15 K at a total pressure up to 10 MPa. The reactions were conducted in a continuous fixed-bed reactor with palladium on Deloxan as proprietary catalyst. For the case of the carbon dioxide used as reaction solvent, the authors observed significantly improved space-time yields compared to hydrogenation in other types of reactors (e.g. conventional trickle bed and slurry), a longer catalyst life, higher linoleate selectivity and a significantly decreased *cis/trans* isomerization rate. Propane or propane/ CO₂ mixtures enhance the solubility of fats and oils and decrease the viscosity of the reaction mixture whereas the diffusivity is further increased. Consequently, a higher hydrogenation rate is observed. The results related to selectivity and *cis/trans* isomerization rate were not reported.

Similarly, Härröd and co-workers (1996-1999) succeeded in overcoming the solubility problem and the transport resistance for hydrogen. They used near-critical or supercritical propane, which is miscible with both, oil and hydrogen thus forming a homogeneous phase, and fed it into a continuous fixed-bed reactor packed with a commercial palladium catalyst. The researchers used a fractional factorial design to study the effect of operating variables on rate and *trans*-fatty acid formation. Their results suggest that both temperature and hydrogen pressure have a strong positive effect on the reaction rate. The *trans*-fatty acid formation decrease when the temperature is increased and the residence time shortened at high hydrogen pressure. Under the experimental conditions studied, they achieved extremely high reaction rates, according to the authors, about 400 times higher, for the partial hydrogenation of fatty acid methyl esters compared to the traditional technique. The tremendous rate enhancement was attributed to the elimination of gas/liquid mass transfer as a consequence of the

essentially homogeneous phase under supercritical conditions, which facilitated the increase in the hydrogen concentration at the catalyst surface. Another benefit of supercritical conditions was that the concentration of *trans*-fatty acids was considerably reduced compared to conventional processes using the same catalyst and the same degree of hydrogenation. However, the problem of catalyst deactivation remained unresolved. Despite of the fact of the incredible results reported by these authors, the kinetics of the oil hydrogenation are poorly studied.

Comparison of the reactions in presence of different supercritical solvents indicates that the kind of supercritical fluid plays an important role on the overall conversion. Härröd and Møller (1996) found that the space velocity for the hydrogenation of triglycerides is increased by a factor of 60 in presence of carbon dioxide and by a factor of 700 in presence of propane. Related to this matter, Brake *et al.* (2002) studied the role of supercritical fluids in the hydrogenation of triglycerides in presence of carbon dioxide, propane and dimethyl ether (DME) at pressures up to 180 bar and temperatures up to 403.15 K. They have found that the region of complete miscibility between hydrogen, propane and oil is much larger than that in the carbon dioxide system whereas is smaller than that in DME which could be indicated that it would be a slightly better solvent than propane to performance the hydrogenation reaction.

Macher and Holmqvist (2001) carried out the hydrogenation of palm oil in near critical and supercritical propane using a small (5 cm³) continuous fixed reactor and 1% Pd/C as catalyst. Temperature (338.15-408.15 K), H₂/Triglyceride mol ratio (4-50) and residence time (0.2-2 s) were varied in order to assess the iodine value (IV) as a function of the operating variables. The authors observed high reaction rates even using a residence time of 2 s at 393.15 K, which indicates that the reaction could also be run successfully at lower temperatures. Unexpectedly, the hydrogen concentration was of minor importance, which can be a sign of either H₂ saturation of the catalyst or a phase-split of the reaction mixture with resulting mass transport limitation for the hydrogen.

King *et al.* (2001) studied the hydrogenation of soybean oil using pure hydrogen mixed with supercritical carbon dioxide at 14 MPa and 393.15-413.15 K, in a conventional nickel catalyst in a slurry reactor. They found that depending on the chosen reaction conditions, a wide variety of end products can be produced having different iodine values, percentages of *trans* fatty acid content, and dropping points or solid fat indices. Although addition of carbon dioxide to the fluid phase containing hydrogen retards the overall reaction rate in most of the studied cases, the majority of products have low *trans* fatty acid content, consistent with a non-selective mode of hydrogenation.

In a previous work (Ramírez and Larrayoz, 2002), we presented preliminary experimental data from a continuous, single-phase hydrogenation of sunflower oil on Pd/C carried out in a Robinson-Mahoney type of reactor, with a fixed bed catalyst using propane as SC solvent. The results show that it is possible to predict the formation of several hydrogenation products with certain characteristics for different industrial applications by changing the operating conditions, since the final product distribution depends on temperature, pressure and feed mixture composition.

Though partial hydrogenation of fatty oils is one of the oldest industrial processes and a large number of paper, patents and books have been published in the subject, only few papers have been devoted to the kinetics of this reaction as shows above either in the case of using nickel or palladium catalyst. Furthermore, chemistry and kinetics of the hydrogenation of the unsaturated oils are normally studied using simplified reaction systems such as, for example, the methyl ester of linoleic acid. As a consequence, the results of these studies can hardly extended to the interpretation of the behaviour of natural oils, that is, a mixture of polyunsaturated triglycerides.

The preceding literature review shows that the kinetic parameters for oil hydrogenation are not completely well understood and that there is a need to develop a kinetic model that involves the rates of reaction of the di- and mono-unsaturated triglycerides during continuous hydrogenation process especially under supercritical conditions. On the other hand, nickel is the catalyst universally employed in industry but the search is still on for a catalyst operating under milder conditions and producing lower levels of *trans* isomers. In this respect, palladium catalysts seem to be promising in addition to its very high activity.

3.2 Objectives.

This chapter aims to establish a better understanding of how operating variables affect sunflower oil hydrogenation on palladium-based catalysts in combination with a supercritical fluid as reaction medium in a continuous recycle reactor.

The operating variables were varied according to a statistical or sequential experimental design in order to study their influence on rate of reaction, conversion and final product distribution and to establish the experimental conditions where a potential CSTR process could be operated to obtain a certain outlet iodine value (IV) with a minimum *trans* and stearic final content in comparison to those reported for the traditional process.

As an extension of these results, the determination of the kinetic constants and their temperature-dependence for the multiple reactions of hydrogenation-isomerization network involving triglyceride species based on a kinetic formalism proposed early for vegetable oil hydrogenations was achieved by means of the analysis of the CSTR reaction rate.

3.3 Sunflower Oil Hydrogenation on Pd/C using SC Propane as Reaction Solvent.

In this case, the hydrogenation reaction study (Ramírez *et al.*, 2004) was composed of two parts: to build an empirical modeling in order to determine the effects of operating variables on the reaction as well as defining their practical operating ranges, using experimental design concepts, with the objective of getting low *trans* isomer % for a moderate IV reduction and finally to determine hydrogenation kinetic using a reaction scheme proposed early by Albright (1967).

3.3.1 Study of the Effect of Operating Variables on Hydrogenation Reaction by means of the Experimental Design.

3.3.1.1 Creating the Central Composite Experimental Design.

All the experiments carried out in order to determine the SC continuous sunflower oil hydrogenation kinetic were performed in the experimental apparatus described in Chapter 5 as well as the analytical methods used to determine the reaction rate and the distribution of the hydrogenated products.

In order to construct the experimental design, it must be chosen the operating variables which will be measured under different process conditions. From the discussion presented above, the classical operating variables that have effect on the hydrogenation process are temperature, total system pressure, hydrogen concentration, stirring intensity, catalyst concentration, nature of catalyst and oil concentration.

The phase behaviour depends on the mixture composition, temperature and pressure. Thus, by choosing the appropriate operating conditions, a substantially homogeneous supercritical phase can be achieved. From the phase behaviour study developed in the previous chapter, the inlet reaction mixture composition was chosen as follows: 1 mol% of sunflower oil, 2-10 mol % of H₂ and 89 -97 mol% of solvent as well as the operating pressure and temperature. With regard to process economy, the solvent (either propane or DME) addition has to be kept to a minimum to avoid high recycle volumes of this

solvent. Also excess hydrogen has to be recycled. Thus, the composition of the reaction mixture is very important for industrial practice. High substrate loadings and low concentration of hydrogen are desirable. However, the concentration of substrate in the reaction mixture is limited because the viscosity of the reaction mixture increases fast as more substrate is dissolved in the reaction solvent causing that the single-phase conditions can not be secured in the reactor (Richter, 2000). In addition, hydrogen is an anti-solvent in the reaction mixture and reduces the solubility of both substrate and product as reported Van den Hark and Härröd (2001) who have suggested that hydrogen/substrate mol ratios must be around 10 or lower. A similar conclusion was reached by Hitzler *et al.* (1998) who found that at any temperature, the miscibility of the reaction system (cyclohexane + hydrogen + CO₂) always improved when the concentration of H₂ was reduced.

To achieve homogeneity for the chosen conditions, it is required to have 8 kg propane/kg oil fed, according to the calculations of Pereda *et al.* (2003). The values used here (12-15 kg/kg) are well above. From an experimental viewpoint undue phase separation were unobserved in agreement with the calculations and with the ternary system calculations.

Hitzler *et al.* (1998) have found that the most dramatic changes in the hydrogenated product composition happened near and just below the critical pressure of the solvent (in the case of propane $P_c=4.25$ MPa and for the DME $P_c=5.37$ MPa). On the other hand, the total system pressure in the process must be above the critical pressure (P_c) of the mixture (about 6.2 MPa for the mixture with propane) to ensure single-phase conditions. The mixture critical values were estimated using the Chueh-Prausnitz (Reid *et al.*, 1987) approximation. Thus, if the chosen total pressure is 20 MPa, the effect of the total system pressure on the reaction is considered negligible at SC operating conditions as mentioned previously. The technical/economical limit for the standard materials is somewhere around 30 MPa.

The critical temperature (T_c) for the reactant mixture at the chosen feed composition is 389.15 K in the case of propane as reaction solvent and 420.15 K for the DME. The temperature operating range must be higher than these critical values in order to operate in a single-phase condition but not too high as side-products can form (e.g. over-hydrogenation of the reaction products, or product decomposition, or hydrogenation of other functional groups within the substrate molecule, or polymerisation reactions or coke formation).

To check the presence of external mass-transfer limitations, measurements of the product conversion *vs.* the stirring speed (105-209 rad/s) were performed. Even though the maximum agitator speed was 391 rad/s, Autoclave Engineers reduced this value to 235 rad/s in order to ensure the safe operation with flammable substances under high pressure and high temperature experimental conditions.

The hydrogenation reaction occurred on 0.1085 g of an industrial 2% Pd/C catalyst with uniform metal distribution, average particle size of 0.55 mm (Degussa). Hydrogenation runs were done after the catalyst activity had become stable (for further details, see chapter 5).

Finally, in order to get different degrees of hardening, the space velocity (LHSV), defined by the oil volume processed per hour by catalyst volume, was included as one of the studied operating variables. Space velocity in traditional discontinuous oil hydrogenation reactions with nickel on kieselguhr and activated carbon supported precious metal catalyst are below 1 m³ oil/h*m³ reactor volume. The LHSV values reported for the continuous trickle bed and fixed bed are between 30 – 60 m³ oil/h*m³ reactor volume (Tacke *et al.*, 1997).

Based on the considerations explained above, the ranges of operating conditions are shown in Table 3-2 as follows:

Table 3-2: Scope of variables of reaction.

VARIABLES	Low level (-1)	High level (+1)
Reaction temperature (K)	443.15	473.15
Liquid hourly space velocity (LHSV) (h ⁻¹)	40	60
H ₂ mol %	4	8
Fan speed (rad/s)	105	209

The total system pressure, the molar oil concentration and the catalyst mass were kept constant at 20 MPa, 1 mol % and 0.1085 g, respectively.

To evaluate the effect of the process variables and their interactions on the hydrogenation reaction, a second order polynomial model similar to Box *et al.* (1978) was employed:

$$y = \beta_0 + \sum_{i=1}^k \beta_i x_i + \sum_{i=1}^k \beta_{ii} x_i^2 + \sum_{i < j} \beta_{ij} x_i x_j + \epsilon \quad (3.30)$$

This describes the correlations between the significant predictor reaction variables (x_i) and the predicted responses (y).

The experiments were carried out at different operating conditions according to a 4-variables, two-levels, central composite design (2^4 factorial design + 8 star points (SP) + 1 center point (CP) = 25 experiments). The coded experimental design matrixes are shown in Table 3-3 and Table 3-4.

Table 3-3: Coded 2^4 factorial design matrix.

RUN	Temperature	LHSV	H ₂ %	Fan Speed
1	-1	-1	-1	-1
2	1	-1	-1	-1
3	-1	1	-1	-1
4	1	1	-1	-1
5	-1	-1	1	-1
6	1	-1	1	-1
7	-1	1	1	-1
8	1	1	1	-1
9	-1	-1	-1	1
10	1	-1	-1	1
11	-1	1	-1	1
12	1	1	-1	1
13	-1	-1	1	1
14	1	-1	1	1
15	-1	1	1	1
16	1	1	1	1

Table 3-4: Coded centre and star points design matrix.

RUN	Temperature	LHSV	H ₂ %	Fan speed
17 (CP)	0	0	0	0
18 (SP)	-2	0	0	0
19 (SP)	2	0	0	0
20 (SP)	0	-2	0	0
21 (SP)	0	2	0	0
22 (SP)	0	0	-2	0
23 (SP)	0	0	2	0
24 (SP)	0	0	0	-2
25 (SP)	0	0	0	2

The observed responses were the iodine value (proportional to conversion) and *trans* C18:1. A lined out activity catalyst was employed. The data processing was done using the statistical package Minitab (Applegate and Minitab, 1996).

3.3.1.2 Results and Discussion.

After collecting response data, the experimental factors that have a large effect on the reaction were determined using the *p*-values (which represent the probability of rejecting non-significant experimental variables) of the estimated effects and the table of coefficients for the initial regression from the experimental results. Then, the second order polynomial models were constructed. The significance of the results is indicated by the estimated standard deviations (*s*) of the model, which is used as a measure of dispersion.

The collected response data were fit to a full mathematical model using Minitab, which includes the four main factors (% H₂, LHSV, T, fan speed), six two-way interactions and four quadratic-way interactions.

Using the values in the *p* factor (<0.05), we determined the factors that were significant for the responses under study (IV and *trans* content). So it is observed that the main effect was due to T. The LHSV- H₂ % interaction and T- H₂ % interaction came next and were more important than the effects of LHSV or H₂ % alone. The stirrer speed was the least important factor. From these facts, the polynomial model was reduced and fitted to the experimental data again.

The final polynomial regression equations for the Iodine Value (proportional to conversion) and *trans* C18:1 are respectively:

$$IV = -34.571 + 0.482T + 1.280LHSV + 29.132H_2 - 0.113T H_2 - 0.182LHSV H_2 \quad (3.31)$$

$$trans \text{ C18:1} = -18.521 + 0.074T + 0.696LHSV - 0.003T LHSV - 1.858H_2 - 0.027LHSV H_2 + 0.018T H_2 \quad (3.32)$$

The estimated standard deviations (*s*) of each final polynomial regression models (*s* = 6 for the iodine value (IV) and *s* = 0.73 for the *trans* C18:1 content) were considered to be low. These deviations were mainly due to some experimental instability of the flow rates (e.g. fluctuations in the gas feed flow) or to analytical variability (lack of precision) problems.

From the experiments performed, it could be observed that an increase either in the temperature, the LHSV or the %H₂ (for the mean values of the other variables) involves an increase in conversion and in the *trans* acid content (see experiments 17-23 on Table 3-5). Although the response of conversion is as expected, the effect of %H₂ on the *trans* content is opposite to what is observed at low pressure vegetable hydrogenations (Farrauto and Bartholomew, 2000). This was probably due to the following reason: at the beginning of a hydrogenation, i.e. while the IV is still high, the *trans* content is low. As the IV decreases with the increase of H₂ content at constant temperature and LHSV mean values, the *trans* concentration increases and reaches a maximum. This maximum value is about IV=50 as being suggested by Macher *et al.* (1999). From IV=50 down to IV=0 (i.e. full hydrogenation), the *trans* content decreases, due to the formation of more and more saturates.

Table 3-5: Effects of the increase either in the temperature, the LHSV or the %H₂ for the mean values of the other variables on the responses.

Run	IV	<i>trans</i> wt %	C18:1 wt%
17	117.6	2.3	12.7
18	120.3	1.1	9.9
19	95.17	4.6	23.0
20	113.1	2.4	11.8
21	119.4	2.1	11.4
22	121.3	2.2	8.9
23	110.7	3.1	13.1

For other values of the operating variables, the effect of temperature is not as clear because of the interactions between variables. That is, the effect of one variable on the response of interest depends on the values taken by the other variables. For example, at high temperature, an increase of H₂ % causes a decrease in % *trans*, for any LHSV, whereas the opposite effect is observed at low temperature.

When LHSV is increased (for any %H₂) the same behaviour is observed depending on the value of temperature. If the temperature is low, % *trans* increases and if temperature is high, the *trans* content goes down (See Figs 3-2a and 3-2b). For short contact times (high LHSV), an increase in temperature decreases the *trans* content (for %H₂ < 6%) whereas for low LHSV the opposite effect is observed, irrespective of % H₂ in the feed.

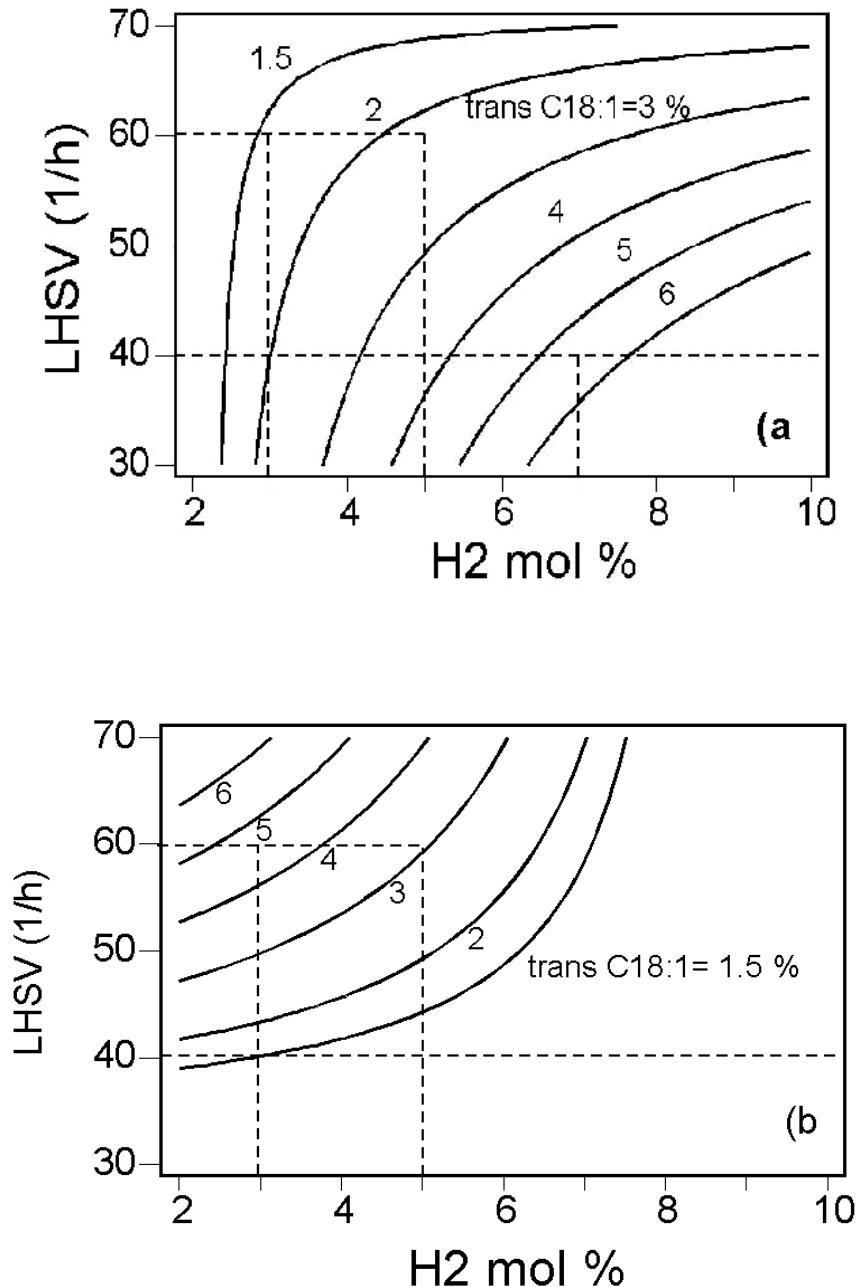


Figure 3-2: Contour map based on empirical quadratic model. High fan speed: a) LHSV vs %H₂ at 488.15 K; b) LHSV vs %H₂ at 428.15 K.

Quite surprisingly, it is observed that at high space velocities, an increase in temperature or H₂ concentration makes hydrogenation extension larger than at low space velocities. This is seen in Figs 3-3a and 3-3b, respectively. Kinetically, this is not the expected behaviour. A possible explanation is that for low LHSV an increase in H₂ produces a decrease in solubility of oil in the reaction medium, which brings about some condensation in the catalyst pores, thus increasing internal mass transfer resistance.

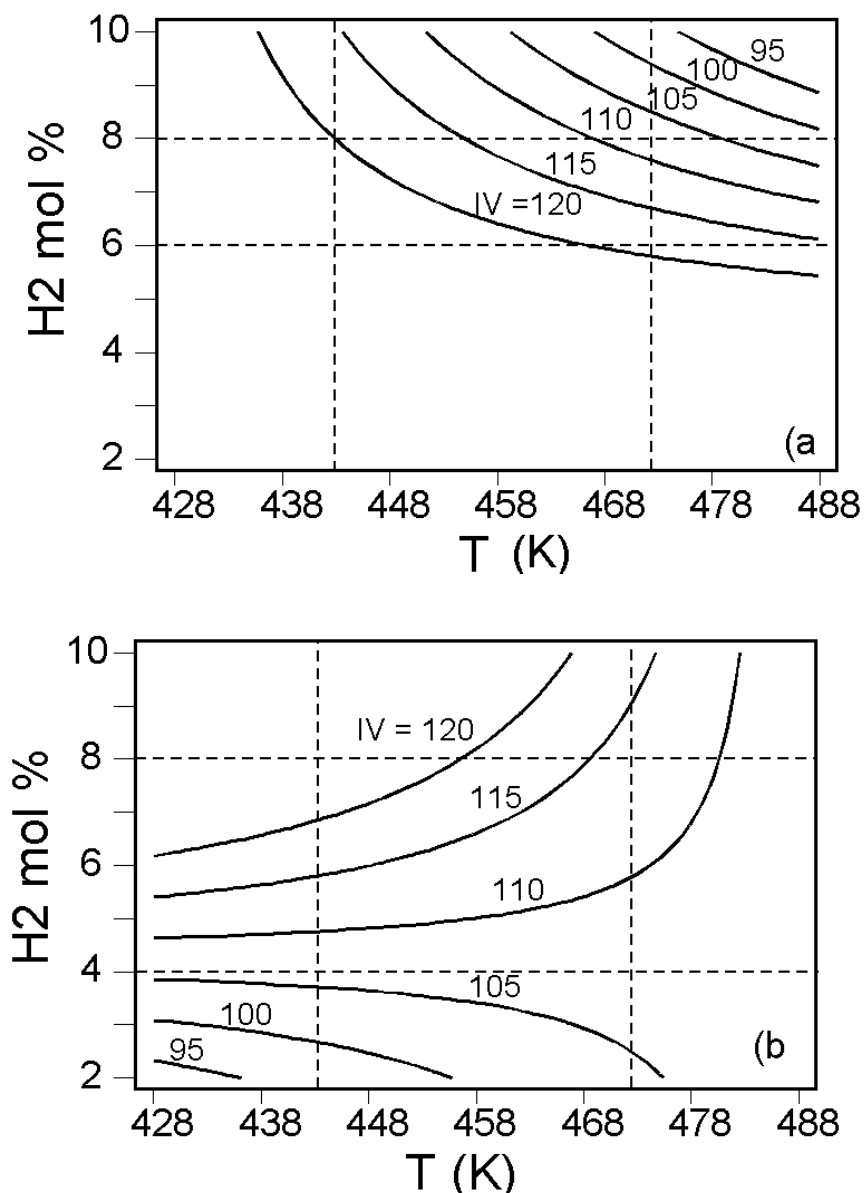


Figure 3-3: Contour map based on empirical quadratic model. High fan speed: a) %H₂ vs T at LHSV=70 h⁻¹ b) %H₂ vs T at LHSV=30 h⁻¹.

The effect of the recycle rate was also considered in the design. An increase in operating fan speed from 52 rad/s to 262 rad/s produces a slight increase in rate (higher conversion). The effect of stirring speed on the *trans* content is similar to that on the IV. The physical effect of increasing fan speed on *trans* content is consistent with the effect of removing some of the diffusion resistance in a net of multiple reactions (Smith, 1981), which improves the yield in intermediates. While in the present reactor is small, its effect cannot be overlooked in a packed bed reactor without recycle and with larger size of catalyst, particularly if very low *trans* isomer is wanted in industrial production. As shows the following figure:

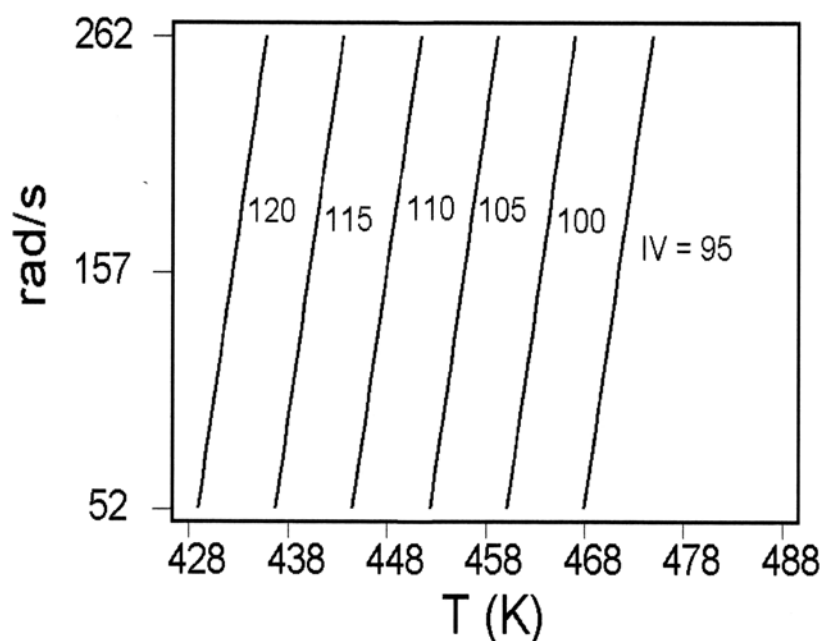


Figure 3-4: Contour maps on the effect of the reactor recycle speed at different temperatures at constant high space velocity and large %H₂.

From the study of the operating variables on IV reduction and *trans* content and their interactions, it is possible to derive different sets of reaction conditions leading to increased conversion while at the same time lowering the *trans* C18:1 isomer content. So in principle, one set of possible reaction conditions would be to operate the reactor at the high temperature range and high H₂ % range together with a high space velocity (LHSV). By contrast, a second combination would be to use a low LHSV, a low T and a H₂ % less than 4. There are other possibilities as well.

In practice, a final hydrogenation product can be obtained that exhibits a low *trans* C18:1 at conversion by letting some increase in the content of saturates (in the form of stearic chains) or by having a low degree of mono-unsaturated. In the former case, the final product could have suitable plastic properties, but could be objectionable from a health viewpoint. In the second case, the necessary plasticity would not be suitable for other applications.

From the results of this study, it is possible to determine the optimum operating conditions to obtain a final hydrogenated product of immediate food application (for example for margarine/shortenings production), such that it has a low *trans* content (<3%) and a moderate IV reduction (final 90<IV<110) together with a stearic content relatively low (<20%). Figs 3-a and 3-b show different alternative operating conditions

(clear colored), that allow simultaneously meeting the above specifications. For example a good combination of operating conditions would be on the upper settings of the variables ($T=473.15$ K, $LHSV=60h^{-1}$, $H_2 \%=9$ fan speed= 262 rad/s) among other possibilities as shown Figs 3-5a y 3-5b.

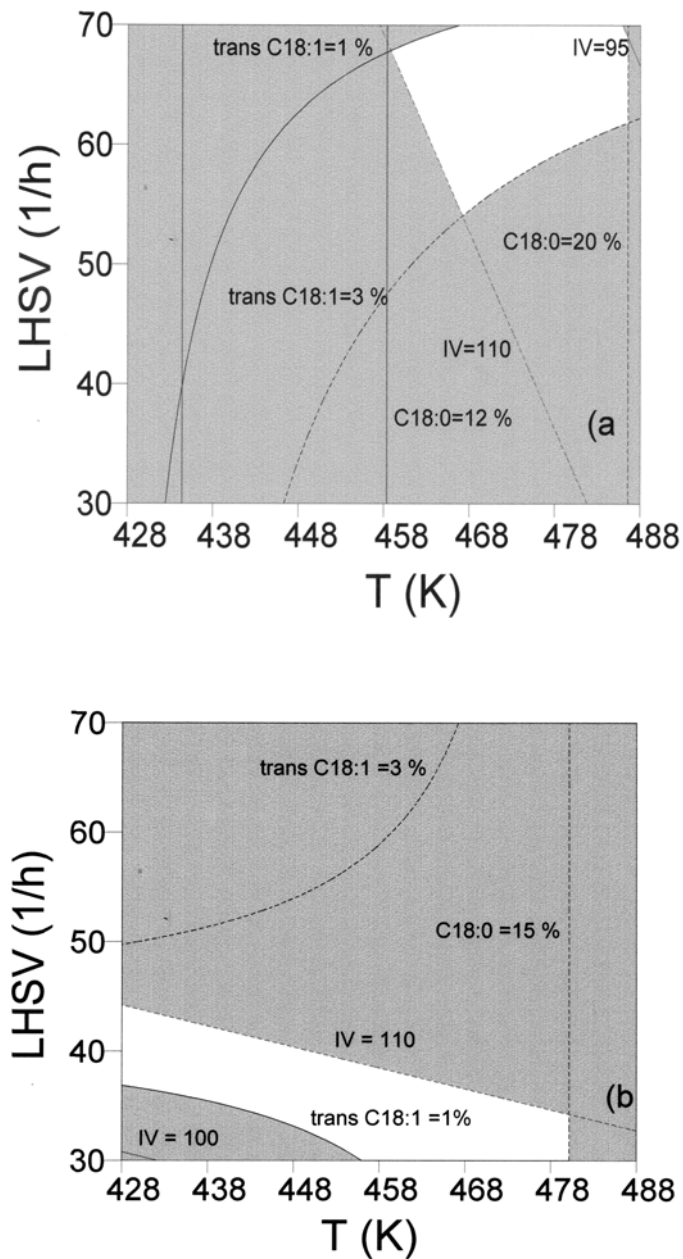


Figure 3-5: Operating zones in the LHSV-T plane a) in the high H_2 composition range between 1-3 *trans* wt %, for IV = 95-110 and stearic content % = 12-2 b) in the low H_2 composition range.

Some of the experimental results are presented in Figs 3-6 and 3-7 together with typical data corresponding to the conventional low-pressure process, as well as those results

reported by King *et al.* (2001) for the hydrogenation of soybean oil in a high-pressure, slurry reactor using SC CO₂ and H₂.

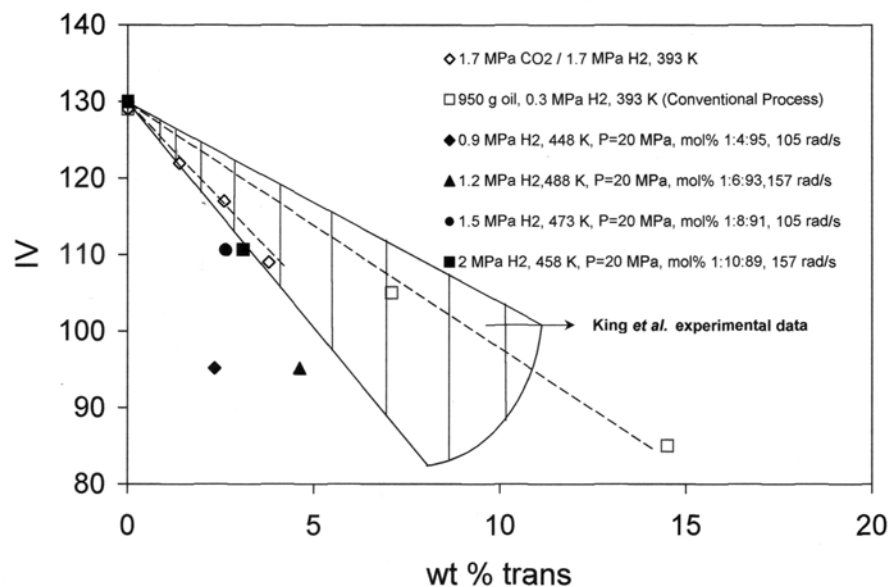


Figure 3-6: Plot showing *trans* C18:1 formed *vs* reduction in iodine value in the continuous hydrogenation of sunflower oil over Pd. Initial IV = 130. Data by King *et al.* (2001) lie within dashed region.

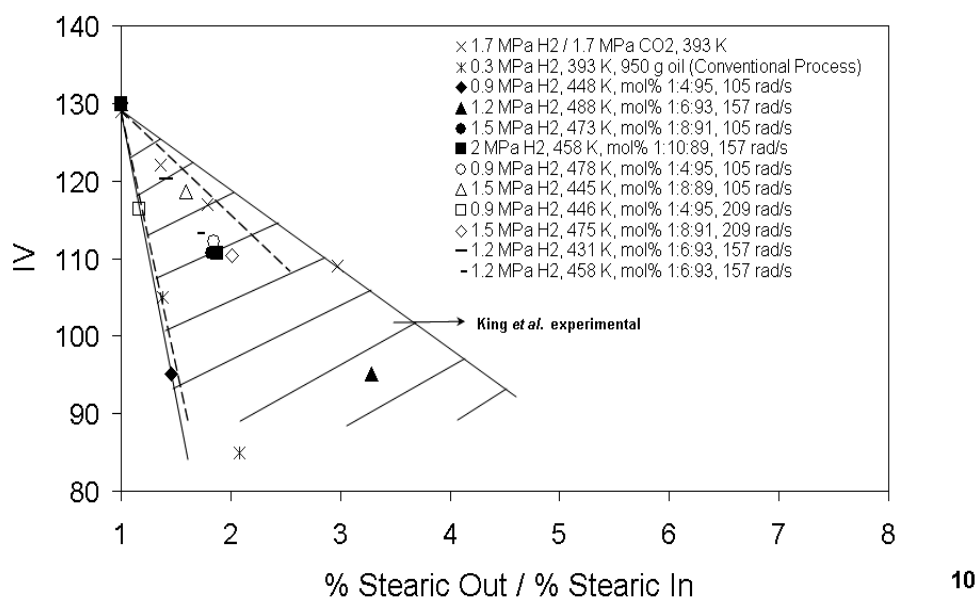


Figure 3-7: Plot showing stearic ester *vs* reduction in iodine value in the continuous hydrogenation of sunflower oil over Pd, Initial IV = 130. Data by King *et al.* (2001) lie within dashed region.

It is seen that for the same degree of hydrogenation, the *trans* % obtained in the runs is quite lower than that obtained in the conventional process and that reported by King *et al.*, whereas the stearic ester content (expressed as the percentage of newly stearic formed, based on initial stearic feed) is slightly higher than that obtained in the conventional process, and quite similar to that published by King *et al.* (2001).

Table 3-6 shows the characteristics of the commercial raw materials used in margarines and shortenings, together with the experimental results of King *et al.* as well as the results obtained in the present work. It is worth mentioning the great potential of SC hydrogenation as compared with the conventional process, as it allows using a final product with the required plasticity as well as a low *trans* % value by properly choosing the reaction conditions.

Table 3-6: Partially hydrogenated vegetable oils vs. commercial margarine feed stocks (DP. 305.15-312.15 K). Data on Iodine Value, *trans* content and stearic production.

Process	IV	<i>trans</i> wt %	% C18:0 Out/% C18:0 In	Substrate
Conventional process	90-110	11 - 30	1.4 - 2.1	Soybean Oil
King <i>et al.</i> (2001)*	108-114	2.5 - 5	1.7 - 2.6	Soybean Oil
Present study (SC propane)	95-110	2 - 5	1 - 3.3	Sunflower Oil

* Experimental SC conditions: 393.15 K, 0.02 wt% Ni catalyst, 1.7 MPa H₂ + 1.7 MPa CO₂.

3.3.2 Kinetic Analysis of CSTR Data: Modeling and Results.

The experimental design approach presented allows also the calculation of the main kinetic parameters provided that kinetic expressions are assumed for the reactions of scheme proposed early by Albright (1967).

Mechanistic kinetic models for the hydrogenation-isomerization reaction network of the proposed scheme are available for vegetable triglycerides on either Raney-type or supported nickel. For supported Pd or Ni catalysts, studies are more recent (for example Santacesaria *et al.*, 1994; Fillion *et al.*, 2000). The important feature is that hydrogenation and isomerization take place on the same sites, since mono-unsaturated adsorption plays a key role in both reactions. From the concepts of Horiuti and Polanyi (1934) and Allen and Kiess (1956), it is accepted that hydrogenation occurs by reaction of adsorbed atomic hydrogen next to a fatty acid adsorbed on an adjacent site. The controlling mechanism is the surface reaction between adsorbed species (linoleic (L), oleic (O) or elaidic (E) fatty acids) and adsorbed hydrogen atoms, therefore reactions are

half order in the dissociating species. *Cis-trans* isomerization takes place through the hydrogenation to a saturated intermediate therefore that is also expected to be half order in H_2 .

In the kinetic hydrogenation modeling was assumed that adsorption and desorption steps at equilibrium as well as the catalyst surface was sparsely covered by adsorbed components and thus the concentration of unoccupied sites was essentially independent of the amount of the catalyst.

The above features have been put in terms of fluid phase concentrations for the case of cottonseed oil hydrogenation proposed by Hashimoto *et al.* (ibid) as follows:

$$r_L = -(k_{12} + k_{13})C_L\sqrt{C_{H_2}} \quad (3.33)$$

$$r_O = k_{12}C_L\sqrt{C_{H_2}} - k_{23}C_O\sqrt{C_{H_2}} + k_{32}C_E\sqrt{C_{H_2}} - k_{24}C_OC_{H_2} \quad (3.34)$$

$$r_E = k_{13}C_L\sqrt{C_{H_2}} + k_{23}C_O\sqrt{C_{H_2}} - k_{32}C_E\sqrt{C_{H_2}} - k_{34}C_OC_{H_2} \quad (3.35)$$

$$r_S = k_{24}C_OC_{H_2} + k_{34}C_EC_{H_2} \quad (3.36)$$

$$r_{H_2} = -3k_{12}C_L\sqrt{C_{H_2}} - 3k_{13}C_L\sqrt{C_{H_2}} - 3k_{24}C_OC_{H_2} - 3k_{34}C_EC_{H_2} \quad (3.37)$$

in which an order one-half with respect to hydrogen was considered for the reactions involving di- and mono-unsaturates and first order for the formation of saturates from oleic or elaidic fatty acids.

The last equation gives the total hydrogen uptake rate. Note that for low concentrations of mono-unsaturates (O and E) and large concentrations of linoleic fatty acid (L), the last two terms will be small; therefore the overall H_2 consumption rate will be half order in H_2 and proportional to C_L . The half-order is observed in Fig. 3-8., where log rate data as a function of log hydrogen partial pressure, is shown. The bottom line corresponds to 448.15 K. The slope of the regression line is 0.48, very near to the theoretical value 0.5. The upper line corresponds to a higher temperature (460.15 K) both for 262 rad/s, and 20 MPa. The slope for the upper line is 0.52. These results suggest an order 0.5 with respect to hydrogen concentration, so it lends some confidence on the kinetic formulation given above.

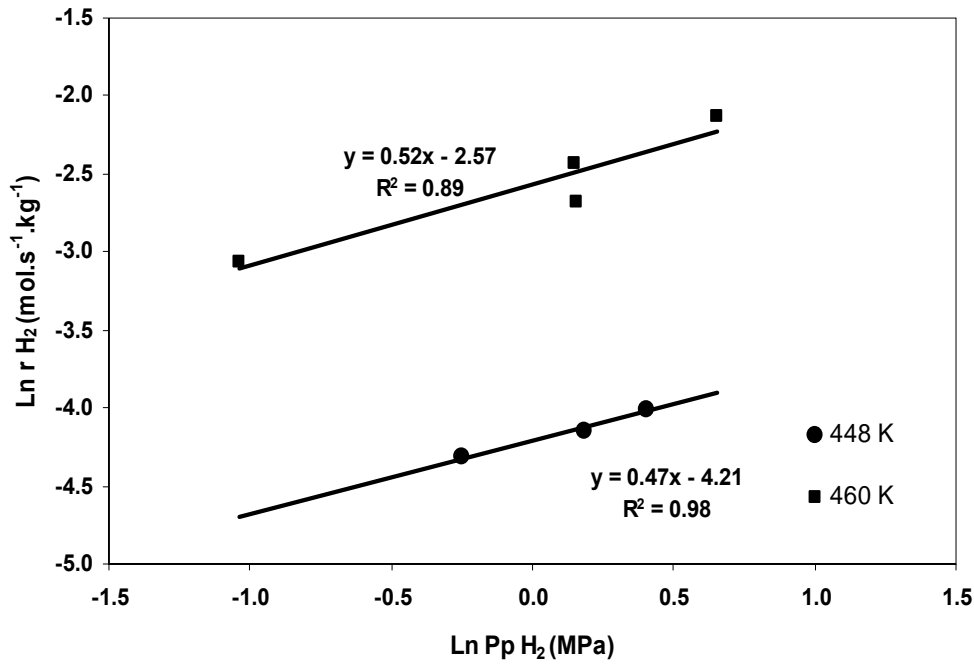


Figure 3-8: Linearised plot of hydrogen uptake rate: $\text{Ln } r_{\text{H}_2}$ vs $\text{Ln } p_{\text{H}_2}$, for 448.15 K and 460.15 K. Upper line slope is 0.52, bottom line slope = 0.48.

Given the above kinetic scheme it is possible to fit the kinetic constants for the multiple reaction system as follows. The steady state conservation equations for multiple reactions in a CSTR are described by the following system of equations:

$$F_{i0} - F_i + r_i W = 0 \quad i = 1 \text{ to } 5 \quad (3.38)$$

where W is the mass of catalyst in the CSTR and r_i is the global rate of formation for species i (L, O, E, S and H₂). Substitution of the rate expressions given before in the balance equations provides a system of equations in the concentrations and in terms of parameters k_{ij} . So, in principle there would be 6 parameters to fit for every temperature. But since reaction runs are made at different temperatures, allowance should be made for variable temperature from one run to the other, from 431.15 K to 490.15 K.

The final expression results in a non-linear problem to fit the reactor outlet concentrations by guessing the six (k_{ij}) parameters. The system of equations for the CSTR was solved for the concentrations using the nonlinear Newton-Raphson method along with simultaneous optimization of the parameters using a nonlinear least squared method with restrictions in order to minimize a χ^2 -target function, defined as the deviation between experimental and model concentrations for $N_{q,d}$ experimental points of the N_q hydrogenation runs with $N_{q,l}$ components:

$$\chi^2 = \frac{1}{N_q} \sum_{q=1}^{N_q} \frac{1}{N_{q,i} N_{q,d}} \sum_{i=1}^{N_{q,i}} \sum_{d=1}^{N_{q,d}} \frac{(C_{q,i,d}^{\text{exp}} - C_{q,i,d}^{\text{mdl}})^2}{C_{q,i,d}^{\text{exp} 2}} \quad (3.39)$$

Here, $C_{q,i,d}^{\text{exp}}$ and $C_{q,i,d}^{\text{mdl}}$ are the experimentally observed and the calculated model concentration values for the q th experiment and the i th component and d th data point, respectively.

Table 3-7 summarizes the values of the optimized parameters with their χ^2 .

Table 3-7: Fitted parameters values for the kinetic model.

Parameter	T(K)				
	431.15	444.15	459.15	477.15	490.15
k_{12} [mol ^{-1/2} .(m ³) ^{3/2} .kg ⁻¹ .s ⁻¹]	7.73x10 ⁻⁵ ± 4.87x10 ⁻⁶	1.00x10 ⁻⁴ ± 5.92x10 ⁻⁸	1.30x10 ⁻⁴ ± 3.93x10 ⁻⁶	1.83x10 ⁻⁴ ± 1.22x10 ⁻⁵	2.76x10 ⁻⁴ ± 8.43x10 ⁻⁶
k_{13} [mol ^{-1/2} .(m ³) ^{3/2} .kg ⁻¹ .s ⁻¹]	2.84x10 ⁻⁶ ± 5.64x10 ⁻⁸	2.90x10 ⁻⁶ ± 3.53x10 ⁻⁸	2.99x10 ⁻⁶ ± 2.24x10 ⁻⁷	3.05x10 ⁻⁶ ± 3.15x10 ⁻⁷	3.15x10 ⁻⁶ ± 7.95x10 ⁻⁸
k_{24} [mol ⁻¹ .(m ³) ² .kg ⁻¹ .s ⁻¹]	2.78x10 ⁻⁶ ± 1.99x10 ⁻⁷	2.86x10 ⁻⁶ ± 1.23x10 ⁻⁷	3.54x10 ⁻⁶ ± 1.07x10 ⁻⁶	6.07x10 ⁻⁵ ± 2.54x10 ⁻⁶	2.38x10 ⁻⁴ ± 9.23x10 ⁻⁶
k_{34} [mol ⁻¹ .(m ³) ² .kg ⁻¹ .s ⁻¹]	3.14x10 ⁻⁶ ± 5.23x10 ⁻⁷	4.17x10 ⁻⁶ ± 2.94x10 ⁻⁷	7.09x10 ⁻⁶ ± 5.91x10 ⁻⁶	1.99x10 ⁻⁵ ± 4.97x10 ⁻⁶	2.63x10 ⁻⁵ ± 9.21x10 ⁻⁶
k_{23} [mol ^{-1/2} .(m ³) ^{3/2} .kg ⁻¹ .s ⁻¹]	1.44x10 ⁻⁴ ± 1.00x10 ⁻⁴	3.33x10 ⁻⁴ ± 1.15x10 ⁻⁵	4.36x10 ⁻⁴ ± 2.03x10 ⁻⁴	5.27x10 ⁻⁴ ± 5.23x10 ⁻⁵	8.05x10 ⁻⁴ ± 6.33x10 ⁻⁵
k_{32} [mol ^{-1/2} .(m ³) ^{3/2} .kg ⁻¹ .s ⁻¹]	7.59x10 ⁻⁴ ± 5.22x10 ⁻⁴	8.44x10 ⁻⁴ ± 4.39x10 ⁻⁴	1.41x10 ⁻³ ± 6.35x10 ⁻⁴	2.18x10 ⁻³ ± 2.82x10 ⁻⁴	2.62x10 ⁻³ ± 4.23x10 ⁻⁴
χ^2 [mol ² .m ⁻⁶]	2.103x10 ⁻⁵	7.839x10 ⁻⁵	4.227x10 ⁻⁵	2.276x10 ⁻⁵	1.988x10 ⁻⁴

Figure 3-9 depicts the predicted and experimental data for the fatty acid compositions using the optimized values of the kinetic constants.

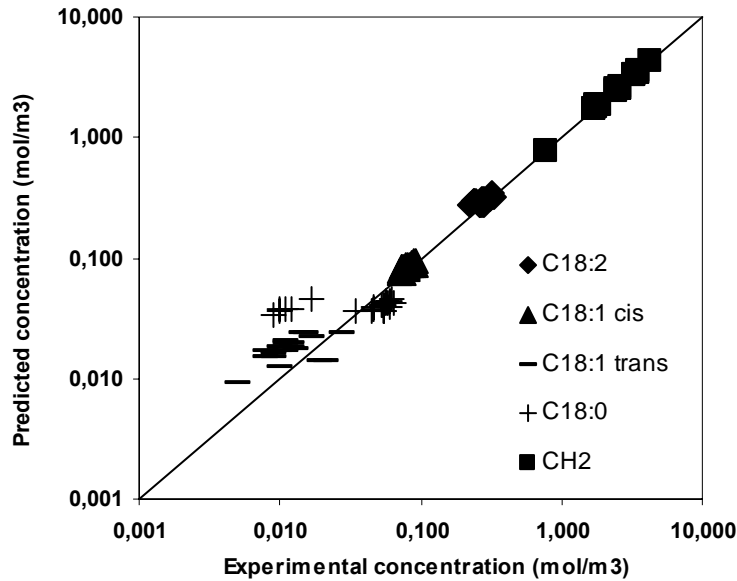


Figure 3-9: Parity plot of component concentrations in CSTR *vs* those predicted by kinetic model.

Despite the fact of the selection of the experiments for the kinetic studies should cover conversion ranges between 30 and 80% (González *et al.*, 1999), in the case of selective hydrogenation of vegetables oils for margarines production, the expected conversion is around 50%. In the present case study the maximum conversion reached was around 31%.

In the 25 runs performed, the accuracy is different depending on the species; for example, hydrogen uptake is very accurately fitted while stearic ester is less well predicted. The *trans*-content is also well predicted with the present kinetic model (see Fig. 3-9). It is seen that due to a little reduction in iodine values (inlet IV = 130, exit IV=90), the kinetic constants for stearic ester formation may have more error.

Based on the literature already cited there was reason to assume that k_{24} and k_{34} are equal. From the results of these calculations, this assumption seems to be invalid. Rase (1977) had difficulty in adjusting these values too. He suggested that the lack of fit with the model for the values of k_{24} and k_{34} would suggest the need for independent evidence to establish the true magnitudes of these constants. The model seems not very sensitive to these values as measured by overall performance such as iodine value and reaction time.

Estimated rate constant values confirm that *trans* isomer is more reactive than *cis* mono-unsaturated specie. The majority of the values of the equilibrium ratio of the mono-

unsaturated fatty acids ($K=k_{32}/k_{23}$) obtained from these calculations are in agreement with those reported by Albright (1962) and Gut (1979) for the hydrogenation of sunflower oil. These authors reported K values between 2 and 4. In the same way, the behaviour of K with the reaction temperature is as being expected in the case of an exothermic reaction.

The temperature dependence of the reaction rate constants was assumed to obey the Arrhenius equation as:

$$k_i(T) = A_i e^{-E_i/RT} \quad (3.40)$$

where A_i is the pre-exponential factor, E_i is the apparent activation energy, R is the gas constant and T is the absolute temperature. Table 3-8 presents E_i values obtained from a plot of $\ln k_i$ versus $1/T$.

Table 3-8: Kinetic parameters, according to equation (3.40), for the hydrogenation of sunflower oil over Pd/C as catalyst and propane as solvent.

Reaction	E_i (J/mol)	A_i [mol ^{-1/2} .(m ³) ^{3/2} .kg ⁻¹ .s ⁻¹]
12	35892.43	1.61
13	1472.15	4.25x10 ⁻⁰⁶
24	265761.48	7.08x10 ^{+24†}
34	148844.39	3.25x10 ^{+11†}
23	34962.05	3.84
32	69.72	1.48x10 ⁻³

†[mol⁻¹.(m³)².kg⁻¹.s⁻¹]

From the results presented above, it could be realized that poly-unsaturated specie (L) is hydrogenated substantially faster than the mono-unsaturated species (O or E) as suggest their apparent activation energy values.

A later discussion about the kinetic parameters obtained will be presented in the last section of this chapter along with the results obtained for the other kinetic case study (oil hydrogenation over Pd/Al₂O₃ using DME) and with those reported in the available literature.

3.4 Sunflower Oil Hydrogenation over Pd/Al₂O₃ using SC DME as Reaction Solvent.

In this case, SC oil hydrogenation was performance on eggshell Pd/Al₂O₃ in order to study the effect of a less adsorptive catalysts support on conversion and product distribution in combination with a “slightly” better reaction solvent: DME. A small set of high pressure experiments were carried out in order to build a kinetic hydrogenation model. The data treatment to determine the hydrogenation kinetic parameters was made in a similar way to the propane case using the reaction scheme proposed by Albright (1967).

3.4.1 Experimental Considerations.

Based on the preliminary experience with propane, the idea of performance another experimental design study was rejected because it would take a long time and would be too expensive because the DME is not a common solvent. On the other hand, Brake *et al.* (2002) and Weidner *et al.* (2004) have reported that the principal thermodynamic behaviour of DME in the triglycerides hydrogenation is similar to that in the propane system but DME is a slightly better solvent due to its larger region of complete system miscibility.

A set of preliminary runs under equal experimental conditions except the reaction solvent used (propane or DME) suggests that the rate of reaction is fairly higher (around 3%) in the case of DME which is in agreement with the results of Brake *et al.* (2002) and Weidner *et al.* (2004) mentioned above.

As in the former case study, all the experiments carried out in order to determine the SC continuous sunflower oil hydrogenation kinetic were performed in the experimental apparatus described in Chapter 5 as well as the analytical methods used to determine the reaction rate and the distribution of the hydrogenated products. Hydrogenation runs were done after the catalyst activity had become stable.

The hydrogenation reaction occurred over an industrial 0.5% Pd on alumina supported catalyst (Johnson Matthey). Eggshell spheres of 2 mm nominal size were used to reduce internal mass-transfer limitations. The amount of catalyst was varied between 0.4 and 1 g in order to obtain a conversion degree similar to that of the propane case and to introduce the mixture-weight-hourly-space-velocity (WHSV) as experimental variable instead of LHSV. The WHSV is defined by the mass of reactant mixture processed per

hour per gram of catalyst. This can be assumed as a space velocity, which might at first sight be regarded as the reciprocal of the apparent residence time. The WHSV variation made by varying the amount of catalyst instead of the mass of reactant mixture was due to the expansion valve, which did not allow setting low solvent volumetric flows.

From the phase behaviour study developed in the previous chapter, the inlet reaction mixture composition for this case was chosen as follows: 1 mol% of sunflower oil, 4-14 mol % of H₂ and 85-95 mol% of DME as well as the operating pressures and temperatures which ensure single-phase reaction conditions. The critical pressure and temperature for the chosen molar compositions was 8 MPa and 420.15 K respectively. These values were estimated using the Chueh-Prausnitz (Reid *et al.*, 1987) approximation. Therefore, the operating total pressure was selected equal to 20 MPa in order to eliminate its possible effect on the hydrogenated product composition as mentioned by Hitzler *et al.* (1998).

The stirrer speed was 131 rad/s for all experimental runs because after this threshold value, the kinetic becomes independent of agitation.

The experimental ranges for the experimental variables, temperature, H₂ mol% and WHSV were as follows:

Temperature: 456.15-513.15 K

H₂ mol%: 4-9

WHSV: 200-600 h⁻¹

Catalyst weight: 0.4 to 1 g

They were varied according to a sequential design, where the experiments were chosen each one of them depending on the obtained results from the previous one. This type of design is especially appropriate for building kinetic studies because it reduces the number of experiments to performance. A summary of experimental operating conditions carried out is presented in Table 3-9.

Table 3-9: Operating experimental conditions used in the sunflower oil hydrogenation over Pd/Al₂O₃ with DME as reaction solvent.

RUN	Reaction Temperature (K)	H ₂ mol %	WHSV (h ⁻¹)	Catalyst Weight (g)
1	483.15	4	567.2	0.4
2	456.15	4	567.2	0.4
3	483.15	4	283.6	0.9
4	456.15	4	283.6	0.9
5	483.15	4	203.0	0.9
6	483.15	8	203.3	1
7	483.15	9	203.5	1
8	456.15	4	204.5	1
9	456.15	7	204.7	1
10	456.15	9	204.9	1
11	513.15	4	203.1	1
12	513.15	7	203.3	1
13	513.15	9	203.5	1
14	513.15	4	283.8	1
15	513.15	7	284.2	1

3.4.2 Kinetic Analysis of CSTR Data: Results and Modeling.

The results from the fifteen experimental runs are presented in Table 3-10.

Table 3-10: Effect of reaction conditions on sunflower oil hydrogenation. Oil concentration: 1 mol%; P=20 MPa; catalyst: 0.5% Pd/Al₂O₃; solvent: DME.

RUN	IV	<i>trans</i> wt %	C18:0 wt%
1	116.7	0.4	7.4
2	128.7	0.3	7.4
3	108.7	2.4	7.9
4	117.9	0.9	7.5
5	104.6	4.7	9.8
6	102.8	4.0	9.1
7	100.2	3.8	10.9
8	112.9	2.4	9.4
9	111.7	2.3	9.3
10	110.4	2.0	9.1
11	101.5	6.1	15.2
12	99.0	5.8	15.5
13	94.0	5.0	19.3
14	109.7	5.7	15.7
15	104.7	5.2	17.8

Based on the collected experimental data, it could be realized that a rise in temperature and/or apparent rise time increases the reaction rate and, consequently, lowers the IV (see Figure 3-10).

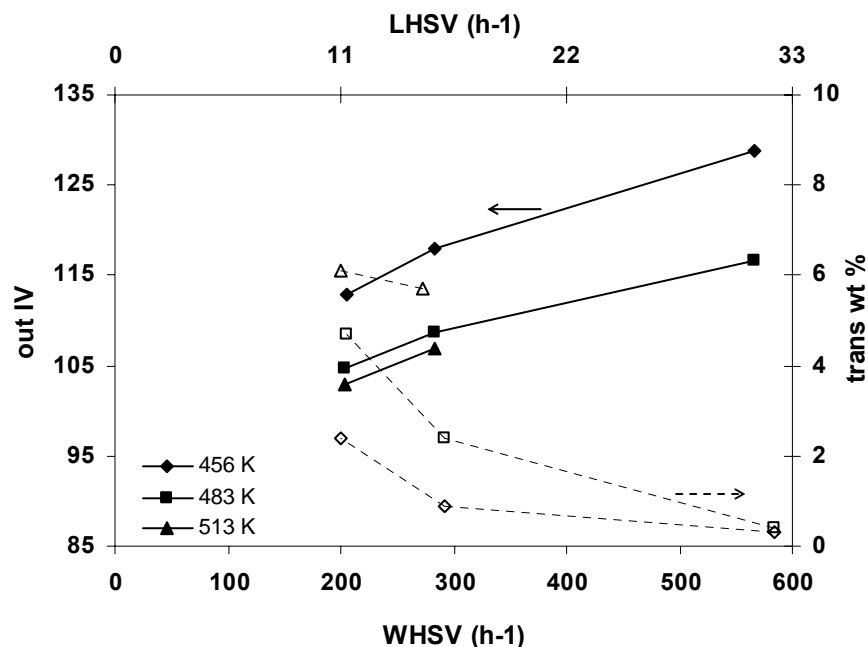


Figure 3-10: Iodine value (IV) and *trans* content as a function of temperature and space velocity at 4% H₂ mol content. Solid line= IV, dashed line= *trans* content.

The effect of H₂ content is depending on the temperature. At high temperature, an increase in H₂ content increases the reaction rate, but this effect decreases with decreasing temperature. This behaviour can be explained with the changing activity of the catalyst at different temperatures: At high temperature the catalyst activity is high, thus, if more hydrogen is added, this results in higher reaction rate. At low temperature the catalyst activity is lower: the catalyst is saturated with hydrogen already at low H₂ contents and cannot convert additional hydrogen (Macher *et al.*, 1999 and Van den Hark *et al.*, 2001). Therefore, an increase in H₂ content has a low effect at low temperature as shows the Figure 3-11.

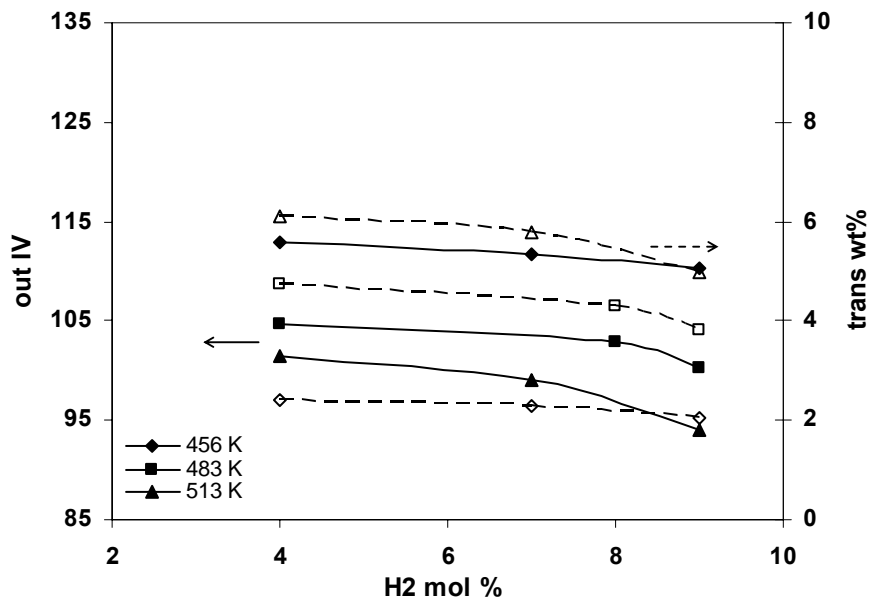


Figure 3-11: Iodine value (IV) and *trans* content as a function of temperature and H₂ mol content at WHSV= 200 h⁻¹. Solid line= IV, dashed line= *trans* content.

The *trans* content increased, when the temperature and/or the residence time was increased as could be observed in Figure 3-10. At high apparent residence time, the *trans* content decreases with increasing H₂ content at any temperature (see Figure 3-11). The trends in Fig. 3-10 and 3-11 indicate that the *trans* formation can be further reduced, if the temperature, as well as the residence time, are decreased. Since the effect of hydrogen pressure was not significant at low temperatures, this indicates that a low *trans* contents can perhaps even be obtained at low hydrogen pressures.

For the same degree of hydrogenation (IV=95-110), the *trans* content obtained in the experimental runs is similar than that obtained in the former case study (Pd/C in combination with propane) whereas the stearic content (expressed as % newly formed stearic based on initial stearic in feed) is slightly lower (<2.7) as well as the overall hydrogenation rate.

These facts are possibly derived from the catalyst type employed in each case. In the former, the catalyst is supported on activated carbon, which adsorbs the reactants very strongly producing spillover of the species from the metal to the support and *vice-versa*. On the other hand, activated carbon has a pore size distribution consisting of micropores ($d_{\text{pore}} < 3$ nm). This combination added to the fact that the metal location is uniform, lead to a decrease of the linoleic selectivity (S_i) because of the presence of pore

diffusional resistance which increases saturated compounds production as suggested by Coenen (1976).

In the latter case, the catalyst support was Al_2O_3 and the metal location is eggshell type. This kind of support is less adsorptive than activated carbon and its pore size distribution is mainly mesopores ($3 \text{ nm} < d_{\text{pore}} < 5 \text{ nm}$). This fact along with the eggshell distribution, which minimizes pore diffusion resistance, common in the processing of large organic molecules, makes the employed catalyst more selective.

A catalyst with a uniform metal location is more active at high pressures than an eggshell catalyst as shows Figure 3-12. This is the possible explanation to the less hydrogenation rate obtained in the case of eggshell catalyst.

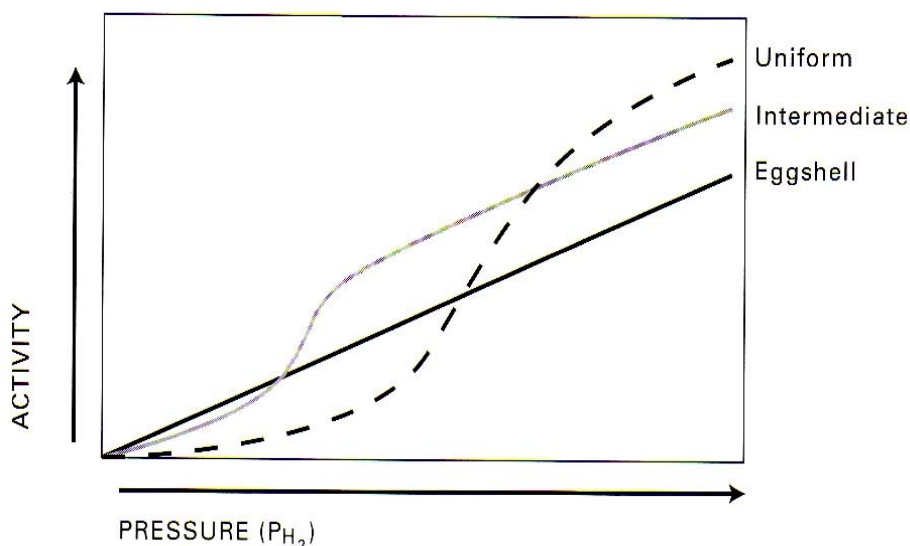


Figure 3-12 Effect of hydrogen pressure on the hydrogenation activity of the catalyst.

The kinetics for sunflower oil hydrogenation using a commercial $\text{Pd}/\text{Al}_2\text{O}_3$ catalyst and DME as reaction solvent, were investigated using the same approach than that in the former case study.

First at all, the reaction order was checked with respect to overall hydrogen consumption rate by means of plotting $\log(\text{rate data})$ as a function of $\log(\text{hydrogen partial pressure})$. The slope of the regression line is 0.42 as shows Figure 3-13. The obtained value is close to the expected value, 0.5.

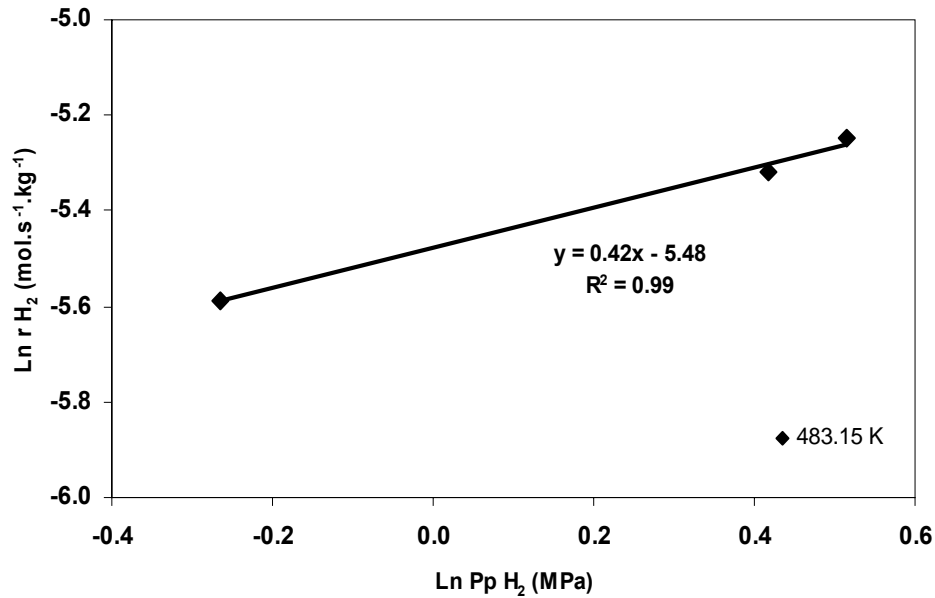


Figure 3-13: Linearised plot of hydrogen uptake rate: $\ln r_{H_2}$ vs $\ln p_{H_2}$, for 483.15 K.

The kinetic expressions are assumed for the reaction scheme proposed by Albright (1967) using the same assumptions. The obtained results for the kinetic parameters are presented in Table 3-11.

Table 3-11: Fitted kinetic parameters values for Pd/Al₂O₃ – DME reaction system.

Parameter	T(K)		
	456.15	483.15	513.15
k_{12} [mol ^{-1/2} .(m ³) ^{3/2} .kg ⁻¹ .s ⁻¹]	4.09x10 ⁻⁶ ± 5.29x10 ⁻⁷	4.54x10 ⁻⁶ ± 1.77x10 ⁻⁶	9.76x10 ⁻⁶ ± 8.78x10 ⁻⁷
k_{13} [mol ^{-1/2} .(m ³) ^{3/2} .kg ⁻¹ .s ⁻¹]	3.32x10 ⁻⁶ ± 8.38x10 ⁻⁷	5.69x10 ⁻⁶ ± 3.56x10 ⁻⁶	2.21x10 ⁻⁵ ± 3.89x10 ⁻⁶
k_{24} [mol ⁻¹ .(m ³) ² .kg ⁻¹ .s ⁻¹]	1.10x10 ⁻⁵ ± 1.94x10 ⁻⁶	1.85x10 ⁻⁵ ± 2.15x10 ⁻⁶	2.05x10 ⁻⁵ ± 2.08x10 ⁻⁶
k_{34} [mol ⁻¹ .(m ³) ² .kg ⁻¹ .s ⁻¹]	2.78x10 ⁻⁶ ± 5.12x10 ⁻⁷	2.48x10 ⁻⁵ ± 2.94x10 ⁻⁶	8.99x10 ⁻⁵ ± 4.21x10 ⁻⁵
k_{23} [mol ^{-1/2} .(m ³) ^{3/2} .kg ⁻¹ .s ⁻¹]	4.03x10 ⁻⁶ ± 9.40x10 ⁻⁷	6.94x10 ⁻⁵ ± 2.40x10 ⁻⁵	2.39x10 ⁻⁴ ± 4.78x10 ⁻⁵
k_{32} [mol ^{-1/2} .(m ³) ^{3/2} .kg ⁻¹ .s ⁻¹]	5.69x10 ⁻⁶ ± 1.83x10 ⁻⁶	3.43x10 ⁻⁴ ± 1.25x10 ⁻⁴	8.79x10 ⁻⁴ ± 2.37x10 ⁻⁵
χ^2 [mol ² .m ⁻⁶]	8.233x10 ⁻⁵	1.913x10 ⁻⁴	2.594x10 ⁻⁴

Figure 3-14 shows a comparison between experimental and predicted data for the fatty acid compositions.

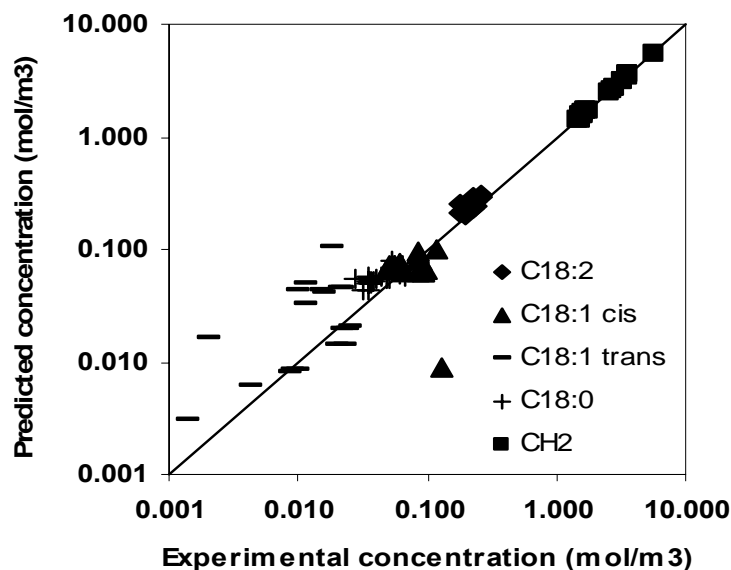


Figure 3-14 Parity plot of component concentrations in CSTR *vs* those predicted by kinetic model.

As can be observed in this figure, the accuracy data for the *trans* content is not completely good whereas the other components are well predicted with the kinetic model. The explanation to these deviations (which are mainly at 483.15 K) could come from the lack of analytical precision.

As in the former case, the model seems not very sensitive to k_{11} and k_{12} . These values are not equal which would suggest that *cis* and *trans* mono-unsaturated species are not equally hydrogenated to the stearate. The obtained K values agree with those early mentioned.

Obeying the Arrhenius law, Table 3-12 shows the apparent activation energies E_i obtained from a plot of $\ln k_i$ *versus* $1/T$.

Table 3-12: Kinetic parameters, according to equation (3.40), for hydrogenation of sunflower oil using Pd/Al₂O₃ as catalyst and DME as solvent.

Reaction	E_i (J/mol)	A_i [mol ^{-1/2} .(m ³) ^{3/2} .kg ⁻¹ .s ⁻¹]
12	19283.59	5.56x10 ⁻⁴
13	64069.94	67.96
24	19025.84	1.71x10 ^{-3†}
34	106382.75	5.64x10 ^{+6†}
23	152444.52	8.97x10 ⁺¹¹
32	194615.16	1.09x10 ⁺¹⁷

†[mol⁻¹.(m³)².kg⁻¹.s⁻¹]

In this case, the double bond isomerization is found to be the slowest reaction whereas the hydrogenation of poly-unsaturated to *cis*-mono-unsaturated species is the fastest along with its consecutive hydrogenation to stearate.

3.5 Final Discussion.

Table 3-13 presents the activation energies reported for several researchers for the oil hydrogenation.

Table 3-13: Activation energies reported in the available literature.

General Kinetic Schemes									
$T \xrightarrow{1} B \xrightarrow{2} \begin{matrix} \text{---} \\ \text{---} \\ \text{---} \end{matrix} \xrightarrow{3} S$									
Author	Oil type	Catalyst	E _i (J/mol)						
			1	2	3	12	13	24	34
Bern <i>et al.</i> (1975)	Rapeseed	Ni	61488	65010	75070				
Snyder <i>et al.</i> (1978)	Soybean	Ni	31549	36481					
Gut <i>et al.</i> (1979)	Sunflower	Ni/ Spherosil			9033	15941	21799		
Chen <i>et al.</i> (1981)	Soybean	Ni	44164	78454	30837				
Santacesaria <i>et al.</i> (1994)	Rapeseed	Pd/Silica- Al ₂ O ₃	12700	12500	14700				
Jonker <i>et al.</i> (1998)	FAMES	Supported Ni						32200	28100
Fillion <i>et al.</i> (2001)	Soybean	Ni/Al ₂ O ₃	70156		45627	68180	65258		
Gonzalez <i>et al.</i> (1998)	Sunflower	Ni/Silica				122000	102000		
						60000	50000		
This work, Case 1	Sunflower	Pd/C				35892	1472	265761	148844
This work Case 2	Sunflower	Pd/Al ₂ O ₃				19284	64070	19026	106383

As can be seen in Table 3-13, the apparent activation energies for the hydrogenation of the di-unsaturated species are lower than those reported by Bern *et al.*(1975), Chen *et al.* (1981), Fillion *et al.* (2001) and Gonzalez *et al.* (1998) but are comparable with those reported by Snyder *et al.* (1978) and Gut *et al.* (1979) for nickel catalysts. However, these values are quite higher than those reported by Santacesaria *et al.* (1994) with a Pd catalyst. The possible explanation of these low values could be the nature of the palladium catalyst along with the presence of internal mass-transfer limitations as suggested Veldinsk *et al.* (1997).

The activation energies obtained for the hydrogenation of mono-unsaturated species are the highest reported. This behaviour could be interpreted, assuming that in the case of poly-unsaturated compounds, conjugated double bonds are formed before hydrogenation, resulting in a very different reactivity compared to mono-unsaturated compounds as mentioned Santacesaria *et al.* (1994).

3.6 Conclusions.

Single-phase, continuous hydrogenations of sunflower oil on supported Pd catalysts were carried out in an internal recycle, well-mixed, packed-bed microreactor (50 cm³) using propane or DME as supercritical-fluid solvent. Because of the gradientless nature of this type reactor, reaction kinetics were studied as well as the effect of operating variables on sunflower hydrogenation process to assess both the reduction in iodine value and the formation of *trans* C18:1 isomer, parameters that are necessary for further industrial food application.

Operating conditions were chosen well above the two-phase region to avoid condensation so that a single fluid phase was present. For the time-on stream values used here catalyst deactivation effects were not observed. The experimental runs were carried out according to a four-variable, two-level, central composite design or using a sequential experimental design.

A wide range of hydrogenation products were obtained with certain plastic characteristics for further food application by tuning the reaction conditions. The experimental results show that one principal advantage of using a supercritical fluid as reaction solvent is the low *trans* acid content, as well as low stearic acid, compared with that reported for conventional process.

A formal kinetic analysis of the reactor rate data allowed to determinate the kinetic constants at several operating temperatures for the multiple reactions of

hydrogenation–isomerization network proposed by Albright (1967). The apparent activation energies were obtained for both cases under study (2% Pd/C with propane as solvent and 0.5% Pd/Al₂O₃ in combination with DME) and compared to those reported in the available literature. The activation energies values for the hydrogenation of the di-unsaturates were lower than those reported for nickel catalyst. The possible explanation of these low values could be the nature of the palladium catalyst along with the presence of internal mass-transfer limitations. For mono-unsaturated species, the activation energies were the highest reported.

3.7 Nomenclature.

A	pre-exponential factor [(m ^{4.5})/(mol ^{0.5} kg s)] or [(m ⁶)/(mol kg s)]
C _i	molar concentration of fatty ester i [mol/m ³]
$C_{q,i,d}^{\text{exp}}$	experimental observed concentration of the specie i [mol/m ³]
$C_{q,i,d}^{\text{mdl}}$	calculated model concentration of specie I [mol/m ³]
F _i	molar flow of species i [mol/ s]
E	apparent activation energy [J/mol]
k _A , k _B ...	rate constants for adsorption of components A, B, etc. (See Eqs. 3.9-3.16)
k _{-A} , k _{-B} ..	rate constants for desorption of components A, B, etc. (See Eqs. 3.9-3.16)
k ₀ , k ₁ ..	forward-reaction rate constants (See Eqs. 3.9-3.16)
k ₋₀ , k ₋₃ ..	reverse-reaction rate constants (See Eqs. 3.9-3.16)
k _{ij}	kinetic rate constant [(m ^{4.5})/(mol ^{0.5} kg s)] or [(m ⁶)/(mol kg s)]
k'ij	pseudo first order rate constants, see Eqs. 3.3-3.8
K	adsorption equilibrium constant, see Eqs. 3.25-3.29
K	equilibrium ratio of the monounsaturated fatty acids, K=k ₃₂ /k ₂₃
LHSV	liquid oil feed [cm ³ /h] divided by catalyst volume [cm ³], [1/h]
IV	iodine value [g I ₂ /100 g oil]: 1 IV =36 mol H ₂ /m ³ oil

N_q	number of hydrogenation runs
$N_{q,d}$	number of experimental points
$N_{q,i}$	number of components
p	probability of making a Type 1 error (that is, rejecting the null hypothesis when it is true)
P	pressure [MPa]
P_c	critical pressure [MPa]
R	gas-law constant [8.314 J/(mol K)]
r_i	global reaction rate of species i per mass of catalyst [mol/s kg]
s	estimated standard deviation [IV or <i>trans</i> wt % units]
S_i	Specific Isomerization, gives the number of <i>trans</i> double bonds formed for double bond hydrogenated
S_l	linoleic selectivity, see Eq. 3.1
S_{ll}	linolenic selectivity, see Eq. 3.2
SR	selectivity ratio defined as the ratio of the reaction rate constant for linoleic to oleic, divided by the reaction rate constant for oleic to stearic
T	temperature [K]
T_c	critical temperature [K]
W	mass of catalyst [kg]
x_i	significant predictor reaction variables, see Table 3.2
y	predicted responses in Eq. 3.30 [IV or <i>trans</i> wt % units]

Greek letters

B	regression coefficients in Eq. 30
-----	-----------------------------------

ε	error term in Eq. 30
σ	unoccupied active center on catalyst surface
χ^2	Chi-squared optimization function, see Eq. 3.39

Acronyms

A	hydrogen
B	diunsaturated fatty acid
CO ₂	dioxide carbon
C ₃ H ₈	propane
CP	center point
CSTR	continuous stirred-tank reactor
DME	dimethyl ether
E	elaidic fatty acid, <i>trans</i> C18:1
FAME	fatty acid methyl ester
H ₂	hydrogen
H ₂ %	hydrogen molar composition
i	component, i=L, O, E, S, H ₂
IV	iodine value
L	linoleic fatty acid, C18:2
LHSV	liquid oil hourly space velocity
O	oleic fatty acid, <i>cis</i> C18:1
R ₁	<i>cis</i> monounsaturated fatty acid
R ₂	<i>trans</i> monounsaturated fatty acid

S stearic fatty acid, C18:0

SC supercritical

SP star point

Sub- and Superscripts

c critical

d data point

exp experimental

i component

mdl predicted

q experiment

0 entering

Chapter Four

Intraparticle Diffusion in Porous Catalyst Particles used in Supercritical Sunflower Oil Hydrogenation.

4.1 Introduction.

It was assumed that each site of the entire catalyst surface was accessible to the same reactant concentration in surface reactions. However, where the reactants diffuse into the pores of the catalyst pellet, the concentration at the pore mouth will be higher than that inside the pore, and it can be seen that the entire catalytic surface is not accessible to the same concentration. To account for variations in concentration throughout the pellet, a parameter known as the effectiveness factor is introduced.

The pores in the pellet are not straight and cylindrical; they consist of a network of tortuous, interconnecting paths of varying cross sectional-areas. It would not be feasible to describe the diffusion within each and every one of the tortuous pathways individually; consequently, it shall define an effective diffusion coefficient so as to describe the average diffusion taking place at any position r in the pellet. It shall consider only radial variations in the concentration; the radial flux W_{ir} will be based on the total area (voids and solid) normal to diffusion direction rather than void area alone. These basis for W_{ir} are made possible by proper definition of the effective diffusivity D_e .

The effective diffusivity is taken into account since:

- 1 Not all of the area normal to the direction of the flux is available (i.e., void) for the molecules to diffuse.
- 2 The paths are tortuous.
- 3 The pores are of varying cross-sectional area.

An equation that relates D_e to either the bulk or the Knudsen diffusivity is

$$D_e = \frac{D\varepsilon_p}{\tau} \quad (4.1)$$

where D is the global molecular diffusivity, ε_p is the pellet porosity and τ is the tortuosity factor. τ is defined as the ratio of the distance through which the species have to diffuse in the porous media to the linear distance between the two points. Equation

4.1 is valid when the diffusion in pores occurs by molecular diffusion and when the diameter of the diffusing molecule is sufficiently small compared to the average pore diameter so the Knudsen diffusion is negligible.

In the absence of experimental data, it is necessary to estimate D_e from the physical properties of the catalyst. In this case the first step is to evaluate the diffusivity for a single cylindrical pore. Then a geometric model of the pore system is used to convert D to D_e for the porous pellet. A model is necessary because the geometry of the void spaces is quite complex. The optimum model is a realistic presentation of the geometry of the voids (with tractable mathematics) that can be described in terms of easily measurable physical properties of the catalyst pellet. These properties are the surface area and pore volume per gram, the density of the solid phase, and the distribution of void volume according to the pore size.

The random-pore model was originally developed for pellets containing a bidisperse pore system. It is supposed that the pellet consists of an assembly of small particles. When the particles themselves contain pores (micropores), there exists both a macro and a micro void-volume distribution. The voids are not imagined as capillaries, but more as an assembly of short void regions surrounding and between individual particles, as indicated in Figure 4-1.

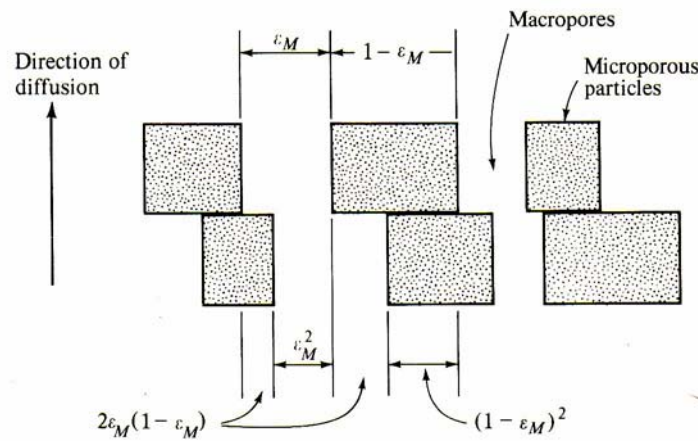


Figure 4-1: Random-pore model.

The nature of the interconnection of macro and micro voids regions is the essence of the model. Transport in the pellet is assumed to occur by a combination of diffusion through the macro regions (of voids fraction ϵ_M), the micro regions (of void fraction ϵ_μ), and a series of contributions involving both regions. It is supposed that both micro and macro regions can be represented as straight, short cylindrical pores of average radii \bar{a}_M

and \bar{a}_μ . The magnitude of individual contributions is dependent on their effective cross-sectional areas (perpendicular to the direction of diffusion): The details of the development are given elsewhere (Wakao and Smith, 1962 and 1964) but in general these areas are evaluated from the probability of pore interconnections. The resultant expression for D_e may be written as follows:

$$D_e = \bar{D}_M \varepsilon_M^2 + \frac{\varepsilon_\mu^2 (1 + 3\varepsilon_M)}{1 - \varepsilon_M} \bar{D}_\mu \quad (4.2)$$

where \bar{D}_M and \bar{D}_μ for macro and micro regions in terms of the bulk diffusivity D_{AB} and Knudsen diffusivity D_K are:

$$\frac{1}{\bar{D}_M} = \frac{1}{D_{AB}} + \frac{1}{(\bar{D}_K)_M} \quad (4.3)$$

$$\frac{1}{\bar{D}_\mu} = \frac{1}{D_{AB}} + \frac{1}{(\bar{D}_K)_\mu} \quad (4.4)$$

Note that neither the tortuosity factor nor other fitting parameter is involved in this model. The actual path length is equal to the distance coordinate in the direction of diffusion. To apply equation 4.2 requires void fractions and mean pore radii for both macro and micro regions. The mean pore radii can be calculated for the micro region from porosimetry data.

The random-pore model can also be applied to monodisperse systems. For a pellet containing only macropores, $\varepsilon_\mu=0$. Consequently, equation 4.2 becomes:

$$D_e = \bar{D}_M \varepsilon_M^2 \quad (4.5)$$

Similarly, for a material as silica gel, where $\varepsilon_M=0$, the effective diffusivity is:

$$D_e = \bar{D}_\mu \varepsilon_\mu^2 \quad (4.6)$$

Comparison of these last two equations with equation 4.1 indicates that $\tau=1/\varepsilon$. The significance of this model is that the effective diffusivity is proportional to the square of the porosity. From experimental data for various catalysts, it has been found that τ varies from less than unity to more than 6.

Tortuosity factors less than unity can occur when the surface diffusion is significant. Satterfield (1970) has summarized data for catalysts from the literature and recommended the use of $\tau=4$ when surface diffusion is insignificant. Only a few authors have measured τ directly in high-pressure, high-density non-reactive systems (Lai and Tan, 1993; Stüber *et al.*, 1997 and Abaroudi *et al.*, 1999). On the other hand, this has been

measured for many catalysts under low-pressure and medium-pressure conditions as summarized in Table 4-1.

Table 4-1: Tortuosity factors for diffusion in catalysts at 6.5 MPa (Butt,1999).

Catalyst	Internal Porosity	Tortuosity Factor τ
Harshaw MeOH synthesis catalyst (pre-reduced)	0.49	6.9
Haldor-Topsoe MeOH synthesis catalyst (pre-reduced)	0.43	3.3
BASF MeOH synthesis catalyst (pre-reduced)	0.50	7.5
Girdler G-52 cat., 33% Ni on refractory oxide support	0.44	4.5
Girdler G-58 catalyst Pd/Al ₂ O ₃ (0.6 MPa)	0.39	2.8

The role of Knudsen diffusion D_K in dense media seems to be negligible (Lai and Tan, 1993). However, since molecules are closer to each other in a dense medium (liquid or compressed gas), diffusivities are difficult to predict (Smith, 1981). Direct measurements of D_e values in dense gas have been obtained in situations where the intra-particle rate was controlling. In such cases, the tortuosity factors obtained are very small indeed, as reported by some of the values in Table 4-1. Knaff and Schlünder (1987) were the first to note an abnormally low ratio of D/D_e (~ 1.5) that was also variable with temperature.

Tortuosity factors less than unity have been often been reported for three-phase catalytic reactors where a reactant gas diffuses in a liquid- (or dense) medium. Many examples are available. A discussion of the possible causes of the abnormal tortuosity factors is given by Stüber *et al.* (1997). These are related to the possible existence of co-operative surface diffusion with bulk pore fluid diffusion.

When sorption of the diffusing species occurs, two additional complications may arise. First, the sorbed phase can have an accumulation of solute sufficiently large that it must be included in the mass balance equations. Second, the sorbed phase could be mobile, which would be added to the diffusion flux. The former case has been extensively considered in a series of papers by Weisz *et al.* (1967, 1968, and 1973). The mass transfer equation becomes:

$$\varepsilon_p \frac{\partial C_A}{\partial t} + \rho_p \frac{\partial C_{Al}}{\partial t} = \frac{\partial}{\partial z} D_e \frac{\partial C_A}{\partial z} \quad (4.7)$$

where $C_{Al} = C_{Al}(C_A)$ through the adsorption process. If instantaneous adsorption equilibrium is assumed, the functional form is found from the isotherm, and (for constant D_e)

$$\frac{\partial C_A}{\partial t} = D_a \left(\frac{\partial^2 C_A}{\partial z^2} \right) \quad (4.8)$$

where D_a is a modified diffusivity that does not have the same value as the steady-state value D_e even the usual diffusion results can be used with this equation. This D_a is defined as:

$$D_a = \left(\frac{D_e}{\varepsilon_p + \rho_p \frac{dC_{Al}}{dC_A}} \right) \quad (4.9)$$

The second situation of "surface diffusion" is less well understood. It is usually represented by a Fickian-type flux expression, using the adsorbed concentration as the driving force:

$$N_s = -D_s \rho_p \frac{dC_{Al}}{dz} \quad (4.10)$$

If instantaneous adsorption equilibrium is again assumed, the total flux is:

$$N_A = -(D_L + D_s \rho_p \frac{dC_{Al}}{dC_A}) \left(\frac{dC_A}{dz} \right) \quad (4.11)$$

where D_L is the effective pore-volume diffusivity and D_s is the effective surface diffusivity.

Thus, except for a simple linear isotherm, $C_{Al} = (C_t K_A) C_A$, the diffusivity is concentration dependent. The mass balance now becomes:

$$\frac{\partial C_A}{\partial t} = \frac{1}{\varepsilon_p + (\rho_p \frac{dC_{Al}}{dC_A})} \frac{\partial}{\partial z} \left(D_L + D_s \rho_p \frac{dC_{Al}}{dC_A} \right) \left(\frac{\partial C_A}{\partial z} \right) \quad (4.12)$$

which, for a linear isotherm, reduces to:

$$\frac{\partial C_A}{\partial t} = \left(\frac{D_L + D_s \rho_p C_t K_A}{\varepsilon_p + \rho_p C_t K_A} \right) \left(\frac{\partial^2 C_A}{\partial z^2} \right) \quad (4.13)$$

From this equation, the overall effective diffusivity D_e can then be viewed as a result of combination of two effects: (a) a pore volume diffusion with an effective coefficient defined by Equation 4.1, and (b) a surface diffusion contribution. When the adsorption follows a linear isotherm, the effective diffusivity can be expressed as:

$$D_e = \frac{D\varepsilon_p}{\tau} + \frac{\rho_p K_A D_s}{\tau} \quad (4.14)$$

where K_A is the adsorption equilibrium constant on the solid from the high-pressure fluid and D_s is the common surface diffusion coefficient. Since these quantities are seldom available, an average or apparent tortuosity factor is employed (see the values in Table 4-2) indicating that a change in temperature may largely affect K_A , which may lower the effective diffusivity with increasing temperature, thus showing a reverse-temperature effect.

Table 4-2: Tortuosity factors for high-pressure extraction of porous solids (Stüber *et al.*, 1997).

Authors	Operating Conditions	Solid Matrix	Tortuosity Factor τ
Knaff and Schlünder (1987)	308.15-328.15 K 12-22.6 MPa	Bronze, $\varepsilon_p=0.3$ Pore size 8- 20x10 ⁻⁶ m	τ indep. of d_p and P $\tau=0.4$ to 0.54
Recasens <i>et al.</i> (1989)	Desorption EtAc 300.15-338.15 K, $P<13$ MPa [†]	Regeneration of activated carbon	Linear driving force model $\tau=4$
Madras <i>et al.</i> (1994)	Naphthalene adsorption, 298.15-318.15 K 8-31 MPa	Micro- and macroporous alumina	τ const. w/ P and T $\tau=3.29$ (av)
Lai and Tan (1993)	Toluene adsorption	Micro- and macroporous activated carbon $\varepsilon_p=0.45$	τ depends on pressure $\tau\sim 0.2$ to 0.6
Stüber <i>et al.</i> (1997)	DiCl-benzene extraction	Bronze, macropores $\varepsilon_p=0.20$ to 0.25 pore size $\sim 15\times 10^{-6}$ m	τ const. w/ P but varies w/ T $\tau\sim 0.22$ to 0.62

Some discussions of the theoretical bases were presented by Ya and Sladek *et al.* (1974) for gases and by Dedrick and Beckman (1967) and Koriyama and Smith (1974) for liquids. Values of D_s have been collected by Schneider and Smith (1968) and Sladeck *et al.* (1974). For hydrocarbon gases in the usual catalyst substrate materials, values in the range $10^{-9} - 10^{-7}$ m²/s are observed. The contribution to the mass flux is more important for microporous solids, and it can be appreciable under some conditions, especially in liquids.

Another phenomenon observed is the restricted diffusion. This occurs when the dimensions of the solute molecule and the pore are comparable. A number of

investigators (Satterfield and Katzer, 1971; Satterfield and Cheng, 1972; Moore and Katzer, 1972; Satterfield *et al.*, 1973, etc.) have shown that such restricted diffusion occurs in silica-alumina and zeolite catalyst with pore diameters of less than 5 nm. Satterfield *et al.* (1973) obtained experimental data on diffusion in silica-alumina catalyst with a very fine pore diameter of the order of 3.2 for a number of solutes, such that the ratio of the critical molecule diameter of the solute to the pore diameter varied from 0.088 to 0.506. The experimental data were correlated by the following equation:

$$\frac{D_e}{D} = \frac{\varepsilon}{\tau} 10^{\frac{-2d_s}{d_e}} \quad (4.15)$$

where d_s is the solute critical diameter defined as the diameter of the smallest cylinder through which the solute molecule can pass without distortion and d_e is the pore diameter. The ratio of d_s to d_e is known as the hindered diffusion factor (λ). Satterfield *et al.* (1973) considered that this factor is in the range 0.1-0.5.

Information from the open literature on the possible role of intraparticle diffusion limitation in oil hydrogenation in slurry reactors is very limited (Veldsink *et al.*, 1997). For low pressure hydrogenation of cottonseed oil, D_{e,H_2} is approximately 70 times as large as $D_{e,Triglycerides}$ in cottonseed oil (Bern *et al.*, 1975). Intraparticle diffusion limitation of triglycerides has, among others, a pronounced effect on linoleate selectivity (S_l), as can be seen from the decrease of S_l with increasing particle diameter (Cordova and Harriot, 1975).

Coenen (1986) summarized the data on diffusion limitation and reported for a narrow pore catalyst (mean pore diameter $\langle d_p \rangle \sim 4$ nm) a 50% decrease in activity relative to a medium ($\langle d_p \rangle \sim 6$ nm) and wide pore ($\langle d_p \rangle \sim 8$ nm) catalyst. Coenen *et al.* (1988) observed intraparticle diffusion in trioleate hydrogenation from which they calculated intraparticle triglycerides diffusion coefficient $D_{e,Triglycerides} = 2 \times 10^{-11}$ m²/s (wide pore catalyst) and 4×10^{-12} m²/s (medium pore catalyst) at 373.15 K and an absence of hydrogen limitation.

For methyl ester hydrogenation over Pd/C catalyst, Tsuto *et al.* (1978) could verify the observed shunt reactions by incorporating intraparticle hydrogen diffusion limitation, though not very accurately because of the insensitivity of the curves for the value of $D_{e,H_2} = 3.6 \times 10^{-9}$ m²/s at 443.15 K. An estimated value of $D_{e,H_2} = 4 \times 10^{-9}$ m²/s at 443.15 K was obtained from the experimental data by Andersson *et al.* and Ganguli and Van den Berg (1978), which is in agreement with the data of Tsuto *et al.* (1978).

Jonker *et al.* (1998) investigated the intraparticle diffusion limitation in the hydrogenation and isomerization of fatty acid methyl esters (FAMES) and soybean edible oil (TAG) in porous nickel catalyst under reactive and inert conditions. They found that FAME hydrogenation reaction at 443.15 K appears to be controlled by intraparticle diffusion of hydrogen ($D_{e,H_2}=1.6\times 10^{-10}$ m²/s). In the case of triglycerides hydrogenation, the triglycerides appear to be diffusion limited ($D_{e,Triglycerides}=3.3\times 10^{-12}$ m²/s) rather than H₂, which agrees the literature. Veldsink (2001) proposes the effective triglyceride coefficient equal to the liquid-phase triglyceride diffusion coefficient divided by 10.

It is surprising that the scarcity of the experimental data in light of the substantial effects intraparticle diffusion limitation may have on the selectivity of the hydrogenation reaction. In the case of SCF systems, the situation is not different: there is a great lack of diffusion data available. The knowledge and the ability to predict transport properties in SCFs and the ability to predict them are of considerable importance in the design and efficiency of the process operation. Due to the high pressure involved, these systems are highly non-ideal and are not readily described by predictive mathematical models. In the numerous reviews of SCFs, specific mention is made on the lack of experimental diffusion data. As a consequence, few theoretical and empirical models exist to predict diffusion coefficients.

Liong *et al.* (1991), developed a simple experimental method that has been used to determine diffusion coefficients in several SCF systems mainly in SC CO₂. Diffusion and thermodynamic measurements by SFC are reviewed by Roth (1991) as well as Suárez *et al.* (1992). Van den Hark (2000) made a rough estimate of the effective FAME diffusivity in SC propane based on measured diffusivities in SC CO₂ (Liong *et al.*, 1992) in the order of 10⁻⁹ m²/s at 553.15 K and 15 MPa. For hydrogen in SC propane, diffusivity was considered in the range of 10⁻⁷ m²/s from the estimation proposed by Satterfield (1970) at low pressure.

As mentioned above, there are currently very few sets of data of diffusivity in supercritical hydrogenation systems. Therefore, the aim of this chapter was to study the intraparticle diffusivity of triglycerides and hydrogen under SC hydrogenation reaction conditions in order to determine the effective diffusion coefficients in the porous catalyst particle. The objective is to have an insight about the mass transport mechanisms in SC fluids.

4.2 Objectives and Strategy.

The objective is to study the intraparticle diffusion coefficients of triglycerides and hydrogen in SC propane under hydrogenation reaction conditions on 2% Pd/C catalyst. The true intrinsic hydrogenation kinetics from several experiments in the absence of diffusion limitation was determined from small particle diameters. The diffusion coefficients were determined from the best fits of the steady-state diffusion and chemical reaction in porous catalyst particle model under isothermal conditions, applied to the previously available kinetic constants to experiments carried out under diffusion limited conditions. The rate equations are used to investigate the effects of intraparticle hydrogen and triglycerides diffusion on the hydrogenation rate. Finally, the ratio of molecular diffusivity, estimated by means of correlations, to effective diffusivity were determined under several operating conditions for triglycerides as well as hydrogen in order to establish which type of diffusivity predominates within the porous catalyst particle.

4.3 Detection of the Internal Mass Transport Resistance.

At the end of chapter 3, the possibility that mass transport controls the reaction rate was put forward. Mass transport resistance might result in concentration gradients within the porous catalyst (internal mass-transfer limitation). These gradients reduce the reactant concentrations at the catalyst surface, which results in lower reaction rates (Note: gradients over gas-liquid interfaces do not exist because of the single-phase reaction mixture).

To test whether internal mass transport has influence on the reaction rate, the catalyst diameter was changed in preliminary runs, see Table 4-3.

Table 4-3: Effect of particle diameter on the conversion at constant apparent residence time (4.2 s). Experimental conditions: 0.25 g of 2% Pd/C at 20 MPa, feed composition (Oil:H₂:Propane):1:4:95 mol %.

Run	Reaction Temperature (K)	Particle size (mm)	Conversion %	Global H ₂ Reaction Rate (mol s ⁻¹ kg _{cat} ⁻¹ × 10 ⁴)
1	456.15	0.92	30.67	1.23
2	456.15	0.47	36.86	2.16
3	484.15	0.92	36.54	2.26
4	484.15	0.47	43.64	3.48

As seen, for constant temperature the rate of reaction is reduced on larger particles. The results in Table 4-3 thus indicate that internal substrates transport limitation exists at these low concentrations using large catalyst particles.

4.4 Determination of Effective Diffusion Coefficients.

In this part, a few experimental measurements were used to achieve two simultaneous goals: 1) to obtain the intrinsic kinetics of supercritical oil hydrogenation on Pd/C catalyst; 2) to determine the effective diffusivities of triglycerides and H₂ in supercritical propane by means of the adjustment of a simple steady-state diffusion and chemical reaction model in porous catalyst under isothermal conditions.

The intrinsic kinetic was determined from the smallest particle diameter where the intraparticle resistance was considered negligible. Based on the values obtained, the effective diffusivities of oil and H₂ were obtained for the largest catalyst particle. The sensitivity of the proposed model with the H₂ and oil effective diffusivity values was proved for several particle diameters.

Finally, the linoleate selectivity (S_i) along with the specific isomerization (S_i) were defined in terms of the overall reaction rates obtained from the fitted concentration profiles in the entire catalyst.

4.4.1 Experimental Measurements.

For the determination of the effective diffusivity coefficient for triglycerides and hydrogen under different operating conditions, the preliminary experimental runs used for intraparticle resistance detection along with a few intraparticle diffusion-limited hydrogenation runs (see Table 4-4.) were employed.

Table 4-4: Experimental reaction runs on 2% Pd/C for determination of intraparticle diffusion at constant final IV (80-100). Feed composition (Oil:H₂:Propane): 1:4:95 mol %.

RUN	Temperature (K)	Pressure (MPa)	Catalyst Particle size (mm)	Catalyst Mass (g)	Global H ₂ Reaction rate (mol s ⁻¹ kg ⁻¹ × 10 ⁴)
5	456.15	20	2	0.8	0.87
6	456.15	27.5	2	0.8	0.58
7	483.15	20	2	0.8	1.14
8	483.15	27.5	2	0.8	0.82

All the runs carried out were performed in the experimental apparatus described in Chapter 5 along with the analytical methods used to determine the reaction rate and the distribution of the hydrogenated products.

4.4.2 Steady-State Diffusion and Chemical Reaction in Porous Catalyst Particle Model under Isothermal Conditions.

The catalyst particle can be approximated by a slab of thickness L . The hydrogenation reaction is catalyzed within the porous matrix with an intrinsic reaction rate (r) expressed in $\text{mol.kg}^{-1}.\text{s}^{-1}$. It is assumed that the mass-transport process is in one direction though the porous structure and may be represented by a normal diffusion-type expression, so that there is no net convective transport contribution, there is not fluid-particle external resistance and the medium is isotropic (see Appendix F). For this case, a steady-state mass balance of the hydrogenation species inside, an elemental volume of catalyst of slab of thickness dx , gives:

$$D_{e,\text{triglycerides}} \frac{d^2 C_i}{dx^2} + r_i \rho_p = 0 \quad i = L, O, E, S \quad (4.16)$$

$$D_{e,H_2} \frac{d^2 C_{H_2}}{dx^2} + r_{H_2} \rho_p = 0 \quad (4.17)$$

Here, $D_{e,\text{Triglycerides}}$ and D_{e,H_2} are the effective diffusion coefficients for oil and hydrogen in the reaction medium and C_i and C_{H_2} are the concentrations of the reactants respectively. In this case, the effective diffusivities for the components of the oil were assumed to be the same because the components are of similar structure and molecular weight (Brunner, 1994).

The zero flux boundary conditions at the particle center plane are given by:

$$\frac{dC_i}{dx} = \frac{dC_{H_2}}{dx} = 0 \quad \text{at } x = 0 \quad (4.18)$$

and the boundary conditions for the mixture concentrations at the particle surface ($x=\pm L/2$) are considered equal to the bulk gas concentration, as a result:

$$C_i \Big|_{\frac{L}{2}} = C_{i_s} \quad i = L, O, E, S, H_2 \quad (4.19)$$

The kinetic expressions for the intrinsic reaction rate (r) for each component obeys the hydrogenation scheme proposed early by Albright (1967) and are taken from equations 3.33 to 3.37 of Chapter 3.

The differential equations 4.16 and 4.17 are two point boundary conditions value problems and are solved numerically using a shooting-type method (Riggs, 1988). These second-order ordinary differential equations (ODEs) are converted to coupled pairs of first-order ODEs where z is the new function as follows:

$$z_i = \frac{dC_i}{dx} \quad i = L, O, E, S \quad (4.20)$$

$$z_{H_2} = \frac{dC_{H_2}}{dx} \quad (4.21)$$

$$D_{e, \text{triglycerides}} \frac{dz_i}{dx} + r_i \rho_p = 0 \quad i = L, O, E, S \quad (4.22)$$

$$D_{e, H_2} \frac{dz_{H_2}}{dx} + r_{H_2} \rho_p = 0 \quad (4.23)$$

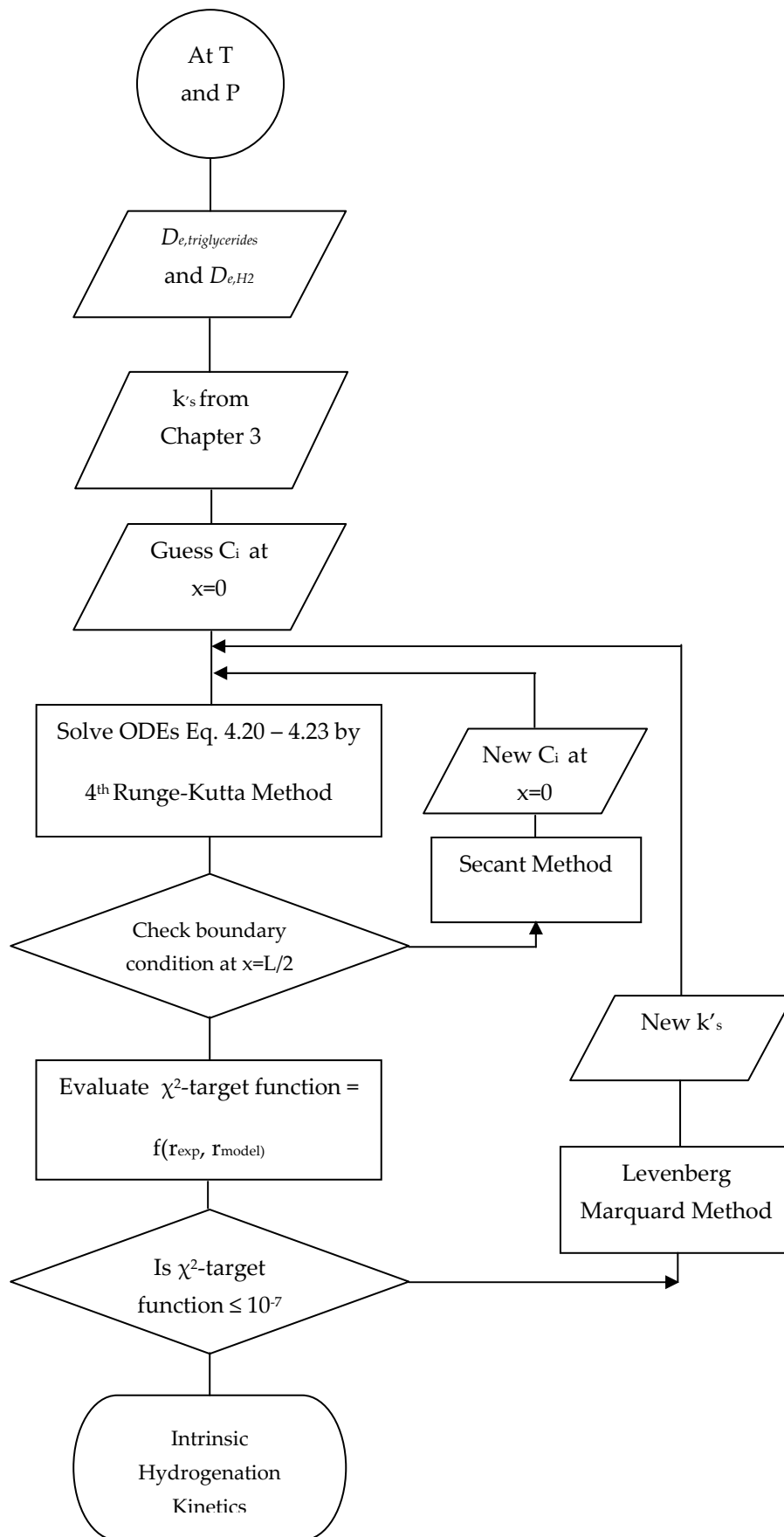
An initial-value problem is created by guessing a concentration value for the species at the center of the catalyst slab ($x=0$). The set of ten ODEs are solved sequentially in each section of the catalyst pellet using a fourth order Runge-Kutta method with a small step size (Riggs, 1988). The guessed value of the concentrations at the center is adjusted using the secant method, until the value of the concentrations at the external surface ($x=\pm L/2$) as computed by the integration, converges to the stated boundary condition. These concentration conditions correspond to the CSTR outlet concentrations.

After the concentration profiles are calculated, the actual observed rates can be obtained. The calculated rates can be determined from the internal concentration profiles as:

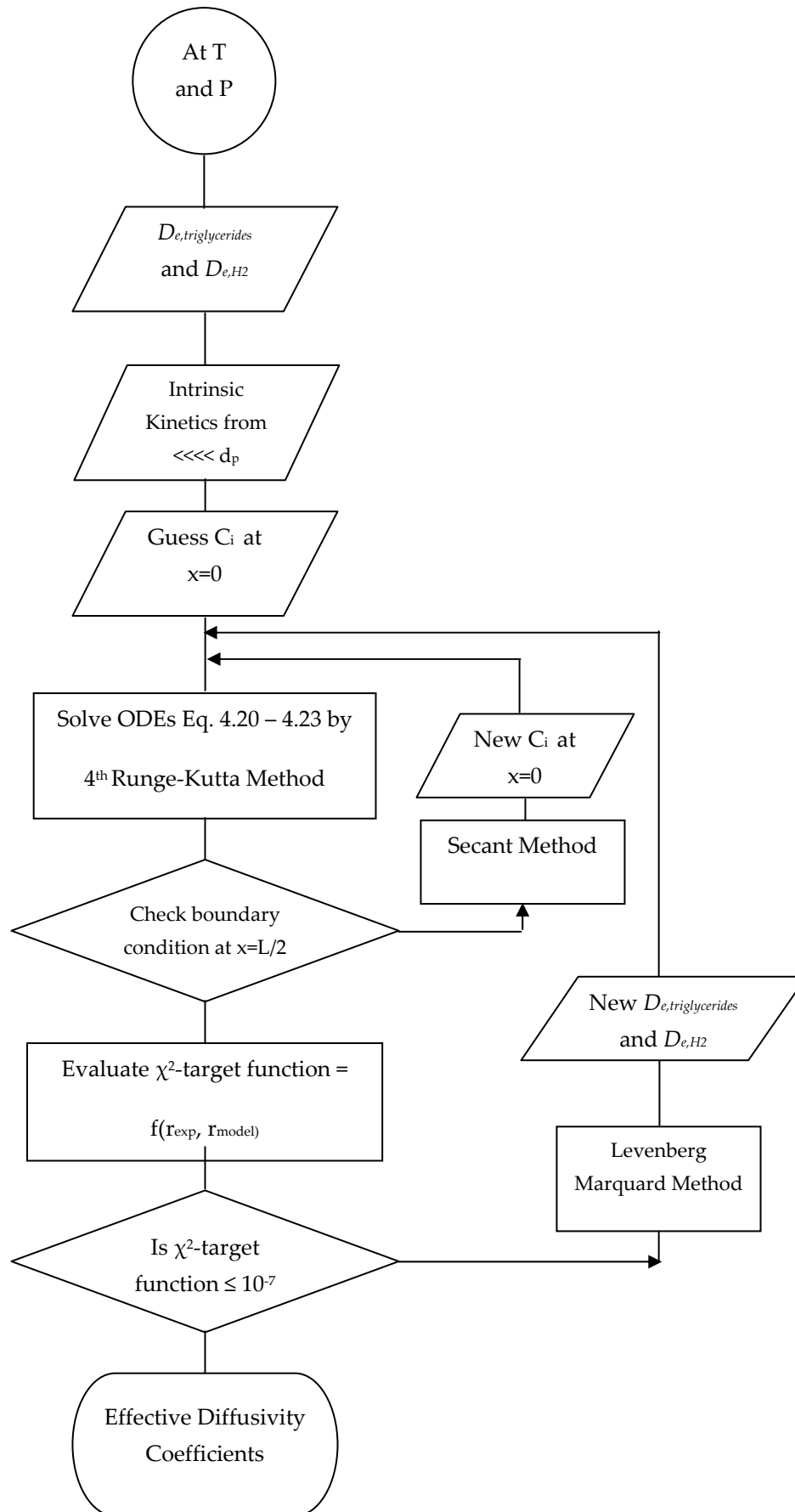
$$r_{p,i} = \left[\frac{D_{e,i}}{x \cdot \rho_p} \left(\frac{dC_i}{dx} \right) \Big|_{x=\frac{L}{2}} \right] \quad i = L, O, E, S, H_2 \quad (4.24)$$

where $r_{p,i}$ is the rate per pellet expressed in $\text{mol.kg}^{-1}.\text{s}^{-1}$.

The differential equations 4.20 to 4.23 were solved for several estimated values for the intraparticle effective diffusivities $D_{e, \text{triglycerides}}$ and D_{e, H_2} and using the intrinsic kinetic rate constants obtained previously. The optimization of these values was achieved by means of the minimization of χ^2 -target function using a Levenberg-Marquardt method. This objective function was the residual sum of squares of the experimentally observed and the predicted model rates of reaction for the hydrogenation species. Optimization was done simultaneously with the numerical integration of the model equations. For a better understanding of the employed mathematical solution strategy, see Schemes 4.1 and 4.2.



Scheme 4-1: Flow chart for the parameter fitting procedure for the smallest particle diameter catalyst ($d_p = 0.47$ mm, 2% Pd/C).



Scheme 4-2: Flow chart for the parameter fitting procedure for the largest particle diameter catalyst ($d_p = 2 \text{ mm}$, 2% Pd/C).

4.4.3 Results and Discussion.

The concentration profiles for each hydrogenation species inside the catalyst particle under different operating conditions are shown from Figure 4-2 to Figure 4-4.

Under 484.15 K and 20 MPa, the concentration profiles are steeper at the largest diameter particles (0.92 and 2 mm) than at the smallest one (0.47 mm) as can be seen in Figure 4-2. In the later case, the flat concentration profiles suggest that the internal diffusion could be considered negligible. The same behaviour occurred at 457.15 K and 20 MPa.

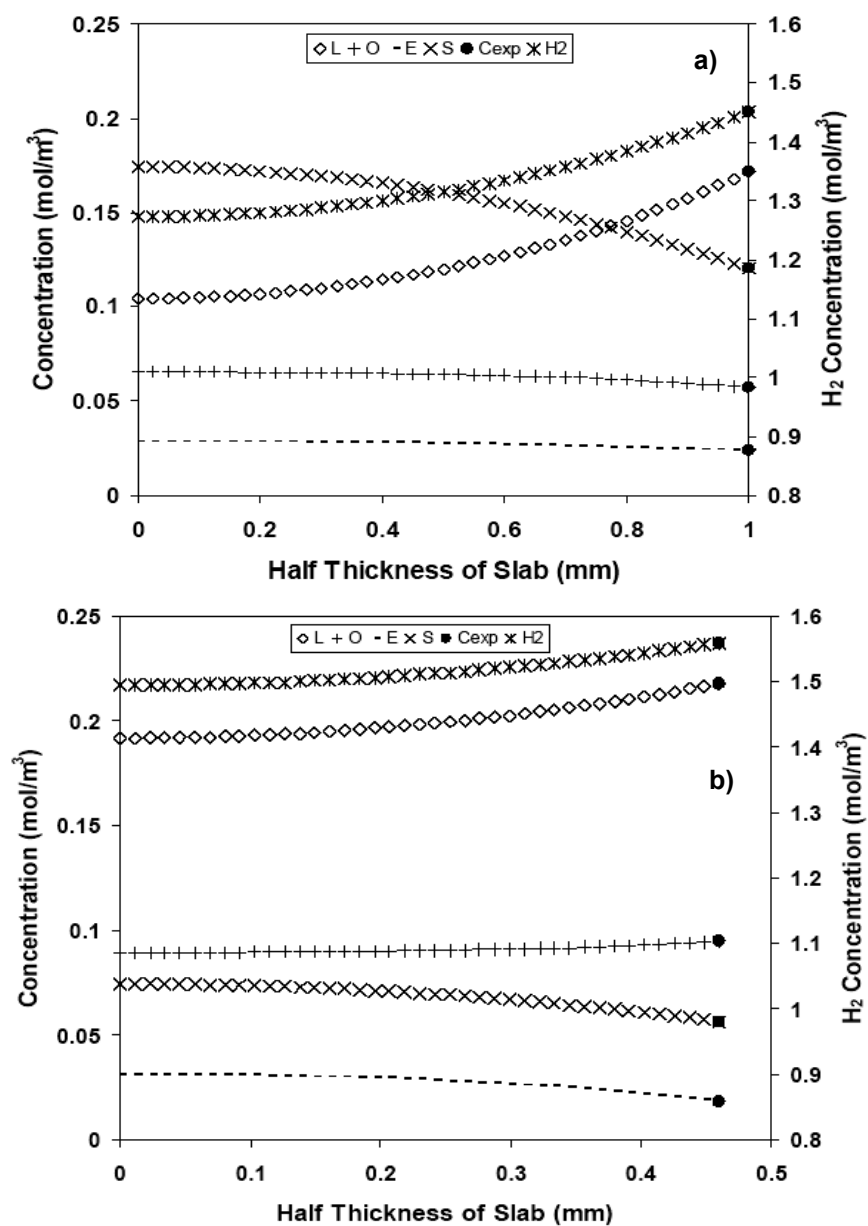


Figure 4-2: Concentration profiles of hydrogen and sunflower oil components in 2% Pd/C at 484.15 K, 20 MPa, feed composition (Oil:H₂:C₃H₈): 1:4:95 mol %. a) $d_p = 2$ mm b) $d_p = 0.92$ mm.

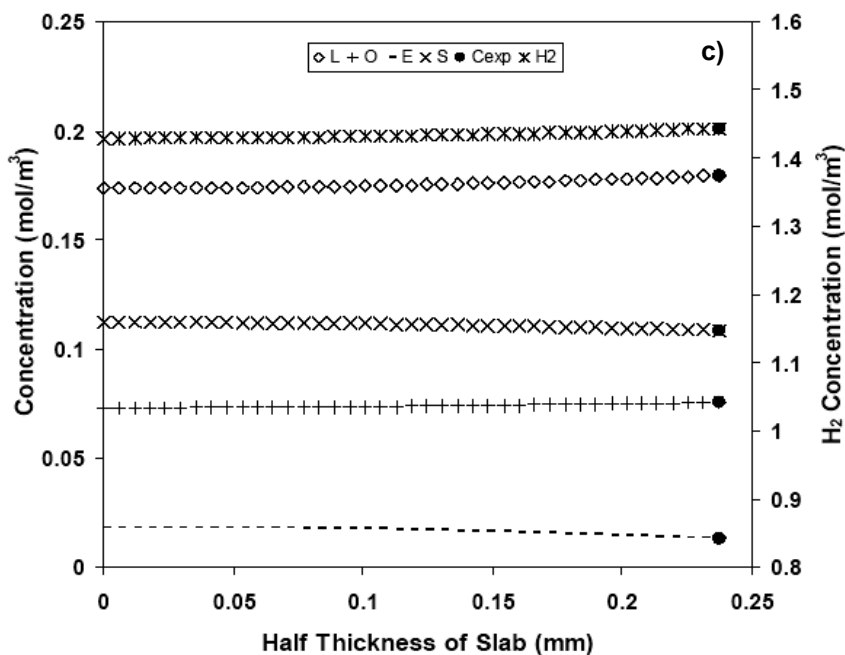


Figure 4-2: Intraparticle concentration profiles of hydrogen and oil components in 2% Pd/C at 484.15 K, 20 MPa, feed composition (Oil:H₂:Propane): 1:4:95 mol %. c) $d_p = 0.47$ mm.

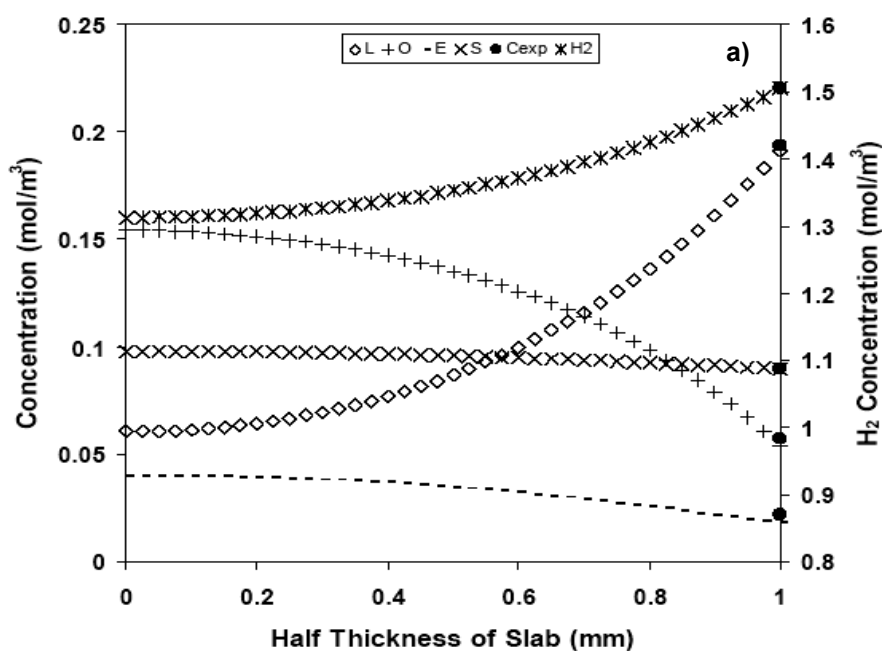


Figure 4-3: Intraparticle concentration profiles in oil hydrogenation in SC propane at 457.15 K, feed composition (Oil:H₂:Propane): 1:4:95 mol % and $d_p = 2$ mm. a) $P = 20$ MPa

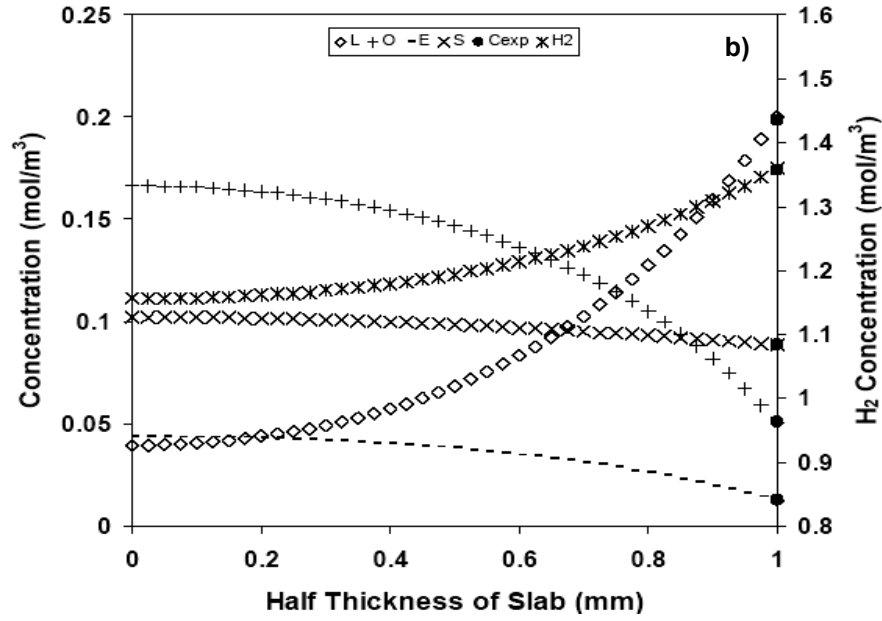


Figure 4-3: Intraparticle concentration profiles in oil hydrogenation in SC propane at 457.15 K, feed composition (Oil:H₂:Propane): 1:4:95 mol % and d_p= 2 mm. b) P= 27.5 MPa.

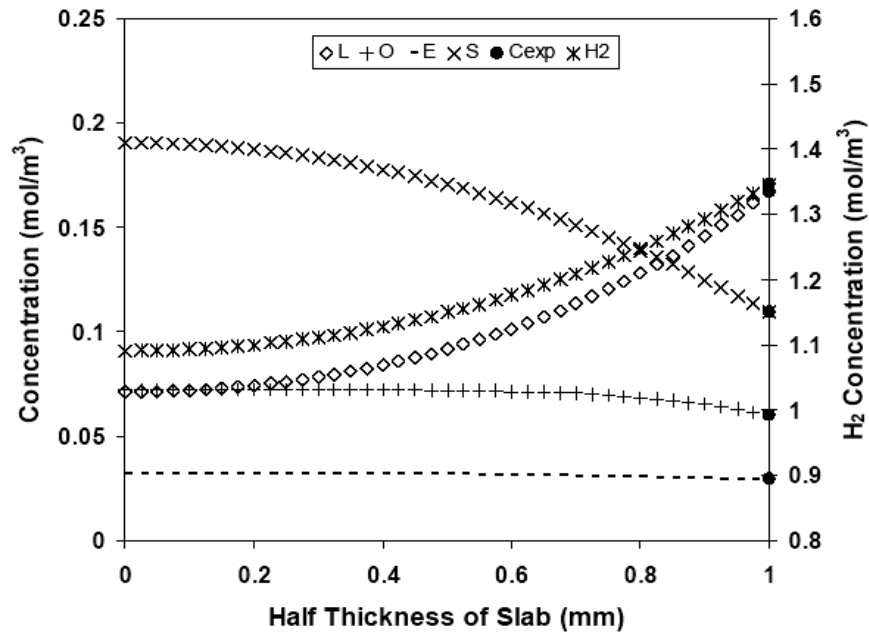


Figure 4-4: Intraparticle concentration profiles in oil hydrogenation in SC propane at 484.15 K, P= 27.5 MPa. Feed composition (Oil:H₂:Propane): 1:4:95 mol %, d_p= 2 mm.

For this reason, the model seems to be insensitive at small particle diameters as expected because the intraparticle diffusional resistance is considered negligible. The total average absolute deviation (AAD %) is defined by:

$$AAD\% = \frac{100}{N_q \cdot N_{q,i}} \sum_{i=1}^{N_{q,i}} \left| \frac{D_{q,i}^{exp} - D_{q,i}^{pred}}{D_{q,i}^{exp}} \right| \text{ where } i = L, O, E, S, H_2 \quad (4.25)$$

where N_q is the number of hydrogenation runs with $N_{q,i}$ components, $D_{q,i}^{exp}$ and $D_{q,i}^{pred}$ are the optimized and predicted reaction rate squared deviation for each component respectively.

For large particle diameters the model sensitivity was larger with respect to the diffusivities values. The variation of ± 10 times the optimized H_2 effective diffusivity value ($2 \times 10^{-7} \text{ m}^2/\text{s}$), generated a variation on predicted H_2 rates of reaction between 8 and 43% in comparison with the experimental values as shown in Figure 4-5.

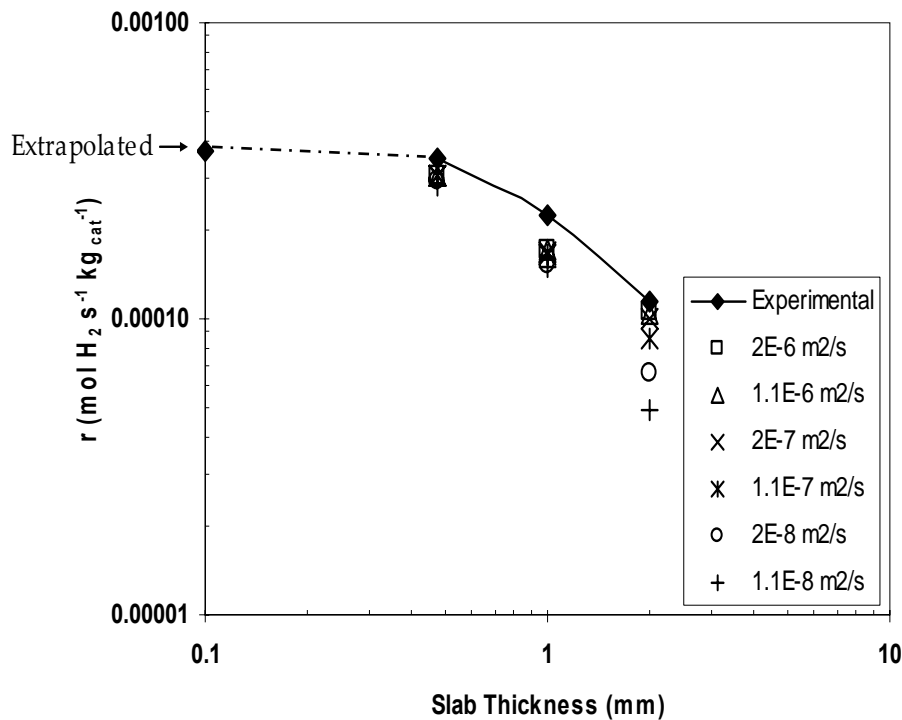


Figure 4-5 Sensitivity of the proposed model with H_2 effective diffusivity values at 484.15 K, 20 MPa. Feed composition (Oil: H_2 :Propane) of 1:4:95 mol %.

The sensitivity of the model to all fitted parameters (intrinsic kinetic constants and effective diffusivities increased 10 times) for both particle diameters is presented in Table 4-5. As can be observed, at the smallest particle diameter, the less AAD % values are obtained with a change of effective diffusivities rather than with the kinetic parameters. The situation is opposite for the largest particle diameter.

Table 4-5 Model sensitivity with fitted parameters at 484.15 K, 20 MPa and feed composition (Oil:H₂:Propane) of 1:4:95 mol %.

Parameters	Optimized	Tested	AAD %	
			L=2 mm	L=0.1 mm
k_{12} [mol ^{-1/2} .(m ³) ^{3/2} .kg ⁻¹ .s ⁻¹]	1.5625x10 ⁻⁴	1.5625x10 ⁻³	1.10	5.86
k_{13} [mol ^{-1/2} .(m ³) ^{3/2} .kg ⁻¹ .s ⁻¹]	0.00	1.5625x10 ⁻⁷	0.02	0.01
k_{24} [mol ⁻¹ .(m ³) ² .kg ⁻¹ .s ⁻¹]	1.8225x10 ⁻⁴	1.8225x10 ⁻³	3.71	14.50
k_{34} [mol ⁻¹ .(m ³) ² .kg ⁻¹ .s ⁻¹]	3.1608x10 ⁻⁵	3.1608x10 ⁻⁴	3.92	3.23
k_{23} [mol ^{-1/2} .(m ³) ^{3/2} .kg ⁻¹ .s ⁻¹]	6.6595x10 ⁻⁴	6.6595x10 ⁻³	2.87	87.48
k_{32} [mol ^{-1/2} .(m ³) ^{3/2} .kg ⁻¹ .s ⁻¹]	1.9279x10 ⁻³	1.9279x10 ⁻²	4.42	71.60
$D_{e, \text{triglycerides}}$ (m ² .s ⁻¹)	9.8000x10 ⁻⁸	9.8000x10 ⁻⁷	69.99	0.006
D_{e, H_2} (m ² .s ⁻¹)	2.0000x10 ⁻⁷	2.0000x10 ⁻⁶	70.22	0.003

Figure 4-6 shows the internal effectiveness factor found for several particle diameters.

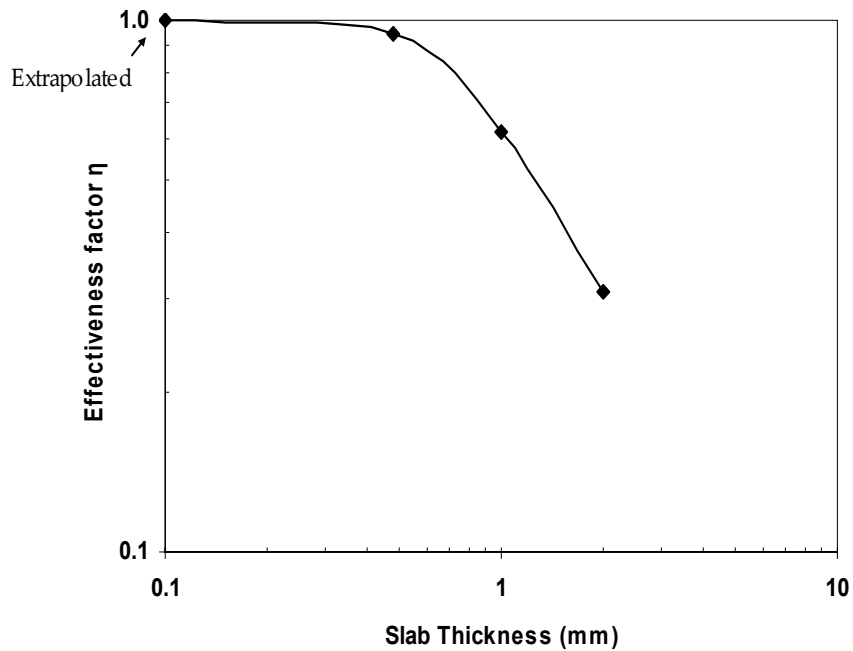


Figure 4-6: Effectiveness factor with respect to hydrogen for several slab catalyst particles thickness.

From Figure 4-6, it can be observed that as the particle diameter becomes very small (0.1 mm), the effectiveness factor approaches 1 due to the fact that the reaction is surface-reaction limited. On the other hand, when the particle diameter increases, the internal effectiveness factor η becomes very low (i.e., $\ll 1$), so the catalyst is not fully utilized.

Table 4-6 presents the intrinsic kinetic parameters for the supercritical sunflower hydrogenation determined from the solution of the combined diffusion-reaction model for the smallest particle diameter.

Table 4-6: Intrinsic kinetic parameters for the SC sunflower oil hydrogenation on Pd/C.

T(K)	Kinetic Constants					
	k_{12}^*	k_{13}^*	k_{24}^\dagger	k_{34}^\dagger	k_{23}^*	k_{32}^*
457.15	1.3076×10^{-4}	0.00	3.2001×10^{-6}	3.2854×10^{-6}	3.9129×10^{-4}	1.4564×10^{-3}
484.15	1.5625×10^{-4}	0.00	1.8225×10^{-4}	3.1608×10^{-5}	6.6595×10^{-4}	1.9279×10^{-3}

* [mol^{-1/2}.(m³)^{3/2}.kg⁻¹.s⁻¹] † [mol⁻¹.(m³)².kg⁻¹.s⁻¹]

The minimized χ^2 -target function (Spiegel, 1987) is defined by Equation 4.26 defined as the square deviation between experimental and model rate of reaction for $N_{q,d}$ experimental points of the N_q hydrogenation runs with $N_{q,i}$ components:

$$\chi^2 = \frac{1}{N_q} \sum_{q=1}^{N_q} \frac{1}{N_{q,i} N_{q,d}} \sum_{i=1}^{N_{q,i}} \sum_{d=1}^{N_{q,d}} \frac{(r_{q,i,d}^{\text{exp}} - r_{q,i,d}^{\text{mdl}})^2}{(r_{q,i,d}^{\text{exp}})^2} \quad i = L, O, E, S, H_2 \quad (4.26)$$

Here, $r_{q,i,d}^{\text{exp}}$ and $r_{q,i,d}^{\text{mdl}}$ are the experimentally observed and the calculated model rate of reaction values for the q th experiment and the i th component and d th data point, respectively.

So the weighting factors are already taken into account as the inverse of the expected values of r_i . Other objective functions, based on probability laws can be used (Froment and Bischoff, 1990). The kinetic parameters are obtained by the algorithm of Levenberg-Marquardt using the χ^2 -test. The values of $k_{i,j}$ are in the range of 10^{-3} - 10^{-6} , thus very widely apart (see the standard deviation in Chapter 3).

In the algorithm of Levenberg-Marquardt, the following constrains used are those of Table 4-7.

Table 4-7: Constrains of Levenberg-Marquardt algorithm.

Parameters	C_L	C_O	C_E	C_S	C_{H_2}
Constrain	$<C_{L0}$	$>1 \times 10^{-5}$	$>1 \times 10^{-5}$	$>C_{S0}$	$<C_{H0}$

The obtained kinetic constants were used in the steady-state diffusion and chemical reaction model in order to obtain the effective diffusivities of oil and H_2 respectively. Table 4-8 presents the estimated values under different reacting conditions.

Table 4-8: Fitted effective diffusion coefficients for hydrogenation species on 2% Pd/C catalyst (d_p range=0.47-2 mm).

T(K)	P (MPa)	Oil opt. D_e ($m^2 \cdot s^{-1} \times 10^8$)	H_2 opt. D_e ($m^2 \cdot s^{-1} \times 10^7$)
457.15	20	2.94	0.64
457.15	27.5	1.72	0.44
484.15	20	9.80	2.00
484.15	27.5	6.25	1.30

The effective diffusivities results confirm that hydrogen diffuse much more readily (10-100 times) than the triglycerides due to its lower molecular size.

It is also seen that the increase in temperature or the decrease of system pressure leads to an increase in the effective diffusion coefficients but the effect of temperature on them seems to be greater than the effect of the pressure. The increment in effective diffusion coefficients with temperature does follows the trend suggested by Satterfield (1970) who considered that it is proportional to T^m with m between 1.5 and 2. In our case the exponent m is around 21 whereas the increment of effective diffusivities with decreasing pressure is directly proportional to P . The trend suggests that the pronounced temperature dependence may be due to the strong effect of temperature on the adsorption equilibrium constants, as we will see later on. The influence of system pressure on the effective diffusivities was less significant at higher pressures in the supercritical region away from the mixture critical points (See Chapter 2) in agreement with the results reported by Suárez *et al.* (1993) and Arunajatesan *et al.* (2003). It is clear, that the effective diffusivity coefficients for triglycerides and hydrogen in the liquid-phase traditional hydrogenation reaction are much lower than those in the supercritical-phase.

The obtained effective triglycerides diffusivities values agree with those expected for mixtures of a supercritical gas and a low volatile component (10^{-8} m²/s) as suggested by Brunner (1994). They are about one order of magnitude higher than that for liquids and about two orders of magnitude lower than that for gases. In the case of hydrogen dissolved in a SC propane, it is expected that the effective diffusivity can be one order of magnitude higher than that in liquids (effective diffusivity is around 10^{-8} m²/s) because even though a gas phase is present, the wetting of the catalyst particles by the supercritical fluid means that the pores will be essentially filled with the supercritical fluid, which has a liquid-like density. Therefore diffusive properties should resemble those in liquid-filled pores.

From the concentration profiles in the entire catalyst, the overall reaction rates can be calculated. Then the overall linoleate selectivity (S_l) of the catalyst is defined here as the ratio of the net rate of formation of *cis*-monounsaturated compound to the net rate of formation of saturated species:

$$\text{Linoleate Selectivity } (S_l) = D_{e, \text{triglycerides}} \cdot \left. \frac{-\left(\frac{dC_o}{dx}\right)}{-\left(\frac{dC_s}{dx}\right)} \right|_{x=\frac{L}{2}} \quad (4.27)$$

The S_l was determined for 484.15 K, 20 MPa and a molar feed composition (Oil:H₂:Propane) of 1:4:95 for both, the smallest and the largest diameter particle. These values were compared to those from the classical definition of selectivity based on the kinetic constants. Following the kinetic scheme of hydrogenation reactions proposed by Albright (1967), the linoleate selectivity was defined as:

$$S_l = \frac{k_{12} + k_{32}}{k_{24} + k_{34}} \quad (4.28)$$

which is obviously valid only in the chemical kinetic regime.

At the same time, the *Specific Isomerization* defined as the ratio of the rate of formation of *trans*-monounsaturated compound to the net rate of uptake hydrogen (see equation 4.29) was determined and compared with the values from the definition suggested by Coenen (1986) as the ratio of the percentage increase in *trans*-isomer content and the decrease in iodine value (IV).

$$\text{Specific Isomerization } (S_i) = \frac{D_{e, \text{triglycerides}}}{D_{e, \text{H}_2}} \cdot \frac{-\left(\frac{dC_E}{dx}\right)}{-\left(\frac{dC_{\text{H}_2}}{dx}\right)} \Bigg|_{x=\frac{L}{2}} \quad (4.29)$$

Table 4-9 presents the obtained values for S_i and *trans* selectivity.

Table 4-9: Estimated selectivities for SC sunflower oil hydrogenation on 2% Pd/C at 487.15K, 200 MPa and a feed composition (Oil:H₂:Propane) of 1:4:95 mol %.

Particle size (mm)	Linoleate Selectivity (S_i)		Specific Isomerization (S_i)	
	Eq. 4.27	Classical kinetic definition*	Eq. 4.29	Coenen definition
0.1	7.82	7.55	0.05	0.04
2	2.11	7.55	0.08	0.02

*Albright (1967)

As can be observed in the case of the smallest particle diameter, the S_i value obtained from the kinetic constants agrees well with that from Eq. 4.27 because the surface reaction is rate limiting. When the particle diameter is large, the diffusion usually limits the overall rate of reaction and for this reason, the S_i values do not agree.

The selectivity results are in concordance with those reported by Tsuto *et al.* (1978), Coenen (1986), Westerterp *et al.* (1987), Colen *et al.* (1988) and Veldsink *et al.* (1997), who have found that in the hydrogenation of edible oils on porous catalyst, intraparticle mass-transfer limitations not only reduce the catalyst effectivities but also may change the product selectivities.

Having measured the kinetic parameters and the diffusive properties within the catalyst particle, we examined the possible mass transfer mechanism. We based the analysis on the abnormal tortuosity factor (or D_e/D) observed in SCF solvent.

In order to determine the ratio D_e/D , which is related with the tortuosity factor (τ) by equation 4.1, the molecular diffusivities for oil and H₂ in SC propane were estimated. In the case of triglycerides, the Catchpole - King (1994) and the Sun-Chen (1987) correlations were employed in near critical fluids (For more details see Appendix G).

Table 4-10 shows the estimated molecular diffusivity coefficients for C₃H₈-Triglycerides and C₃H₈-H₂ pairs found by means of the correlations explained above.

Table 4-10: Molecular diffusivities for C₃H₈-Triglycerides and C₃H₈-H₂ under several operating conditions.

Temperature (K)	Pressure (MPa)	$\rho_{C_3H_8}$ (kg/m ³)	Molecular Binary Diffusion Coefficient D_{12} (m ² /s)		
			C ₃ H ₈ -Triglycerides $\times 10^8$		C ₃ H ₈ -H ₂ $\times 10^7$
			Catchpole and King	Sun and Chen	Satterfield
457.15	20.0	377	1.62	1.51	3.21
457.15	27.5	448	0.83	0.85	2.34
484.15	20.0	300	1.92	1.80	3.58
484.15	27.5	408	1.25	1.11	2.61

As expected, the molecular diffusivity coefficients for C₃H₈-Triglycerides and C₃H₈-H₂ pairs increase with temperature at constant pressure. This rise is proportional to T^m where m is around 2 for C₃H₈-H₂ and 3 for C₃H₈-Triglycerides pair and may be due to the decrease in the solvent density associated with the increase in system pressure (Arunajatesan *et al.*, 2003).

The molecular diffusivity coefficients are inversely proportional to the molar volume of the solute. As can be realized from Table 4-10, the triglycerides seem to diffuse at a slower rate than hydrogen in SC propane under similar experimental conditions.

The general trend observed is that the molecular diffusivities decrease with increasing pressure at constant temperature. It was found that the molecular diffusivities are inversely proportional to the system pressure ($D_{12} \propto P^{-1}$). The influence of pressure is essentially the combination of changes in the fluid density and viscosity. As the density of the fluid increases, the molar volume decreases. In such situation, collision transfer, rather than molecular transfer, becomes the dominant transport mechanism. This results in a more erratic path taken by the solute molecule and consequently in a sharp decline in diffusivity suggesting an inverse relationship between diffusion coefficient and solvent density, as shows in Figure 4-7.

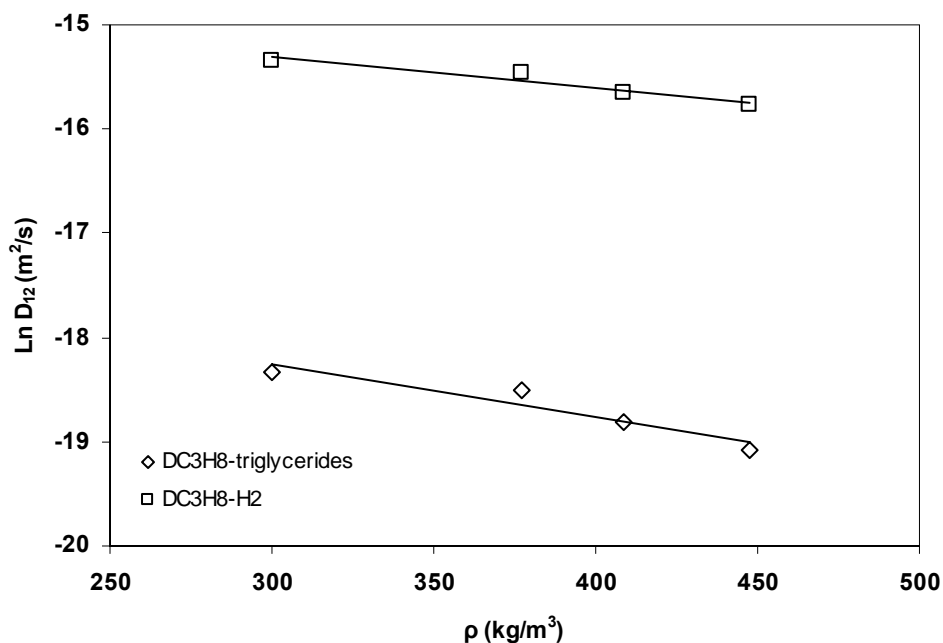


Figure 4-7: Estimated molecular diffusivity of hydrogen and triglycerides in SC C₃H₈.

Using the estimated molecular diffusivity values for C₃H₈-Triglycerides and C₃H₈-H₂ pairs, the ratio of the molecular diffusivity to the effective diffusivity under several operating conditions was determined with the fitted experimental effective diffusivities. The obtained values are shown in Table 4-11.

Table 4-11: D_e/D ratio for triglycerides and hydrogen in SC propane on 2% Pd/C.

Reaction Temperature (K)	Pressure (MPa)	$(D_e/D)_{\text{Triglycerides}}$	$(D_e/D)_{\text{H}_2}$
457.15	20.0	1.95	0.20
457.15	27.5	2.03	0.19
484.15	20.0	5.44	0.56
484.15	27.5	5.63	0.50

As can be seen from Table 4-11, the $(D_e/D)_{\text{H}_2}$ is much less than the unity which suggests that for hydrogen only the bulk diffusion contributes to the mass transport rate within the particle. This is a logical consequence because hydrogen can diffuse much more freely than the triglycerides due to its lower molecular size (see Figure 4-8). The average values of $(D_e/D)_{\text{H}_2}$ (between 0.07-0.14) obtained from Table 4-1 for several hydrogenations at 6.5 MPa over a wide range of temperatures (Butt,1999) are quite similar to those reported in this study.

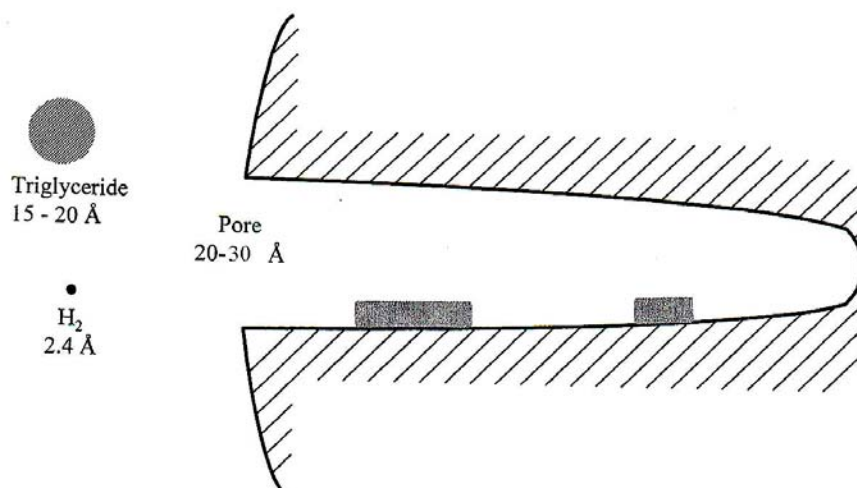


Figure 4-8 Relative sizes of reactants taking place in the pores of 2% Pd/C catalyst during the hydrogenation.

The strong influence of temperature on (D_e/D) ratio rather than pressure is reflected in Figure 4-9. This fact is a consequence of the strong influence of temperature on the effective diffusion coefficients that has been presented previously.

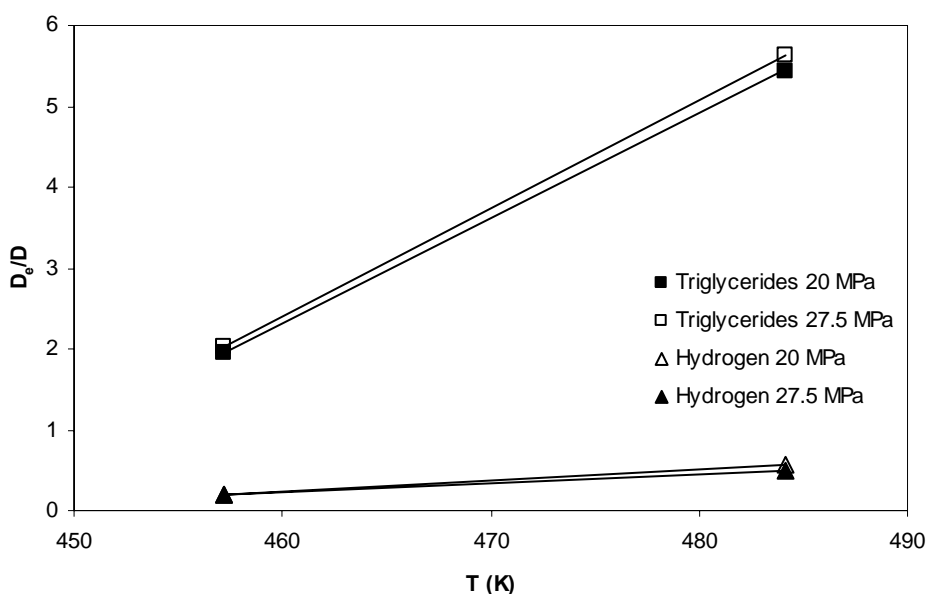


Figure 4-9: Influence of temperature and pressure on (D_e/D) ratio.

Considering the random-pore model developed by Wakao and Smith (1962 and 1964) for a pellet containing micropores, the D_e/D ratio would be equal to the square of the catalyst porosity (see equation 4.6). In the case of 2% Pd/C catalyst, which its pore volume consists predominantly of micropores and its porosity is 0.45, the $(D_e/D)_{H_2}$ ratio

would be 0.25. The obtained results for hydrogen in Table 4-11 are in a good agreement with this value.

Comparison of equation 4.6 with equation 4.1 indicates that $\tau=1/\epsilon$. In our case, the estimated value of τ is around 2 which is a “normal” tortuosity value because τ values usually range between 2 and 6, averaging about 4 when surface diffusion is insignificant (Satterfield, 1971, Smith, 1981 and Froment and Bischoff, 1990).

For the case of triglycerides, D_e/D ratio lay between 1.95-5.63, which is considerably too high to believe that the intraparticle diffusion was contributed by bulk diffusivity only because if the bulk diffusivity predominates within the porous particle, the ratio (D_e/D) generally exists in the range of 0.083-0.25 (Smith, 1981). Such high values of (D_e/D)_{triglycerides} (or $\tau < 1$) would mean that triglycerides would diffuse faster through the net of random pores than in a straight line joining two points. This is clearly impossible. So, to explain these results, we postulated that a parallel path for diffusion should be available to reactants. A potential alternative candidate, parallel diffusion mechanism is surface diffusion. If a molecule can diffuse in the bulk fluid of the pore and on the surface, the superposition of these two mechanisms would enhance the transport significantly. Therefore, surface diffusion plays an important role in the system presently studied as a mechanism of transport; a prerequisite for surface diffusion is a strong adsorption of solute on the walls (Komiya *et al.*, 1978). The trend suggests that the triglycerides preferably are absorbed in the pore's wall and then scout along the wall at a faster rate than it moves in the bulk. A similar range of D_e/D ratio was observed by Lai and Tan (1993) for toluene in SC CO₂ over activated carbon pellets and under non-reaction conditions.

As a consequence, the tortuosity factor is expected to be less than unity when surface diffusion is significant (Smith, 1981), possibly among other cases. In this study, the tortuosity τ could not be determined because the overall effective diffusivity D_e is a result of a combination of two effects: (a) a pore volume or bulk diffusion with an effective coefficient defined by Equation 4.1 and (b) a surface migration contribution, as shows Equation 4.14. In order to evaluate the surface diffusion coefficient D_s , it would be necessary to use a model based on both, pore-volume and surface transport, in a similar way to that Komiya and Smith (1974) have employed, as well as to measure the adsorption rate data under several operating conditions.

The estimation of the importance of surface diffusion to pore volume diffusion under several operating conditions is given by the ratio obtained from Equation 4.14 and presented in Table 4-12.

Table 4-12: $(\rho_p K_A D_s)/D$ ratio for triglycerides in SC propane on 2% Pd/C.

Temperature (K)	Pressure (MPa)	$(\rho_p K_A D_s)/D$
457.15	20.0	3.88
457.15	27.5	4.05
484.15	20.0	11.65
484.15	27.5	12.06

The $(\rho_p K_A D_s)/D$ ratio is a weak function of the pressure and increases remarkably with increasing temperature as can be notice from Table 4-12. The variation of $(\rho_p K_A D_s)/D$ ratio with temperature is indicated in the following equation:

$$\frac{d(\rho_p K_A D_s / D)}{d(1/T)} = \frac{-\Delta H - E_s - E_D}{R} \quad (4.30)$$

where ΔH is the adsorption heat, E_s is the activation energy of superficial diffusivity, E_D is the activation energy of molecular diffusivity, R is the gas constant and T is the absolute temperature. A plot of $(\rho_p K_A D_s)/D$ versus $1/T$ is presented in Figure 4-10.

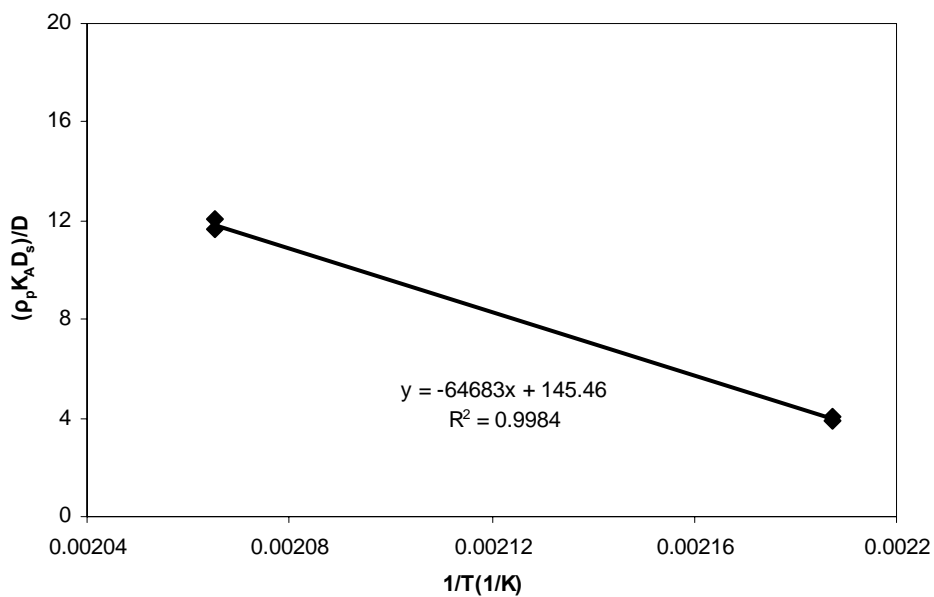


Figure 4-10: Variation of $(\rho_p K_A D_s)/D$ with temperature.

From the slope of the regression line, it is possible to obtain a rough value of the heat of adsorption (ΔH) of 50.2 kJ/mol assuming E_D value around 10.5 kJ/mol for diffusion (Levenspiel, 1996) and E_s value 34.8 kJ/mol from Komiyama *et al.* (1978).

Sladek *et al.* (1974) proposed a correlation for the diffusivities of physically and chemically adsorbed species directly related to the heat of adsorption ΔH . The D_s values for triglycerides on activated carbon are determined from this correlation using the heat of adsorption estimated previously. Figure 4-11 presents the Sladek's correlation with several experimental points along with the predicted values of this study.

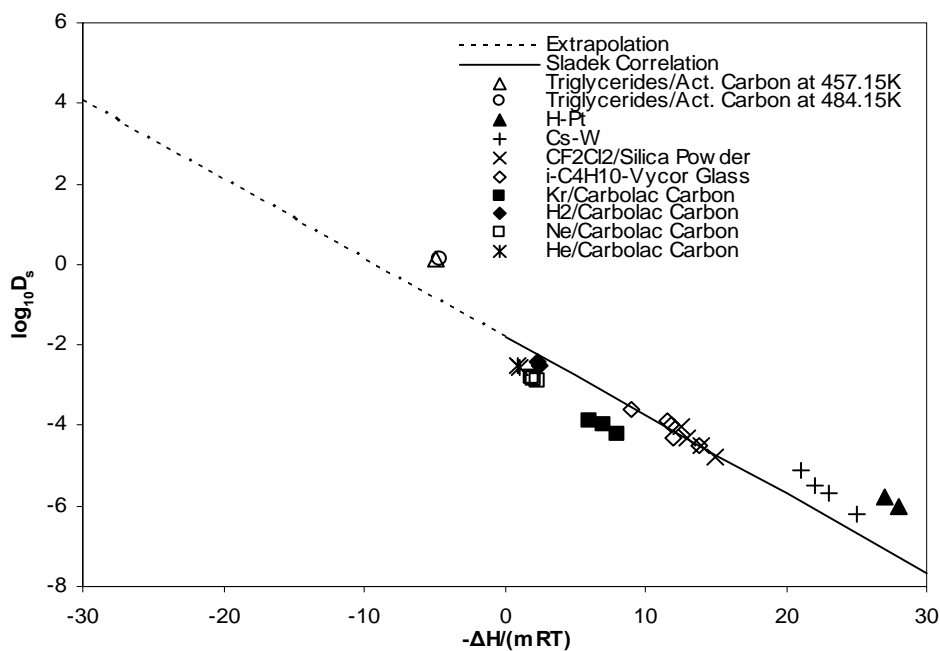


Figure 4-11: General correlation of surface diffusivities from Sladek *et al.* (1974).

The magnitude of estimated D_s values ($1.58 \times 10^{-5} \text{ m}^2/\text{s}$ at 457.15K and $1.26 \times 10^{-5} \text{ m}^2/\text{s}$ at 484.15K) are quite similar to those characteristic of physical adsorption systems, which typically range from 10^{-9} to $10^{-6} \text{ m}^2/\text{s}$ and are considerably higher than those reported for surface diffusion in chemisorption systems (Sladek *et al.*, 1974). From these results, taking into account the $(\rho_p K_A D_s)/D$ ratio, the importance of surface diffusion of triglycerides is mainly due to its adsorption on activated carbon rather than due to the D_s values, because the latter seem to be a weak function of temperature. Consequently, the triglycerides molecules may exhibit a high mobility associated with their low energies of physical bonding to the surface in comparison with that typical chemically adsorbed molecules.

Another phenomenon which could be present in the case of the triglycerides is the restricted diffusion. This occurs when the dimensions of the solute molecule (1.5 - 2 nm for triglycerides) and the pore (2 - 3 nm for 2% Pd/C catalyst) are comparable. In this case, a hindered diffusion factor (around 0.7) has to be taken into account. It depends on the diameter ratio of molecule and pore, d_s/d_e . Using equation 4.15, it is possible to make a rough estimation of the tortuosity factor. The obtained values are much less than the unity therefore it confirms that the hypothesis of the surface diffusion is significant.

4.5 Conclusions.

The study of intraparticle diffusion of triglycerides and hydrogen in SC propane under hydrogenation reaction conditions on 2% Pd/C catalyst, were carried out after intraparticle mass transport resistance was detected.

The true intrinsic hydrogenation kinetics from several experiments in the absence of diffusion limitation was determined from small particle diameters at 457.15 and 484.15 K. The diffusion coefficients for triglycerides and hydrogen in SC propane were determined from the best fits of the steady-state diffusion and chemical reaction in porous catalyst particle model under isothermal conditions, applied to the previously available kinetic constants to experiments carried out under diffusion limited conditions.

The pressure does not seem to have a significant effect on the concentration profiles for hydrogenation species inside the catalyst particle as the temperature, which would suggest that the adsorption equilibrium constant for hydrogen as well for sunflower oil is strongly dependent on temperature.

The effective diffusivities values showed that hydrogen diffuses two times more rapidly than the triglycerides due to its lower molecular size. The effective triglycerides diffusivities values agree with those expected for mixtures of a supercritical gas and a low volatile component. The effective diffusivity values for both components in SC propane are around 10^{-8} m²/s, about one order of magnitude higher than that for liquids and about two orders of magnitude lower than that for gases because even though a gas phase is present into the reactor, the wetting of the catalyst particles by the supercritical fluid means that the pores will be essentially filled with the supercritical fluid, which has a liquid-like density. Therefore diffusive properties should resemble those in liquid-filled pores.

Linoleate selectivity (S_i) was determined and compared to that value obtained by classical kinetic definition. In the case of the smallest particle, the values agreed well which is obvious if only the chemical kinetic regime controls the reaction.

The ratio of molecular diffusivity, estimated by means of correlations, to effective diffusivity was determined under several operating conditions for triglycerides as well as hydrogen. The values for hydrogen were much less than the unity with suggest that only the bulk diffusion contributes to the mass transport rate within the particle.

For the case of triglycerides, D_e/D value ranged 1.95-5.63 which was considerably too high to believe that the intraparticle diffusion was contributed by bulk diffusivity only. To explain these results, it was postulated that a parallel path for diffusion should be available to reactants: surface diffusion. A prerequisite for surface diffusion is a strong adsorption of solute on the walls. This suggests that the triglycerides preferably are absorbed in the pore's wall and then scout along the wall at a faster rate than it moves in the bulk.

A rough estimation of the surface diffusion coefficient (D_s) was made employing a correlation proposed by Sladek *et al.* (1974). The D_s values were quite similar to those characteristic of physical adsorption systems.

4.6 Nomenclature.

AAD	average absolute deviation, see Eq. 4.25
a_M	average radii of cylindrical pores of macroregions [m]
a_μ	average radii of cylindrical pores of microregions [m]
C_{is}	concentration of i at catalyst surface [mol/m ³]
C_i	mol concentration of component i [mol/m ³]
C_{A1}	concentration of A at catalyst surface [mol/m ³]
D	molecular diffusion coefficient [m ² /s]
D_a	modified diffusivity [m ² /s]
D_{AB}	bulk diffusivity [m ² /s]
D_e	effective diffusivity [m ² /s]

$D_{e,Triglycerides}$	effective diffusivity of triglycerides [m^2/s]
D_{e,H_2}	effective diffusivity of hydrogen [m^2/s]
d_e	pore diameter [m]
D_K	Knudsen diffusivity [m^2/s]
D_M	molecular diffusivity of macroregions [m^2/s]
d_p	spherical diameter of particle [m]
D_s	surface diffusion coefficient [m^2/s]
d_s	solute molecule diameter [m]
D_{12}	binary diffusion coefficient [m^2/s]
D_μ	molecular diffusivity of microregions [m^2/s]
$D_{q,i}^{exp}$	optimized reaction rate squared deviation for component i
$D_{q,i}^{pred}$	predicted reaction rate squared deviation for component i
E	activation energy [J/ (mol K)]
E_s	activation energy for surface diffusion [J/ (mol K)]
E_D	activation energy for molecular diffusion [J/ (mol K)]
ΔH	enthalpy change on adsorption [J/(mol K)]
IV	iodine value [g I ₂ /100 g oil]
K_A	adsorption equilibrium constant on the solid from the high-pressure fluid
k_{ij}	kinetic rate constant in the network of Scheme 3-4 [$(m^{4.5})/(mol^{0.5} kg s)$] or [$(m^6)/(mol kg s)$]
L	slab thickness [m]
m	coefficient in Sladek correlation
N_q	number of hydrogenation runs
$N_{q,d}$	number of experimental points

$N_{q,i}$	number of components
N_s	molal rate per unit per meter of pore surface
R	gas-law constant [8.314 J/(mol K)]
r_i	global reaction rate of species i per mass of catalyst [mol/s kg]
$r_{p,i}$	reaction rate of formation per mass of pellet [mol i/(kg s)]
$r_{q,i,d}^{\text{exp}}$	experimentally observed rate of reaction per mass of pellet [mol /(kg s)]
$r_{q,i,d}^{\text{mdl}}$	calculated model rate of reaction per mass of pellet [mol /(kg s)]
S_l	linoleate selectivity, see Eqs. 4.27-4.28
S_i	specific Isomerization, see Eq. 4.29
T	temperature [K]
W_{ir}	molar radial flux of species i [mol/(m ² s)]
x	coordinate perpendicular to slab [m]
z_i	concentration gradient = dC_i/dx [mol/m ⁴]

Greek Symbols

ϵ_M	void fraction of macroregions
ϵ_p	pellet void fraction
ϵ_μ	void fractions of microregions
ρ_p	pellet density [kg/m ³]
χ^2	Chi-squared, see Eq. 4.26
τ	tortuosity factor

Acronyms

E	elaidic fatty acid, <i>trans</i> C18:1
---	--

FAME	fatty acid methyl ester
H ₂	hydrogen
L	linoleic fatty acid, C18:2
O	oleic fatty acid, <i>cis</i> C18:1
ODES	ordinary differential equations
S	stearic fatty acid, C18:0
SC	supercritical
SCF	supercritical fluid
TAG	triglycerides
C ₃ H ₈	propane

Sub- and Superscripts

c	critical
d	data point
exp	experimental
i	component, i=L, O, E, S
M	macroregions
mdl	predicted
pred	predicted
q	experiment
0	entering
μ	microregions

Chapter Five

Experimental.

5.1 Introduction.

All the experiments described in this Thesis were performed using a supercritical continuous flow apparatus. The raw materials used are described at the beginning of this chapter. Then, safety systems of the experimental device are described. A detailed scheme of the flow apparatus is given in Section 5.4. A brief explanation of the individual components of the continuous flow apparatus is included along with the operating procedure of the apparatus. The remainder of the Chapter describes the analytical methods used in earlier Chapters.

5.2 Raw Materials.

5.2.1 Sunflower Seed Oil.

A sunflower seed oil from *Helianthus annuus* from Sigma-Aldrich (Barcelona, Spain) that had an initial iodine value (IV) of 135 and a fatty acid composition (0.4 wt% C14:0, 6.6 wt% C16:0, 0.1 wt% C16:1, 4.5 wt% C18:0, 18.4 wt% *cis* C18:1, 67.6 wt% C18:2, 0.8 wt% C18:3, 0.1 wt% C20:0, 0.06 wt% C20:2) was used in all experiments. The specification data sheet for sunflower oil is presented in Appendix H.

5.2.2 Hydrogen.

Hydrogen (99.999% minimum purity grade) was purchased from Praxair (Barcelona, Spain). Appendix H contains the specification data sheet.

5.2.3 Propane.

Propane (99.5% minimum purity grade) was purchased from Praxair (Barcelona, Spain). The specification data sheet is presented in Appendix H.

5.2.4 Dimethyl ether (DME).

The dimethyl ether used in this thesis was supplied by Grit S. L. (Barcelona, Spain) with a minimum guaranteed purity greater than 99.9%. In Appendix H, the specification data sheet is presented.

5.2.5 Catalysts.

The catalysts used were 0.5% Pd on alumina (eggshell spheres of 2 mm nominal diameter) from Johnson Matthey (Barcelona, Spain) and 2% Pd on activated C (uniform metal loading, 2 mm pellets, pore volume = 1.3 cm³/g mostly in micropores), from Degussa AG (Frankfurt, Germany). Before the hydrogenation, the latter catalyst was crushed and sieved to 0.50 mm and then small pellets were activated in situ. The specification data sheet for both catalysts is presented in Appendix H.

5.2.5.1 Activation Procedure.

The catalyst is load carefully into the reactor, and then it is flushed with nitrogen (99.999% minimum purity grade) at ambient temperature in order to remove oxygen from the system (safety!) ensuring that the volume of nitrogen exceeds five times the volume of the reactor. Nitrogen is replaced gradually by hydrogen (99.999% minimum purity grade, 105 STP cm³/min) and the temperature and pressure are increased up to the desired reaction conditions. A time of 2 hours is employed for the catalyst activation. After this time, the solvent is slowly introduced into the reactor.

5.2.5.2 Test of the Stability of Catalyst Activity.

Hydrogenation runs (duration of about 5 h) were done after the catalyst activity had become stable (see Figure 5-1). Conversion in terms of IV, *trans* C18:1 content, and stearic ester content showed an initial decrease, but were stable during reaction runs.

5.3 Safety Procedures and Devices.

The leaks in the experimental setup are checked with soapy water in combination with CO₂ because it is a not toxic substance. In the case of hydrogen line, helium was employed. For removing oxygen from the system, nitrogen is flushed into the reactor before starting the reaction.

Due to hydrogen is a flammable high pressure-gas that can form explosive mixtures with air, the gas containers are located in a special explosion-proof compartment outside of the laboratory (see Figure 5-2) where the temperature does not exceed 312.15 K.

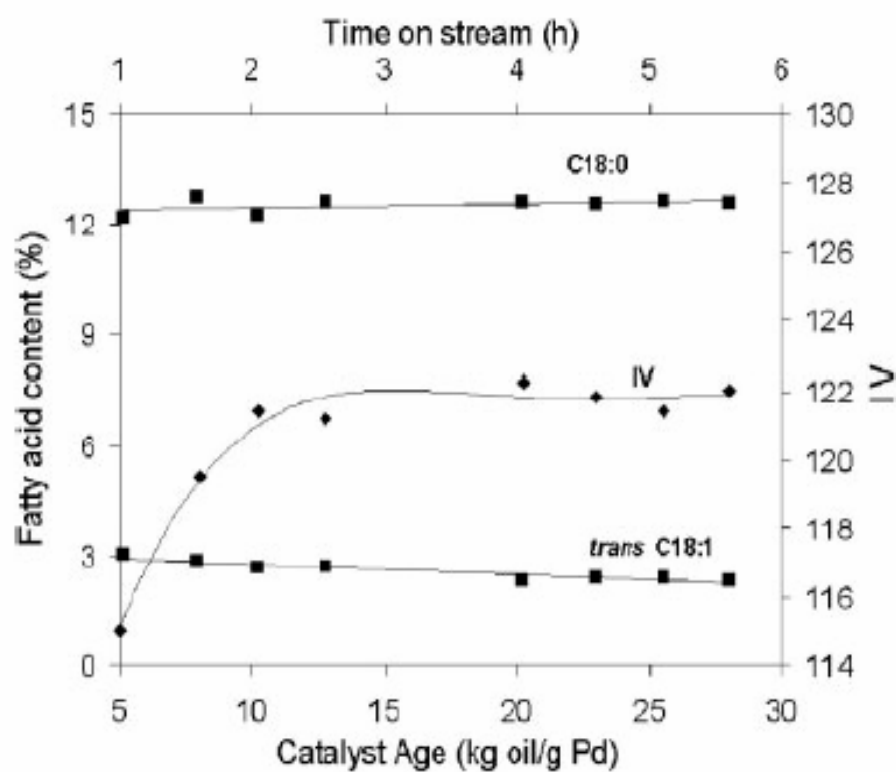


Figure 5-1: Change in product distribution and iodine value (IV) during short term operation ($P = 20$ MPa $T = 444.15$ K, feed mol composition.: sunflower oil = 1%, $H_2 = 8\%$, $C_3H_8 = 91\%$).



Figure 5-2: Explosion-proof compartment for gases.

On the other hand, propane and DME are extremely flammable substances too. These gases are located in areas with adequate ventilation where “No Smoking or Open Flames” signs are posted. Because these gases can be ignited by heat, pilot lights or sparks, all electrical equipment in the system is non-sparking. Furthermore, use and storage areas have approved explosion meters (Polytron Sensing Head SE ExPRM, Dräger) for hydrogen as well as propane and DME. These meters are controlled with a safety device, which consist of one channel gas detection control unit (Quadgard, Dräger) which has a master alarm with visual and acoustic (>90 dBA) signals. The detection is based on the principle of heat-of-combustion (pellistors). The meters are designed for the detection of combustible gases and vapours in the range of the lower explosive limit (LEL) at normal temperature. The mixture of gases (unreacted hydrogen and SC solvent) which is left after separating reaction products is sent to an explosion-proof fume cupboard to remove these exhaust gases from the use area and in this way avoid the risk of working in a stuffy atmosphere especially in confined areas.

The experimental apparatus is equipped in all lines with several pressure relief devices. More details will be given in section 5.4.

5.4 Supercritical Fluid Continuous Flow Apparatus.

A simplified process diagram is presented in Figure 5-3.

5.4.1 Process and Instrumentation Diagram (P&ID).

Figure 5-4 shows a schematic diagram of the supercritical fluid continuous flow apparatus used to carry out all the experiments herein presented.

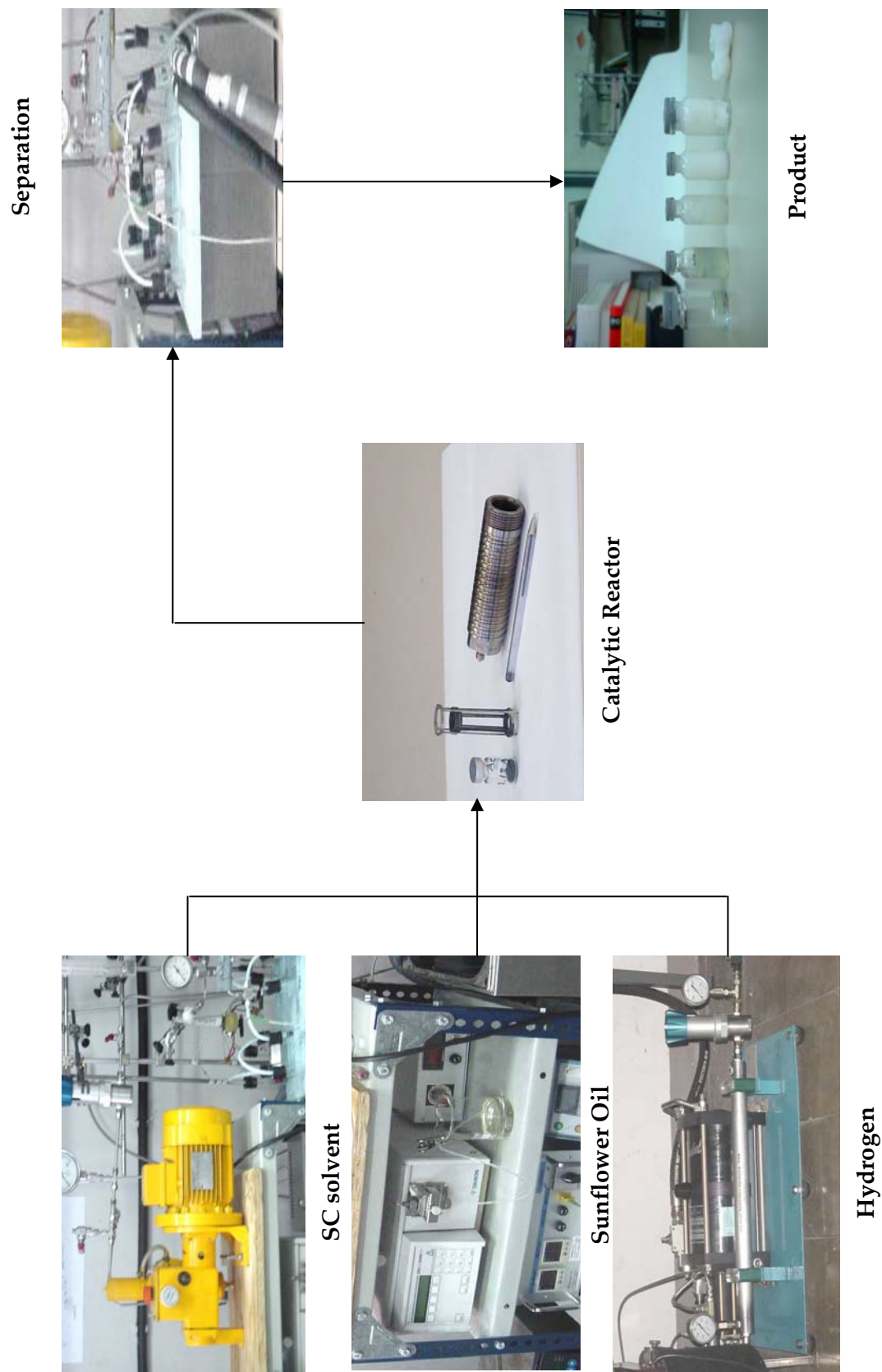


Figure 5-4: Schematic of the supercritical fluid continuous flow apparatus.

5.4.2 Equipment List.

The main equipment is resuming in Table 5-1.

Table 5-1: Equipment list of the supercritical experimental apparatus.

It	Description	Main Characteristics
1	Oil Sunflower Feed Vessel	
2	Oil Sunflower Pump	Gilson, HPLC pump model 305 Q-rate _{max} = 10ml/min, ΔP_{max} = 62 MPa
3	SC Solvent Pump	Dosapro Milton Roy, Diaphragm Pump Milroyal D, Q-rate _{max} =4,17 l/h at 35 MPa
4	Thermocouples	Type K, Stainless Steel.
5	Pressure Gauges	Wika, plastic dial cover/solid front stainless steel case
6	Rupture Disc	Autoclave Engineers, Stainless Steel, P_{max} = 35 MPa
7	Relief Valves	Haskel, model 27741-6, Stainless Steel body, P_{max} = 35 MPa
8	Expansion Valve	Autoclave Engineers Needle valve, model 10VRMM2812, Stainless Steel, T_{max} =403.15 K at 30 MPa, C_{vmax} =0.004
9	Air Compressor	ABAC model B4900LN/T4, 514 l/min at 1.1 MPa
10	Pressure Regulators	GO, Model PR57, stainless Steel body, P_{max} =69 MPa
11	H ₂ Mass Flow Controller	Brooks Instruments, model 5850S, Stainless Steel Body, Q-rate _{max} = 150 mlN/min, P_{max} =28 MPa, T_{max} =343.15 K
12	Gas-Booster System	Haskel, model AG-62, P_{max} =62 MPa
13	Static Mixer	Kenics, model 37-04-065, 20-cm long, 1/4-in. OD, P_{max} =24 MPa at 423.15 K
14	Pre-heater	Kosmon S.A., model 43000, Stainless Steel, T_{max} =545.15 K, P_{max} =30 MPa, 600W
15	Micro Catalytic Reactor Autoclave Engineers	Gradientless with Internal Recycle. Equipped with a MagneDrive Agitator and with a furnace-temperature controller. Made of Hastelloy C-276, Vessel volume=50 cm ³ , Basket volume= 7.15 cm ³ , T_{max} =616.15 K at 35 MPa
16	MagneDrive Agitator	Autoclave Engineers, Hastelloy C, Speed _{max} = 300 rad/s, Power Capacity _{max} =0.5 Hp Cooling requirement= 11 l/h of water
17	Reactor Pressure Gauge	Autoclave Engineers, K-Monel Bourdon tube
18	Reactor Thermowell	Autoclave Engineers, Hastelloy C, type K
19	Control Thermostat	Huber, model 230, thermoregulation liquid= ethylene glycol-water (40% v/v), temperature range= 243.15 – 473.15 K, volume=5 l
20	Rotameter	Tecfluid, model 2300, 20 – 140 l/h C ₃ H ₈ , P_{max} =1.5 MPa, T_{max} = 3935.1 K

5.4.3 Experimental Apparatus Description.

Liquefied propane or DME was pumped using a high-pressure diaphragm pump (Dosapro Milton Roy, France) to the reactor, to provide and maintain a system downstream pressure of 18–25 MPa, which was manually set with a high pressure regulator (GO, Euroval, Barcelona, Spain). The sunflower oil was pumped at a constant flow rate using a high-performance liquid chromatography (HPLC) pump (Gilson, France) and H₂ was compressed by a gas-booster system (Haskel, Barcelona, Spain) equipped with a high-pressure gas reservoir. H₂ flow was metered from the constant pressure reservoir through a mass-flow-indicating controller (Brooks Instruments, Euroval, Barcelona, Spain).

The oil substrate was mixed with propane in a static mixer (Kenics, Barcelona, Spain). H₂ was added downstream of mixer. The reactant mixture was preheated to the desired operating temperature before entering the reactor. The reactor (Robinson-Mahoney reactor, Autoclave Engineers, Erie, PA) was equipped with a fan shaft (MagneDrive, Autoclave Engineers), and a fixed annular catalyst basket (52 X 52 mesh, 0.005 diameter wire). The reactor was heated with an electrical heating jacket. Control thermocouples were located in the outside skin of the reactor body. The internal reactor temperature was monitored with a thermowell located in the bottom. The temperature increment in the reactor, relative to the feed, was seldom more than 274.15 K above the temperature of the inlet heater. This is certainly attributed to the relatively small adiabatic temperature increase for reactions in SC solvents.

After leaving the reactor, the effluent was continuously expanded to atmospheric pressure on an externally heated needle-type valve (Autoclave Engineers, Erie, PA) in order to control the total flow of the reactor mixture. This effluent was then sent to a series of glass U-tubes, immersed in an ethylene glycol–water (40% v/v) bath held at 249.15 K to condense the oil from the propane and unreacted H₂ mixture. The flow rate of exhaust gas was measured with a rotameter (Tecfluid, Spain) and sent to an explosion-proof fume cupboard.

5.4.3.1 The Gradientless Reactor.

Chemical kinetic data, free from mass- and heat-transfer effects, are essential in designing large chemical reactors, but eliminating these effects in heterogeneous catalytic reactions is difficult because of the existence of concentration and temperature gradients between the catalyst and its surroundings fluid stream. To avoid mass- and

heat-transfer effects most catalysis studies are conducted in flow systems that resemble such commercial processes as fixed bed, fluid bed, and continuous stirred-tank reactors (CSTR). Recycle reactors systems which approximate CSTR behavior by employing either external or internal recirculation are probably the most useful for obtaining catalytic kinetic data. The CSTR behavior (perfect mixing) can be achieved in a recycle reactor only if the recycle ratio is greater than 25.

The Robinson-Mahoney “micro” stationary catalyst basket reactor employ internal recycle (recycle ratio higher than 60) to minimize physical effects. In this type of reactor, the reactant mixture moves through a small amount of stationary catalyst (see Figure 5-5). This type of reactor is mainly employed for liquefaction, hydrotreating and catalyst testing where the reactants are liquid/solids or gas/liquid/solids.

Hydrogenation runs were carried out in this type of reactor which has the catalyst held in an annular basket made of mesh screens with baffles inside and outside the basket to prevent vortexing. Recycle flow was delivered by a variable-speed stirring-shaft, which created a flow through the basket to the reactor wall for upward/downward deflection. Because of the large fan speeds used (up to 105 rad/s), well mixed conditions prevailed.

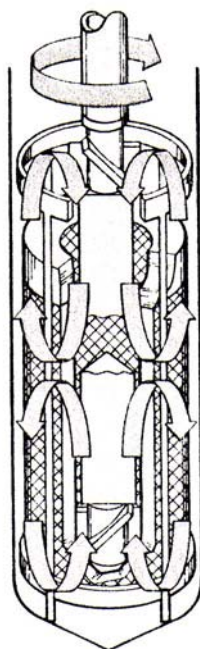


Figure 5-5: Robinson-Mahoney “micro” stationary catalyst basket reactor (Robinson, 1986).

Because the gradientless reactor permits reaction studies at isothermal conditions with uniform concentrations, it eliminates the need for integral or partial-differential

equations. Instead, each steady-state experiment with integral conversion yields a reaction rate that is simply calculated from the ordinary differential equation:

$$\frac{W}{F} = \frac{X_0 - X_i}{r_p} \quad (5.1)$$

where r_p is the global rate of reaction per unit mass of catalyst, F is the feed rate of reactant, W is the mass of catalyst, X is the concentration of the reactant, and subscripts 0 and i refer to outlet and inlet concentration.

5.4.4 Modifications Made to the Supercritical Flow Apparatus.

A number of improvements were carried out by modifying the experimental setup with respect to the beginning of the research. The MagneDrive agitator speed was limited to 300 rad/s for safety reasons due to high operating pressures and temperatures. All electrical equipment in the system was changing by non-sparking equipments in order to avoid the risk of fire and explosion.

Several devices were tested for measuring and controlling hydrogen feed without success until the Brooks mass controller because employed hydrogen flow was too small at high pressure. The expansion of the effluent to atmospheric pressure was problematic too because the valve became frozen lead to system plug. On the other hand, employed expansion valves were too high for controlling the total flow of the reactor mixture. The solution was using an external heated micrometering needle valve by Autoclave Engineers.

In order to improve the mixing of sunflower oil with the SC solvent (propane or DME) at high pressure, a static mixer by Kenics was inserted in line after making the determination of the mixing elements needed to improve the mixing efficiency.

The most relevant was the change of the reactor material.

5.4.4.1 The Replacement of the Reactor.

During the preliminary blank runs, catalytic activity of the reactor was observed. Comparing experiments with and without catalyst, up to 6% of total yield was attributed to the reactor wall because the reactor was made of Hastelloy C-275, an alloy which is rich in nickel, a metal that can catalyze the hydrogenation reaction.

To avoid this reactor-wall effect, the reactor body had to be fabricated with the same dimensions of that of Autoclave Engineers using another material which not only did

not catalyze the reaction but also was resistant to the particular process conditions: high pressure (up to 25 MPa), high temperature (up to 500.15 K), high stirring speed (up to 205 rad/s) and the presence of hydrogen.

At elevated temperatures and significant partial pressures, hydrogen will penetrate carbon steel, reacting with the carbon in the steel to form methane. The pressure generated causes a loss of ductility (hydrogen embrittlement) and failure by cracking or blistering of the steel. The removal of the carbon from the steel (decarburization) results in decreasing strength. Resistance to this type of attack is improved by alloying with molybdenum or chromium because the former improves strength at elevated temperatures and the latter improves the hardness as well as increases corrosion resistance (Perry, 1984).

Accepted limits for the use of carbon and low steels are shown in Figure 5-6, which is adapted from American Petroleum Institute (API) Publication 941, *Steels for Hydrogen Service at Elevated Temperature and Pressures in Petroleum Refineries and Petrochemical Plants*.

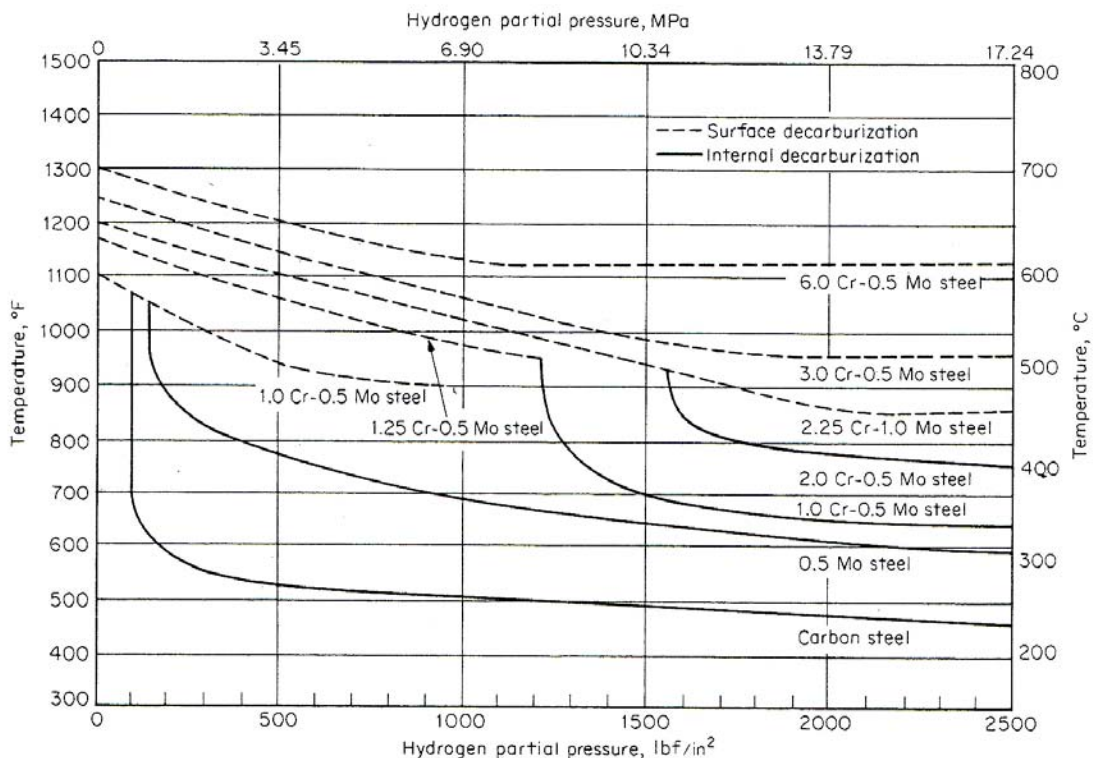


Figure 5-6: Operating limits for steels in hydrogen service. Each steel is suitable for use under hydrogen-partial-pressure-temperature conditions below and to the left of its respective curve (Perry, 1984).

The reactor material chose for hydrogen service was an improved carbon steel (F-126) alloyed with small quantities of molybdenum and chromium. The composition and the mechanical properties of F-126 steel are presented in Table 5-2.

Table 5-2: F-126 steel characterization.

Composition %							Mechanical Properties [†]			
C	Mn	Si	P (max)	S (max)	Cr	Mo	Hardness HB	Elongation %	Yield Strength (MPa)	Tensile Strength (MPa)
0.3- 0.4	0.4- 0.7	0.1- 0.35	0.035	0.035	0.9- 1.5	0.2- 0.4	260-380	45	882- 1074	>900

[†] Typical room-temperature properties

Later blank runs showed no catalysis due to the wall of the new nickel-free vessel.

5.4.5 Standard Operating Procedure for the Supercritical Continuous Flow Apparatus.

This Section describes the general operating procedures which were employed to carry out reactions using the supercritical continuous flow apparatus described in Section 5.4.3.

The day before to the reaction, a known amount of catalyst was loaded within the reactor; the charged reactor was then fitted into the apparatus and the activation procedure was carried out. Before starting, the fume cupboard was turned on.

1. All the power supplies to the apparatus were turned on as well as the heating (pre-heater, reactor jacket and expansion valve) and cooling devices. The SC solvent pump must be left on for at least 20 minutes to allow the refrigerator of the pump to liquefy the solvent. In the meantime, the heating/cooling devices were ready.
2. The system pressure regulator (located in solvent line after piston pump) was kept half open. The expansion valve was nearly closed.
3. The CO₂ cylinder was opened as well as on-off valve and the pump was turn on. Solvent pressure was raised to approximately 5-10 MPa above the required reaction pressure. The solvent was into the system. The pressure regulator was then adjusted slowly to the operating pressure.
4. The expansion valve was opened to set the required gas flow rate on the flow meter.

5. After 30 minutes when desired operating conditions (total pressure, reactor temperature and gas flow rate) were reached and stable, the air compressor was turned on. The hydrogen cylinder valve was open and hydrogen pressure was regulated at 1 MPa. Immediately, the gas-booster system compresses the hydrogen to 25 MPa.
6. When the reservoir with hydrogen was full, the pressure of hydrogen is regulated to 1 MPa above the required reaction system. Next, the on-off valve was open. The mass-flow indicator controller was turned on and the flow rate was set up. Hydrogen was entering slowly into the system.
7. After 10 minutes without fluctuations in operating conditions, the HPLC pump was primed with the liquid sunflower oil and the desired flow rate was set.
8. The reaction was started by turning on the HPLC pump and by opening the on-off valve to allow the organic substrate to flow through the reactor.
9. After noticing the small increment of temperature in the reactor, the operating conditions (reactor temperature, reactor pressure and flow rates) were observed for at least 30 minutes.
10. Once the first product was detected, sample collection was started. Samples were then collected every 20 minutes approximately.
11. The first two samples were discarded to give the reaction system time to reach a steady state and therefore the first of sample will not be representative of the bulk sample.
12. After the collection of six fractions under constant reaction conditions, the reaction parameters can be altered.
13. Once the reaction was finished, the starting materials were switched off by turning off sunflower oil pump as well as hydrogen mass flow indicator controller. Then their respectively on-off valves were closed. The heating/cooling controller devices were switched off. The solvent was flowed for at least 30 minutes; this was to flush any remaining organic material out of the reactor system.
14. After this time, the solvent pump was switched off and the expansion valve was fully open in order to release the pressure from the equipment.

15. The solvent cylinder valve was closed and all the power supplies were switched off.

5.5 Analytical Techniques.

Knowledge of the composition of fats and oils is very important in nearly every phase of fat chemistry and technology although, often, its importance is not fully realized. In fact, progress in the utilization of commercial fats and oils as raw materials in the manufacture of useful products is dependent to a large degree on knowledge of the composition of the starting material and the products derived from it. Methods for determining the composition of fats and oils are important not only because of the fatty acids contents and the pattern of glyceride distribution elaborated by plants and animals, but also because the physical character and end-use performance of fats and oils are directly related to composition.

Catalytic hydrogenation rates were calculated by measuring the decrease in iodine value (IV) using the Wijs titration method following AOCS Official Method Cd 1-25. Fatty acid compositions of the resultant products were determined on a silver-ion column (Varian, Madrid, Spain) in an HPLC system (Waters, Spain) using the isocratic method as described by Adlof (1994). The HPLC analysis was performed on the methyl ester form of the samples. Methyl esters were prepared by the method described in AOCS Official Method Ce 2-66. Occasionally melting points of products were occasionally determined using differential scanning calorimetry (Piris 1 DSC Perkin-Elmer, Spain).

5.5.1 Iodine Value.

The iodine value is a simple and rapidly determined chemical constant for a fat and oil. It is a valuable characteristic in fat analysis, which measures unsaturation but does not define the specific fatty acids. Iodine value analyses are very accurate and provide near theoretical values, except in the case of conjugated bonds or when the double bond is near a carboxyl group. Even with inadequacies, iodine value is a useful tool for process control and product specifications.

Iodine value is defined as the grams of iodine that, added to 100 grams of the fat or oil sample, or in other words, the weight percentage of iodine based on the weight of the sample, adds to the sample. Determination of the iodine value is carried out following AOCS method Cd 1-25 (See Appendix H).

5.5.2 Preparation of Methyl Esters of Fatty Acids.

This procedure (AOCS Official Method Ce 2-66) was employed for preparing methyl esters from the fat or oil sample for further analysis by HPLC using the isocratic method (Adlof, 1994). For further details about AOCS Official Method Ce 2-66 can be found in Appendix H. The sample weight employed was 350 mg because this is the smallest sample amount needed to analyze by gas chromatography (French Standard, NF T 60-233, 1977). Before starting the methylation of esters contained in the sunflower oil, this weight of sample was diluted in heptane until reach an approximate fatty material concentration of 7 wt %.

5.5.3 Silver ion High-Performance Liquid Chromatography.

Fatty acid compositions of the resultant products were determined on a silver-ion column (Chromspher 5 lipids CP28313, Varian, Madrid, Spain) in an HPLC system (Waters, Spain) using the isocratic method described by Adlof (1994). The advantage of the HPLC method over the GC method is that it allows a more complete separation of the *cis* and *trans* C18:1 isomers (López, 2002).

The HPLC equipment consisted of a Waters 515 HPLC pump, a Rheodyne injector (7125) with a 20 μ l injection loop and a Waters 2487 dual λ absorbance detector (210 nm). The ChromSper 5 Lipids column (250 mm x 4.6 mm I.D. stainless steel; 5 μ m) was used as received. The elution solvent was heptane/acetonitrile 99.7:0.3% v/v (both HPLC grade from Panreac, Spain). Solvent flow was standardized at 1.0 ml/min and run temperatures at 295.15-296.15 K. A small furnace (Waters 038040) was used to minimize column temperature fluctuations.

The samples after the preparation of methyl esters were injected immediately. To carry out qualitative and quantitative analysis using HPLC, the equipment must be calibrated using standards of known concentrations of all the components of the reaction mixture (see Figure 5-7). The external standards (Fluka, Spain) provided very useful information, such as the retention times at which the compounds are eluted, and also the relationship between the concentration and the area % on the chromatogram. The calibration curves are shown in Figures 5-8a to 5-8d.

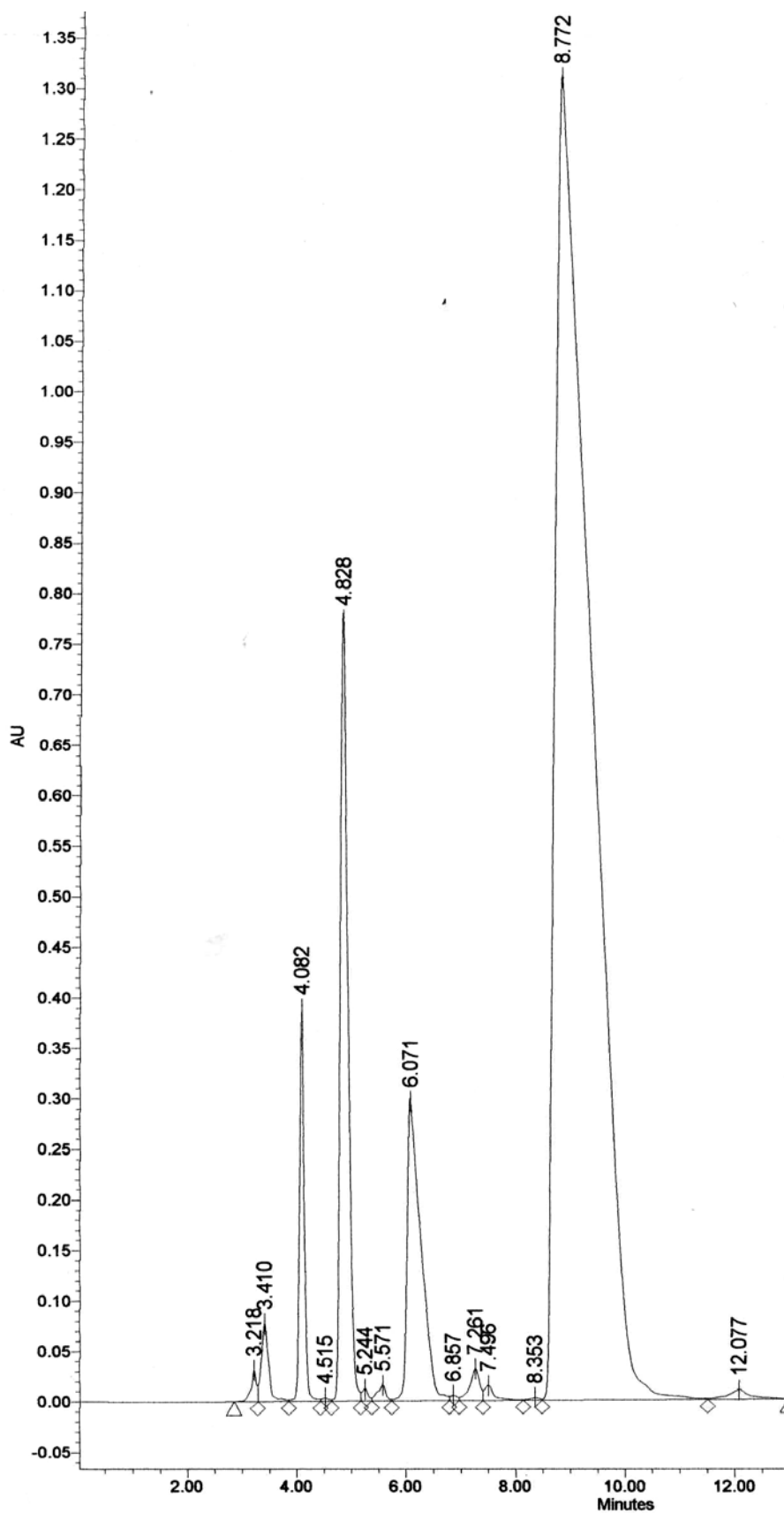


Figure 5-7: Separation of fatty acid methyl ester standards of known concentrations.

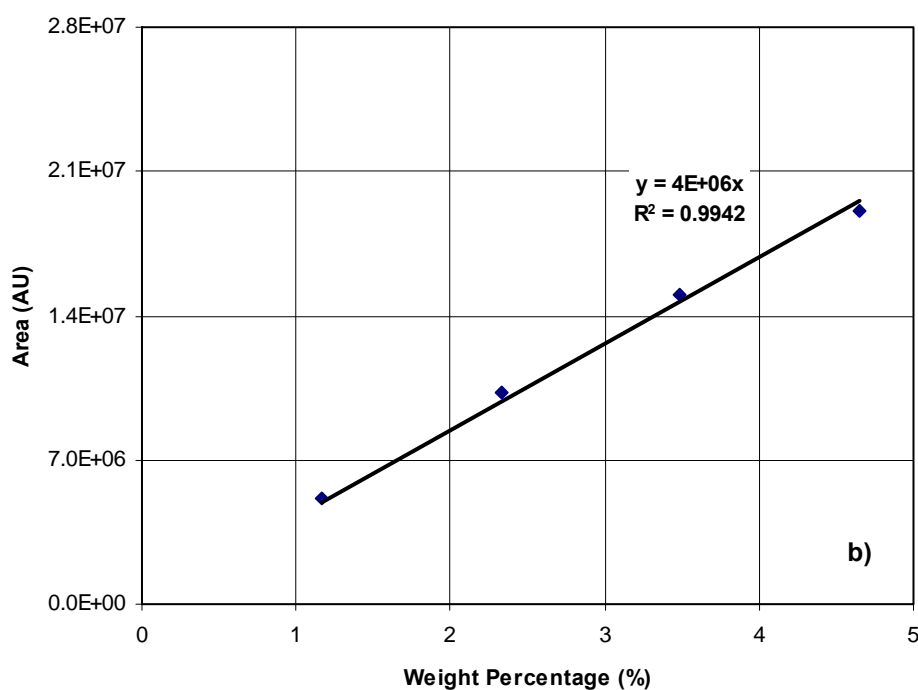
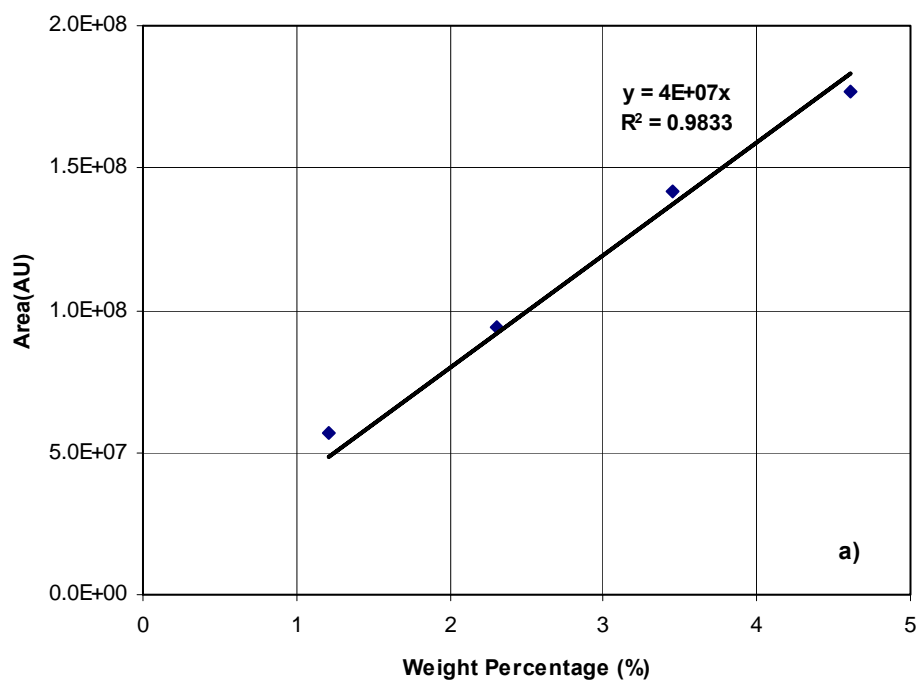


Figure 5-8: Calibration curves for main components of sunflower oil using HPLC (210 nm). a) Methyl linoleate and b) Methyl oleate.

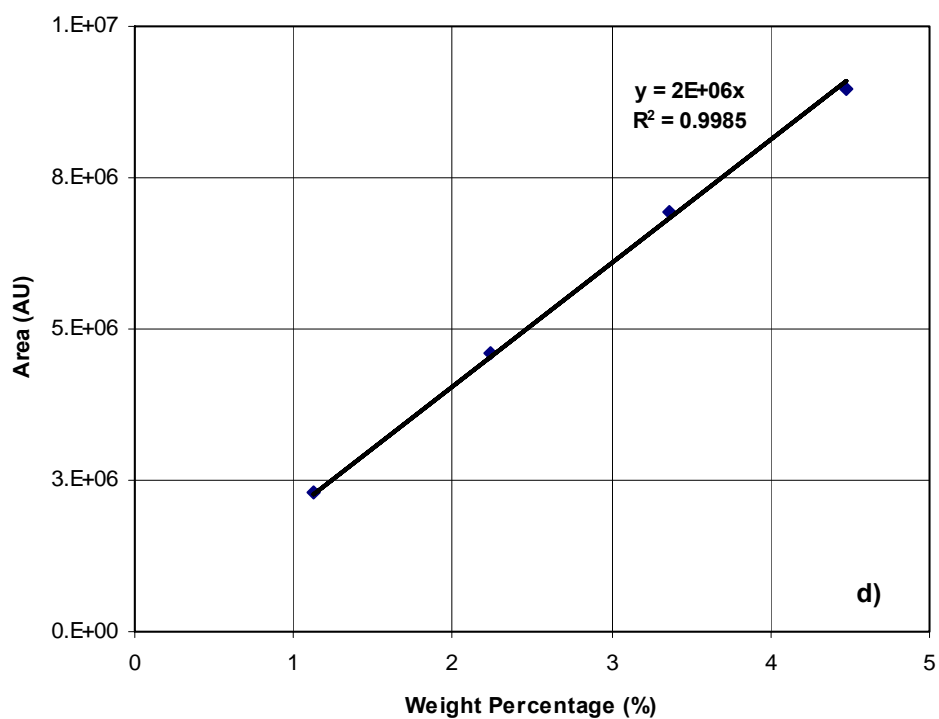
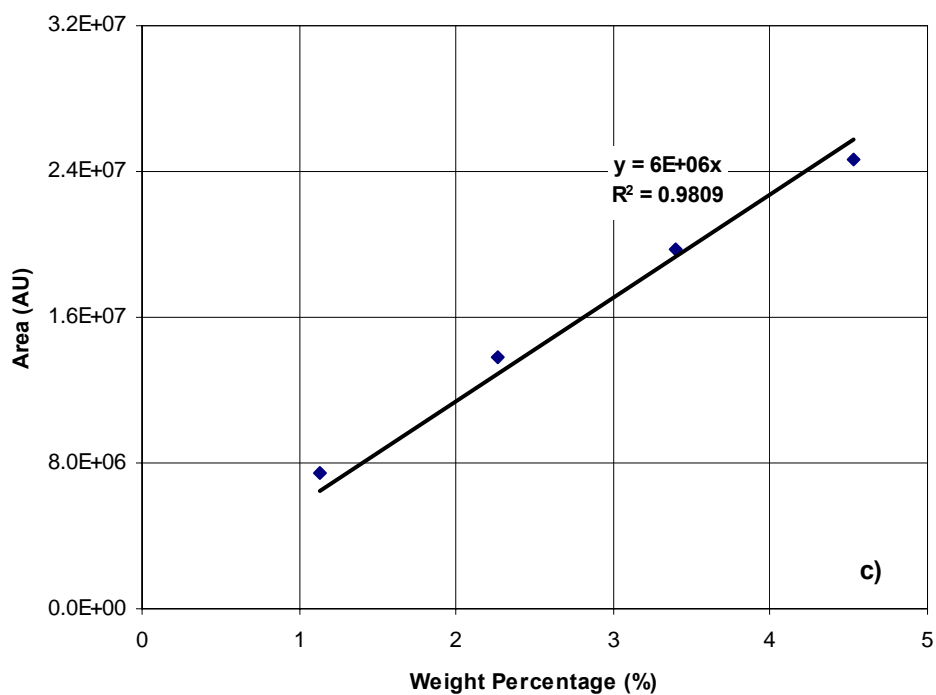


Figure 5-8: Calibration curves for main components of sunflower oil using HPLC (210 nm). c) Methyl elaidate and d) Methyl stearate.

The following example show how the calculations were carried out for all the reactions described in this thesis. The final compositions were calculated for the sunflower oil raw material using the calibration curves and the equation as follows:

$$\text{weight percentage of } i \text{ (\%)} = \frac{\text{area of } i}{\text{calibration curve slope of } i} \times \frac{100}{7} \quad (5.2)$$

The reason of multiply by 100 and divide by 7 is to obtain the real product composition because the original sample for analyzing was diluted 7 times (see Section 5.5.2).

Equation 5.2 was applied for all components but methyl linoleate. This compound presents a strong absorbance in the wavelength (210 nm) used, this fact leads to the detector saturation. For this reason, its determination was made with a sample diluted 10 times more. In this case, the division was by 0.7 instead of 7.

Figure 5-9 presents the separation of FAMES contained in sunflower oil raw material. As can be noticed, this chromatograph presents a lot of peaks without previous identification. This fact is due to the HPLC ChromSpher Lipids column separates fatty acids by positional isomers as well as by degree of unsaturation in isocratic elution mode. For example, in the case of *cis* C18:1, the column separates this compound in its isomers n12, n9, and n7 as shows Figure 5-9. This fact could lead to lack of precision in quantitative analytical determination.

Table 5-3 shows retention times, areas and weight percentages of sunflower oil components.

Table 5-3: Chromatographic analysis of sunflower oil raw material.

Compound	Retention Time (min)	Area (AU)	wt %
Methyl Sterarate	4.273	1105069	7.88
Methyl Elaidate	5.130	40968	0.01
Methyl Oleate	5.738-6.272	6658821	21.16
Methyl Linoleate	8.558	1780901	63.60

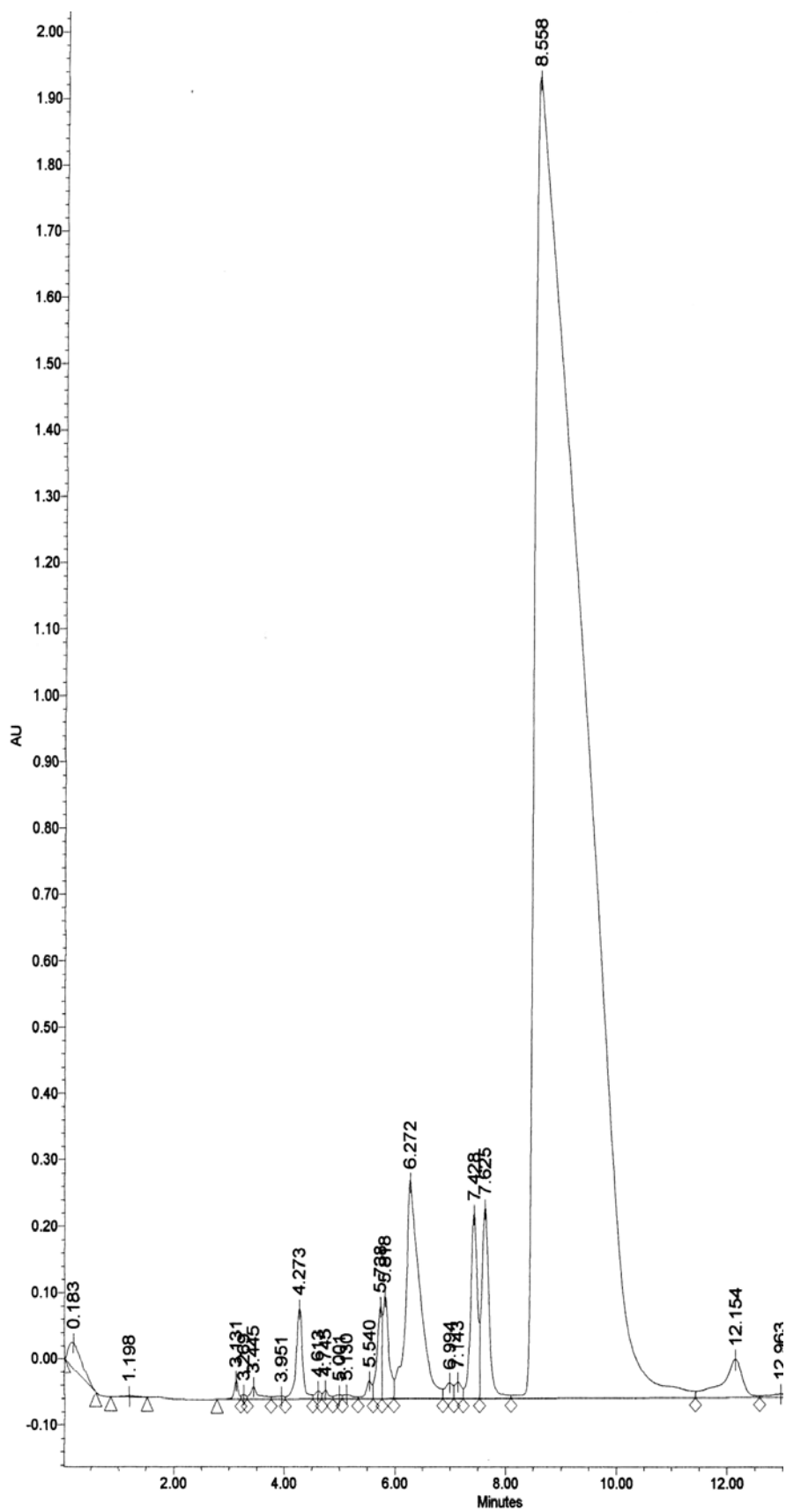


Figure 5-9: Separation of fatty acid methyl esters of sunflower oil before hydrogenating.

5.6 Nomenclature.

F	feed rate of reactant [mol/s]
P	pressure [MPa]
Q-rate	volumetric rate [ml/min] or [l/h]
r_p	global rate of reaction per unit mass of catalyst
T	temperature [K]
W	mass of catalyst [kg]
X	concentration of the reactant [mol/m ³]

Acronyms

AOCS	American Oil Chemist's Society
AE	Autoclave Engineers
C ₃ H ₈	propane
C14:0	myristic fatty acid
C16:0	palmitic fatty acid
C16:1	palmitoleic fatty acid
C18:0	stearic fatty acid
C18:2	linoleic fatty acid
C18:3	linolenic fatty acid
<i>cis</i> C18:1	oleic fatty acid
C20:0	arachidic fatty acid
C20:2	eicosadienoic fatty acid
C	carbon

CO ₂	dioxide carbon
DME	dimethyl ether
H ₂	hydrogen
HPLC	high-performance liquid chromatography
I.D.	internal diameter
IV	iodine value [g I ₂ /100 g oil]: 1 IV =36 mol H ₂ /m ³ oil
LEL	lower explosive limit
N	nitrogen
Pd	palladium
SC	supercritical
STP	Standard temperature and pressure
<i>trans</i> C18:1	elaidic fatty acid

Sub- and Superscripts

0	outlet concentration
i	inlet concentration.
max	maximum
N	normal

Chapter Six

Conclusions and Prospects for Further Investigations.

- The capability of the Peng-Robinson (PR) equation of state in combination with the one-fluid Van der Waals-1 mixing rules to model sunflower oil/H₂/SCF systems was studied. The results suggest that this method can be used as an adequate phase equilibrium predictive tool to explore the SC solvent properties and phase equilibrium behavior of the reactive mixture over a wide range of conditions. However, direct experimental evidence for phase equilibrium was not developed.

With the VLE predictions from PR-EOS and taken into account some experimental considerations, it is possible to determinate in a simple way the range of feasible operating conditions that guarantee the existence of a single fluid phase in the reactor.

- The hydrogenation–isomerization network employed for determining the kinetics seems not very sensitive to k_{24} and k_{34} values. A possible explanation is that the conversion reached in the kinetic studies is less than that expected for selective partial vegetable oil hydrogenation (around 50%) which leads to the conclusion that kinetic constants for stearic ester formation might be incorrect. For further investigations, it should be taken into account an increase in the conversion range in order to obtain hydrogenation kinetics more accurate.
- For the same degree of hydrogenation (IV=95-110), the *trans* content obtained in the experimental runs in DME using Pd/Al₂O₃ as catalyst was similar than that obtained in the case of the hydrogenation reactions over Pd/C and using propane as solvent whereas the stearic content was slightly lower (<2.7) as well as the overall hydrogenation rate. These facts were possibly derived from the type of catalyst employed in each case.

Support type and micropores size distribution in Pd/C catalyst can lead to an increase of saturated compounds production because of spillover of the species as well as possible presence of pore diffusional resistance as suggested by Coenen (1986). In the case of eggshell Pd/Al₂O₃, the support is less adsorptive than activated carbon and its mesopores size distribution as well as the metal

location minimize diffusion resistance, common in the processing of large organic molecules, making this catalyst slightly more selective.

- It is worth mentioning the great potential that SC hydrogenation exhibits compared to the conventional low-pressure hydrogenation process, as it allows to obtain a product with a potential application in food industry with lower *trans* fatty acid content (3 wt%) and having similar final IV value ($90 < IV < 110$) by properly tuning the reaction conditions. The level of saturated species is slightly elevated compared to the levels found in commercial shortening basestocks. These facts are particularly attractive since lower *trans* and saturates contents in foodstuffs have an appeal to a health-conscious public.
- Despite of the fact that the hydrogenation experimental conditions described in this study offer a potential versatility in producing different hydrogenated products with a potential use for margarine or shortening, it is necessary to develop a simultaneous study on how this operating hydrogenation conditions affects physical end product properties (e.g. plasticity, melting behavior, etc.). In this way, it would be possible to optimize reaction conditions to produce an array of products having different physical and chemical properties.
- The study of intraparticle diffusivity of triglycerides and hydrogen under SC hydrogenation reaction conditions allowed to determine the effective diffusion coefficients in the porous catalyst particle. For hydrogen, diffusion properties and tortuosity factors are normal. However, for triglycerides the ratio of D_e/D is larger than unity. This is interpreted in terms of surface diffusion for the heavier oil components that they tend to be adsorbed/desorbed to the pore walls and hence diffuse along them in a parallel path to bulk pore diffusion.

As a consequence, the tortuosity factor for triglycerides is expected to be less than unity when surface diffusion is significant (Smith, 1981). In this study, this tortuosity could not be determined because the overall effective diffusivity (D_e) is a result of the combination of two effects: (a) a pore volume or bulk diffusion and (b) a surface migration contribution. In order to determine more accurately surface diffusion coefficient (D_s), it would be necessary to use a model based on both, pore-volume and surface transport, in a similar way to that Komiyama and Smith (1974) have employed, as well as to measure adsorption rate data under several operating conditions.

- The large effect of temperature on $(\rho_p K_A D_s)/D$ ratio rather than pressure suggests that adsorption of reactants on the catalyst, controls diffusion, so that surface migration would be a key mechanism for diffusion in pores filled with a supercritical fluid, at least for heavy solutes (MW>800).
- Despite of the fact that linoleate selectivity (S_i) for SC continuous single-phase hydrogenation of sunflower oil over supported Pd is slightly lower than that reported for conventional low-pressure process (> 10), the SC single-phase process exhibits a great potential due to promising results previously reported and also due to the following advantages:
 - The product quality can be dramatically improved e.g. much lower *trans* fatty acid content with a slightly increase in saturates has been achieved. The low specific isomerization (S_i) value obtained for SC process supports this idea.
 - Reaction rates have been enhanced compared to those for conventional low-pressure process due to the presence of a single-phase reactive mixture into the reactor.
 - Reaction times in the scale of seconds improves productivity compared to conventional process; therefore continuous small reactors are suitable for this type of reactions which allows process intensification and increases safety compared to high pressure equipment.
 - The presence of a SCF as reaction solvent makes possible to control the temperature in the reactor despite of the exothermic character of hydrogenation reactions and high reaction rates because the solvent acts as an internal cooling medium. At the same time, SCF can improve the catalyst life. This means reduced consumption of catalyst and reduced production costs.
 - Although noble-metal catalysts may appear to be cost-prohibitive, their extremely high activities, their more selective character as well as the possibility of recycling may offset the cost limitation and could be a viable alternative to Ni.

- A non-toxic product is obtained by means of easy separation of the product from the supercritical fluid just by reducing the pressure in the reactor effluent stream.
- Based on the determination of the SC hydrogenation kinetics free of external and pore diffusional resistances in the gradientless reactor, a formal analysis of the process in a catalytic integral reactor should be undertaken in order to determine which reactor/catalyst should be used in an industrial scale to take advantage of the full reaction rate and the potential selectivities. On the other hand, solvent recovery must be developed for scale-up as the economy of the whole high-pressure process is an important aspect to take into consideration when the feasibility is under study.

Chapter Seven

Bibliography.

Abaroudi, K., F. Trabelsi, B. Calloud-Gabriel, and F. Recasens, "Mass Transport Enhancement in Modified Supercritical Fluid", *Ind. Eng. Chem. Res.*, 38, 3505 (1999).

Adlof, R. O., "Separation of *cis* and *trans* Unsaturated Fatty Acid Methyl Esters by Silver Ion High-Performance Liquid Chromatography," *J. Chromatogr. A.*, 659, 95 (1994).

Albright, L. F., and J. Wisniak, "Selectivity and isomerization during partial hydrogenation of cottonseed oil and methyl oleate: Effect of operating variables", *J. Am. Oil Chem. Soc.*, 39, 14 (1962).

Albright, L. F., *Chem. Eng.*, 9, 197 (1967).

Albright, L. F., *Modern Chemical Technology*, a reprint from *Chemical Engineering*, McGraw-Hill, New York (1967).

Albright, L. F., "Quantitative Measure of Selectivity of Hydrogenation of Triglycerides", *J. Am. Oil Chemists' Soc.*, 42, 250 (1965).

Allen, R. R., *Hydrogenation*, in *Bailey's Industrial Oil and Fat Products*, 4th edition, ed. D. Swern, Wiley, New York (1982).

Allen, R. R., "Hydrogenation", *J. Am. Oil Chem. Soc.*, 58, 166 (1981).

Allen, R. R. and, A. A. Kiess, "Isomerization during hydrogenation. I. Oleic acid", *J. Am. Oil Chemists' Soc.*, 33, 355 (1956).

Ambrose, D., "Correlations and Estimation of Vapor-Liquid Critical Properties I: Critical Temperatures of Organic Compounds", National Physical Laboratory, Teddington, NPL Rep. Chem.92, September 1978, corrected March 1980.

Ambrose, D.:"Correlations and Estimation of Vapor-Liquid Critical Properties II: Critical Pressures and Volumes of Organic Compounds", National Physical Laboratory, Teddington, NPL Rep. Chem.99 (1979).

Amelse, J. A., and N. A. Kutz, United States Patent 030788, Amoco Corporation, Chicago, Illinois (1991).

American Oil Chemists' Society, Official Methods and recommended practices of the AOCS, 5th Edition, American Oil Chemists' Society, Champaign (1998).

Anderson, N. G., "Practical Use of Continuous Processing in Developing and Scaling Up Laboratory Processes", *Org. Proc. Res. Dev.*, 5, 613 (2001).

Andersson, K., M. Hell, L. Löwendahl, and N. H. Shöön, "Diffusivities of Hydrogen and Glyceryl Trioleate I Cottonseed Oil at Elevated Temperature", *J. Am. Oil Chem. Soc.*, 51, 171 (1974).

Andersson, M. B. O., J. W. King, and L. G. Blomberg, "Synthesis of fatty alcohol mixtures from oleochemicals in supercritical fluids", *Green Chem.*, 2, 230 (2000).

Applegate, A. D. and MINITAB Inc, MINITAB release 13, MINITAB Inc, State College, PA (1996).

Arunajatesan, A., B. Subramaniam, K. W. Huntchenson, and F. Herkes, "Fixed-bed hydrogenation of organic compounds in supercritical carbon dioxide", *Chem. Eng. Sci.*, 56, 1363 (2001).

Arunajatesan, V., K. A. Wilson, and B. Subramaniam, "Pressure Tuning the Effective Diffusivity of Near-Critical Reaction Mixtures in Mesoporous Catalysts", *Ind & Eng Chem. Res.*, 2004.

Baiker, A., "Supercritical Fluids in Heterogeneous Catalysis", *Chem. Rev.*, 99, 453 (1999).

Bailey, A. E., "Theory and Mechanism of the Hydrogenation of Edible Oils", *J. Am. Oil Chem. Soc.*, 26, 596 (1949).

Baptist-Nguyen, S., and B. Subramaniam, "Coking and Activity of Porous Catalysts in Supercritical Reaction Media", *AIChE J.*, 38 (7), 1027 (1992).

Beckman, E. J., "Green chemical processing using CO₂", *I&ECR*, 42, 1598 (2003).

Bern, L., M. Hell, and N. H. Schöön, "Kinetics of Hydrogenation of Rapeseed Oil:I. Influence of Transport Steps in Kinetic Study", *J. Am. Oil Chem. Soc.*, 52, 182 (1975).

Bertucco, A., P. Canu, and L. Devetta, "Catalytic Hydrogenation in Supercritical CO₂: Kinetic Measurements in a Gradientless Internal-Recycle Reactor", *Ind. Eng. Chem. Res.*, 36, 2626 (1997).

Boelhouwer, C., P. M. Heertjes, J. P. W. Houtman, J. Van Steenis, and H. I. Waterman, "Hydrogenation Mechanism", *Rec. trav. Chim.*, 69, 771 (1950).

Bohnen, L. J. M., "Update & Review of Dimethylether Propellant, 1986," *Aerosol Age*, 1 (9), 30 (1986).

Bohnen, L. J. M., "Dimethylether Pure—A Review," *Aerosol Age*, 26, 1, 26 (1981).

Box, G., and N.R. Draper, *Empirical Model-Building and Response Surfaces*, J. Wiley, New York (1987).

Box, G., W. G. Hunter and J. S. Hunter, *Statistics for experimenters. An Introduction to Design, Data Analysis and Model Building*, John Wiley & Sons, New York (1978).

Brake, C., D. Richter and E. Weidner. "Thermodynamic study of the hydrogenation fatty acid esters in presence of supercritical fluids", *Proceedings of 4th International Symposium on High Pressure Process Technology and Chemical Engineering*, Venice, Italy, electronic document, (2002).

Brunner, G., (ed.), *Supercritical Fluids as Solvents and Reaction Media*, Elsevier, Amsterdam, The Netherlands (2003).

Brunner, G, *Gas Extraction- An introduction to fundamentals of supercritical fluids and the application to separation processes*, Steinkopff and Springer, Germany (1994).

Bryson, T. A., J. M. Jennings, and J. M. Gibson, "A green and selective reduction of aldehydes", *Tetrahedron Lett.*, 41, 3523 (2000).

Bukur, D. B., A. Akgerman, X. Lang, and Z. Feng, "Production of Alpha-Olefins via Fisher-Tropsch Synthesis in Supercritical Propane", *Proceedings of The 4th Italian Conference on Supercritical Fluids and their Applications*, Capri, Italy, p.291 (1997).

Burk, M. J., S. Feng, M. F. Gross, and W. Tumas, "Asymmetric catalytic hydrogenation reactions in supercritical carbon dioxide", *J. Am. Chem. Soc.*, 117, 8277 (1995).

Butt, J. B., *Reaction Kinetics and Reactor Design*, 2nd Edn. Marcel Dekker. Inc., New York (2000).

Catchpole, O. J., and M. B. King. "Measurement and Correlation of Binary Diffusion Coefficients in near Critical Fluids", *Ind. Eng. Chem. Res.*, 33, 1828 (1994).

Cecchi, G., J. Castano, and E. Ucciani, "Catalyse par les métaux précieux en lipochimie. I: hydrogénation de l'huile de soja catalysée par les métaux précieux supportés", *Rev. Fr. Corps. Gras.*, 26, 391, 1979.

Chen, A. H., D. D. McIntire, and R. R. Allen, "Modeling of Reaction Rate Constants and Selectivities in Soybean oil Hydrogenation", *J. Am. Oil Chem. Soc.*, 58, 816 (1981).

Chouchi, D., D. Gourgouillon, M. Courel, J. Vital, and L. Nunes da Ponte, "The Influence of Phase Behavior on Reactions at Supercritical Conditions: The Hydrogenation of α -Pinene", *Ind. & Eng. Chem. Res.*, 40, 2551 (2001).

Chueh, P. L., and J. M. Prausnitz. *AIChE J.* 13: 1099 (1967).

Clark, M. C., and B. Subramaniam, "1-hexene isomerization on a Pt/ γ -Al₂O₃ catalyst: The dramatic effects of feed peroxides on catalyst activity", *Chem. Eng. Sci.*, 51, 2369 (1996).

Clark, M. C., and B. Subramaniam, "Extended Alkylate Production Activity during Fixed-Bed Supercritical 1-Butene/Isobutane Alkylation on Solid Acid Catalysts Using Carbon Dioxide as a Diluent", *Ind. Eng. Chem. Res.*, 37, 1243 (1998).

Clark, M.C., and B. Subramaniam, "Kinetics on a Supported Catalyst at Supercritical, Non Deactivating Conditions", *AIChE J.*, 47(7), 1559 (1999).

Clifford, A. A., *Fundamentals of Supercritical Fluids*, Oxford University Press, Oxford (1998).

Coenen, J. W. E., "Catalytic Hydrogenation of Fatty Oils", *Ind. Eng. Chem. Fundam.*, 25, 43 (1986).

Colen, G. C. M., G. Van Duijn and H. J. Van Oosten, "Effect of Pore Diffusion on the Triacylglycerol Distribution of Partially Hydrogenated Trioleoylglycerol", *App. Cat.*, 43, 339 (1988).

Collins, N. A., P. G. Debenedetti, and S. Sundaresan, "Disproportionation of toluene over ZSM-5 under near-critical conditions", *AIChE J.*, 34, 1211 (1998).

Coorens, H. G. A., C. J. Peters, and J. Swaan Arons, "Phase equilibria in binary mixtures of propane and tripalmitin", *Fluid Phase Equilib.*, 40, 135 (1998).

Cordova, W. A. and P. Harriot, "Mass Transfer Resistances in the Palladium-Catalyzed Hydrogenation of Methyl Linoleate", *Chem. Eng. Sci.*, 30, 1201 (1975).

Cussler, E. L., *Diffusion: Mass Transfer in Fluid Systems*, Cambridge Univ. Press, Cambridge, UK, (1997).

Dardas, Z., M. G. Suër, Y. H. Ma, and W. R. Moser, "High-Temperature, High-Pressure in Situ Reaction Monitoring of Heterogeneous Catalytic Processes under Supercritical Conditions by CIR-FTIR", *J. Catal.*, 159, 204 (1996).

De Jong, A., A. Eftaxias, F. Trabelsi, F. Recasens, J. Sueiras, and F. Stüber, "Solvent screening for the supercritical hydrogenation of polyunsaturated hydrocarbons using VLE calculations", *Ind. Chem. Res.*, 40, 3225 (2001).

De la Fuente, J., G. D. Mabe, E. A. Brignole and S. B. Botini, "Phase equilibria in binary mixtures of ethane and propane with sunflower oil", *Fluid Phase Equilib.*, 101, 247 (1994).

Dedrick, R. L. and R. B. Beckman, "Diffusion in porous particles", *Chem. Eng. Prog. Symp. Ser.*, 74, 63 (1967).

Devetta, L., A. Giovanzana, P. Canu, A. Bertucco, and B. J. Minder, "Kinetic experiments and modeling of a three-phase catalytic hydrogenation reaction in supercritical CO₂", *Catal. Today*, 48, 337 (1999).

Devetta, L., P. Canu, A. Bertucco, and K. Steiner, "Modeling of a trickle-bed reactor for a catalytic hydrogenation in supercritical CO₂", *Chem. Eng. Sci.*, 52, 4163 (1997).

Dooley, K. M. and F. C. Knopf, "Oxidation catalysis in a supercritical fluid medium", *Ind. Eng. Chem. Res.*, 26, 1910 (1987).

EC, EC directive 84/344/EEC, 1984.

Edgar, T. F., D. M. Himmelblau and L. S. Lasdon, *Optimization of chemical processes*, 2nd edition, McGrawHill, Singapore (2001).

Eftaxias, A.; F. Trabelsi, F. Recasens, J. Sueiras, and F. Stüber "Preselection of supercritical solvent for hydrogenation reactions via VLE calculations" *Proceedings of II Jornadas de Ingeniería Química*", Tarragona, Spain, p.200 (2001).

Elbid, I. A., and L. F. Albright, "Operating Variables in Hydrogenating Cottonseed Oil", *Industrial and Engineering Chemistry*, 49, 5, 825 (1957).

Engelhard Corporation, *Fats and Oils Manual*, Engelhard Corporation, Iselin, NJ (1992).

Fall, D. J., J. L. Fall, and K.D. Luks, "Liquid-liquid-vapor immiscibility limit in carbon dioxide + n-paraffins mixtures", *J. Chem. Eng. Data*, 32, 201 (1985).

Fan, L. K. Yoshii, S. Yan, J. Zhou, and K. Fujimoto, "Supercritical-phase process for selective synthesis of wax from syngas: Catalyst and process development", *Catal. Today*, 36, 295 (1997).

Fan, L., and K. Fujimoto, *Heterogeneous catalysis in: P. G. Jessop, W. Leitner (Eds), Chemical Synthesis Using Supercritical Fluids*, Wiley-VCH, Weinheim (1999).

Fan, L., I. Nakamura, S. Ishida, and K. Fujimoto, "Supercritical-Phase Alkylation Reaction on Solid Acid Catalysts: Mechanistic Study and Catalyst Development", *Ind. Eng. Chem. Res.*, 36, 1458 (1997).

Fan, L., I. Nakamura, S. Ishida, and K. Fujimoto, "Supercritical-Phase Alkylation on Solid Acid Catalysts: Mechanistic Study and Catalyst Development", *Ind. Eng. Chem. Res.*, 37, 298 (1998).

Fan, L., K. Yokota, and K. Fujimoto, "Supercritical phase Fischer-Tropsch synthesis: Catalyst pore-size effect", *AIChE J.*, 38, 1639 (1992).

Fan, L., S. Yan, and K. Fujimoto, *Chem. Eng. Jpn.*, 30, 557 (1997).

Fan, L., T. Watanabe, and K. Fujimoto, "Reaction phase effect on tertiary butyl alcohol synthesis by air oxidation of isobutane", *Appl. Catal. A*, 158, 41 (1997).

Fan, L., Y. Nakayama, and K. Fujimoto, "Air oxidation of supercritical phase isobutane to tert-butyl alcohol", *Chem. Commun.*, 11, 1179 (1997).

Farrauto, R. J. and C. H. Bartholomew, *Fundamentals of industrial catalytic processes*, Chapman & Hall, Great Britain (1997).

Feng, C. F., and W. E. Steward. "Practical Models for Isothermal Diffusion and Flow of Gases in Porous Solids", *Ind. Eng. Chem. Fun.*, 12, 143 (1973).

Fillion, B., B. Morsi, K. R. Heier, and R. M. Machado, "Kinetics, gas-Liquid Mass Transfer, and Modeling of Soybean Oil Hydrogenation Process", *I&ECR*, 41 (4), 697 (2002).

Fitch Haumann, B., "Hydrogenation, interestification", *INFORM*, 5, 668 (1994).

Florusse, F. L.; C. J. Peters, T. Fornari, S. B. Bottini and E. A. Brignole, "Phase Behavior of the Binary System Near-Critical Dimethylether and Tripalmitin: Measurements and Thermodynamic Modeling", *Proceedings of Fifth Conference on Supercritical Fluids and their Applications*, Garda, Italy, p.611 (1999).

Fornari, T., S. B. Bottini, and E. A. Brignole, "Application of a Group Contribution Equation of State to Mixtures of Supercritical Gases with Natural Fatty Oils and Derivatives," *Latin American Appl. Res.*, 31, 287 (2001).

Freemantle, M., "Cleaning up Hydrogenations", *C & EN*, 28, 30 (2001).

Froment, G. F., and K. B. Bischoff, *Chemical Reactor Analysis and Design*, 2nd Ed. J. Wiley: New York (1990).

Gaffney, A. M., and J. A. Sofranko, *Catalytic Selective Oxidation*, Washington, DC (1992).

Gaffney, A. M., and J. A. Sofranko, United States Patent 5210336, ARCO Chemical Technology, L. P., Wilmington, DE. (1993).

Ganguli, K. L. and H. J. van den Berg, "Measurements of hydrogen-edible oil interfacial area using a homogeneous Zeigler-Natta catalyst in an agitated reactor", *Chem. Eng. J.*, 16, 193 (1978).

Gao, Y., H.-Z. Liu, Y. F. Shi, and W. K. Yuan, "Deactivation in Alkylation of Benzene for Ethylbenzene on Y-type Zeolite under Second Kind Supercritical Condition", *Proceedings of The 4th International Symposium on Supercritical Fluids*, Sendai, Japan, p.531 (1997).

Gao, Y., Y. F. Shi, Z. Zhu, and W. K. Yuan, "Cooking Mechanism of Zeolite for Supercritical Fluid Alkylation of Benzene", *Proceedings of The 3rd International Symposium on High-Pressure Chemical Engineering*, Zurich, Switzerland, p.151 (1996).

Ginosar, D. K., and B. Subramaniam, In *Catalyst Deactivation*; Delmon, B., Froment, G. F., Eds.; Elsevier, New York, (1994).

Ginosar, D. M., and B. Subramaniam, "Olefinic Oligomer and Cosolvent Effects on the Coking and Activity of a Reforming Catalyst in Supercritical Reaction Mixtures", *J. Catal.*, 152, 31 (1995).

González Velasco, J. R., J. A. González de Marcos, M. P. González Marcos, J. I. Gutiérrez Ortiz, and M. A. Gutiérrez Ortiz, *Cinética química aplicada*, Editorial Síntesis, Madrid (1999).

González-Marcos, M. Pilar, José I. Gutiérrez-Ortiz, Cristina González-Ortiz de Elguea, Jon I. Alvarez, Juan R. and González-Velasco, "Control of the Product Distribution in the Hydrogenation of Vegetable Oils over Nickel on Silica Catalyst", *Can. J. Chem. Eng.*, 76, 927 (1998).

Grau, R. J., A. E. Cassano, and M. A. Baltanás, "Kinetics of methyl oleate catalytic hydrogenation with quantitative evaluation of *cis-trans* isomerization equilibrium", *Catal. Rev. Sci. Eng.*, 30, 1 (1988).

Gray, J. I., and L. F. Russell, "Hydrogenation catalysts-Their Effect on selectivity", *JAOCS*, 56, 36 (1979).

Gut, G., J. Kosinka, A. Prabucki, and A. Schuerch, "Kinetics of the Liquid-Phase Hydrogenation and Isomerization of Sunflower Seed Oil with Nickel Catalyst", *Chem. Eng. Sci.*, 34, 1051 (1979).

Hansen, J. B.; B.Voss, F. Joensen, and I. Sigurdardottir, "Large Scale Manufacture of Dimethyl Ethers A New Alternative Diesel Fuel from Natural Gas" SAE Paper No. 950063 (1995).

Härröd, M., and P. Møller, "Hydrogenation of fats and oils at supercritical conditions", *Proceedings of High Pressure Chemical Engineering, Process Technology*, Amsterdam, Netherlands, p.43 (1996).

Härröd, M., and P. Møller, "Hydrogenation of fats and oils at supercritical conditions", *Proceedings of The 3rd International Symposium on High-Pressure Chemical Engineering*, Zurich, Switzerland, p.43 (1996).

Härröd, M., M. Macher, J. Hogberg and P. Moller, "Hydrogenation of lipids at supercritical conditions", *Proceedings of the Fourth Italian Conference on Supercritical Fluids and their Applications*, Capri, Italy, p.319 (1997).

Härröd, M., M. Macher, S. Van den Hark, and P. Moller, "Hydrogenation at supercritical conditions" Proceedings of Fifth Conference on Supercritical Fluids and their Applications, Garda, Italy, p.319 (1999).

Härröd, M., S. Van den Hark, M.-B. Macher and P. Moller, Hydrogenation at supercritical single-phase conditions, In High Pressure Process Technology: Fundamentals and Applications, Eds. Bertucco and Vetter, Elsevier, New York (2001).

Hashimoto, K., K. Muroyama, and S. Nagata, "Kinetics of the Hydrogenation of Fatty Oils", J. Am. Oil Chem. Soc., 48, 291 (1971).

Hashimoto, K., M. Teramoto, and S. Nagata, "Effect of Mass Transfer on the Selectivity in the Hydrogenation of Fatty Oils", J. Chem. Eng. Japan., 4, 150 (1971).

Hashimoto, K., K. Muroyama, and S. Nagata, "Kinetics of the Hydrogenation of Fatty Oils", J. Am. Oil Chem. Soc., 48, 291 (1971).

Hitzler, M. G. and M. Poliakoff, "Continuous hydrogenation of organic compounds in supercritical fluids", Chem. Commun., 17, 1667 (1997).

Hitzler, M. G., F. R. Smail, S. K. Ross, and M. Poliakoff, "Friedel–Crafts alkylation in supercritical fluids: continuous, selective and clean", Chem. Commun., 5, 359 (1998).

Hitzler, M. G., F. R. Smail, S. K. Ross, and M. Poliakoff, "Selective Catalytic Hydrogenation of Organic Compounds in Supercritical Fluids as a Continuous Process", Org. Process Res. Dev., 2 (3), 137 (1998).

Horiuti, J., and M. Polanyi. "Exchange reactions of hydrogen on metallic catalysts", Trans. Faraday Soc., 30, 1164 (1934).

Hougen, O. A., K. M. Watson, and R. A. Ragatz, Principios de los procesos químicos, Vol. 2, Editorial Reverté, S. A., Madrid (1954).

Howdle, S. M., M. A. Healy, and M. Poliakoff. "Organometallic chemistry in supercritical fluids. The generation and detection of dinitrogen and nonclassical dihydrogen complexes of Group 6, 7, and 8 transition metals", J. Am. Chem. Soc., 112, 4804 (1990).

Hsu, N., L. L. Diosady, W. F. Graydon, and L. J. Rubin, "Heterogeneous Catalytic hydrogenation of canola oil using palladium", JAOCS, 63, 1036 (1986).

Hui, Y. H. (ed.), *Bailey's Industrial Oil and Fat Products*, 5th Edn. John Wiley & Sons Inc., New York (1996).

Hyde R., and M. Poliakoff, "Supercritical hydrogenation and acid-catalysed reactions without gases", *Chem. Commun.*, 13, 1482 (2004).

Hyde, J. R., P. Licence, D. N. Carter, and M. Poliakoff, "Continuous catalytic reactions in supercritical fluids", *Appl, Catal, A-Gen.*, 222, 119 (2001).

Applegate, A. D. and MINITAB Inc, MINITAB release 13, MINITAB Inc, State College, PA (1996).

Hyprotech Ltd., HYSYS 2.4.1 Build 3870, USA (1995).

J. Garcia, E. Garcia-Verdugo, E. Ramírez, P. Hamley and M. Poliakoff. "Sodium formate and Formic acid: Green Feedstock for Hydrogenation. Screen of different compounds", *Proceedings of Green Solvent for Synthesis, Bruchsal, Germany*, p.56 (2004).

Jessop, P. G. and W. Leitner, *Chemical Synthesis Using Supercritical Fluids*, Wiley-VCH, Weinheim (1999).

Jessop, P. G., T. Ikariya, and R. Noyori, "Homogeneous catalytic hydrogenation of supercritical carbon dioxide", *Nature*, 368, 231 (1994).

Jessop, P. G., Y. Hsiano, T. Ikariya, R. Noyori, "Homogeneous Catalysis in Supercritical Fluids: Hydrogenation of Supercritical Carbon Dioxide to Formic Acid, Alkyl Formates, and Formamides", *J. Am. Chem. Soc.*, 118, 344 (1996).

Joback, K. G., S. M. thesis in chemical engineering, Massachusetts Institute of Technology, Cambridge, Mass. (1984).

Johnson, M. F. L., and W. E. Stewart. "Pore structure and gaseous diffusion in solid catalysts", *J. Catalysis*, 4, 248 (1965).

Jonker, G. H., J. W. Veldinsk, and A. A. C. M. Beenackers, "Intrinsic of 9-monoenic Fatty Acid Methyl Esters Hydrogenation over Nickel-based Catalyst", *Ind. Eng. Chem. Res.*, 36, 1567 (1997a).

Jonker, G. H., J. W. Veldsink, and A. A. C. M. Beenackers, "Intraparticle Diffusion Limitations in the Hydrogenation of Monounsaturated Edible Oils and Their Fatty Acid Methyl Esters", *Ind. Eng. Chem. Res.*, 37, 4646 (1998).

Kelley, F.D., and E.D. Chimowitz, "Near-Critical Phenomena in Supercritical Fluid Chromatography", *AIChE J.*, 36, 1163 (1990).

King, J. W., R. L. Holliday, G. R. List and J. M. Snyder, "Hydrogenation of vegetable oils using mixtures of supercritical carbon dioxide and hydrogen", *JAOCS*, 78 (2), 107 (2001).

Klen, T., and S. Shulz, "Measurements and model prediction of vapor-liquid equilibria of mixtures of rapeseed oil and supercritical carbon dioxide", *Ind. Eng. Chem. Res.*, 28, 1073 (1989).

Knaff, G., and E.U. Schlünder, "Mass Transfer for Dissolving Solids in Supercritical Carbon Dioxide, Part I. Resistance of the the Boundary Layer", *Chem. Eng. Process*, 21, 151 (1987).

Koriyama, H. and J. M. Smith "Intraparticle Mass Transport in Liquid-Filled Pores", *AIChE J.*, 20, 4, 728 (1974).

Krane, H. G., "Study of Rate Factors in Liquid Phase Hydrogenation", Ph.D. Thesis, Ohio University, Columbus, Ohio (1953).

Kröcher, O., R. A. Köppel, and A. Baiker, "Sol-gel derived hybrid materials as heterogeneous catalysts for the synthesis of N,N-dimethylformamide from supercritical carbon dioxide", *Chem. Commun.*, 1497 (1996).

Kröcher, O., R. A. Köppel, and A. Baiker, "Highly active ruthenium complexes with bidentate phosphine ligands for the solvent-free catalytic synthesis of N,N-dimethylformamide and methyl formate", *Chem. Commun.*, 453 (1997).

Kröcher, O., R. A. Köppel, and A. Baiker, "Synthesis of N,N-Dimethylformamide by Heterogeneous Catalytic Hydrogenation of Supercritical Carbon Dioxide", *Proceedings of The 3rd International Symposium on High-Pressure Chemical Engineering*, Zurich, Switzerland, p.91 (1996).

Kröcher, O., R. A. Köppel, and A. Baiker, *Chimia*, 51, 48, (1997).

Kröcher, O., R. A. Köppel, and A. Baiker, Switzerland Patent 3103/96, ETH Zürich, (1996).

Kröcher, O., R. A. Köppel, M. Froba and A. Baiker, "Silica Hybrid Gel Catalysts Containing Group(VIII) Transition Metal Complexes: Preparation, Structural, and

Catalytic Properties in the Synthesis of N,N-Dimethylformamide and Methyl Formate from Supercritical Carbon Dioxide", *J. Catal.*, 178, 284 (1998).

Lai, C. and C. Tan, "Measurements of Effective Diffusivities of Toluene in Activated Carbon in the Presence of Supercritical Carbon Dioxide", *Ind. Eng. Chem. Res.*, 32 (8), 1717 (1993).

Landert, J. P., and T. Scubla, "Make the most of catalytic hydrogenations", *Chem. Eng.*, 3, 118 (1995).

Levenspiel, O. *Chemical Reaction Engineering*. John Wiley: New York, 1999.

Liong K. K., P. A. Wells, and N. R. Foster, "Diffusion of Fatty Acid Esters in Supercritical Carbon Dioxide", *Ind. Eng. Chem. Res.*, 31, 390 (1992).

Liong, K. K., P. A. Wells, and N. R. Foster. "Diffusion in Supercritical Fluids", *J. Supercrit. Fluids*, 4, 91 (1991).

Litchfield, C., J. Lord, J. E. Isbell, and A. F. Reiser, "Cis-trans isomerization of oleic, linoleic and linolenic acids", *J. Am. Oil Chem. Soc.*, 40, 553 (1963).

López Gómez, C., "Métodos aplicados a la determinación de muestras obtenidas por hidrogenación catalítica en solvente supercrítico," Thesis Report on file at Dept. of Chemical Engineering, EUTIT, UPC (2002).

Macher, M., and A. Holmqvist, "Hydrogenation of palm oil in near-critical and supercritical propane", *Eur. J. Lipid Sci. Technol*, 103, 81 (2001).

Macher, M., J. Högberg, P. Moller and M. Harröd, "Partial hydrogenation of fatty acid methyl esters at supercritical conditions", *Fett/Lipid*, 101 (8), 301 (1999).

Marangozis, J., O. B. Keramidias, and G. Pappas, "Rate and Mechanism of Hydrogenation of Cottonseed Oil in Slurry Reactors", *Ind. Eng. Chem. Proc. Des. Dev.*, 16 (3), 361 (1977).

McCoy, B. J., and B. Subramaniam, "Continuous-mixture kinetics of coke formation from olefinic oligomers", *AIChE J.*, 41, 317 (1995).

McCoy, M., *Chem. Eng. News*, 77, 11 (1999).

McHugh M., and V. Krukonis, *Supercritical Fluid Extraction*, 2nd Edition, Butterworth-Heinemann, Stoneham, UK (1994).

Mielke, S., "Oil demand forecast to rise 32% during decade", *INFORM*, 3, 695 (1992).

Minder, B., T. Mallat, and A. Baiker, "Enantioselective hydrogenation in supercritical fluids. Limitations of the use of supercritical CO₂", *Proceedings of The 3rd International Symposium on High-Pressure Chemical Engineering*, Zurich, Switzerland, p.139 (1996).

Minder, B., T. Mallat, K. H. Pickel, K. Steiner, and A. Baiker, *Catal.Lett.*, 34, 1 (1995).

Moore, H, K., G. A. Richter, and W. B. Van Arsdel, "The Incomplete Hydrogenation of Cottonseed Oil", *Ind. Eng. Chem.*, 9, 451 (1917).

Moore, R. M., and J. R. Katzer, "Counterdiffusion of liquid hydrocarbons in type Y zeolites. Effect of molecular size, molecular type, and direction of diffusion", *AIChE J.*, 18, 816 (1972).

Neff, W. E., R. O. Adlof, G. R. List, and M. El-Agaimy, "Analyses of vegetable oil triacylglycerols by silver ion high performance liquid chromatography with flame ionization detection", *J. Liq. Chromatogr.*, 17 (18), 3951, (1994).

Niboer, E., F. E. Rossetto, and K. R. Menan, *Toxicity of Nickel Compounds*. In *Concepts of Metal Ion Toxicity*; Sigel, H., Sigel, A., Eds., MIR, Moscow (1993).

Niu, F., and H. Hofmann, *Can. J. Chem. Eng.*, 75, 346 (1997).

Niu, F., and H. Hofmann, "Studies on deactivation kinetics of a heterogeneous catalyst using a concentration-controlled recycle reactor under supercritical conditions", *Appl. Catal. A*, 158, 273 (1997).

Niu, F., and H.Hofmann, "Investigation of Various Zeolite Catalyst Under Supercritical Conditions", *Proceedings of The 3rd International Symposium on High-Pressure Chemical Engineering*, Zurich, Switzerland, p.145 (1996).

Norme Francaise NFT 60-233, "Préparation des esters méthyliques d'acides gras", edited by Association Française de Normalisation (AFNOR), Paris, (1977).

O'Brien, R.D., *Fats and Oils*, Technomic Publishing Co., Inc., United States of America (1998).

Oomen, C. M., and M. C. Ocke, "Association between *trans* fatty acid intake and 10-year risk of coronary heart disease in the Zutphen elderly study: A prospective population-based study", *Lancet*, 357, 746 (2001).

Patel, P. V., and J. B. Butt. "Multicomponent Diffusion in Porous Catalysts", *Ind. Eng. Chem. Proc. Des. Dev.*, 14, 298 (1974).

Patterson, H. B.W., *Hydrogenation of Oils and Fats*, Applied Science Publishers, London (1983).

Pereda S., S. B. Bottini and E. A. Brignole, "Gas-liquid reactions under supercritical conditions-phase equilibria and thermodynamic modelling", *Fluid Phase Equilibria*, 194, 493 (2002).

Pereda, S., L. Roveto, S. B. Botini, and E. A. Brignole, "Modeling Phase Equilibria for Hydrogenation Processes at Supercritical Conditions", *Proceedings of 4th International Symposium on High Pressure Process Technology and Chemical Engineering*, Venice, Italy, electronic document, (2002).

Pereda, S., L., S. B. Rovetto, and E. A. Brignole, "Modeling phase equilibria for hydrogenation processes at supercritical conditions", *Proceedings of 5th International Symposium on Supercritical Fluids*, Atlanta, GA (2000).

Pereda, S., S. Bottini, and E. Brignole, "Phase Equilibrium Engineering of Supercritical Hydrogenation Reactors," *AIChE J.*, 48 (11), 2635 (2003).

Perry, R. H., D. W. Green, and J. O. Maloney (Eds), *Perry's Chemical Engineering Handbook*, 6th Ed., McGraw-Hill, Inc., United States of America (1984).

Peters, C. J., H. J. van der Kooi, J. L. de Roo, J. de Swaan Arons, J. S. Gallagher, and J. M. H. Levelt Sengers, "The search for tricritically in binary mixtures of near-critical propane and normal paraffins", *Fluid Phase Equilibria*, 51, 339 (1989).

Plourde, M., K. Belkacemi, and J. Arul, "Hydrogenation of Sunflower Oil with Novel Pd Catalysts Supported on Structured Silica", *Ind. Eng. Chem. Res.*, 43 (10), 2382 (2004).

Poliakoff, M., N. J. Meehan, and S. K. Ross, "A supercritical success story", *Chem. & Ind.*, 4, 750 (1999).

Prausnitz, J. M., R. N. Lichtenthaler and E. Gomes de Azevedo, *Molecular Thermodynamics of Fluid-Phase Equilibria*, 2nd Edition, Prentice Hall Inc., New Jersey (1986).

Puiggené, J., M. A. Larrayoz, and F. Recasens. "Free Liquid-to-Supercritical Fluid Mass Transfer in Packed Beds", *Chem. Eng. Sci.*, 52 (2), 195 (1997).

Ramírez, E., and M. A Larrayoz, " Sunflower oil hydrogenation in SCF in a continuous reactor: Preliminary experimental results", *Proceedings of 4th International Symposium on High Pressure Process Technology and Chemical Engineering*, Venice, Italy, electronic document, (2002).

Ramírez, E., F. Recasens, M. Fernández, and M. A. Larrayoz, "Hydrogenation of Sunflower Oil on Pd/C in Supercritical Propane: Operating Conditions in a Continuous Internal Recycle Reactor", *AIChE Journal*, 50, 6 (2004).

Ramírez, E., S. Zgarni, M. A. Larrayoz, and F. Recasens, "Short compilation of published rate data for catalytic hydrogenations in supercritical fluids", *Chem. Eng. Technol.: Engineering in Life Science*, 2 (9), 257 (2002).

Ramírez, Eliana. "Hydrogenation of Aromatic Compounds in High-Temperature Water", Pre-doctoral Internship Report on file at Clean Technology Research Group, University of Nottingham (2004).

Rase, H. F., *Chemical Reactor Design for Process Plants, Vol II: Case Studies and design Data*, John Wiley, New York (1977).

Rase, H. F., *Handbook of Commercial Catalysts: Heterogeneous Catalysts*, CRC Press, Boca Raton, FL (2000).

Rathke, J. W., R. J. Klinger, and T. R. Krause, "Propylene hydroformylation in supercritical carbon dioxide", *Organometallics*, 10, 1350 (1991).

Rautanen, P. A., J. R. Aittamma, and A. O. I. Krause, "Solvent Effect in Liquid-Phase Hydrogenation of Toluene", *AIChE J.*, 49 (6), 1508 (2000).

Ray, J. D., "Behaviour of hydrogenation catalysts I: Hydrogenation of Soybean Oil with Palladium", *JAOCs*, 62, 1243 (1985).

Recasens, F., E. Velo, M. A. Larrayoz, and J. Puigggené, "Endothermic Character of Toluene Adsorption from SC Carbon Dioxide onto Activated Carbon at Low Coverage", *Fluid Phase Equilibria*, 90, 265 (1993).

Reid, R., J Prausnitz, and B. Poling, *The properties of gases & liquids*, 4th edn, McGraw Hill, New York (1987).

Richardson, A. S., C. A. Knuth, and C. H. Milligan, "Heterogeneous Catalysis", *Ind. Eng. Chem.*, 16, 519 (1924).

Richter, D., and E. Weidner, E. "Influence of Supercritical Carbon Dioxide and Propane on the Solubility and Viscosity of systems containing Hydrogen and Triglycerides (Soybean Oil)", *Proceedings of 6th Meeting on Supercritical Fluids - Chemistry and Materials*, Nottingham, UK, p.651 (1999).

Richter, D., "Phasenverhalten und Viskosität In Systemen aus Triglyceriden, Wasserstoff, Kohlendioxid, Propan und Dimethylether", Ph.D. Thesis, University of Erlangen-Nürnberg, Germany (2000).

Riggs, J. B., *An Introduction to Numerical Methods for Chemical Engineers*, Texas Tech University Press (1988).

Robinson, K. K., "Performance of gradientless microreactors", *Proceedings of Symposium on Laboratory Reactor – AIChE Annual Meeting*, Miami Beach, Fl, (1986).

Roth, T. H., "Diffusion and Thermodynamic Measurements by Supercritical Fluid Chromatography", *J. Microcol. Sep.*, 3, 173 (1991).

Rovetto, L. J., S. B. Bottini, and C. J. Peters, "Phase equilibrium data on binary and ternary mixtures of methyl palmitate, hydrogen and propane", *J. Supercrit. Fluids*, 31, 111 (2004).

Rylander, P. N. *Hydrogenation Methods*, Academic Press, New York (1985).

Saim, S., and B. Subramaniam, *J. Supercrit. Fluids*, 3, 214 (1990).

Saim, S., and B. Subramaniam, "Chemical reaction equilibrium at supercritical conditions", *Chem. Eng. Sci.*, 15, 43 (1998).

Saim, S., and B. Subramaniam, "Isomerization of 1-Hexene over Pt/ γ -Al₂O₃ catalyst: Reaction mixture density and temperature effects on catalyst effectiveness factor, coke laydown, and catalyst micromeritics ", *J. Catal.*, 131, 445 (1991).

Saim, S., D. M. Ginosar, and B. Subramaniam, In *Supercritical Fluid Science and Technology*; Johnston, K. P., Penninger, J. M. L., Eds., American Chemical Society: Washington DC, 1989.

Sandler, S. I., *Chemical and Engineering Thermodynamics*, 3rd Edition, Wiley, New York (1999).

Sans Solé, J., "Hidrogenació d'oli en condicions supercri'tiques," Chemical Engineering MS Thesis, Chemical Engineering Dept., ETSEIB-UPC, Barcelona, Spain (2003).

Santacesaria, E., P. Parrilla, M. Di Serio, and G. Borelli, "Role of mass transfer and kinetics in the hydrogenation of rapeseed oil in supported palladium catalyst", *Appl. Catal. A: Gen.*, 116, 269 (1994).

Sardesai, A., "Catalytic Conversion of Dimethyl Ether to Lower Olefins: Process and Catalyst Deactivation Studies", Ph.D. Thesis, The University of Akron, EUA (1997).

Satterfield, C. N. and C. S. Cheng, "Liquid counter diffusion of selected aromatic and naphthenic hydrocarbons in type Y zeolites", *AIChE J.*, 18, 724 (1972).

Satterfield, C. N. and J. R. Katzer, "The counterdiffusion of liquid hydrocarbons in type Y zeolites," *Adv. Chem. Ser.*, 102, 193 (1971).

Satterfield, C. N., C. K. Colton and W. H. Pitcher, "Restricted diffusion in liquids within fine pores", *AIChE J.*, 19, 628 (1973).

Satterfield, C. N., *Mass Transfer in Heterogeneous Catalysis*, MIT Press, Cambridge, Mass. (1970).

Savage, P. E., S. Gopalan, T. I. Mizan, C. J. Marino, and E. E. Brock, "Reactions at Supercritical Conditions: Applications and Fundamentals", *AIChE*, 41 (7), 1723 (1995).

Schieman, H., "Interfacial tension of lipids in the presence of dense gases", Ph.D. Thesis, Univ. Erlangen-Nuremberg, Erlangen, Germany (1993).

Schiemann, H, E. Weidner, and S. Peter. "Interfacial Tension in Binary Systems Containing a Dense Gas", *J. Supercrit. Fluids*, 6, 181 (1993).

- Schmidt, S., "Formation of *trans* unsaturation during partial catalytic hydrogenation", Eur. J. Lipid Sci., 102, 646 (2000).
- Schneider, P. and J. M. Smith, "Chromatographic Study of Surface Diffusion", AIChE J., 14, 886 (1968).
- Singh, U. K. and M. A. Vannice. "Liquid-Phase Hydrogenation of Citral over Pt/SiO₂ Catalyst I. Temperature Effects on Activity and Selectivity", J. Catal., 191, 165 (2000).
- Sladeck, K. J., E. R. Gilliland and R. F. Baddour, "Diffusion on Surfaces II. Correlation of Diffusivities of physically and Chemically Adsorbed Species", Ind. Chem. Fundam., 13, 2, 100 (1974).
- Smeds, S., T. Salmi, L. P. Lindfors and O. Krause, "Chemisorption and TPD Studies of Hydrogen on Ni/Al₂O₃", Appl. Catal., 144, 177 (1996).
- Smith, J. M., Chemical Engineering Kinetics, 3rd Edn. McGraw-Hill, New York (1981).
- Snavely, K., and B. Subramaniam, "On-Line Gas Chromatographic Analysis of Fischer-Tropsch Synthesis Products Formed in a Supercritical Reaction Medium", Ind. Eng. Chem. Res., 36, 4413 (1997).
- Snyder, J. M., H. J. Dutton, and C. R. Scholfield, "Laboratory-Scale Continuous Hydrogenation", J. Am. Oil Chem. Soc., 55, 383 (1978).
- Sourelis, S. G., JAOCS, 33, 492 (1956).
- Straver, E. J. M., J. L. De Roo, C. J. Peters and J. Swaan Arons. "Phase behavior of the binary system propane and tristearin", J. Supercritical Fluids, 11, 139 (1998).
- Stüber, F., S. Julien and F. Recasens, "Internal mass transfer in sintered metallic pellets filled with supercritical fluid", Chem. Eng. Sci., 52, 3527 (1997).
- Suárez, J. J., J. L. Bueno and I. Medina, "Determination of Binary Diffusion Coefficients of Benzene and Derivates in SC Carbon Dioxide", Chem. Eng. Sci., 48, 2419 (1993).
- Suárez, J. J., J. L. Bueno, I. Medina and J. Dizy, "Aplicaciones de la cromatografía supercrítica: Determinación de Difusividades Moleculares", Afinidad, 438, 101 (1992).
- Subramaniam, B. "Enhancing the stability of porous catalysts with supercritical reaction media" Appl. Catal. A-Gen., 212, 199 (2001).

Subramaniam, B., and B. J. McCoy, "Catalyst Activity Maintenance or Decay: A Model for Formation and Desorption of Coke", *Ind. Eng. Chem. Res.*, 33, 504 (1994).

Subramaniam, B., and D. Ginosar, "Enhancing the Activity of Solid Acid Catalysts with Supercritical Reaction Media: Experiments and Theory", *Proceedings of The 3rd International Symposium on High-Pressure Chemical Engineering, Zurich, Switzerland*, p.3 (1996).

Subramaniam, B., and M. McHugh, "Reactions in Supercritical Fluids-A Review", *Ind. Eng. Chem. Res.*, 25, 1 (1985).

Subramaniam, B., and S. Saim, United States Patent 5690809, Center for Research, Inc., Lawrence, KS (1997).

Subramaniam, B., and S. Saim, United States Patent 5725756, Center for Research, Inc., Lawrence, KS (1998).

Subramaniam, B., C. J. Lyon, and V. Arunajatesan, "Environmentally-Benign Multiphase Catalysis", *Appl. Catal. B-Environ*, 37, 279 (2002).

Subramanian B. and M. A. McHugh, "Reactions in Supercritical Fluids-A Review", *Ind. Eng. Chem. Process Des. Dev.*, 25, 1 (1985).

Sun, C. K. J., and S. H. Cheng, "Tracer Diffusion in Dense Methanol and 2-Propanol up to Supercritical Region: Understanding of Solvent Molecular Association and Development of an Empirical Correlation", *Ind. Eng. Chem. Res.*, 26, 815 (1987).

Tacke, T., "Fetthärtung mit Festbettkatalysatoren", *Die Ernährungsindustrie*, 12, 50 (1995).

Tacke, T., S. Wieland, and P. Panster, "Hardening of fats and oils in supercritical CO₂", *Proceedings of High Pressure Chemical Engineering, Process Technology, Amsterdam, The Netherlands*, p.17 (1996).

Tacke, T., S. Wieland, and P. Panster, "Selective and complete hardening of edible oils and free fatty acids in supercritical fluids", *Proceedings of the 4th International Symposium on Supercritical Fluids, Sendai, Japan*, p. 511 (1997).

Tacke, T., S. Wieland, and P. Panster, "Hardening of Fats and Oils", *Proceedings of The 3rd International Symposium on High-Pressure Chemical Engineering, Zurich, Switzerland*, p.17 (1996).

Tacke, T., Wieland, S. and Panster, P. Selective and Complete Hydrogenation of Vegetable Oils and Free Fatty Acids in Supercritical Fluids, in *Green Chemistry Using Liquid and Supercritical Carbon Dioxide*, ed. J. M. De Simone, Oxford University Press, Oxford (2003).

Tiltscher, H., and H. Hofmann, "Trends in high pressure chemical reaction engineering", *Chem. Eng. Sci.*, 42, 959 (1987).

Tiltscher, H., H. Wolf, and J. Schelchshorn, "", *Ber. Bunsen-Ges. Phys.Chem.*, 88, 897 (1984).

Tiltscher, H., H. Wolf, J. Schelchshorn, and K. Dialer, United States Patent 4605811 (1986).

Tiltscher, H., J. Schelchshorn, F. Westphal, F., and K. Dialer, *Chem.Ing. Technol.*, 56, 42 (1984).

Tsuto, K., Harriott, P., and Bischoff, K. B. "Intraparticle Mass Transfer Effects and Selectivity in the Palladium-Catalyzed Hydrogenation of Methyl Linoleate", *Ind. Eng. Chem. Fundam.*, 17, 3, 199 (1978).

Tundo, P., *Continuous Flow Methods in Organic Synthesis*, Ellis Horwood, Great Britain (1991).

Van den Hark, S., and M. Härröd, "Fixed-Bed Hydrogenation at Supercritical Conditions to Form Fatty Alcohols: The Dramatic Effects Caused by Phase Transitions in the Reactor", *Ind. Eng. Chem. Res.*, 40, 5052 (2001).

Van den Hark, S., and M. Härröd, "Hydrogenation of oleochemicals at supercritical at supercritical single-phase conditions: influence of hydrogen and substrate concentrations on the process", *Appl. Catal. A: Gen.*, 210, 207 (2001a).

Van den Hark, S., M.Härröd, and P. Möller, "Hydrogenation of fatty acid methyl esters to fatty alcohols at supercritical conditions", *J. Am. Oil Chem. Soc.*, 76, 1363 (1999).

Veldsink, J. W., "Selective Hydrogenation of Sunflower Seed Oil in a Three-Phase Catalytic Membrane Reactor", *JAOCS*, 78, 5, 443 (2001).

Veldsink, J. W., M. J. Bouma, N. H. Schön, and A. A. C. M. Beenackers, "Heterogeneous Hydrogenation of Vegetable Oils: A Literature Review", *Catal. Rev.-Sci. Eng.*, 39, 253 (1997).

Vieville, C., and Z. Mouloungui, Proceedings of The 3rd International Symposium on Supercritical Fluids, Strasbourg, France, p.19 (1994).

Vieville, C., Z. Mouloungui, A. Gaset, "Esterification of oleic acid by methanol catalyzed by p-toluenesulfonic acid and the cation-exchange resins K2411 and K1481 in supercritical carbon dioxide", *Ind. Eng. Chem. Res.*, 32, 2065 (1993).

Wakao, N., and J. Smith, "Diffusion in Catalyst Pellets", *Chem. Eng. Sci.*, 17, 825 (1962).

Wakao, N., and J. Smith, "Diffusion in Catalyst Pellets", *Ind. Eng. Chem. Fund. Quart.*, 3, 123 (1964).

Wei, J., "Intraparticle Diffusion Effects in Complex Systems of First Order Reactions", *J. Catal.*, 1, 526 (1962).

Weidner, E., C. Brake and D. Richter. Thermo- and fluid dynamic aspects of the hydrogenation of triglycerides and esters in presence of supercritical fluids, in *Supercritical Fluids as Solvents and Reaction Media*, 1st edition, ed. G. Brunner, Elsevier, The Netherlands (2004).

Weisz, P. B., and H. Zollinger, "Sorption-diffusion in heterogeneous systems. Part 4.—Dyeing rates in organic fibres", *Trans. Faraday Soc.*, 64, 1693 (1968).

Weisz, P. B., "Sorption-diffusion in heterogeneous systems. Part 1.—General sorption behaviour and criteria", *Trans. Faraday Soc.*, 63, 1801 (1967).

Weisz, P. B., and H. Zollinger, "Sorption-diffusion in heterogeneous systems. Part 3.—Experimental models of dye sorption", *Trans. Faraday Soc.*, 63, 1815 (1967).

Weisz, P. B., and J. S. Hicks, "Sorption-diffusion in heterogeneous systems. Part 2.—Quantitative solutions for uptake rates", *Trans. Faraday Soc.*, 63, 1807 (1967).

Westerterp, K. R., W. P. M. Van Swaaij, and A. A. C. M. Beenackers, "Chemical Reactor Design and Operation", John Wiley and Sons: New York (1987).

Wheeler A. "Reaction Rates and Selectivity in Catalyst Pores", *Adv. Catal.*, 3, 323 (1952).

Wisniak, J. and L. F. Albright, "Hydrogenating Cottonseed Oil at Relatively High Pressure", *Ind. Eng. Chem.*, 53 (5), 375 (1961).

Wisniak, J., and L. F. Albright, "Hydrogenating Cottonseed Oil at Relatively High Pressure", *Ind. Eng. Chem. Res.*, 40, 5052 (1961).

Yang, R. T., J. B. Fenn, and G. L. Haller, "Modification to the Higashy model for surface diffusion", *AIChE J.*, 19, 1052 (1973).

Yaws, C. L., *Chemical Properties Handbook*, McGraw Hill, New York (1999).

Yokota, K., and K. Fujimoto, "Supercritical-phase Fischer-Tropsch synthesis reaction. 2. The effective diffusion of reactant and products in the supercritical-phase reaction", *Ind. Eng. Chem. Res.*, 30, 95 (1991).

Yokota, K., Y. Hanakata, and K. Fujimoto, "Supercritical phase Fischer-Tropsch synthesis", *Chem. Eng. Sci.*, 45, 2743 (1990).

Yu, Z. R., S. Bhajmohan, S. H. Rizvi and J. A. Zollweg, "Solubilities of Fatty Acids, Fatty Acid Esters, Triglycerides, and Fats and Oils in Supercritical Carbon Dioxide", *J. Supercrit. Fluids*, 7 (1), 54 (1994).

Zalc, J. M., S. C. Reyes, and E. Iglesia, "The effects of diffusion mechanism and void structure on transport rates and tortuosity factors in complex porous structures", *Chem. Eng. Sci.*, 59, 2947 (2004).

Zgarni, Sara. "Etude d'amélioration d'un procédé d'hydrogénation d'huile de tournesol en solvant supercritique", Internal report on file at Dept. of Chemical Engineering, ETSEIB, UPC (2000).

Zosel, K., "Process for the Simultaneous Hydrogenation and Deodorization of Fats and Oils", US Patent 3969382 (1976).

Zwahlen, A. G., and A. Bertucco, "CSTR-System for Kinetic Investigation for Hydrogenation Reaction", *Proceedings of The 3rd International Symposium on High-Pressure Chemical Engineering*, Zurich, Switzerland, p.37 (1996).

Appendix A

Survey of Heterogeneous Catalytic Reactions carried out under SC Conditions or in SCF solvents (Baiker, 1999, Ramírez *et al.* 2002).

Table A-1: General overview of catalytic heterogeneous reaction in SCFs.

reaction	catalyst	solvent	T, K	P, MPa	r ^a	S ^b	a ^c	Ref(s)
Alkylation								
benzene and ethylene	Y-type zeolites		523-558	3.5-7.0	↑	↑	↑	Gao <i>et al.</i> (1996, 1997)
isopentane and isobutene	H-USY, Y-type zeolite	isopentane	323-473	3.5-4.6	↑		↑	Fan <i>et al.</i> (1997, 1998)
isobutane and isobutene	H-USY, Y-type zeolite	isobutane	323-413	3.5-5.0	↑		↑	Fan <i>et al.</i> (1997, 1998)
1-butene and isobutane	zeolite H-USY, sulfated zirconia	CO ₂	323-413	3.4-15.5			↑	Clark and Subramaniam (1998)
mesitylene and propene	polysiloxane (DELOXAN) supported solid acid	propene	433-453	20.0				Hitzler <i>et al.</i> (1998)
mesitylene and propan-2-ol	polysiloxane (DELOXAN) supported solid acid	CO ₂	473-573	15.0-20.0				Hitzler <i>et al.</i> (1998)
Amination								
amino-1-propanol	Co-Fe	NH ₃	468	5.0-13.5			↑	Fischer <i>et al.</i> (1998)
Cracking								
heptane	promoted Octacat (H-Y zeolite)	heptane	598	3.4			↑	Dardas <i>et al.</i> (1996)
Disproportionation								
toluene to <i>p</i> -xylene and benzene	zeolite (ZSM-5)		593-598	3.36-5.6			↑	Collins <i>et al.</i> (1988)

reaction	catalyst	solvent	T, K	P, MPa	r ^a	S ^b	a ^c	Ref(s)	
Disproportionation									
1,4-diisopropylbenzene to cumene and 1,3,5-triisopropylbenzene	zeolite (type 13 NaHX)	benzene, <i>n</i> -pentane	533	20.0			↑	Tiltscher <i>et al.</i> (1984, 1987)	
ethylbenzene to benzene and diethylbenzene	zeolites (USY, H-ZSM-5, H-mordenite), zeolite-HY	butane, pentane	573-673	5.0			↑	Niu and Hofmann (1996, 1997)	
Esterification									
oleic acid and methanol	K2411 sulfonic macroporous ion exchange resin	CO ₂	>823	0.95-1.3	↑			Vieville <i>et al.</i> (1993, 1994)	
Reaction	catalyst	solvent	T, K	P, MPa	r ^a	S ^b	a ^c	Ref(s)	
Fisher-Tropsch Synthesis									
CO and H ₂ to liquid hydrocarbons	Ru 2% on Al ₂ O ₃ , Co on SiO ₂ , Fe	<i>n</i> -hexane	313-341	4.5	↓	d	e	↑	Yokota <i>et al.</i> (1990, 1991) Fan <i>et al.</i> (1992, 1997)
CO and H ₂ to liquid hydrocarbons with addition of 1-olefins	Co-La or Co on SiO ₂ gel, Ru/Al ₂ O ₃	<i>n</i> -pentane	513	4.5	↓	d	↑	↑	Fan <i>et al.</i> (1997)
CO and H ₂ to liquid hydrocarbons	100 Fe/5 Cu/4.2 K/25 SiO ₂	propane	523	5.5			↑		Bukur <i>et al.</i> (1997)
CO and H ₂ to liquid hydrocarbons	Fe	<i>n</i> -hexane	513	7.0-8.0					Snaveley and Subramaniam (1998)
Isomerization									
1-hexene to 2-hexene (<i>cis/trans</i>) and 3-hexene	γ-Al ₂ O ₃ /Al-metal shell catalyst		493-523	5.0-80.0	↑	↑	↑	↑	Tiltscher <i>et al.</i> (1984-1987)
1-hexene	Pt/γ-Al ₂ O ₃	CO ₂ and cosolvents <i>n</i> -pentane, <i>n</i> -hexane	291	18.0	↑	↑	↑	↑	Subramaniam works (1989-1998)
1-hexene to olefinic oligomers	Pt/γ-Al ₂ O ₃		300.7	27.7					McCoy and Subramaniam (1995)
xylene isomerization to <i>p</i> -xylene	solid acid catalyst,		276.2	3.2	↑		↑		Amelse and Kutz (1991)

reaction	catalyst	solvent	T, K	P, MPa	r ^a	S ^b	a ^c	Ref(s)
Oxidations								
toluene to benzaldehyde	Co/Al ₂ O ₃	CO ₂	281	8.0		↑		Dooley and Knopf (1987)
propene to propylene glycol	CaI ₂ /CuI/Cu ₂ O on MgO or γ -alumina		>280	>7	↓	↑		Gaffney and Sofranko (1992, 1993)
isobutane to <i>tert</i> -butyl alcohol	SiO ₂ -TiO ₂ , Pd on C		426	4.4-5.4	↑		↑	Fan <i>et al.</i> (1997)
Hydrogenation								
fats and oils fatty methyl esters	5% Pd on C, 3% Pd on aminopolysiloxan	propane	323-373	7.0-12.0	↑	↑		Harrod <i>et al.</i> (1996-1999)
fats and oils	Pd or Pt on DELOXAN support	CO ₂	333-433	8.0-16.0	↑	↑		Tacke <i>et al.</i> (1995-1997, 2003)
Hydrogenation								
fats and oils	Pd on DELOXAN support	propane	323	10	↑	↑	↑	Tacke <i>et al.</i> (1997, 2003)
acetophenone	5% Pd APII DELOXAN	CO ₂	363-573	12.0	↑	↑		Hitzler and Poliakoff (1997)
cyclohexene	5% Pd APII DELOXAN, 5% Pt APII DELOXAN	CO ₂ , propane	313-593	6.0-12.0	↑			Hitzler and Poliakoff (1997)
cyclohexene	5% Pd/C	CO ₂	343	13.6		↑	↑	Arunajatesan <i>et al.</i> (2001)
1,2-(methylenedioxy)-4-nitrobenzene	1% Pd DELOXAN	CO ₂	363	14.0	↑			Hitzler and Poliakoff (1997)
<i>m</i> -cresol, benzaldehyde, propionaldehyde, acetophenone, cyclohexanone, cyclohexanole, furan, nitrobenzene, <i>N</i> -benzylidenemethylamine, 2-butanone oxime, 1-octyne, 1-octene, cyclohexene, isophorone	various noble metal catalysts on DELOXAN aminopolysiloxane support	CO ₂ , propane	363	14.0	↑	↑		Hitzler <i>et al.</i> (1998)

reaction	catalyst	solvent	T, K	P, MPa	r ^a	S ^b	a ^c	Ref(s)
Hydrogenation								
ethyl pyruvate to (R)-ethyl lactate	Pt/ γ -Al ₂ O ₃ and cinchonidine as modifier	ethane, propane	313-373	7.0-25.0	↑	↑		Minder <i>et al.</i> (1995, 1996)
double bonds of unsaturated ketone	Pd/Al ₂ O ₃	CO ₂	323-493	12.0-17.5	↑	↑		Zwahlen and Bertuccio (1996) Bertuccio <i>et al.</i> (1997) Devetta <i>et al.</i> (1999)
dimethylamine to dimethylformamide	sol-gel RuCl ₂ X ₂ , X) PMe ₂ (CH ₂) ₂ Si(OEt) ₃	CO ₂						Kröcher <i>et al.</i> (1996-1998)
fatty acid methyl esters	Chromium free copper based catalyst	propane	473-573	15	↑	↑		Van den Hark <i>et al.</i> (1999-2001)
fatty acid methyl esters	Chromium free and copper chromite	CO ₂ , propane	483-523	15-25	↑	↑		Andersson <i>et al.</i> (2000)
α - Pinene	10% Pd/ C	CO ₂	323	14	↑	↑		Chouchi <i>et al.</i> (2001)
palm oil	1% Pd/C	propane	338-408	15	↑	↑		Macher and Holmqvist (2001)
reaction	catalyst	solvent	T, K	P, MPa	r ^a	S ^b	a ^c	Ref(s)
Hydrogenation								
soybean oil	0.25 wt% supported Ni	CO ₂	393-413	14	↑	↑		King <i>et al.</i> (2001)
Nitrobenzene, cyclohexanone, Acetophenone, benzaldehyde	---	H ₂ O	428-478	15-20	↑	↑		Garcia <i>et al.</i> (2004) Ramírez (2004)
sunflower oil	2% Pd/C	Propane	428-488	20	↑	↑	↑	Ramírez <i>et al.</i> (2004)

^aChange of reaction rate in the supercritical region with respect to subcritical conditions (↑ increase, ↓ decrease). ^b Change of selectivity in the supercritical region with respect to subcritical conditions (↑ increase, ↓ decrease). ^c Change of catalyst lifetime in the supercritical region with respect to subcritical conditions (↑ increase, ↓ decrease). ^d Higher olefin content. ^e Versus gas. ^f Changes *cis/trans*, double bond and side reactions. ^g Oxidation in supercritical water (SCWO) have intentionally been omitted since they have been omitted.

Appendix B

Hydrogenation of Aromatic Compounds in High-Temperature Water.



Clean Technology Research Group

ELIANA RAMÍREZ RANGEL

Supervisors:

EDUARDO GARCIA-VERDUGO

MARTYN POLIAKOFF

Introduction.

Hydrogenation of petroleum feed stocks and other derivatives for commercial purposes are a common process. For example, large amounts of fatty alcohols (FOH), 1 million ton/year, and their derivatives are used in detergents. FOH are mostly produced by catalytic hydrogenation of fatty acid methyl esters (FAME), at severe conditions, i.e. 523.15 K and 30 MPa. In the same way 20 million ton per year of vegetable oils are hydrogenated, mostly for the production of margarine and shortenings.

Recent impacts of environmental legislation are pushing chemical companies to develop new synthetic routes to fine chemicals. One of the alternative technologies that comply with these restrictions is supercritical fluids (SCFs).

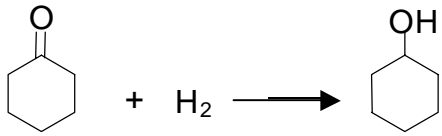
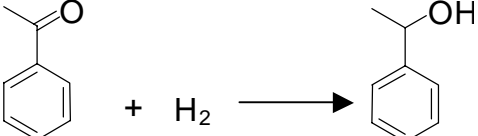
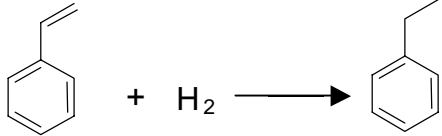
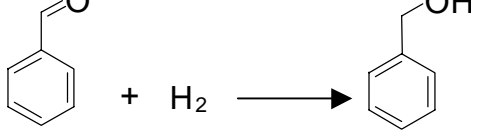
Great attention has been drawn to the use of SCFs for organic syntheses. Supercritical carbon dioxide has played an important role as a reaction medium and/or reactant. In the past supercritical water has been deemed destructive, yet supercritical water has been proven to be a synthetically useful tool. Under sub- to super-critical conditions, organic materials have greatly enhanced solubility in water and the hydrogen-bonding network of water is minimized. The weakening of hydrogen bonding is thought to induce the evolution of protons, further increasing its acidity.

In this research, the reduction of a variety of organic substrates has been studied using a green process achievable with very simple equipment. Aqueous solutions of formic acid (HCO₂H), sodium formate (NaCO₂H) or ammonium formate (NH₄CO₂H) are used as a hydrogen source by thermal decomposition. No catalyst is required.

Objectives.

To study the behaviour of different cyclic and aromatic ketones, olefins and aldehydes under hydrogenating conditions in sub-critical water without catalyst in a continuous flow reactor. Hydrogen is supplied by the decomposition of formic acid, sodium formate or ammonium formate aqueous solutions.

Table B-1: Screening hydrogenation reactions.

<p style="text-align: center;"><i>Cyclic ketone</i></p>  <p style="text-align: center;">Cyclohexanone Cyclohexanol</p>	<p style="text-align: center;"><i>Aromatic ketone</i></p>  <p style="text-align: center;">Acetophenone 1-phenylethanol</p>
<p style="text-align: center;"><i>Aromatic olefin</i></p>  <p style="text-align: center;">Styrene Ethylbenzene</p>	<p style="text-align: center;"><i>Aromatic aldehyde</i></p>  <p style="text-align: center;">Benzaldehyde Benzyl Alcohol</p>

Experimental.

Conditions.

1. Aqueous solutions of HCO₂H, HCO₂Na and HCO₂NH₄
2. Organic diluted in 100 cm³ of ethanol
3. The maximum allowable pressure and temperature of the equipment employed are 40 MPa and 623 K.

Apparatus.

A schematic flow diagram of the apparatus is presented in figure B-1.

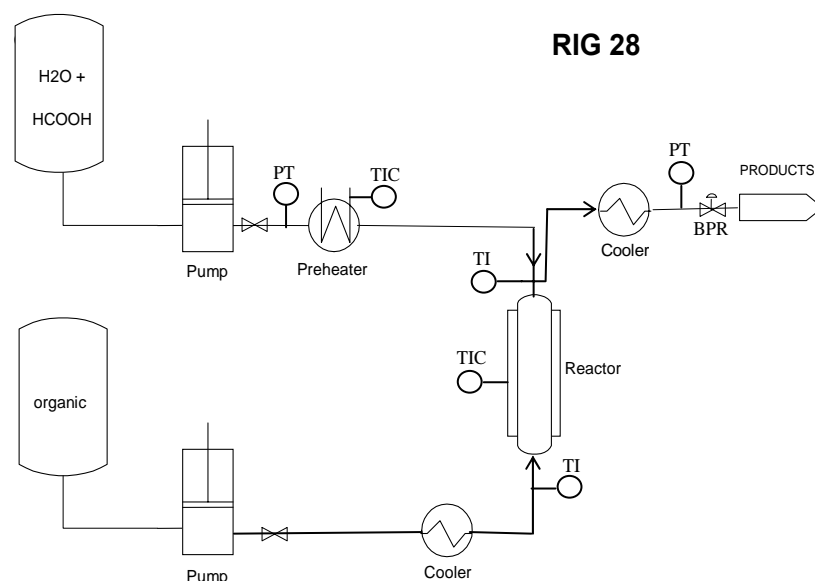


Figure B-1: Experimental setup for hydrogenation reactions.

The supercritical fluids continuous flow equipment employed mainly consists of three HPLC pumps, a pre-heater, a reactor, two water coolers and a Back Pressure Regulator (BPR) (Tescom). The pre-heater and reactor are supported on heatproof bricks and are insulated with a jacket rated to 773.15 K.

Two pressure transducers (PT) are used to monitor the pressure before the pre-heater and in the reactor. The temperature is monitored throughout the equipment to ensure the pressure transducers do not get hot.

A 10ml/min HPLC pump is used to feed either aqueous solutions of HCO_2H , HCO_2Na or HCO_2NH_4 via the pressure transducer to the pre-heater. Pumps and heaters are tripped off therefore, if the pressure exceeds 41 MPa, the pumps and heaters are switched off automatically.

The aqueous solution of sodium or ammonium formate were prepared as follows: in a 1000 cm^3 volumetric flask, formic acid and an aqueous sodium or ammonia solution (35% v/v) were mixed until the desired pH was obtained.

The pre-heater consists of 1/16 inch tubing (approx. 3m) coiled around an aluminium block. A cartridge and a band, which are both powered from a temperature indicator controller (TIC) set at 230V, are used to supply heat. An earth lead, surrounded by a heatproof sleeve, is attached to the aluminium plate and wired to the heaters. The

temperature is controlled by a thermocouple (T_1) placed at the bottom of the aluminium block, which needs to be set at higher value (~ 283.15 K) than desired temperature to allow the heat transfer through the aluminium and into the steel pipe.

Another 5ml/min HPLC pump is used to pump the organic reagents which are diluted in ethanol. The reactor unit is identical to the pre-heater, except that the tubing coiled around it is shorter (1.15 m from the organic T-piece to the cooler). The temperature controller is fitted with a trip unit (West 6700) in case of an exothermic reaction producing an over temperature. The temperature (T_2) is set substantially lower than T_1 as the aqueous solution flow is already hot and only needs to maintain the temperature into the reactor. To monitor the outlet reactor temperature, a thermocouple located at the top of the reactor (T_4) is used.

A T-piece in the reactor bottom measures the inlet temperature of the organic stream (T_3) after being cooled in order to avoid the decomposition of the starting material by high temperature. The BPR is set to the desired pressure and the knurled nut is adjusted as necessary to stabilize the pressure.

After leaving the reactor, the products are cooled and collected.

Study.

To screen the hydrogenation reactions in near-critical water a number of 22 experiments have been carried out.

The following variables have been studied:

Pressure: 16 and 20 MPa.

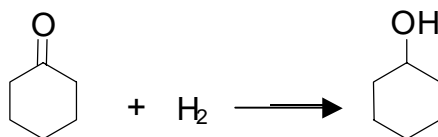
Reactor Temperature: 413, 463, 523 and 563 K.

Effect of the nature of hydrogen source: HCO_2H , HCO_2Na and HCO_2NH_4

Effect of pH of ammonium formate aqueous solutions: 2.7, 4, 8 and 11.

Mol Organic/Hydrogen ratio: From 1:5 to 1:50.

Residence time (RT): Between 6 to 30 s.

Results.**Cyclohexanone.****Scheme B-1: Hydrogenation of cyclohexanone.**

Starting material and reaction product were analyzed by Gas Chromatography. The column used was Altech ECONO-CAT™-EC™-1 (30m*0.32mm ID*1mm). The standards were diluted in ethanol whereas reactor samples were injected without any dilution. The analysis method is described as follows:

Method 5

Initial Column Temperature=	423 K
Time 1=	10 min
Rate 1=	278.15 K/min
Time 2=	10 min
Rate 2=	End
Detector Temperature=	573.15 K
Injector Temperature=	523.15 K
Pressure 1=	0.1 MPa
Volume Injection=	5 μ l

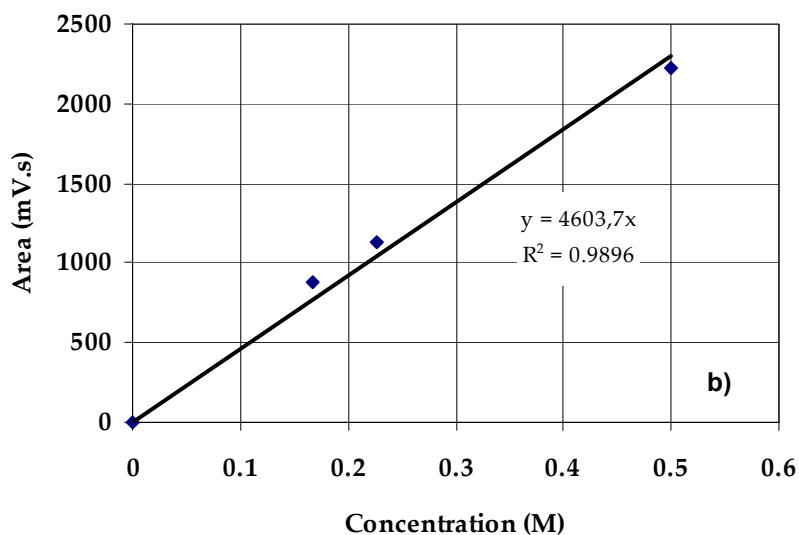
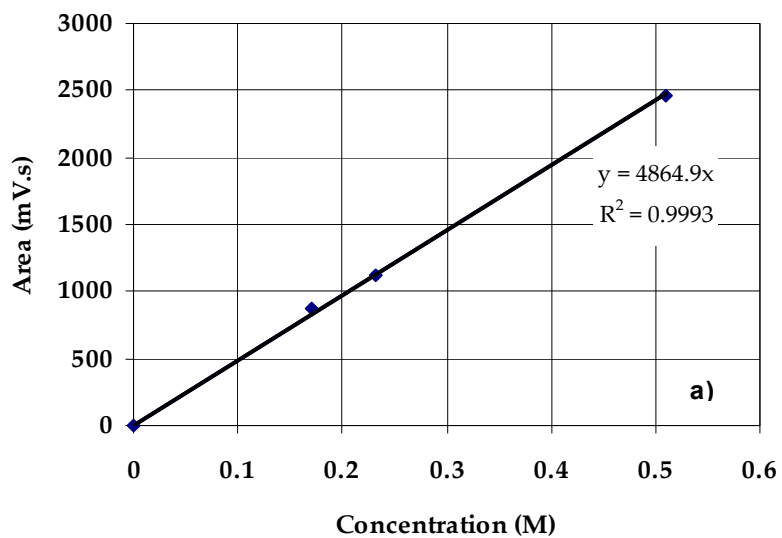


Figure B-2: GC calibration of a) Cyclohexanone and b) Cyclohexanol.

The effect of the reaction variables on cyclohexanol yield is presented in Table B-2.

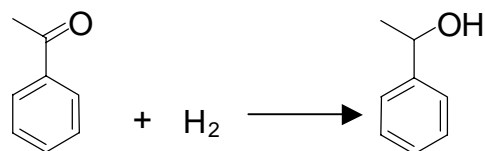
Table B-2: Effect of operating variables on cyclohexanol yield.

Aqueous Reducing Reagent	mol Org/H ₂ Ratio	T (K)	P (MPa)	Residence time (s)	Yield (%)
HCO ₂ Na (pH=12)	1/5	523	16	9	14±0.1
	1/12	523		10	17±1
	1/9	523		24	28±0.2
	1/12	292		9	23±1
HCO ₂ H (pH=1)	1/12	250		10	1.7±0.1

The cyclohexanone yield obtained from formic acid decomposition is poor.

In the case of sodium formate, temperature rise leads to an increase in the cyclohexanone yield as well as higher mol Organic-H₂ ratio or residence time but the latter seems to have stronger influence on yield.

Acetophenone.



Scheme B-2: Hydrogenation of acetophenone.

Starting material and reaction product were calibrated by HPLC. The column used was Water XTerra Column (3*150mm), which contains inorganic (silica) and organic (organosiloxane) components that allow a high efficiency of separation and offers improved pH stability. The reactor samples were analysed using instrumental method called Hydro254.m.

Method Hydro254.m

UV Signals 254.4, 230.4, 280.4, 300.4 nm

Solvent 30% ACN

70% buffer (AcOH/AcONa/H₂O)

Pressure Limit 400 bar maximum

Flow= 0.7 ml/min

Stop time= 7 min

Post time= 2 min

Injection Volume= 5 μ l

Dilution= Standards were diluted in ACN whereas reactor products were diluted in water (1:10)

The following two figures show the calibration of the acetophenone and 1-phenylethanol respectively.

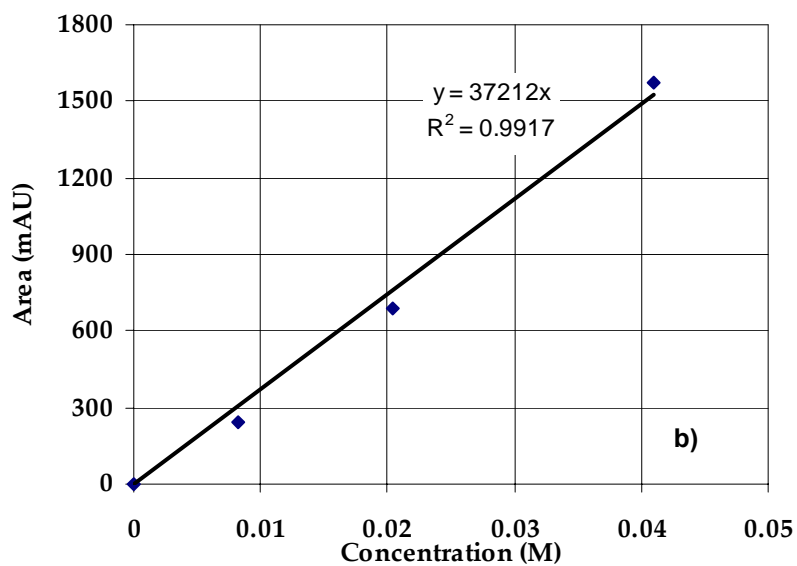
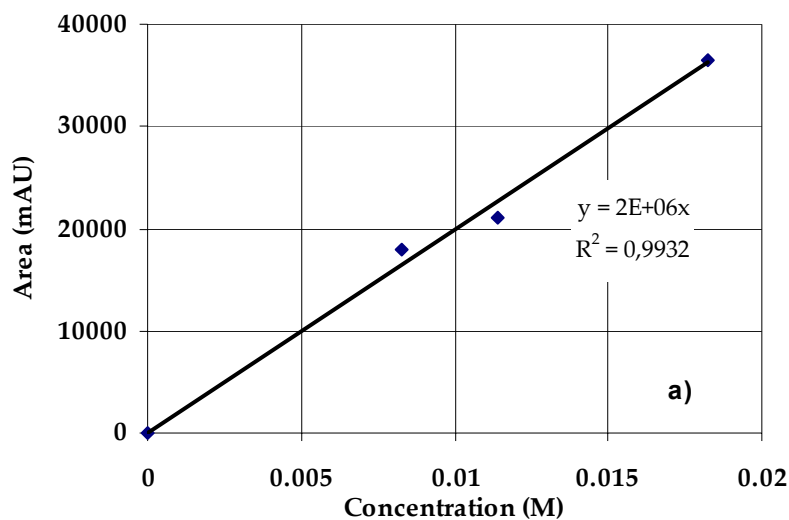


Figure B-3: GC calibration of a) Acetophenone and b) Phenylethanol.

The effect of the reaction variables on 1-phenylethanol yield is presented in Table B-3.

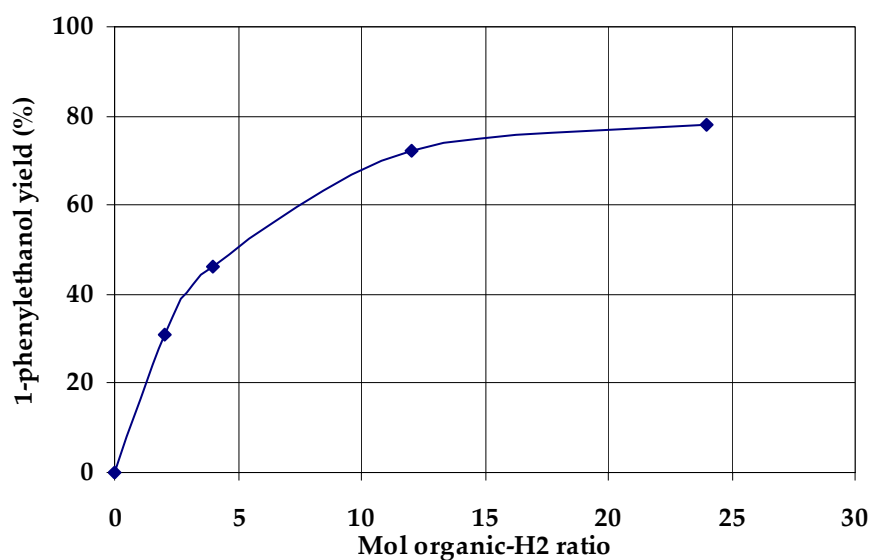
Table B-3: Effect of operating variables on 1-phenylethanol yield.

Aqueous Reducing Reagent	mol Org/H ₂	T (K)	P (MPa)	Residence time (s)	Yield (%)
HCO ₂ Na (pH=12)	1/32	523	16	10	57±2
	1/24			19	78±1
	1/2			19	31±1
	1/4			19	46±1
				38	57±2
	1/12			19	72±1
HCO ₂ H (pH=1)	1/32	523	16	10	0

Acetophenone yield increases with the increment of residence time or mol organic-hydrogen ratio.

The optimal mol organic-H₂ ratio for achieve high 1-phenylethanol yield under the reaction conditions chosen, was 12 as shows the figure below. A higher ratio than 12 did not improve significantly the yield.

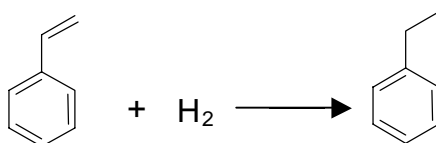
On the other hand, it could be possible to obtain an increase on reaction yield using a lower mol organic-H₂ ratio but increasing the residence time in the reactor.

**Figure B-4: Effect of mol organic-H₂ ratio on yield (523.15 K, 16 MPa and 19 s.).**

As in the case of cyclohexanone, the hydrogenation of acetophenone reaction does not work well with the use of formic acid but at the same reaction conditions, product yield from acetophenone hydrogenation is higher than cyclohexanone reaction due to its higher reactivity.

HCO₂H seems to be poorly decomposed in the experimental conditions used but addition of NaOH to the formic acid solution helps dramatically the reactivity.

Styrene



Scheme B-3: Hydrogenation of styrene.

Collected samples from the reactor and starting material were analyzed by HPLC using instrumental method explained above. Standard samples were diluted in ethanol whereas reaction products in water (1:10). Calibration curves for the reactant and product are presented below.

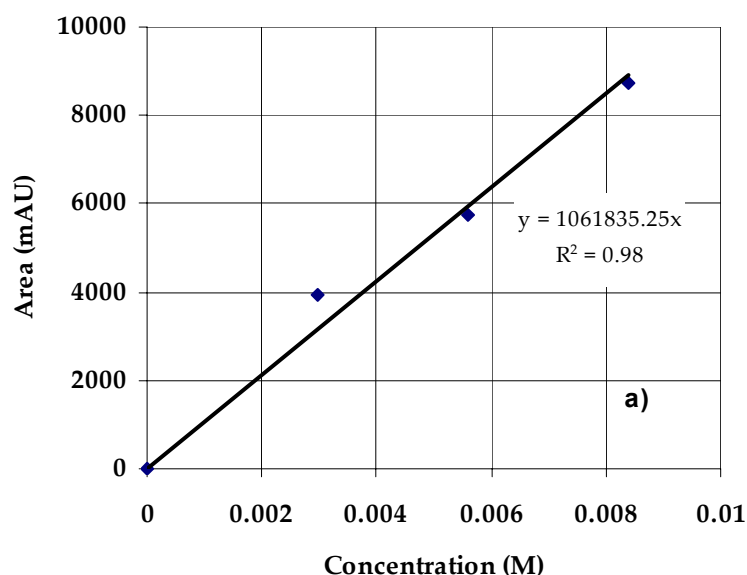


Figure B-5a: GC calibration of Styrene.

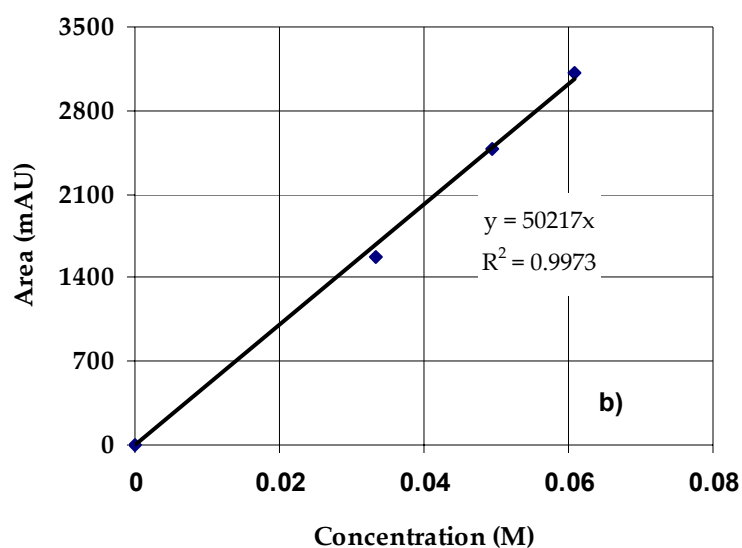


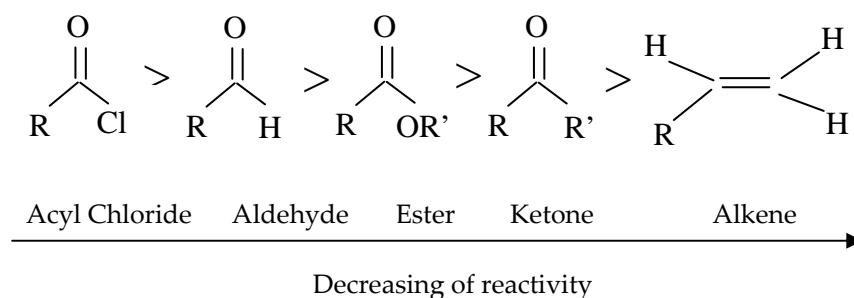
Figure B-5b: GC calibration of Ethylbenzene.

The effect of the reaction variables on ethylbenzene yield is presented in Table B-4.

Table B-4: Effect of operating variables on ethylbenzene yield.

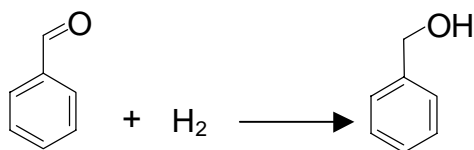
Aqueous Reducing Reagent	mol Org/H ₂ ratio	T (K)	P (MPa)	Residence time (s)	Yield (%)
HCO ₂ Na (pH=12)	1/49	523	16	6	0
HCO ₂ H (pH=1)					

Formic acid decomposition does not hydrogenate styrene neither does sodium formate. This fact is possibly explained by the high activation energy of this chemical reaction and by the low reactivity of the alkenes in comparison with aldehydes and ketone carbonyl groups and for instance, it must be necessary to add a hydrogenation catalyst. The reactivity of carbonyl groups and alkenes can be clarified as follows:



Scheme B-4: Reactivity of organic groups.

Benzaldehyde



Scheme B-5: Hydrogenation of benzaldehyde.

Like acetophenone and styrene calibration, benzaldehyde and benzyl alcohol were calibrated by HPLC analysis using Hydro254.m method. The standards and reactor samples were diluted in methanol.

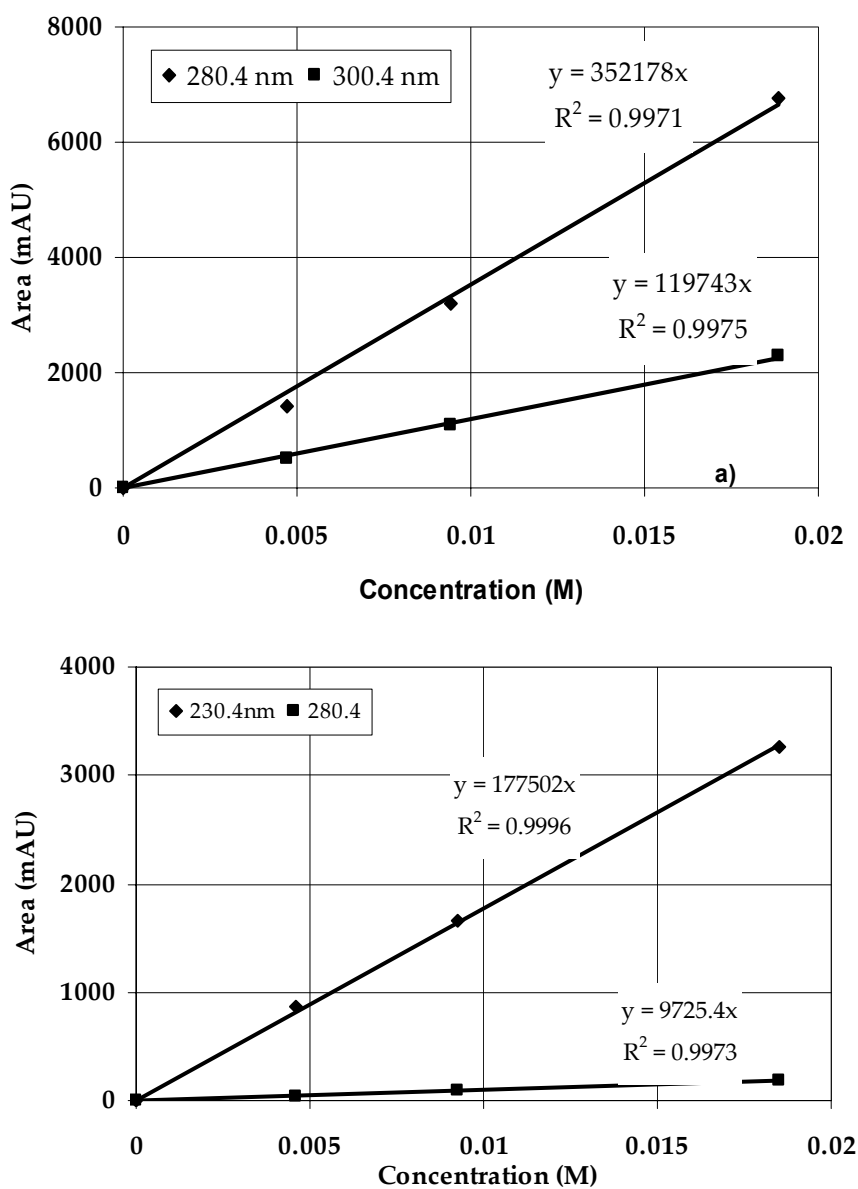


Figure B-6: GC calibration of a) Benzaldehyde and b) Benzyl Alcohol.

The effect of the reaction variables on benzyl alcohol is presented in Table B-5.

Table B-5: Effect of operating variables on benzyl alcohol yield.

Aqueous Reducing Reagent	mol Org/H ₂ ratio	T (K)	P (MPa)	Residence time (s)	Yield (%)
HCO ₂ Na (pH=12)	1/19	520	16	19	65±1
	1/13	463	16	29	54±0.7
	1/13	463	21	29	48±1
	1/13	414	15	31	40±0.2
H ₂ O (pH=7)	1/0	521	16	19	0
HCO ₂ H (pH=1)	1/32	523	16	19	0
HCO ₂ NH ₄ (pH=2.7)	1/10	522	15	24	94±3
HCO ₂ NH ₄ (pH=4)	1/33				88±2
HCO ₂ NH ₄ (pH=8)	1/33				56±1
HCO ₂ NH ₄ (pH=11)	1/33				11±1

Benzyl alcohol yield could be improved by rising the reaction temperature. On the other hand, the increase of pressure has a negative influence on it.

Like in the other organic compounds studied before, hydrogenation reaction using formic acid aqueous solution did not work but if a small amount of ammonia solution is added to the formic acid aqueous solution in order to change the pH, the benzyl alcohol yield dramatically increases at low pH (from pH=1 to 2.7).

As shows in the following figure, the rise of solution pH decreases reaction yield due to the large ammonium excess used at high pH an leads presumably to side reactions as the HPLC analysis suggested (many small peaks could not be identified).

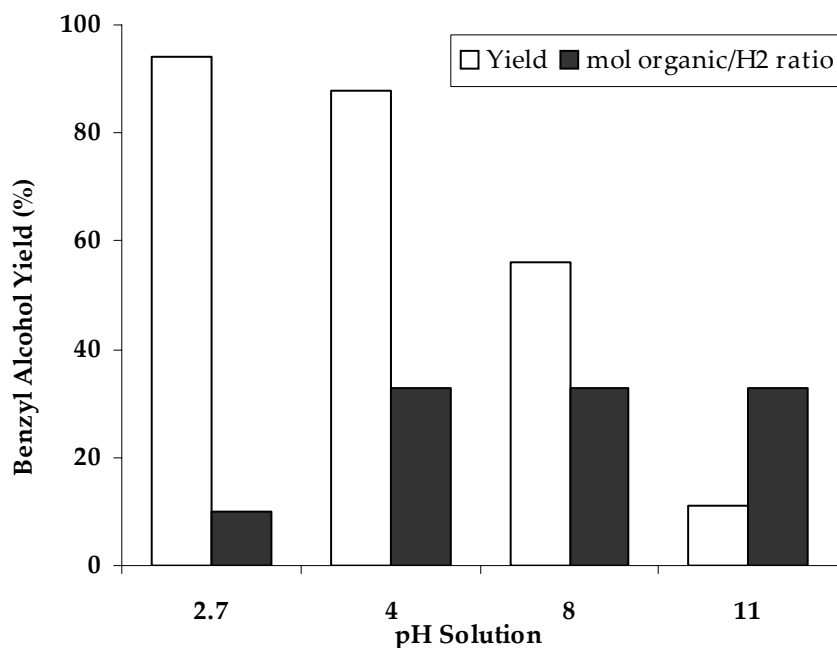


Figure B-7: Effect of pH of HCO₂NH₄ solution on reaction yield.

The results obtained in this research are comparable as those reported by Bryson *et al.* (2004), who have reduced aldehydes and a number of ketones using aqueous sodium formate without adding any catalyst.

Table B-6: Research results in comparison with those of Bryson *et al.* (2004).

Author	Reaction conditions	Cyclohexanone Yield %	Benzyl Alcohol Yield %
Bryson <i>et al.</i>	588 K 8 MPa 3 h (batch) 1:3 mol org-H ₂ ratio	34	74
This research	523 K 15 MPa 19-24 s (continuous) 1:9/19 mol org-H ₂ ratio	28	65

The advantage of our research compared to Bryson *et al.* are:

- Continuous reaction
- Lower temperature
- Much less residence time

- Comparable yields.

Conclusions and further plans.

Aldehydes and ketones are effectively reduced to alcohol with sodium or ammonium formate in near critical water without a co-solvent or added catalyst.

Aldehyde hydrogenation yield is higher than those obtained from ketone reactions. This fact is easily explained by the chemical reactivity as well as the fact of no reaction of styrene (even it is stable in these reaction conditions), was observed, and the use of a hydrogenation catalyst is needed.

Increase of temperature or mol organic-H₂ ratio or residence time produces an increase in yield of products even the latter seems to have stronger influence on it. The total system pressure increment has a negative effect on reaction yield.

The amount of ammonia solution to change the pH of acid formic solution and to produce ammonium formate has a strong influence on benzyl alcohol yield because with a small amount is enough to obtain a good yield whereas an ammonium exceeds lead to the decrease of it because of no-reactant ammonia originate side reactions.

Once the studies on:

- Decomposition of formic acid, sodium formate and ammonium formate to produce H₂.
- Screening of different organic compounds have been carried out, the main aspects for the further study are:
 1. Kinetics study on temperature and pressure for each compound with residence time (RT).
 2. Heterogeneous catalysis study.
 3. Attempt other functional groups to be hydrogenated.

Nomenclature

P pressure [MPa]

RT residence time [s]

T Temperature [K]

Acronyms

CAN acetonitrile

AcONA acetone

BPR back pressure regulator

FAME fatty acid methyl ester

FAO fatty alcohols

H₂ hydrogen

H₂O water

HCO₂H formic acid

HPLC high-performance liquid chromatography

ID internal diameter

NaCO₂H sodium formate

NaOH sodium hidroxide

NH₄CO₂H ammonium formate

Org organic

PT pressure transducer

RT retention time

SCF supercritical fluid

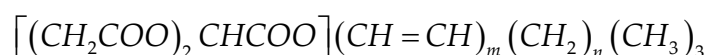
T thermocouple

TIC temperature indicator controller

Appendix C

Estimation of Thermodynamic Properties for Sunflower Vegetable Oil.

Natural vegetable oils consist mainly of mixtures of saturated and unsaturated triglycerides of long-fatty acid chains; i.e. slightly polar molecules, with molecular weights in the order of 850. A vegetable oil can be represented through a pseudo-component of this type:



Scheme C-1: Pseudo-component which represents a vegetable oil (Pereda *et al.*, 2002).

The number of double bonds (m) and the length of the fatty chains (n) in the pseudo-component molecule have to satisfy the degree of unsaturation and the molecular weight of the natural oil, obtained from its fatty acid composition.

Vegetable sunflower oil triacylglycerol composition was reported by Neff *et al.* (1994) as follows:

Table C-1: Sunflower oil triacylglycerol composition by reversed-phase high performance liquid chromatography with flame ionization detection (Neff *et al.* (1994).

Resolution			Quantitation (wt %)
Triacylglycerol saturated, monoenic, dienoic, trienoic fatty acid species*	Number of double bonds	Triacylglycerol molecular species reversed phase [†]	
SSS	0	PPP, PPS, PSS, SSS	0.3
SSM	1	POP, SPO, SOS	0.7
SSD	2	PLP, SLP, SLS	1.7
SMM	2	POO, SOO	1.8
SMD	3	LOP, LOS	8.1
MMM	3	OOO	1.5
SDD	4	LLS, LLP	20.4
MMD	4	LOO	6.0
DDM	5	LLO	23.4
DDD	6	LLL	35.8
TDD	7	LnLL	0.3

*S, M, D, T = saturated (palmitic and stearic acids); monoenoic (oleic); dienoic (linoleic) and trienoic (linolenic) acids, respectively, attached to the triacylglycerol glycerol moiety.

^tS, P, O, L, Ln = stearic, palmitic, oleic, linoleic and linolenic acids, respectively, attached to the triacylglycerol moiety.

First of all, the thermodynamic constants for each pure component of sunflower oil are estimated by means correlations of the *group contribution* type because the scarcity of experimental data. Even though the Ambrose method is somewhat more complicated than other estimate methods, it yields the smaller error for critical properties estimation. The mean of the absolute error for T_C , P_C and V_C estimation are 0.7 K, 0.18 MPa and 8.5 cm³/mol respectively.

In the method of Ambrose (Reid, *et al.*, 1987), the three critical properties T_C , P_C and V_C are estimated by a group contribution technique using the following relations:

$$T_C = T_b \left[1 + \left(1.242 + \sum \Delta_T \right)^{-1} \right] \quad \text{(C.1)}$$

$$P_C = M \left(0.339 + \sum \Delta_p \right)^{-2} \quad \text{(C.2)}$$

$$V_C = 40 + \sum \Delta_v \quad \text{(C.3)}$$

The units are kelvins, bars, and cubic centimetres per mole. The Δ quantities are evaluated by summing contributions for various atoms or groups of atoms as shown in Table C-2.

To employ these equations, the normal boiling point T_b (at 0.1 MPa) and the molecular weight M are needed. Yu *et al.* (1994) report the boiling point for several triglycerides (tripalmitin, triolein and tristearin). The boiling point values for the other components were estimated using the group contributions for T_b proposed by Joback (Reid, *et al.*, 1987) with the relation:

$$T_b = 198 + \sum \Delta_b \quad \text{(C.4)}$$

where T_b is in kelvins. The average absolute error found with this equation was 12.9 K and the standard deviation of the error was 17.9 K. Although these errors are not small, this simple technique may be useful as a guide in obtaining approximate values of T_b for which no experimental value is available.

Table C-2: Ambrose group contributions for critical constants (Reid *et al.*, 1987).

	Δ values for		
	T_c	P_c	V_c
Carbon atoms in alkyl groups	0.138	0.226	55.1
Corrections:			
>CH- (each)	-0.043	-0.006	-8
>C< (each)	-0.120	-0.030	-17
Double bonds (nonaromatic)	-0.050	-0.065	-20
Triple bonds	-0.200	-0.170	-40
Delta Platt number, ¹ multiply by	-0.023	-0.026	—
Aliphatic functional groups:			
-O-	0.138	0.160	20
>CO	0.220	0.282	60
-CHO	0.220	0.220	55
-COOH	0.578	0.450	80
-CO-O-OC-	1.156	0.900	160
-CO-O-	0.330	0.470	80
-NO ₂	0.370	0.420	78
-NH ₂	0.208	0.095	30
-NH-	0.208	0.135	30
>N-	0.088	0.170	30
-CN	0.423	0.360	80
-S-	0.105	0.270	55
-SH	0.090	0.270	55
-SiH ₃	0.200	0.460	119
-O-Si(CH ₃) ₂	0.496	—	—
-F	0.055	0.223	14
-Cl	0.055	0.318	45
-Br	0.055	0.500	67
-I	0.055	—	90
Halogen correction in aliphatic compounds:			
F is present	0.125	—	—
F is absent, but Cl, Br, I are present	0.055	—	—
Aliphatic alcohols ²			15
Ring compound increments (listed only when different from aliphatic values):			
-CH ₂ -, >CH-, >C<	0.090	0.182	44.5
>CH- in fused ring	0.030	0.182	44.5
Double bond	-0.030	—	-15
-O-	0.090	—	10
-NH-	0.090	—	—
-S-	0.090	—	30
Aromatic compounds:			
Benzene	0.448	0.924	5
Pyridine	0.448	0.850	—
C ₂ H ₄ (fused as in naphthalene)	0.220	0.515	—
-F	0.080	0.183	—
-Cl	0.080	0.318	—
-Br	0.080	0.600	—
-I	0.080	0.850	—
-OH	0.198	-0.025	—
Corrections for nonhalogenated substitutions:			
First	0.010	0	—
Each subsequent	0.030	0.020	—
Ortho pairs containing -OH	-0.080	-0.050	—
Ortho pairs with no -OH	-0.040	-0.050	—

One of the more common pure component constants is the acentric factor, w , which represents the acentricity or nonsphericity of a molecule. For monoatomic gases, w is, therefore, essentially zero. However, for higher molecular-weight hydrocarbons, w increases. It also rises with polarity. The acentric factor is defined as follows:

$$w = \frac{3}{7} \frac{\theta}{1-\theta} \log P_c - 1 \quad (\text{C.5})$$

where P_c , in this case, expressed in atmospheres and $\theta = T_b/T_c$.

The critical values for all triacylglycerol molecular species were not estimated due to the great similarity between them. The species for calculation were chosen depending on their structural simplicity as well on their high weight content in the sunflower oil (see Table C-1).

Table C-3 presents the critical values for some of pure components of sunflower oil estimated with Ambrose method as well as the acentric factor values estimated by equation C-5.

Table C-3: Estimated critical properties for pure components of sunflower oil.

Triacylglycerol Specie	Formula	Molecular Weight (g/mol)	T_b (K)	T_c (K)	P_c (bar)	V_c (cm ³ /mol)	w
PPP	C ₅₁ H ₉₈ O ₆	807.3	798.5*	889.1	5.1	2916.8	1.670
SSS	C ₅₇ H ₁₁₀ O ₆	891.5	816.3*	901.0	4.6	3247.4	1.732
SOS	C ₅₇ H ₁₀₈ O ₆	889.46	791.6	874.6	4.7	3207.4	1.733
SOO	C ₅₇ H ₁₀₆ O ₆	887.45	787.5	870.9	4.7	3167.4	1.733
OOO	C ₅₇ H ₁₀₄ O ₆	885.5	783.3*	867.2	4.8	3127.4	1.734
LOO	C ₅₇ H ₁₀₂ O ₆	883.4	779.1	863.5	4.9	3087.4	1.734
LLO	C ₅₇ H ₁₀₀ O ₆	881.4	775.0	859.8	5.0	3047.4	1.733
LLL	C ₅₇ H ₁₉₈ O ₆	879.4	770.8	845.1	5.1	3007.4	1.732

*From Yu *et al.* (1994)

With the values of Table C-3, the critical properties of the oil, which is a triglycerides mixture, are estimated using the empirical methods due to their simplicity.

The true mixture critical temperature is usually not a linear mole fraction average of the pure component critical temperatures. Li (1971) has suggested that if the composition is expressed as

$$\phi_j = \frac{y_j V_{cj}}{\sum_i y_i V_{ci}} \quad (\text{C.6})$$

the true mixture critical temperature can be estimated by

$$T_{CT} = \sum_j \phi_j T_{cj} \quad (\text{C.7})$$

where y_j is the mole fraction of component j , V_{cj} is the critical volume of j , T_{cj} is the critical mixture of j and T_{CT} is the true mixture critical temperature.

Chueh and Prausnitz (1967) have proposed a similar technique. By defining a *surface fraction* θ_j ,

$$\theta_j = \frac{y_j V_{cj}^{2/3}}{\sum_i y_i V_{ci}^{2/3}} \quad (\text{C.8})$$

they then relate θ_j and T_{CT} by

$$T_{CT} = \sum_j \theta_j T_{cj} + \sum_i \sum_j \theta_i \theta_j \tau_{ij} \quad (\text{C.9})$$

where τ_{ij} is an interaction parameter. τ_{ii} is considered to be zero, and τ_{ij} ($i \neq j$) can be estimated for several different binary types by

$$\psi_T = A + B\delta_T + C\delta_T^2 + D\delta_T^3 + E\delta_T^4 \quad (\text{C.10})$$

where

$$\psi_T = \frac{2\tau_{ij}}{T_{ci} + T_{cj}} \quad (\text{C.11})$$

and

$$\delta_T = \left| \frac{T_{ci} - T_{cj}}{T_{ci} + T_{cj}} \right| \quad (\text{C.12})$$

The coefficients for equation C-10 are shown below for a few binary types, where $0 \leq \delta_T \leq 0.5$:

Table C-4: Coefficients for equation C.10 (Reid *et al.*, 1987).

Binary	A	B	C	D	E
Containing aromatics	-0.0219	1.227	-24.277	147.673	-259.433
Containing H ₂ S	-0.0479	-5.725	70.974	-161.319	
Containing CO ₂	-0.0953	2.185	-33.985	179.068	-264.522
Containing C ₂ H ₂	-0.0785	-2.152	93.084	-722.676	
Containing CO	-0.0077	-0.095	-0.225	3.528	
All other systems	-0.0076	0.287	-1.343	5.443	-3.038

The critical temperature value for sunflower oil was 855 K from Li estimation and 859 K from Chueh and Prausnitz method. As can be noticed, these values are not quite different. For both methods, the average deviation is less than 4 K (Reid, *et al.*, 1987).

Only a few experimental values are available for mixture critical volumes. Thus the range and accuracy of estimation methods are not clearly established but an analytical technique by Chueh and Prausnitz (1967) appears to be more accurate. When the surface fraction θ_j is defined as in equation C-8, the mixture critical volume is given by:

$$V_{CT} = \sum_j \theta_j V_{cj} + \sum_i \sum_j \theta_i \theta_j v_{ij} \quad (\text{C.13})$$

V_{cj} is the critical volume of j and v_{ij} is an interaction parameter such that $v_{ii}=0$ and v_{ij} ($i \neq j$) can be estimated as follows:

$$\psi_v = A + B\delta_v + C\delta_v^2 + D\delta_v^3 + E\delta_v^4 \quad (\text{C.14})$$

$$\psi_v = \frac{2v_{ij}}{V_{ci} + V_{cj}} \quad (\text{C.15})$$

$$\delta_v = \left| \frac{V_{ci}^{2/3} - V_{cj}^{2/3}}{V_{ci}^{2/3} + V_{cj}^{2/3}} \right| \quad (\text{C.16})$$

The coefficients for equation C-14 are given below for a few binary types when $0 \leq \delta_v \leq 0.5$.

Table C-5: Coefficients for equation C.14.

Binary	A	B	C	D	E
Aromatic-aromatic Containing at least one cycloparaffin	0	0	0	0	0
Paraffin-aromatic	0.0753	-3.332	2.220	0	0
System with CO ₂ or H ₂ S	-0.4957	17.1185	-168.56	587.05	-698.89
All other systems	0.1397	-2.9672	1.8337	-1.536	0

The critical volume estimated value for sunflower was 3261 cm³/mol. The average error of this method is around 10.5%.

The dependence of mixture critical pressures on mole fraction is often nonlinear, and estimation of P_{CT} is often unreliable. One of the most general approaches for predicting the critical pressure for mixtures was developed by Chueh and Prausnitz (1967). P_{cm} was related to T_{cm} and V_{cm} by a modified Redlich-Kwong equation of state:

$$P_{CT} = \frac{RT_{CT}}{V_{CT} - b_m} - \frac{a_m}{T_{CT}^{1/2} V_{CT} (V_{CT} + b_m)} \quad (\text{C.17})$$

where T_{CT} and V_{CT} are calculated from the methods presented earlier in this appendix. The mixture coefficients for determining P_{CT} are defined as

$$b_m = \sum_j y_j b_j = \sum_j \frac{y_j \Omega_{bj}^* RT_{cj}}{P_{cj}} \quad (\text{C.18})$$

$$a_m = \sum_i \sum_j y_i y_j a_{ij} \quad (\text{C.19})$$

with

$$\Omega_{bj}^* = 0.0867 - 0.0125w_j + 0.011w_j^2 \quad (\text{C.20})$$

$$a_{ii} = \frac{\Omega_{ai}^* R^2 T_{ci}^{2.5}}{P_{ci}} \quad (\text{C.21})$$

$$a_{ij} = \frac{(\Omega_{ai}^* + \Omega_{aj}^*) RT_{cij}^{1.5} (V_{ci} + V_{cj})}{4 [0.291 - 0.04(w_i + w_j)]} \quad (\text{C.22})$$

$$T_{cij} = (1 - k_{ij}) \sqrt{T_{ci} T_{cj}} \quad (\text{C.23})$$

$$\Omega_{aj}^* = \left(\frac{RT_{cj}}{V_{cj} - b_j} - P_{cj} \right) \frac{P_{cj} V_{cj} (V_{cj} + b_j)}{(RT_{cj})^2} \quad (\text{C.24})$$

The interaction parameter k_{ij} usually ranges from 0.15 to 0.01. Values for a large number of binary systems have been tabulated (Chueh and Prausnitz, 1967). With this estimation, the average deviation is around 1.5 bar.

The estimated critical pressure for sunflower oil was around 2 bar.

Table C-6 presents the critical properties estimated in this appendix for sunflower oil:

Table C-6: Estimated sunflower oil critical constants.

T_{cm} (K)	V_{cm} (cm ³ /mol)	P_{cm} (bar)
859±4	3261±342	2±1.5

Nomenclature

- A..E coefficients of eqs. C-10 and C-14
- D dioenoic (linoleic) acids attached to the triacylglycerol glycerol moiety
- k_{ij} parameter of binary mixture
- L linoleic acids attached to the triacylglycerol moiety
- L_n linolenic acids attached to the triacylglycerol moiety
- M monoenoic (oleic) acids attached to the triacylglycerol glycerol moiety
- M molecular weight [g/mol]
- O oleic acids attached to the triacylglycerol moiety
- P palmitic acids attached to the triacylglycerol moiety
- P_c critical pressure [bar]
- P_{cm} mixture critical pressure [bar]
- P_{CT} true mixture critical pressure [bar]
- R gas-law constant [8.314 J/(mol K)]
- S saturated (palmitic and stearic) acids attached to the triacylglycerol glycerol moiety
- T trienoic (linolenic) acids, attached to the triacylglycerol glycerol
- T_b boiling temperature [K]
- T_c critical temperature [K]
- T_{cm} mixture critical temperature [K]

T_{CT} true mixture critical temperature [K]

V_c critical molar volume [cm³/mol]

V_{cm} mixture critical volume [cm³/mol]

w acentric factor

y mole fraction

Greek letters

Δ increment

θ T_b/T_c

θ_j surface fraction

ϕ composition

τ interaction parameter

v interaction parameter

Sub- and Superscripts

b boiling

c critical

i component

j component

m mixture

m number of double bonds

n length of the fatty chains

t true

Appendix D

Calculating Binary, Vapor-Liquid Equilibria Using The Peng Robinson Equation of State.

The basic scheme for modelling the phase behaviour of binary mixtures consists of first, include the the pure components characteristic parameters T_c , P_c and w , and then determine the binary mixture parameters k_{ij} and η_{ij} , by fitting data such as pressure-composition isotherms by means of analytical solution of the cubic PR-EOS. Normally k_{ij} and η_{ij} are expected to be between ± 0.200 . If the two species are close in chemical size and intermolecular potential, the binary mixture parameters will have values very close to zero. In certain cases a small value of either of these two parameters can have a large influence on the calculated results (McHugh and Krukonis, 1994). The program PR2 is detailed and explained step to step as follows:

PROGRAM PR2

```
PARAMETER (N=2)                                !# of components

IMPLICIT REAL*8 (A-H,O-Z)

DIMENSION H(N,1000),Q(N,1000),FPV(N),FPL(N),TEST(N),PR(N+1,N+1),
ETA(N+1,N+1)

DIMENSION X(N),Y(N),AMW(N),W(N),TC(N),PC(N),U(N),V(N)

COMMON/PENG/AMW,W,TC,PC,PR,ETA

OPEN (Unit=15,File='PR2.DAT',Status='OLD')

OPEN (Unit=16, File='PR2.OUT', Status='UNKNOWN')

CLOSE (16 ,Status='DELETE')

OPEN (Unit=16, File='PR2.OUT', Status='NEW')
```

Variables subscripted #1 designate the volatile component, light (solvent). Variables subscripted #2 designate the non-volatile component, heavy (solute). The second subscript in double subscripted variables is the iteration method number so that $H(2,1)$ is the distribution K value ($K=y/x$) for component #2 for the first iteration. The first part

of the program is set up to read from an external data file, here named PR2.DAT, physical constants (molecular weights, T_c , P_c and w), mixture parameters (k_{ij} -designated 'PR' in this program- and η_{ij} -designated 'ETA' in this program), and pressure ranges (PHIGH, PLOW, and PINC for pressure increment) for the calculation.

```
DO 10 I=1,N                                !Input T(°C), P(bar), Mw, Tc, Pc, w, kij and ηij

READ (15,*) AMW(I)

10 READ (15,*) TC(I),PC(I),W(I)

DO 50 I=1,N-1

    DO 60,J=1,N-1

        READ (15,*) PR(I,J+1),ETA(I,j+1)

        PR(J+1,I)=PR(I,J+1)

        ETA(J+1,I)=ETA(I,J+1)

    60 CONTINUE

50 CONTINUE

WRITE(6,*)'kij=',PR(1,2),'nij=',ETA(1,2)

READ(15,*)T,PLOW,PHIGH,PINC

WRITE(6,*)T

T=T+273.15

WRITE(*,*)'T=',T-273.15

WRITE(*,12)

WRITE(*,13)

WRITE(16,*)"T=",T-273.15

WRITE(16,12)

READ (15,*) PLOW, PHIGH, PINC
```

```
12 FORMAT (24X,'(bar)',8X,'(g/cm3)',4X,'(g/cm3)')
```

```
WRITE(*,12)
```

```
13 FORMAT(3X,'Xheavy',2X,'Y(gas)heavy',3X,'Press',8X,'DENL',4X,'DENV', 5X,'it')
```

The pressure is initialized for the first iteration and initial estimates of the $K = y/x$ are given.

```
H(1,1)=20.0
```

```
H(2,1)=0.05
```

```
P=FLOW
```

```
DP=PINC
```

To calculate the P-x isotherm. ICOUNT is used to flag the method for updating the distribution coefficient, $H(i,j)$, to avoid a singularity. JFLAG= number of iterations per tie line. The DO 20 LOOP is used to calculate the entire P-x isotherm. A very high number of iterations is set, so that the program is expected to reach the mixture's critical pressure (PHIGH) before reaching the maximum number of iterations in this loop. The DO 30 LOOP is used to calculate a single tie line. Again the number of iterations is set high so that the tie line is expected to converge or a warning statement will be printed to the screen before 250 iterations can be performed.

```
DO 20 ICOUNT=1,15000
```

```
    DO 30 JFLAG=1,5000
```

```
        X(2)=(1.-H(1,JFLAG))/(H(2,JFLAG)-H(1,JFLAG))
```

```
        X(1)= 1.-X(2)
```

```
        IF((X(1).LT.0.0).OR.(X(1).GT.1.0)) GOTO 115
```

```
        Y(1)=H(1,JFLAG)*X(1)
```

```
        Y(2)=1.-Y(1)
```

The vapor-phase fugacity coefficient (ϕ) is calculated first, followed by the liquid-phase fugacity coefficient:

```
CALL PHIPR(T,P,Y,FPV,DENV,0,N)
```

```
CALL PHIPR(T,P,X,FPL,DENL,1,N)
```

The following lines test the equilibrium, i.e., if the fugacity (f) of each component is equal in each of the phases.

```
Q(1,JFLAG)=(X(1)*FPL(1))/(Y(1)*FPV(1))
```

```
Q(2,JFLAG)=(X(2)*FPL(2))/(Y(2)*FPV(2))
```

```
TEST(1)=ABS(Q(1,JFLAG)-1.)
```

```
TEST(2)=ABS(Q(2,JFLAG)-1.)
```

If TEST(1) or TEST(2) are not within the adjustable tolerance, the program will do another iteration at this temperature and pressure with a new estimate of the distribution coefficients:

```
IF(TEST(1).GE.0.001.OR.TEST(2).GE.0.001) THEN
```

```
    H(1,JFLAG+1)=H(1,JFLAG)*Q(1,JFLAG)
```

```
    H(2,JFLAG+1)=H(2,JFLAG)*Q(2,JFLAG)
```

```
ELSE
```

```
    GOTO 35
```

```
ENDIF
```

```
30 CONTINUE
```

```
WRITE (*,*) "THE TIE LINE DID NOT CONVERGE"
```

```
GOTO 115
```

Equilibrium has been reached if TEST1 and TEST2 are within the adjustable tolerance. Now the program calculates new x_s and y_s for each component at the next pressure, $P+DP$. The pressure increment is decreased as the mixture's critical point is approached,

which is seen by determining how close $H(2,JFLAG)$ is to unity. The method for calculating the H_s at $P+DP$ can cause the program to crash if the pressure increment is adjusted at low pressures, far from the maximum pressure of the $P-x$ loop. Here we use an arbitrary value of 50 bar to avoid this problem.

```
35 IF(P.LE.50.0) THEN
```

```
DP=2.
```

```
ELSE
```

```
    IF (H(2,JFLAG).GT.0.40) DP=1.0
```

```
    IF (H(2,JFLAG).GT.0.60) DP=1.0
```

```
    IF (H(2,JFLAG).GT.0.70) DP=0.5
```

```
    IF (H(2,JFLAG).GT.0.80) DP=0.5
```

```
    IF (H(2,JFLAG).GT.0.95) GOTO 75
```

This last statement stops the program very near the mixture critical point. Otherwise the program continues until PHIGH is reached.

```
ENDIF
```

Now a first guess for the values of x and y at this new pressure is attained by fitting the straight K-line through the calculated data and extrapolating it to the new pressure:

```
POLD=P-DP
```

```
PNEW=P+DP
```

```
SS2=X(2)+(PNEW-P)*((X(2)-U(2))/(P-POLD))
```

```
IF(ICOUNT.EQ.1) SS2=X(2)
```

```
SS1=1.-SS2
```

```
TT2=Y(2)+(PNEW-P)*((Y(2)-V(2))/(P-POLD))
```

```
IF(ICOUNT.EQ.1) TT2=Y(2)
```

```
TT1=1.0-TT2
```

$$H(1,1)=TT1/SS1$$

$$H(2,1)=TT2/SS2$$

$$U(1)=X(1)$$

$$U(2)=X(2)$$

$$V(1)=Y(1)$$

$$V(2)=Y(2)$$

The program prints the results on the screen and to a datafile named PR2.OUT.

```
WRITE(*,85) X(2),Y(2),P,DENL,DENV,JFLAG
```

```
WRITE(16,85) X(2),Y(2),P,DENL,DENV,JFLAG
```

```
85 FORMAT (1X,F8.6,2X,F8.6,4X,F9.3,2X,F9.3,1X,F7.4,2X,I4)
```

The program will continue calculating a P-x isotherm as long as the upper limit has not been reached and H(2,JFLAG) is less than 0.95

```
IF(P.GE.PHIGH)THEN
```

```
WRITE(*,*)'UPPER PRESSURE BOUND REACHED'
```

```
    GOTO 115
```

```
ENDIF
```

```
    P=P+DP
```

```
20 CONTINUE
```

```
75 WRITE(*,*)'NEAR THE MIXTURE CRITICAL POINT'
```

```
115 WRITE(16,116)
```

```
WRITE(*,116)
```

```
116 FORMAT(////,8X,'THE PROGRAM IS COMPLETED')
```

```
CLOSE(16)
```

END

Subroutine PHIPR calculates the fugacity coefficient, and the phase density from the PREOS and the mole fractions NNN=0 for the liquid phase, NNN=1 for the gas phase.

```
SUBROUTINE PHIPR(T,P,Y,FP,DEN,NNN,N)
```

```
IMPLICIT REAL*8(A-H,O-Z)
```

```
DIMENSION Y(2),FP(2),A(2,2),B(2,2),AMW(2),W(2),TC(2),PC(2),
```

```
PR(3,3),ETA(3,3),TR(2),TERM1(2),TERM2(2),TERM3(2),ROOT(3),G(2)
```

```
COMMON/PENG/AMW,W,TC,PC,PR,ETA
```

```
GASR=83.14
```

```
BM=0.0
```

```
AM=0.0
```

```
SQ2=2.0**0.5
```

```
Q1=1.0+SQ2
```

```
Q2=SQ2-1.0
```

```
Q3=2.0*SQ2
```

These are the mixture terms A and B for the PREOS. The SUM term will be used later to calculate the mixture density.

```
SUM=0.0
```

```
DO 10 I=1,N
```

```
    SUM=SUM+Y(I)*AMW(I)
```

```
    B(I,I)=0.0778*GASR*TC(I)/PC(I)
```

```
    TERM3(I)=0.0
```

```
    TR(I)=T/TC(I)
```

$$G(I)=(1.0+(0.37464+1.54226*W(I)-0.26992*W(I)**2)*(1.0-TR(I)**0.5))**2$$

$$10 A(I,I)=0.45724*(GASR**2)*(TC(I)**2)/PC(I)*G(I)$$

$$J=N-1$$

$$DO 20 I=1,J$$

$$DO 21 K=I,J$$

$$L=K+1$$

$$A(I,L)=(A(I,I)*A(L,L))**0.5*(1.0-PR(I,L))$$

$$A(L,I)=A(I,L)$$

$$B(I,L)=(B(I,I)+B(L,L))/2.0*(1.0-ETA(I,I))$$

$$B(L,I)=B(I,L)$$

21 CONTINUE

20 CONTINUE

$$DO 30 I=1,N$$

$$DO 31 J=1,N$$

$$BM=BM+Y(I)*Y(J)*B(I,J)$$

$$AM=AM+Y(I)*Y(J)*A(I,J)$$

31 CONTINUE

30 CONTINUE

$$AA=AM*P/GASR**2/T**2$$

$$BB=BM*P/GASR/T$$

The PREOS is written as a cubic equation in $Z=PV/RT$. The equation C becomes:
 $RA1*Z^3 + RA2*Z^2 + RA3*Z + RA4 = 0$. Only one of the 3 roots is valid. The following routine calculates the valid root, using the trigonometric solution of the cubic equation

RA1=1.0

RA2=BB-1.0

RA3=AA-2.0*BB-3.0*BB**2

RA4=BB**3+BB**2-AA*BB

A1=(3.0*RA3-RA2**2)/3.0

B1=(2.0*RA2**3-9.0*RA2*RA3+27.0*RA4)/27

TEST1=DABS((A1**3)/27.0)

TEST2=(B1**2)/4.0

PIE=3.14159265

IF(A1.LT.0.0.AND.TEST1.GT.TEST2)THEN

CO=2.0*(((A1)/3)**0.5)

THETA=(DACOS((3.0*B1)/(A1*CO)))/3.0

ROOT(1)=CO*DCOS(THETA)-(RA2/3.0)

ROOT(2)=CO*DCOS(THETA+(2.0*PIE)/3.0)-(RA2/3.0)

ROOT(3)=CO*DCOS(THETA+(4.0*PIE)/3.0)-(RA2/3.0)

DO 300 J=1,3

IF(ROOT(J).LT.0.0.AND.NNN.EQ.1) THEN

ROOT(J)=1.E+10

ENDIF

300 CONTINUE

The largest root is the vapor's z , the smallest is the liquid's. Depending upon the value of NNN (NNN=0 for the vapor, NNN=1 for the liquid) either the largest or the smallest root is used to determine the fugacity coefficients of the 2 components in a particular phase.

IF(NNN.EQ.0) ZM=DMAX1(ROOT(1),ROOT(2),ROOT(3))

IF(NNN.EQ.1) ZM=DMIN1(ROOT(1),ROOT(2),ROOT(3))

But A1 may not be greater than zero, or TEST1 may not be greater than TEST2:

ELSE

DD=DSQRT(TEST2+(A1**3)/27.0)

AL=1.0

ALL=1.0

TEST3=(-B1)/2.0+DD

IF(TEST3.LT.0.0) THEN

AL=-1.0

ENDIF

TEST3=DABS(TEST3)

A2=AL*((TEST3)**0.3333334)

TEST4=(-B1)/2.-DD

IF(TEST4.LT.0.0) THEN

ALL=-1.0

ENDIF

TEST4=DABS((-B1)/2.-DD)

B2=ALL*((TEST4)**0.3333334)

$$ZM=A2+B2-(RA2/3.0)$$

IF(TEST4.LT.1.E-04) GOTO 40

TEST5=DABS(1.0-DABS(A2/B2))

IF(TEST5.LT.5.E-04) THEN

$$ZM=-1.0*((A2+B2)/2.0)-(RA2/3.)$$

ENDIF

40 ENDIF

$$VM=ZM*GASR*T/P$$

$$DEN=(1/VM)*SUM$$

The fugacity coefficients for each component are now calculated.

BRPRIME=0.0

DO 60 I=1,N

$$BP2=0.0$$

DO 61 INN=1,N

$$61 BP2=2.0*Y(INN)*B(I,INN)+BP2$$

$$BPRIME=BP2-BM$$

$$TERM1(I)=BPRIME*(ZM-1.0)/BM-DLOG(ZM-BB)$$

$$TERM2(I)=BPRIME*AA*DLOG((ZM+Q1*BB)/(ZM-Q2*BB))/(BM*BB*Q3)$$

DO 62 J=1,N

$$62 TERM3(I)=TERM3(I)+2.0*Y(J)*A(J,I)$$

$$TERM3(I)=AA*DLOG((ZM+Q1*BB)/(ZM-Q2*BB))*TERM3(I)/(BB*AM*Q3)$$

$$FP(I)=DEXP(TERM1(I)+TERM2(I)-TERM3(I))$$

60 CONTINUE

RETURN

END

This is the input data file for PR2.FOR. The example given here is for ethane and n-octane:

!Molecular weight of ethane (g/mol)

305.4 48.8 0.091 !Tc(K), Pc(bar), acentric factor w

114.23 !Molecular weight of n-octane (g/mol)

568.8 24.8 0.394 !Tc(K), Pc(bar), acentric factor w

0.017 0.000 ! k_{ij} , η_{ij}

40.0 !Temperature ($^{\circ}$ C)

25 300 3 ! Pressures(bar):Starting, Ending, Increment

This is a partial listing of an example printout for PR2.FOR. X-Heavy and Y-Heavy represent the mole fraction of heavy component in the liquid and gas phase. Den-Liquid is the density of the liquid phase and Den-Vapor is the density of the vapor. The number of iterations increases substantially when the mixture-critical point is approached.

$k_{ij}= 1.700E-2$ $\eta_{ij}=0.00E+00$

T=40.0

X-Heavy	Y-Heavy	Pressure(bar)	Den-Liquid(g/cm ³)	Den-Vapor(g/cm ³)	Iterations
0.467603	0.003399	25.00	0.579	0.037	6
0.412496	0.003326	28.00	0.565	0.043	6

X-Heavy	Y-Heavy	Pressure(bar)	Den-Liquid(g/cm ³)	Den-Vapor(g/cm ³)	Iterations
0.358738	0.003303	31.00	0.549	0.049	4
0.306197	0.003326	34.00	0.531	0.056	4
0.254694	0.003392	37.00	0.509	0.065	5
0.204037	0.003504	40.00	0.483	0.074	5

THIS PROGRAM IS COMPLETED

Nomenclature

Den-Liquid density of the liquid phase [g/cm³]

Den-Vapor density of the vapor phase [g/cm³]

f fugacity [MPa]

k_{ij} parameter of binary mixture

K_i VLE constant. $K_i = y_i/x_i$

M_w molecular weight [g/mol]

P pressure [bar]

P_c critical pressure [bar]

T temperature [°C]

T_c critical temperature [K]

w acentric factor

x liquid mol fraction

y vapor mol fraction

Greek letters

η_{ij} parameter of binary mixture

ϕ fugacity coefficient

Acronyms

PR-EOS Peng-Robinson equation of state

Sub- and Superscripts

1 volatile component (light)

2 non-volatile component (heavy)

i component

Appendix E

Calculating Ternary, Vapor-Liquid Equilibria Using The Peng Robinson Equation of State.

The HYSYS 2.4.1 Build 3870 (Hyprotech, USA) software makes possible to predict properties of mixtures using the Peng Robinson equation of state (PR-EOS) (see equations 2.1 to 2.20 in Chapter 2) in order to predict the vapour-liquid phase equilibrium. The software provides the compositions of vapor and liquid of each component as well as total the vapor fraction. The curve of bubble is reached when the fraction of vapor is 0 and the curve of dew when it is 1.

To find dew and bubble points, the pressure and temperature are set and the composition of the ternary mixture is varied. For each point, the composition of solvent is set, and then the compositions of oil and hydrogen are varied until it reaches a vapor fraction value equal to 0 or 1. The same procedure is repeated for several propane composition values until bubble and dew curves are obtained. These curves (bubble and dew) join in a point which will be roughly the critical point.

The sequence employed for making the estimates is presented as follows:

1. Define the fluids and parameters for estimation (*add fluid package*):
 - 1.1 Choose the PR EOS
 - 1.2 Especificy the components of the system to be studied:
 - 1.2.1 Choose propane and hydrogen from software library.
 - 1.2.2 Create a new component: sunflower oil (*quick create a hypothetical component*): Introduce the name, group, chemical formula, structure, molecular weight, boiling temperature, density, critical properties and the acentric factor (Take these properties values from Appendix B)
 - 1.2.3 Introduce the binary coefficients corresponding to interaction parameters for the chosen EOS.
2. Enter to the environment of simulation

3. Create a fluid (*flowsheet* → *add stream*): Define the temperature, pressure as well as the flow composition (specify molar or weight percentages).
4. Start calculations (*Simulation* → *Start calculation*).

Dew and bubble curves data for the ternary system DME + hydrogen + sunflower oil at 453.15 K and 20 MPa are reported in Table E-1 and VLE are plotted in Figure E-1.

Table E-1: Dew and bubble curves data for the ternary system Dimethyl ether (1)/Hydrogen (2)/Sunflower Oil (3) system at 453.15 K and 20 MPa, x denotes either liquid or vapor phase mole fraction.

x (1)	x (2)	x (3)	Vapor Fraction
0.0000	1.0000	0.0000	1
0.1000	0.9000	0.0000	1
0.2000	0.8000	0.0000	1
0.3000	0.6999	0.0001	1
0.4000	0.5999	0.0001	1
0.5000	0.4999	0.0001	1
0.6000	0.3996	0.0004	1
0.7000	0.2965	0.0035	1
0.7100	0.2856	0.0044	1
0.7200	0.2745	0.0055	1
0.7300	0.2623	0.0077	1
0.7400	0.2493	0.0107	1
0.7400	0.2026	0.0574	0
0.7300	0.2027	0.0673	0
0.7200	0.2035	0.0765	0
0.7100	0.2047	0.0853	0
0.7000	0.2060	0.0940	0
0.6000	0.2240	0.1760	0
0.5000	0.2425	0.2575	0
0.4000	0.2596	0.3404	0
0.3000	0.2753	0.4247	0
0.2000	0.2898	0.5102	0
0.1000	0.3034	0.5966	0
0.0000	0.3161	0.6839	0

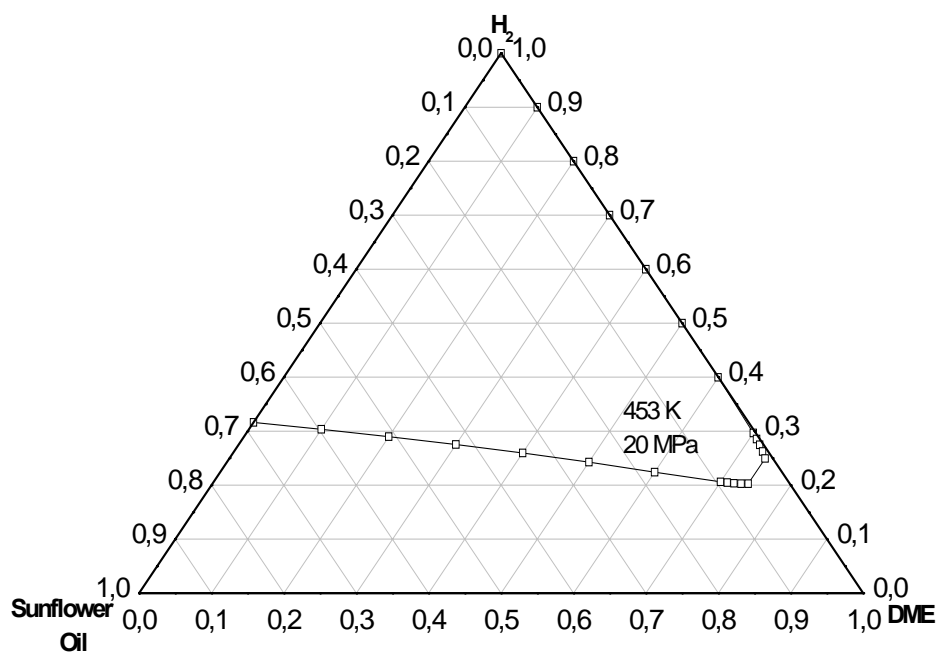


Figure E-1: Dew and bubble curves for the ternary systems estimated with the PR-EOS (see Sandler, 1999): Dimethyl ether (DME)/Hydrogen (H₂)/sunflower oil system at 473.15 K and 20 MPa. In mol %.

Appendix F

Estimation of Transport Effects.

A substantial number of *a priori* criteria for the estimation of transport effects on catalytic reaction rates has been reported by a number of workers. These criteria are generally derived on the premise that one does not desire the net transport effect to alter the true rate by more than some arbitrarily specified amount, normally 5%. Because of the uncertainty involved in knowing some parameters, the philosophy in applying these criteria should be conservative.

A summary of applied intraparticle transport criteria is given as follows. These criteria ensure the absence of any effects (combined) of temperature and concentration gradients but do not guarantee that this may not be due to a compensation between heat- and mass-transport rates.

Required Experimental Data

$$T = 484.15 \text{ K}$$

$$P = 20 \text{ MPa}$$

Particle size = 0.92 mm then $R_p = L/2 = 0.46 \text{ mm}$ for a slab geometry

$$-r'_{\text{H}_2, \text{obs}} = 2.26 \times 10^{-4} \text{ mol}/(\text{kg s})$$

$$D_{e, \text{H}_2} = 2 \times 10^{-7} \text{ m}^2/\text{s}$$

$$\rho_p = 640 \text{ kg}/\text{m}^3$$

$$C_{\text{H}_2, s} = 1.56 \text{ mol}/\text{m}^3$$

$$k_{ef} = 2.09 \times 10^{-4} \text{ (KJ m)}/(\text{s K}) \text{ from Butt (2000)}$$

$$Re = 592.93$$

$$k_g = 1 \times 10^{-2} \text{ m/s from Puiggené et al. (1996)}$$

$$h = 0.2 \text{ (KJ m}^2)/(\text{s K}) \text{ from Velo (2003)}$$

$$\Delta H_r = -121 \text{ KJ/mol from Veldinsk et al. (1997)}$$

Interphase transport temperature gradient (Levenspiel, 1999).

$$\Delta T_{\max, \text{film}} = \frac{L(-r'_{H_2, \text{obs}} \cdot \rho_p)(-\Delta H_r)}{h} = 0.04^\circ \text{C} \quad (\text{F.1})$$

Intraparticle transport temperature gradient (Levenspiel, 1999).

$$\Delta T_{\max, \text{pellet}} = \frac{D_{e, H_2} C_{H_2, s} (-\Delta H_r)}{k_{ef}} = 0.18^\circ \text{C} \quad (\text{F.2})$$

The values estimated above show that the pellet remains practically under a uniform temperature.

Interphase transport (isothermal) concentration gradient (Levenspiel, 1999).

$$\frac{k_{\text{obs}}'' L}{k_g} = \frac{-r'_{H_2, \text{obs}} \rho_p L}{C_{H_2, s} k_g} = \frac{1}{234} \quad (\text{F.3})$$

The obtained ratio allows to conclude that the rate of reaction is not affected by mass transfer resistance through the film.

Intraparticle mass transport limitation (isothermal particle) (Smith, 1981).

Table F-1: Evaluation of intraparticle mass transport limitation.

Particle size d_p (mm)	Global observed H_2 Reaction rate ($\text{mol s}^{-1} \text{kg}_{\text{cat}}^{-1} \times 10^4$)	$r'_{H_2, \text{obs}} \cdot d_p \times 10^4$
0.92	2.26	2.08
0.47	3.48	1.94

As reflects the product between the observed rate and the particle size, it is clear that the diffusion within the porous pellet has influence on the rate of reaction as well as makes it diminishes.

Nomenclature

$C_{H_2, s}$ concentration of hydrogen at catalyst surface [mol/m³]

D_{e, H_2} effective diffusivity of hydrogen [m²/s]

d_p	spherical diameter of particle [mm]
h	heat transfer coefficient [KJ/(m ² s K)]
H_r	heat of hydrogenation reaction [J/(mol K)]
k_{ef}	heat conductivity of the catalyst particle [(KJ m) / (s K)]
k_g	gas-side overall mass transfer coefficient [m/s]
L	slab thickness [m]
P	pressure [MPa]
Re	Reynolds number
R_p	particle radius [mm]
$r'_{H_2,obs}$	observed reaction rate of hydrogen per mass of catalyst [mol/s kg]
T	temperature [K]

Greek Symbols

Q_p	pellet density [kg/m ³]
-------	-------------------------------------

Appendix G

Estimation of Molecular Diffusivities.

The molecular diffusivities for oil and hydrogen in supercritical propane were estimated. In the case of triglycerides was employed the Catchpole and King (1994) as well as the Sun-Chen (1987) correlations in near critical fluids.

From the data obtained under conditions of tracer diffusion of five aromatic hydrocarbons in ethanol and supercritical n-hexane, Sun and Chen (see Reid *et al.* 1987) have developed by multiple regressions an empirical correlation for the molecular diffusivity in the form:

$$\frac{D}{T} = \frac{2.29 \times 10^{-8}}{\mu_c^{0.799} V_c^{0.490}} \quad (\text{G.1})$$

where D is the molecular diffusivity of the solute, μ_c is the viscosity of supercritical fluid and V_c is the critical volume of solute.

The Catchpole and King (1994) correlation can estimate the molecular diffusivities in a range of near critical solvents over the solvent reduced density 1-2.5, with an average error of $\pm 10\%$. The correlation is not suitable for estimating binary diffusion coefficients at the binary mixture critical point where diffusion coefficient tends to zero (Brunner, 1994).

The final binary diffusion coefficient correlation is as follows:

$$D_{12} = 5.152 D_c T_r (\rho_r^{-\frac{2}{3}} - 0.4510) \frac{R}{X} \quad \text{where } 1 < \rho_r < 2.5 \quad (\text{G.2})$$

where T_r and ρ_r are the reduced temperature and density of the solvent respectively, D_c is the self-diffusion coefficient at the critical point, X is the size to mass parameter and R is the correction factor.

The self diffusion coefficient at the critical point, D_c , can be estimated from a modified empirical diffusion coefficient correlation in terms of the critical density (Catchpole and King, 1994):

$$D_c = \frac{4.300 \times 10^{-7} M_c^{\frac{1}{2}} T_c^{0.75}}{\sum v^3 \rho_c} \quad (\text{G.3})$$

where M is the molar mass in $\text{g}\cdot\text{mol}^{-1}$, T_c and ρ_c are the critical temperature and density of the solvent in K and $\text{kg}\cdot\text{m}^{-3}$ respectively and $\sum v$ are the diffusion volumes given in Reid *et al.* (1987).

A size to mass ratio parameter X is defined by

$$X = \frac{\left(1 + \left(\frac{V_{c2}}{V_{c1}}\right)^{\frac{1}{3}}\right)^2}{\left(1 + \frac{M_1}{M_2}\right)^{\frac{1}{2}}} \quad (\text{G.4})$$

where 1 is the solvent, 2 is the solute, V_{ci} is the critical volume and M_i is the molar mass.

R is given by the equations as follows:

$$R = 1.0 \pm 0.1 \quad \text{when } 2 < X \quad (\text{G.5})$$

$$R = X^{0.17} \pm 0.1 \quad \text{when } 2 < X < 10 \quad (\text{G.6})$$

The required data for determining the molecular diffusion coefficient for C_3H_8 -Triglycerides pair is presented as follows:

Required Data

$T_c \text{ C}_3\text{H}_8 = 369.8 \text{ K}$

$\rho_c \text{ C}_3\text{H}_8 = 369.8 \text{ kg/m}^3$

$M \text{ C}_3\text{H}_8 = 44.094 \text{ g/mol}$

$V_c \text{ C}_3\text{H}_8 = 203 \text{ cm}^3/\text{mol}$

$\mu_c \text{ C}_3\text{H}_8 = 228 \text{ }\mu\text{p}$

$D_c \text{ C}_3\text{H}_8 = 6.775 \times 10^{-8} \text{ m}^2/\text{s}$

$M \text{ Sunflower Oil} = 875 \text{ g/mol}$

$V_c \text{ Sunflower Oil} = 3261 \text{ cm}^3/\text{mol}$

For the case of the solvent, the data is taken from Catchpole and King (1994) and for the sunflower oil; the data was estimated in Annex B.

The molecular diffusivity for H_2 in SC propane was determined based on the experimental value reported by Satterfield (1970). For the propane- H_2 gas pair at NTP

conditions, $D_{12}P=0.45 \times 10^{-4}$ m²/s. Therefore, a molecular diffusivity in the range of 10^{-7} m²/s is expected.

The estimated molecular diffusivity coefficients for C₃H₈-Triglycerides and C₃H₈-H₂ pairs found by means the correlations explained above are presented as following:

Table G-1: Molecular diffusivities for C₃H₈-Triglycerides and C₃H₈-H₂ under several operating conditions.

Reaction Temperature (K)	Pressure (MPa)	$\rho_{C_3H_8}$ (kg/m ³)	Molecular Diffusion Coefficient D_{12} (m ² /s)		
			C ₃ H ₈ -Triglycerides $\times 10^8$		C ₃ H ₈ -H ₂ $\times 10^7$
			Catchpole and King	Sun and Chen	Satterfield
457.15	20.0	377	1.62	1.51	3.21
457.15	27.5	448	0.83	0.85	2.34
484.15	20.0	300	1.92	1.80	3.58
484.15	27.5	408	1.25	1.11	2.61

Nomenclature

- D molecular diffusivity of the solute [cm²/s]
- D_{12} diffusion coefficient [m²/s]
- D_c self diffusion coefficient at the critical point [m²/s]
- M molar mass [g/mol]
- P pressure [atm]
- R correction factor
- T temperature [K]
- T_r reduced temperature
- V_c critical volume of solute [cm³/mol]
- X size to mass parameter

Greek letters

μ_c solvent viscosity [P]

ρ_r reduced density [kg/m³]

$\sum v$ difussion volumen

Acronyms

C₃H₈ propane

H₂ hydrogen

NTP normal temperatura and pressure

SC supercritical

Sub- and Superscripts

1 solvent

2 solute

c critical

r reduced

Appendix H

Specification Data Sheets and Analytical Procedures.

Sunflower Seed Oil.

S5007
Sunflower seed oil



Certificate of Analysis

TEST	SPECIFICATION	LOT {SAMPLE} RESULTS
Product Name	Sunflower seed oil	
Product Number	S5007	
CAS Number	8001216	
APPEARANCE	CLEAR YELLOW LIQUID	CONFORMS
SPECIFIC GRAVITY	0.915 TO 0.920	0.919
IODINE VALUE	110 TO 143	135 *
SAPONIFICATION VALUE	188 TO 194	192 *
FREE FATTY ACIDS	<2.5 ML OF 0.02 M SODIUM HYDROXIDE	0.2 ML *
QC ACCEPTANCE DATE		* SUPPLIER'S INFORMATION NOVEMBER 1999

A handwritten signature in black ink, appearing to read "D. Feldker", written over a horizontal line.

David Feldker, Manager
Analytical Services

Hydrogen.

Product: Hydrogen

P-4604-E

Date: June 2000

Praxair Material Safety Data Sheet**1. Chemical Product and Company Identification**

Product Name: Hydrogen, compressed (MSDS No. P-4604-E)		Trade Name: Hydrogen	
Chemical Name: Hydrogen		Synonyms: None	
Formula: H ₂		Chemical Family: Permanent Gas	
Telephone:	Emergencies: 1-800-645-4633* CHEMTREC: 1-800-424-9300* Routine: 1-800-PRAXAIR	Company Name: Praxair, Inc. 39 Old Ridgebury Road Danbury, CT 06810-5113	

* Call emergency numbers 24 hours a day only for spills, leaks, fire, exposure, or accidents involving this product. For routine information, contact your supplier, Praxair sales representative, or call 1-800-PRAXAIR (1-800-772-9247).

2. Composition/Information on Ingredients

This section covers materials of manufacture only. For custom mixtures of this product, request an MSDS for each component. See section 16 for important information about mixtures.

INGREDIENT	CAS NUMBER	CONCENTRATION	OSHA PEL	ACGIH TLV-TWA
Hydrogen	1333-74-0	>99%	None currently established	Simple asphyxiant

* The symbol > means "greater than"; the symbol <, "less than."

3. Hazards Identification**EMERGENCY OVERVIEW**

DANGER! Flammable high-pressure gas.

Can form explosive mixtures with air.

May ignite if valve is opened to air.

Burns with invisible flame.

May cause dizziness and drowsiness.

Self-contained breathing apparatus may be required by rescue workers.

Odor: None

THRESHOLD LIMIT VALUE: TLV-TWA, simple asphyxiant (ACGIH, 1999). TLV-TWAs should be used as a guide in the control of health hazards and not as fine lines between safe and dangerous concentrations.

Product: Hydrogen

P-4604-E

Date: June 2000

EFFECTS OF A SINGLE (ACUTE) OVEREXPOSURE:

INHALATION—Asphyxiant. Effects are due to lack of oxygen. Moderate concentrations may cause headache, drowsiness, dizziness, excitation, excess salivation, vomiting, and unconsciousness. Lack of oxygen can kill.

SKIN CONTACT—No harm expected.

SWALLOWING—An unlikely route of exposure; this product is a gas at normal temperature and pressure.

EYE CONTACT—No harm expected.

EFFECTS OF REPEATED (CHRONIC) OVEREXPOSURE: No harm expected.

OTHER EFFECTS OF OVEREXPOSURE: Hydrogen is an asphyxiant. Lack of oxygen can kill.

MEDICAL CONDITIONS AGGRAVATED BY OVEREXPOSURE: The toxicology and the physical and chemical properties of hydrogen suggest that overexposure is unlikely to aggravate existing medical conditions.

SIGNIFICANT LABORATORY DATA WITH POSSIBLE RELEVANCE TO HUMAN HEALTH HAZARD EVALUATION: None known.

CARCINOGENICITY: This product is not listed by NTP, OSHA, or IARC.

4. First Aid Measures

INHALATION: Remove to fresh air. If not breathing, give artificial respiration. If breathing is difficult, qualified personnel may give oxygen. Call a physician.

SKIN CONTACT: Wash with soap and water. If irritation persists, seek medical attention.

SWALLOWING: An unlikely route of exposure. This product is a gas at normal temperature and pressure.

EYE CONTACT: Flush eyes thoroughly with water for at least 15 minutes. Hold the eyelids open and away from the eyeballs to ensure that all surfaces are flushed thoroughly. See a physician, preferably an ophthalmologist, immediately.

NOTES TO PHYSICIAN: *There is no specific antidote. Treatment of overexposure should be directed at the control of symptoms and the clinical condition of the patient.*

5. Fire Fighting Measures

FLASH POINT (test method):	Flammable gas	
AUTOIGNITION TEMPERATURE:	932°F (500°C)	
FLAMMABLE LIMITS IN AIR , % by volume:	LOWER: 4%	UPPER: 75%

EXTINGUISHING MEDIA: CO₂, dry chemical, water spray, or fog

SPECIAL FIRE FIGHTING PROCEDURES: **DANGER! Flammable high-pressure gas.** Evacuate all personnel from danger area. Immediately deluge cylinders with water from maximum distance until cool, then move them away from fire area if without risk. Continue cooling water spray while moving cylinders. Do not extinguish flames emitted from cylinders; allow them to burn out. Self-contained

Product: Hydrogen

P-4604-E

Date: June 2000

breathing apparatus may be required by rescue workers. On-site fire brigades must comply with OSHA 29 CFR 1910.156.

UNUSUAL FIRE AND EXPLOSION HAZARDS: Flammable gas. Flame is nearly invisible. Escaping gas may ignite spontaneously. Hydrogen has a low ignition energy. Fireball forms if gas cloud ignites immediately after release.

Forms explosive mixtures with air and oxidizing agents. Heat of fire can build pressure in cylinder and cause it to rupture. Hydrogen cylinders are equipped with a pressure relief device. (Exceptions may exist where authorized by DOT.) No part of a cylinder should be subjected to a temperature higher than 125°F (52°C). If venting or leaking hydrogen catches fire, do not extinguish flames. Flammable gas may spread from leak, creating an explosive re-ignition hazard. Vapors can be ignited by pilot lights, other flames, smoking, sparks, heaters, electrical equipment, static discharge, or other ignition sources at locations distant from product handling point. Explosive atmospheres may linger. Before entering area, especially confined areas, check atmosphere with approved explosion meter.

HAZARDOUS COMBUSTION PRODUCTS: None known.

6. Accidental Release Measures

STEPS TO BE TAKEN IF MATERIAL IS RELEASED OR SPILLED: DANGER! Flammable high-pressure gas. Forms explosive mixtures with air. (See section 5.) Immediately evacuate all personnel from danger area. Use self-contained breathing apparatus where needed. Remove all sources of ignition if without risk. Reduce gas with fog or fine water spray. Shut off flow if without risk. Ventilate area or move cylinder to a well-ventilated area. Flammable gas may spread from leak. Before entering area, especially confined areas, check atmosphere with an appropriate device.

WASTE DISPOSAL METHOD: Prevent waste from contaminating the surrounding environment. Keep personnel away. Discard any product, residue, disposable container, or liner in an environmentally acceptable manner, in full compliance with federal, state, and local regulations. If necessary, call your local supplier for assistance.

7. Handling and Storage

PRECAUTIONS TO BE TAKEN IN STORAGE: Store and use with adequate ventilation. Separate hydrogen cylinders from oxygen, chlorine, and other oxidizers by at least 20 ft (6.1 m), or use a barricade of noncombustible material. This barricade should be at least 5 ft (1.53 m) high and have a fire resistance rating of at least ½ hour. Firmly secure cylinders upright to keep them from falling or being knocked over. Screw valve protection cap firmly in place by hand. Post "No Smoking or Open Flames" signs in storage and use areas. There must be no sources of ignition. All electrical equipment in storage areas must be explosion-proof. Storage areas must meet national electric codes for Class 1 hazardous areas. Store only where temperature will not exceed 125°F (52°C). Store full and empty cylinders separately. Use a first-in, first-out inventory system to prevent storing full cylinders for long periods. For full details and requirements, see NFPA 50A, published by the National Fire Protection Association.

PRECAUTIONS TO BE TAKEN IN HANDLING: Protect cylinders from damage. Use a suitable hand truck to move cylinders; do not drag, roll, slide, or drop. Hydrogen is the lightest known gas. It may leak out of systems that are air-tight for other gases and may collect in poorly ventilated upper reaches of buildings. All piped hydrogen systems and associated equipment must be grounded. Electrical equipment must be non-sparking or explosion-proof. Leak check system with soapy water; never use a flame. Do not crack or open disconnected hydrogen cylinder valves; escaping gas may ignite spontaneously. Never

Product: Hydrogen

P-4604-E

Date: June 2000

attempt to lift a cylinder by its cap; the cap is intended solely to protect the valve. Never insert an object (e.g., wrench, screwdriver, pry bar) into cap openings; doing so may damage the valve and cause a leak. Use an adjustable strap wrench to remove over-tight or rusted caps. Open valve slowly. If valve is hard to open, discontinue use and contact your supplier. For other precautions in using hydrogen, see section 16.

8. Exposure Controls/Personal Protection

VENTILATION/ENGINEERING CONTROLS:

LOCAL EXHAUST—An explosion-proof local exhaust system is acceptable. See SPECIAL.

MECHANICAL (general)—Inadequate; see SPECIAL.

SPECIAL—Use only in a closed system.

OTHER—See SPECIAL.

RESPIRATORY PROTECTION: None required under normal use. An air-supplied respirator must be used in confined spaces. Respiratory protection must conform to OSHA rules as specified in 29 CFR 1910.134.

SKIN PROTECTION: Wear work gloves for cylinder handling.

EYE PROTECTION: Select in accordance with OSHA 29 CFR 1910.133.

OTHER PROTECTIVE EQUIPMENT: Metatarsal shoes for cylinder handling. Select in accordance with OSHA 29 CFR 1910.132 and 1910.133. Regardless of protective equipment, never touch live electrical parts.

9. Physical and Chemical Properties

MOLECULAR WEIGHT:	2.016
SPECIFIC GRAVITY (Air = 1) at 32°F (0°C) and 1 atm:	0.06960
GAS DENSITY at 70°F (21.1°C) and 1 atm:	0.00521 lb/ft ³ (0.08342 kg/m ³)
SOLUBILITY IN WATER , vol/vol at 60°F (15.6°C) and 1 atm:	0.019
PERCENT VOLATILES BY VOLUME:	100
BOILING POINT at 1 atm:	-423.0°F (-252.8°C)
MELTING POINT at 1 atm:	-434.55°F (-259.2°C)

APPEARANCE, ODOR, AND STATE: Colorless, odorless, tasteless gas at normal temperature and pressure

10. Stability and Reactivity

STABILITY:	<input type="checkbox"/> Unstable	<input checked="" type="checkbox"/> Stable
INCOMPATIBILITY (materials to avoid):	Oxidizing agents, lithium, halogens	
HAZARDOUS DECOMPOSITION PRODUCTS:	None	
HAZARDOUS POLYMERIZATION:	<input type="checkbox"/> May Occur	<input checked="" type="checkbox"/> Will Not Occur
CONDITIONS TO AVOID:	None known.	

Propane.

Product: Propane

P-4646-F

Date: September 2004

Praxair Material Safety Data Sheet**1. Chemical Product and Company Identification**

Product Name: Propane (MSDS No. P-4646-F)		Trade Name: Liquefied Petroleum Gas
Chemical Name: Propane		Synonyms: Dimethylmethane, N-propane, propyl hydride, propylhydride, refrigerant gas R290
Formula: C ₃ H ₈		Chemical Family: Alkane
Telephone:	Emergencies: 1-800-645-4633* CHEMTREC: 1-800-424-9300* Routine: 1-800-PRAXAIR	Company Name: Praxair, Inc. 39 Old Ridgebury Road Danbury, CT 06810-5113

* Call emergency numbers 24 hours a day only for spills, leaks, fire, exposure, or accidents involving this product. For routine information, contact your supplier, Praxair sales representative, or call 1-800-PRAXAIR (1-800-772-9247).

2. Composition/Information on Ingredients

This section covers materials of manufacture only. See sections 3, 8, 10, 11, 15, and 16 for information on by-products generated during use, especially use in welding and cutting. See section 16 for important information about mixtures.

INGREDIENT	CAS NUMBER	CONCENTRATION	OSHA PEL	ACGIH TLV-TWA (2004)
Propane	74-98-6	>99%*	1000 ppm	1000 ppm**

* The symbol > means "greater than."

** Aliphatic hydrocarbon gases (ACGIH, 2004)

3. Hazards Identification**EMERGENCY OVERVIEW**

DANGER! Flammable liquid and gas under pressure.

Can form explosive mixtures with air.

May cause frostbite.

May cause dizziness and drowsiness.

Self-contained breathing apparatus may be required by rescue workers.

Odor: Faintly disagreeable

THRESHOLD LIMIT VALUE: TLV-TWA, 1000 ppm, aliphatic hydrocarbon gases (ACGIH, 2004). Hazardous fumes may be generated during welding with this product. See section 16 for more information on welding hazards. TLV-TWAs should be used as a guide in the control of health hazards and not as fine lines between safe and dangerous concentrations.

Product: Propane

P-4646-F

Date: September 2004

EFFECTS OF A SINGLE (ACUTE) OVEREXPOSURE:

INHALATION—Asphyxiant. Effects are due to lack of oxygen. Moderate concentrations may cause headache, drowsiness, dizziness, excitation, excess salivation, vomiting, and unconsciousness. Lack of oxygen can kill.

SKIN CONTACT—No harm expected from vapor. Liquid may cause frostbite.

SWALLOWING—An unlikely route of exposure. This product is a gas at normal temperature and pressure, but frostbite of the lips and mouth may result from contact with the liquid.

EYE CONTACT—No harm expected from vapor. Liquid may cause frostbite.

EFFECTS OF REPEATED (CHRONIC) OVEREXPOSURE: No harm expected.

OTHER EFFECTS OF OVEREXPOSURE: At very high concentrations, propane may produce cardiac arrhythmias or arrest due to sensitization of the heart to adrenaline and noradrenalin.

MEDICAL CONDITIONS AGGRAVATED BY OVEREXPOSURE: The toxicology and the physical and chemical properties of propane suggest that overexposure is unlikely to aggravate existing medical conditions.

SIGNIFICANT LABORATORY DATA WITH POSSIBLE RELEVANCE TO HUMAN HEALTH

HAZARD EVALUATION: In a study conducted in 1948, dogs breathed varying mixtures of hydrocarbons and oxygen for 10 minutes. Of a group of dogs exposed to propane, all (3 of 3) showed myocardial sensitivity to injected epinephrine hydrochloride as determined by electrocardiogram (EKG) readings. No direct evidence is known of propane-induced cardiac sensitization in humans.

CARCINOGENICITY: Propane is not listed by NTP, OSHA, or IARC.

4. First Aid Measures

INHALATION: Immediately remove to fresh air. If not breathing, give artificial respiration. If breathing is difficult, qualified personnel may give oxygen. Call a physician.

SKIN CONTACT: For exposure to liquid, immediately warm frostbite area with warm water not to exceed 105°F (41°C). In case of massive exposure, remove contaminated clothing while showering with warm water. Call a physician.

SWALLOWING: An unlikely route of exposure. This product is a gas at normal temperature and pressure.

EYE CONTACT: For contact with the liquid, immediately flush eyes thoroughly with warm water for at least 15 minutes. Hold the eyelids open and away from the eyeballs to ensure that all surfaces are flushed thoroughly. See a physician, preferably an ophthalmologist, immediately.

NOTES TO PHYSICIAN: *This material may be a cardiac sensitizer; avoid the use of epinephrine. There is no specific antidote. Treatment of overexposure should be directed at the control of symptoms and the clinical condition of the patient.*

5. Fire Fighting Measures

FLASH POINT (test method):	-156°F (-104°C) TCC	
AUTOIGNITION TEMPERATURE:	842°F (450°C)	
FLAMMABLE LIMITS IN AIR , % by volume:	LOWER: 2.1%	UPPER: 9.5%

Product: Propane

P-4646-F

Date: September 2004

EXTINGUISHING MEDIA: CO₂, dry chemicals, water spray, or fog.

SPECIAL FIRE FIGHTING PROCEDURES: DANGER! Flammable liquid and gas under pressure. Evacuate all personnel from danger area. Immediately cool cylinders with water spray from maximum distance, taking care not to extinguish flames. Remove ignition sources if without risk. Remove all cylinders from area of fire if without risk, while continuing cooling water spray. Do not extinguish any flames emitted from cylinders. Stop flow of gas if without risk, or allow flames to burn out. Self-contained breathing apparatus may be required by rescue workers. On-site fire brigades must comply with OSHA 29 CFR 1910.156.

UNUSUAL FIRE AND EXPLOSION HAZARDS: Flammable gas. Forms explosive mixtures with air and oxidizing agents. Heat of fire can build pressure in cylinder and cause it to rupture. No part of cylinder should be subjected to a temperature higher than 125°F (52°C). Propane cylinders are equipped with a pressure relief device. (Exceptions may exist where authorized by DOT.) If venting or leaking propane catches fire, do not extinguish flames. Flammable gas may spread from leak, creating an explosive re-ignition hazard. Vapors can be ignited by pilot lights, other flames, smoking, sparks, heaters, electrical equipment, static discharge, or other ignition sources at locations distant from product handling point. Explosive atmospheres may linger. Before entering area, especially confined areas, check atmosphere with an appropriate device.

HAZARDOUS COMBUSTION PRODUCTS: Carbon monoxide, carbon dioxide

6. Accidental Release Measures

STEPS TO BE TAKEN IF MATERIAL IS RELEASED OR SPILLED: DANGER! Flammable liquid and gas under pressure. Forms explosive mixtures with air. (See section 5.) Immediately evacuate all personnel from danger area. Use self-contained breathing apparatus where needed. Remove all sources of ignition if without risk. Reduce vapors with fog or fine water spray. Shut off flow if without risk. Ventilate area or move cylinder to a well-ventilated area. Flammable vapors may spread from leak. Before entering area, especially confined areas, check atmosphere with an approved device.

WASTE DISPOSAL METHOD: Prevent waste from contaminating the surrounding environment. Keep personnel away. Discard any product, residue, disposable container, or liner in an environmentally acceptable manner, in full compliance with federal, state, and local regulations. If necessary, call your local supplier for assistance.

7. Handling and Storage

PRECAUTIONS TO BE TAKEN IN STORAGE: Store and use with adequate ventilation. Separate propane cylinders from oxygen, chlorine, and other oxidizers by at least 20 ft (6.1 m) or use a barricade of noncombustible material. This barricade should be at least 5 ft (1.53 m) high and have a fire resistance rating of at least ½ hour. Firmly secure cylinders upright to keep them from falling or being knocked over. Screw valve protection cap firmly in place by hand. Post "No Smoking or Open Flames" signs in storage and use areas. There must be no sources of ignition. All electrical equipment in storage areas must be explosion-proof. Storage areas must meet national electric codes for Class 1 hazardous areas. Store only where temperature will not exceed 125°F (52°C). Store full and empty cylinders separately. Use a first-in, first-out inventory system to prevent storing full cylinders for long periods.

Product: Propane

P-4646-F

Date: September 2004

PRECAUTIONS TO BE TAKEN IN HANDLING: Protect cylinders from damage. Use a suitable hand truck to move cylinders; do not drag, roll, slide, or drop. All piped propane systems and associated equipment must be grounded. Electrical equipment must be non-sparking or explosion-proof. Leak check system with soapy water; never use a flame. Never attempt to lift a cylinder by its cap; the cap is intended solely to protect the valve. Never insert an object (e.g., wrench, screwdriver, pry bar) into cap openings; doing so may damage the valve and cause a leak. Use an adjustable strap wrench to remove over-tight or rusted caps. Open valve slowly. If valve is hard to open, discontinue use and contact your supplier. For other precautions in using propane, see section 16.

For further information on storage, handling, and use of this product, see NFPA 55, *Standard for the Storage, Use, and Handling of Compressed and Liquefied Gases in Portable Cylinders*, published by the National Fire Protection Association.

8. Exposure Controls/Personal Protection

VENTILATION/ENGINEERING CONTROLS:

LOCAL EXHAUST—An explosion-proof local exhaust system is acceptable. See SPECIAL.

MECHANICAL (general)—Inadequate; see SPECIAL.

SPECIAL—Use only in a closed system.

OTHER—None

RESPIRATORY PROTECTION: Respiratory protection must conform to OSHA rules as specified in 29 CFR 1910.134. Select per OSHA 29 CFR 1910.134 and ANSI Z88.2.

SKIN PROTECTION: Wear work gloves for cylinder handling and to prevent exposure to liquid. Wear welding gloves for welding.

EYE PROTECTION: Wear safety glasses when handling cylinders; for welding, see section 16. Select eye protection in accordance with OSHA 29 CFR 1910.133.

OTHER PROTECTIVE EQUIPMENT: Metatarsal shoes for cylinder handling. For welding, see section 16. Select in accordance with OSHA 29 CFR 1910.132 and 1910.133. Regardless of protective equipment, never touch live electrical parts.

9. Physical and Chemical Properties

MOLECULAR WEIGHT:	44.096
SPECIFIC GRAVITY (H ₂ O = 1) at 77°F (25°C) and 1 atm:	0.5077
SPECIFIC GRAVITY (Air = 1) at 70°F (21.1°C) and 1 atm:	1.523
VAPOR PRESSURE at 70°F (21.1°C):	109.73 psig (756.56 kPa)
SOLUBILITY IN WATER , vol/vol at 100°F (37.8°C) and 1 atm:	0.065
PERCENT VOLATILES BY VOLUME:	100
EVAPORATION RATE (Butyl Acetate = 1):	High
BOILING POINT at 1 atm:	-43.67°F (-42.04°C)
FREEZING POINT at 1 atm:	-305.84°F (-187.69°C)

APPEARANCE, ODOR, AND STATE: Colorless gas at normal temperature and pressure, faintly disagreeable odor.

Product: Propane

P-4646-F

Date: September 2004

10. Stability and Reactivity

STABILITY: Unstable Stable

INCOMPATIBILITY (materials to avoid): Oxidizing agents, chlorine dioxide

HAZARDOUS DECOMPOSITION PRODUCTS: Thermal decomposition and burning may produce CO/CO₂.

HAZARDOUS POLYMERIZATION: May Occur Will Not Occur

CONDITIONS TO AVOID: None known.

11. Toxicological Information

Possible cardiac sensitization to epinephrine; see section 3. The welding process may generate hazardous fumes and gases. (See sections 3, 10, 15, and 16.)

12. Ecological Information

No adverse ecological effects expected. Propane does not contain any Class I or Class II ozone-depleting chemicals. Propane is not listed as a marine pollutant by DOT.

13. Disposal Considerations

WASTE DISPOSAL METHOD: Do not attempt to dispose of residual or unused quantities. Return cylinder to supplier.

14. Transport Information

DOT/IMO SHIPPING NAME: Propane

HAZARD CLASS: 2.1 **IDENTIFICATION NUMBER:** UN 1978 **PRODUCT RQ:** None

SHIPPING LABEL(s): FLAMMABLE GAS

PLACARD (when required): FLAMMABLE GAS

SPECIAL SHIPPING INFORMATION: Cylinders should be transported in a secure position, in a well-ventilated vehicle. Cylinders transported in an enclosed, nonventilated compartment of a vehicle can present serious safety hazards.

Shipment of compressed gas cylinders that have been filled without the owner's consent is a violation of federal law [49 CFR 173.301(b)].

15. Regulatory Information

The following selected regulatory requirements may apply to this product. Not all such requirements are identified. Users of this product are solely responsible for compliance with all applicable federal, state, and local regulations.

Dimethyl Ether (DME).

SAFETY DATA SHEET
According to EC-directive 2001/58/EC

DEMEON D (DME, AEROSOL GRADE)**1. IDENTIFICATION OF THE SUBSTANCE/PREPARATION AND OF THE COMPANY/UNDERTAKING**

Product label name Dimethyl ether
Supplier Akzo Nobel Base Chemicals bv
Stationsplein 4
PO Box 247
NL-3800 AE Amersfoort
Tel.: +31-334676767
Emergency telephone + 31 570679211 (Fax. + 31 570679801)
Akzo Nobel Chemicals-Deventer-NL

2. COMPOSITION/INFORMATION ON INGREDIENTS

This product is to be considered as a substance in conformance to EC directives

Information on hazardous ingredients

Chemical description Dimethyl ether

Composition / information on ingredients

Number	% w/w	CAS-number	Chemical name	Symbol(s)	Risk-phrase(s)
1	approx. 100	115-10-6	Dimethyl ether		
Number	EC-number	Annex-1 number	Symbol(s)		Risk-phrase(s)
1	204-065-8	603-019-00-8	F+		R12

3. HAZARDS IDENTIFICATION

Extremely flammable.

4. FIRST AID MEASURES

Symptoms and effects Irritating to eyes and respiratory system. Causes frost bite.

First aid

General

In all cases of doubt, or when symptoms persist, seek medical attention.

Inhalation

Move to fresh air, rest, half upright position, loosen clothing. Oxygen or artificial respiration if there is difficulty in breathing. Seek medical advice after significant exposure.

Skin

In case of frostbite: DO NOT remove clothing, but first thaw frosted parts with water (never use warm water!). Then remove clothing carefully and seek medical advice.

Eye

Rinse thoroughly with plenty of water. Eyelids should be held away from the eyeball to ensure thorough rinsing. Seek medical advice after significant exposure.

Ingestion

Not likely to occur.

Advice to physician

Symptomatic treatment is advised

5. FIRE-FIGHTING MEASURES

Extinguishing media powder

Unsuitable extinguishing media none known.

Special exposure hazards Vapours may form explosive mixtures with air.
Vapours may travel to a source of ignition and flash back.

Hazardous decomposition/
combustion products No hazardous decomposition products known.

Protective equipment Use self-contained or supplied-air respiratory equipment.

Other information Cool closed containers with water.

6. ACCIDENTAL RELEASE MEASURES

Personal precautions Wear self contained breathing apparatus.
For personal protection see Section 8.

Environmental precautions Do not allow to enter drains or water courses.

Methods for cleaning up Isolate spill area. Ventilate the area.

Other information Take precautionary measures against static discharges.
Keep away from sources of ignition - No smoking.

7. HANDLING AND STORAGE

Handling Use only in well-ventilated areas. When workers are facing concentrations above the exposure limit they must use appropriate certified respirators.

Fire and explosion prevention Keep away from sources of ignition - No smoking.
Take precautionary measures against static discharges.
Vapours are heavier than air and may spread along floors.
Vapours may travel to a source of ignition and flash back.

SAFETY DATA SHEET

According to EC-directive 2001/58/EC

DEMEON D (DME, AEROSOL GRADE)

Storage requirements	Store in a dry well ventilated place away from sources of heat and direct sunlight.
-----------------------------	---

8. EXPOSURE CONTROLS/PERSONAL PROTECTION

Engineering controls	Provide adequate ventilation. Use explosion protected equipment.
Exposure limits	
Name	
Dimethyl ether	In this country no exposure limit has been established
Personal protection	
Respiratory	Use self-contained respiratory equipment
Hand	Wear suitable gloves of neoprene.
Eye	Wear eye/face protection.
Skin and body	Wear suitable protective clothing.

9. PHYSICAL AND CHEMICAL PROPERTIES

Appearance	liquefied gas (25 °C)
Colour	colourless
Odour	almost odourless
Boiling point/range	-25 °C (101.3 kPa)
Melting point/range	-141 °C (freezing point)
Flash point	-41 °C
Flammability	Extremely flammable
Autoignition temperature	350 °C (235 °C, BAM, DIN 51 794)
Explosive properties	Vapours may form explosive mixtures with air
Explosion limits	3 - 18.6 Vol % (ASTM)
Oxidizing properties	not determined
Vapour pressure	510 kPa (20 °C) 1140 kPa (50 °C)
Density	approx. 670: kg/m ³ (20 °C, liquid)
Bulk density	not applicable
Solubility in water	328 g/l (20 °C, 410 kPa)
Solubility in other solvents	Soluble in: methanol, ethanol, Isopropanol, chlorinated hydrocarbons, toluene
pH value	not relevant
Partition coefficient	-0.18
n-octanol/water	
Relative vapour density (air=1)	1.59
Viscosity	not applicable

10. STABILITY AND REACTIVITY

Stability	Stable under recommended storage and handling conditions (see section 7).
Conditions to avoid	Keep away from sources of ignition - No smoking. Avoid contact with Air / O ₂ (Formation of peroxides)
Materials to avoid	Chlorine, Air, hydrochloric acid (HCl), O ₂ , HF, N ₂ O, strong oxidising agents rubber, KEL-F, Viton
Hazardous decomposition products	No hazardous decomposition products known.

11. TOXICOLOGICAL INFORMATION

Name	Dimethyl ether
Acute toxicity	
Oral LD ₅₀	not applicable
Inhalation LC ₅₀	rat, 16,4 Vol % , 4 - hours inhalation (Lit.)
Irritation	
Skin	Causes frost bite
Other toxicological information	Not mutagenic, Not teratogenic, not carcinogenic. 90 days inhalation, rat: No Observed Effect Concentration (NOEC) 10000 ppm

SAFETY DATA SHEET

According to EC-directive 2001/58/EC

DEMEON D (DME, AEROSOL GRADE)**12. ECOLOGICAL INFORMATION**

Name	Dimethyl ether
Ecotoxicity	
fish	Poecilia reticulata: Acute toxicity, 96h-LC50 > 4000 mg/l
daphnia	Daphnia magna: Acute toxicity, 48h-EC50 > 4000 mg/l (Akzo Nobel E-file)
Fate	
Degradation Abiotic	The product can be degraded by chemical or photolytic processes
Degradation Biotic	Not readily biodegradable (Closed bottle test)

13. DISPOSAL CONSIDERATIONS

Product	According to local regulations (most probably controlled incineration)
Contaminated packaging	not restricted. Exclude sources of ignition and ventilate the area.

14. TRANSPORT INFORMATION*Land transport (ADR/ RID)*

ADR class	2	ADR Classification Code	2F / 2F
RID class	2	ADR/RID packing group	not applicable
Hazard Identification No.	23	Substance Identification No.	1033
TREM-Card	CEFIC TEC(R)- 20G2F	UN number	1033
Proper Shipping Name	Dimethyl ether		
Other information	Transport label(s): 2.1		

Sea transport (IMDG-code/ IMO)

IMO/IMDG code		Class	2
Packing group	none	UN number	1033
EMS	2-07	Subsidiary Risk	
Marine pollutant	no		
Proper Shipping Name	Dimethyl ether		
Other information	Transport label(s): 2.1		

Air transport (ICAO-TI/ IATA-DGR)

Class	2.1	Packing group	
Proper Shipping Name	Dimethyl ether		
Other information	Cargo aircraft only		
	Transport label(s): 2.1 (flammable gas)		

15. REGULATORY INFORMATION

Chemical description	Dimethyl ether
----------------------	----------------

Labelling according to EC directives

EC-number	See section 2.
Classification based on	Annex-1



Symbol(s)	HIGHLY FLAMMABLE (F)
R(isk) phrase(s)	R12: Extremely flammable
S(afety) phrase(s)	(S2: Keep out of the reach of children) S9 : Keep container in a well-ventilated place S16: Keep away from sources of ignition - No smoking S33: Take precautionary measures against static discharges
Wassergefährdungsklasse (WGK)	1

0.5% Pd/Al₂O₃ catalyst.

DATASHEET JOHNSON MATTHEY.

0.5% Palladium On Alumina Spheres Type 50B.

TYPICAL INFORMATION	
Reference	0.5R50B
Active Metal/Loading	Palladium (0.5%)
Support (Carrier)	γ-Alumina Spheres
Metal Location	Eggshell
Metal State	Metal
Surface Area	320 m ² /g
Metal Area	1.0 m ² /g
Support Diameter	2 - 4.75 mm
Apparent Bulk Density	0.75 g/cm ³
Pore Volume	0.45 cm ³ /g
TYPICAL APPLICATIONS	
Removal of O ₂ from H ₂ , N ₂ , Ar, Air etc by combination with H ₂ . Vapour Phase Hydrogenations. Vapour Phase Dehydrogenations.	
Reference Number	JM/CPC/0.5R50BDATA02/0695S
Date	01/06/95

2% Pd/C catalyst.

DATA SHEET

Palladium on activated carbon



Fixed bed catalyst, Metal location: Uniform

E 154 XKP/D 2%

Material-No.: 48.7821.4010.00

Characteristic Physicochemical Values

Values	Units	Typical
Palladium content	%	2.0
Tapped density	g/l	360
Attrition	%	1.1
Specific surface area	m ² /g	1530
Total pore volume	ml/g	1.30

Valid from: 07.02.2000 Trial product

Iodine Value of Fats and Oils: Wijs Method (AOCS Cd 1-25).

SAMPLING AND ANALYSIS OF COMMERCIAL FATS AND OILS

AOCS Official Method Cd 1-25

Withdrawn (Historical Interest Only)

Iodine Value of Fats and Oils
Wijs Method

DEFINITION

The iodine value is a measure of the unsaturation of fats and oils and is expressed in terms of the number of centigrams of iodine absorbed per gram of sample (% iodine absorbed).

SCOPE

Applicable to all normal fats and oils that do not contain conjugated double bonds (see Notes, 1).
Applicable to all normal fats and oils with samples having iodine values between 0–15.

APPARATUS

1. Glass-stoppered iodine flasks—500 mL.
2. Glass-stoppered volumetric flasks—1000 mL, for preparing standard solutions.
3. Pipet—25 mL, for accurately dispensing 25.0 mL of Wijs solution.
4. Volumetric dispenser—20 mL, 1-mL adjustability, for 10% potassium iodide (KI) solution.
5. Volumetric dispenser—2 mL, 1-mL adjustability, for starch solution.
6. Volumetric dispenser—50 mL, 1-mL adjustability, for distilled water.
7. Repeater pipet—with filling flask, 20 mL, for cyclohexane.
8. Analytical balance—accurate to ± 0.0001 g.
9. Magnetic stirrer.
10. Filter paper—Whatman no. 41H, or equivalent.
11. Beakers—50 mL.
12. Hot air oven.
13. Timer.

REAGENTS

1. Wijs solution—see Notes, 2 and *Caution*.
2. Potassium iodide (KI)—reagent grade.
3. Carbon tetrachloride—reagent grade (see Notes, *Caution* and Recommendations). The absence of oxidizable matter in this reagent is verified by shaking 10 mL of the reagent with 1 mL of saturated aqueous potassium dichromate solution and 2 mL of concentrated sulfuric acid; no green coloration should appear.
4. Soluble starch solution—recently prepared, tested for sensitivity (see Notes, 3). Make a paste with 1 g of natural, soluble starch (see Notes, 4) and a small amount of cold distilled water. Add, while stirring, to 100 mL of boiling water.

Test for sensitivity—Place 5 mL of starch solution in 100 mL of water and add 0.05 mL of freshly prepared 0.1 N KI solution and one drop of a 50 ppm chlorine solution made by diluting 1 mL of a commercial 5% sodium hypochlorite (NaOCl) solution to 1000 mL. The deep blue color produced must be discharged by 0.05 mL of 0.1 N sodium thiosulfate.

5. Potassium dichromate—primary standard grade. The potassium dichromate is finely ground and dried to constant weight at about 110°C before using.

Note—A standard sample of potassium dichromate with a certificate of analysis may be obtained from the National Bureau of Standards in Washington, D.C., USA. This sample, or equivalent, is strongly recommended for the primary standard for this method. Treat as directed in the certificate of analysis accompanying the sample.

6. Sodium thiosulfate ($\text{Na}_2\text{S}_2\text{O}_3 \cdot 5\text{H}_2\text{O}$)—reagent grade.

SOLUTIONS

1. Potassium iodide (KI) solution—100 g/L (10% solution), prepared by dissolving 100 g of reagent grade KI in 1000 mL of deionized water.
2. Starch indicator solution—prepared and tested as noted in Reagents, 4. Salicylic acid (1.25 g/L) may be added to preserve the indicator. If long storage is required, the solution must be kept in a refrigerator at 4–10°C (40–50°F). Fresh indicator must be prepared when the end point of the titration from blue to colorless fails to be sharp. If stored under refrigeration, the starch solution should be stable for about 2–3 weeks.
3. Sodium thiosulfate ($\text{Na}_2\text{S}_2\text{O}_3 \cdot 5\text{H}_2\text{O}$) solution—0.1 N (see Notes, 5), accurately standardized vs. potassium dichromate primary standard as follows:
 - (a) Sodium thiosulfate solution 0.1 N, prepared by dissolving 24.9 g of sodium thiosulfate in distilled water and diluting to 1 L.
 - (b) Weigh 0.16–0.22 g of finely ground and dried potassium dichromate into a 500-mL flask or bottle by difference from a weighing bottle. Dissolve in 25 mL of water, add 5 mL of concentrated hydrochloric acid, 20 mL of potassium iodide solution and rotate to mix. Allow to stand for 5 min, and then add 100 mL of distilled water. Titrate with sodium thiosulfate solution, shaking continuously until the yellow color has almost disappeared. Add 1–2 mL of starch indicator and continue the titration, adding the thiosulfate solution slowly until the blue color just disappears. The strength of the sodium thiosulfate solution is expressed in terms of its normality.

Normality of $\text{Na}_2\text{S}_2\text{O}_3$ solution =

$$20.394 \times \text{mass of } \text{K}_2\text{Cr}_2\text{O}_7 \text{ in g/mL of sodium thiosulfate}$$

4. Wijs solution—see Notes, 2 and *Caution*.

SAMPLING AND ANALYSIS OF COMMERCIAL FATS AND OILS
Cd 1-25 • Iodine Value of Fats and Oils

Table 1
Sample weights.

Iodine value	Mass of sample		Weighing accuracy
	100% excess	150% excess	
	g	g	g
<3	10	10	± 0.001
3	10.576	8.4613	0.005
5	6.346	5.0770	0.0005
10	3.1730	2.5384	0.0002
20	1.5865	1.2720	0.0002
40	.7935	.6346	0.0002
60	.5288	.4231	0.0002
80	.3966	.3173	0.0001
100	.3173	.2538	0.0001
120	.2644	.2115	0.0001
140	.2266	.1813	0.0001
160	.1983	.1587	0.0001
180	.1762	.1410	0.0001
200	.1586	.1269	0.0001

PROCEDURE

- Melt the sample, if it is not already liquid (the temperature during melting should not exceed the melting point of the sample by more than 10°C), and filter through two pieces of filter paper to remove any solid impurities and the last traces of moisture. The filtration may be performed in an air oven at 80–85°C, but should be completed within 5 min ± 30 sec. The sample must be absolutely dry.
Note—All glassware must be absolutely clean and completely dry.
- After filtration, allow the filtered sample to achieve a temperature of 68–71 ± 1°C before weighing the sample.
- Once the sample has achieved a temperature of 68–71 ± 1°C, immediately weigh the sample into a 500-mL iodine flask, using the weights and weighing accuracy noted in Table 1 (see Notes, 6).
- Add 15 mL of carbon tetrachloride on top of the sample and swirl to ensure that the sample is completely dissolved.
- Dispense 25 mL of Wijs solution using the pipet (Apparatus, 3) into flask containing the sample, stopper the flask and swirl to ensure an intimate mixture. Immediately set the timer for 30 min.
- Immediately store the flasks in the dark for the required reaction time at a temperature of 25 ± 5°C.
- Remove the flasks from storage and add 20 mL of KI solution, followed by 100 mL of distilled water (see Notes, 8 and 9).
- Titrate with 0.1 N Na₂S₂O₃ solution, adding it gradually and with constant and vigorous shaking (see Notes, 10). Continue the titration until the yellow color has almost disappeared. Add 1–2 mL of starch indicator solution and continue the titration until the blue color just disappears.

- Prepare and conduct at least one blank determination with each group of samples simultaneously and similar in all respects to the samples.

CALCULATIONS

$$1. \text{ The iodine value} = \frac{(B - S) \times N \times 12.69}{\text{mass, g of sample}}$$

Where—

- B = volume of titrant, mL of blank
S = volume of titrant, mL of sample
N = normality of Na₂S₂O₃ solution

NOTES

Caution

Wijs solution causes severe burns, and the vapors can cause lung and eye damage. Use of a fume hood is recommended. Wijs solution without carbon tetrachloride is available commercially.

Carbon tetrachloride is a known carcinogen. It is toxic by ingestion, inhalation and skin absorption. It is a narcotic. It should not be used to extinguish fires. It decomposes to phosgene gas at high temperature. The TLV is 5 ppm in air. A fume hood should be used at all times when using carbon tetrachloride.

Hydrochloric acid is a strong acid and will cause severe burns. Protective clothing should be worn when working with this acid. It is toxic by ingestion and inhalation and is a strong irritant to eyes and skin. The use of a properly operating fume hood is recommended. When diluting the acid, always add the acid to the water, never the reverse.

Chlorine is a poisonous gas. The TLV is 1 ppm in air. It is a strong oxidizing agent and should not be allowed to come in contact with organic materials, hydrogen, powdered metals and reducing agents. A fume hood should be used at all times when using chlorine.

Sulfuric acid is a strong acid and will cause severe burns. Protective clothing should be worn when working with this acid. It is an oxidizing agent and should not be stored in the vicinity of organic materials. Use great caution in mixing with water due to heat evolution that can cause explosive spattering. Always add the acid to water, never the reverse.

Acetic acid in the pure state is moderately toxic by ingestion and inhalation. It is a strong irritant to skin and tissue. The TLV in air is 10 ppm.

Potassium dichromate is toxic by ingestion and inhalation. There is sufficient evidence in humans for the carcinogenicity of chromium [+6], in particular lung cancer. It is a strong oxidizing agent and a dangerous fire risk in contact with organic chemicals.

RECOMMENDATIONS

The most satisfactory replacement found to date for carbon tetrachloride has been cyclohexane + acetic acid, 1:1, v/v (see AOCS Cd 1d-92). Because of environmental concerns, 1,1,2-trichloro-1,2,2-trifluoroethane (Freon 113) is not recommended. Acetic acid alone and a mixture of cyclohexane + acetic acid (4:1, v/v), respectively, have been shown to be unsatisfactory replacements for carbon tetrachloride.

Preparation of Methyl Esters of Fatty Acids (AOCS Ce-266).

SAMPLING AND ANALYSIS OF COMMERCIAL FATS AND OILS

AOCS Official Method Ce 2-66

Reapproved 1997

Preparation of Methyl Esters of Fatty Acids

DEFINITION

This method provides a means for preparing methyl esters of long-chain fatty acids for further analysis by GLC, as in AOCS Official Methods Ch 2-91 (olive oil, capillary GC), Ce 1-62 (fats and oils, packed-column GLC), Ce 1b-89 (*cis* and *trans* fatty acid isomers by capillary GC), Ce 1d-91 (n-3 and n-6 fatty acids by capillary GC) and Cd 14-61 (*trans* fatty acids by IR).

SCOPE

The method is applicable to common fats, oils and fatty acids with the exception of milk fats (see Notes, 1). Unsaponifiables are not removed but, if present in large amounts, they may interfere with subsequent analyses. The procedure will result in partial or complete destruction of the following groups: epoxy, hydroperoxy, cyclopropenyl, cyclopropyl and possibly hydroxyl and acetylenic fatty acids, and is not suitable for the preparation of methyl esters of fatty acids containing these groups.

APPARATUS

1. Flasks—50- and 125-mL flat-bottom boiling flasks, or Erlenmeyer flasks with $\text{T}^{24/40}$ outer necks.
2. Water-cooled condensers—Liebig or West design, 20–30-cm jacket, with $\text{T}^{24/40}$ inner joint.
3. Separatory funnels—250 mL.
4. Boiling flask—200 mL, for solvent removal.
5. Boiling chips—free of fat.

REAGENTS

1. BF_3 -methanol reagent, 12% to 15%, available commercially as 14% and 50% solution (see Notes, Caution, Notes, 5) (125 g BF_3 per liter of methanol)—available commercially, or may be prepared using BF_3 gas and methanol [see Section 3 (d) of American Society for Testing and Materials (ASTM) Method D-1983-64T, or References, 1].
2. Sodium hydroxide (NaOH)—0.5 N in methanol.
3. Sodium chloride (NaCl)—saturated solution in water.
4. Petroleum ether—redistilled, bp 30–60°C (see Notes, Caution).
5. Heptane—gas chromatographically clean (see Notes, Caution).
6. Sodium sulfate (Na_2SO_4)—anhydrous, reagent grade.
7. Methyl red indicator—0.1% in 60% ethanol.
8. Nitrogen gas—high purity.

PROCEDURE

1. Accurate weighing is not required. Sample size need be known only to determine the size of flask and amounts of reagents that should be used according to the following table:

Sample, mg	Flask, mL	NaOH 0.5 N, mL	BF_3 -methanol reagent, mL
100–250	50	4	5
250–500	50	6	7
500–750	125	8	9
750–1000	125	10	12

2. For fatty acids—

- (a) Introduce the fatty acids into the 50- or 125-mL reaction flask. Add the specified amount of BF_3 -methanol reagent, attach a condenser and boil for 2 min (see Notes, 1). Add 2–5 mL of heptane through the condenser and boil for 1 min longer. Remove from heat, remove condenser and add about 15 mL of saturated sodium chloride solution (Reagents, 3). Stopper the flask and shake vigorously for 15 sec while the solution is still tepid. Add sufficient saturated sodium chloride solution to float the heptane solution of the methyl esters into the neck of the flask (References, 2). Transfer about 1 mL of the heptane solution into a test tube and add a small amount of anhydrous sodium sulfate. The dry heptane solution may then be injected directly into a gas chromatograph. (See Notes, 2.)

- (b) To recover dry esters, transfer the salt solution and heptane phase to a 250-mL separatory funnel. Extract twice with 50-mL portions of redistilled petroleum ether (bp 30–60°C). Wash the combined extracts with 20-mL portions of water until free of acids (test water with methyl red indicator), dry with sodium sulfate and evaporate the solvent under a stream of nitrogen on a steam bath (see Notes, 3 and 4).

3. For fats and oils—

- (a) Introduce the fat into the 50- or 125-mL reaction flask. Add the specified amount of 0.5 N methanolic sodium hydroxide and add a boiling chip. Attach a condenser and heat the mixture on a steam bath until the fat globules go into solution. This step should take 5–10 min. Add the specified amount of BF_3 -methanol reagent through the condenser, and proceed as directed in the fatty acid section (Procedure, 2).

4. Alternate method for fats and oils (acid value <2) (References, 3)—An alternate method for the preparation of fatty acid methyl esters (FAME) is as follows: Accurately weigh a test portion of sample (approximately 200 mg) into a stoppered-glass centrifuge vial.

drated castor oils and dehydrated castor oil fatty acids, weigh 0.11–0.13 g.

7. The indicated reaction times are those specified in the International Union of Pure and Applied Chemistry (IUPAC) Iodine Value Method 2.205 (References, 1) and were the reaction times used in the IUPAC/ISO validation study of the cyclohexane + acetic acid method (AOCS Official Method Cd 1d-92). Previous AOCS versions of iodine value methods specified a reaction time of 0.5 hr, regardless of the iodine value, but noted that “a longer reaction time may be necessary for oils with high iodine value.” The longer reaction times appear to be particularly critical when cyclohexane is

used as a replacement for carbon tetrachloride.

8. If the reaction is not terminated within 3 min after the reaction time, the sample must be discarded.
9. The sample must be titrated within 30 min of reaction termination, after which the analysis is invalid.
10. Mechanical stirring is recommended for agitation during the addition of thiosulfate.

REFERENCES

1. *Standard Methods for the Analysis of Oils, Fats and Derivatives*, International Union of Pure and Applied Chemistry, 7th edn., Blackwell Scientific Publications, 1987, IUPAC Method 2.205.

Publications.

Conferences Proceedings Articles.

Sodium formate and Formic acid: Green Feedstock for Hydrogenation. Screen of different compounds.

J. Garcia, E. Garcia-Verdugo, **E. Ramírez**, P. Hamley and M. Poliakoff (2004).

Proceedings of International Conference "Green Solvents for Synthesis", DECHEMA, Bruchsal (Germany).

Abstract: Supercritical fluids (SCFs) are one of the alternative technologies which comply with recent impacts of environmental legislation. SCF technology is an environmentally friendly alternative which supports most of the Principles of Green Chemistry. Supercritical water (SCW) as a reaction media for organic synthesis has been reported previously. However, it is normally used as a medium for oxidation (SCWO process) to destroy organic wastes producing water, CO₂, N₂ and precipitated salts as the main products. At lower temperatures (T < 374 °C), near critical water (NCW), is also used for oxidation, and has been shown to be a successful medium for partial oxidation of organic compounds. This work presented here has been focused on screening different reduction reactions in NCW and SCW. H₂ was generated by the decomposition of formic acid (HCO₂H) or sodium formate (NaCO₂H) solutions up to 10% w/w. A maximum yield of H₂+CO₂ (1:1) was obtained at 15 MPa and 350 °C for formic acid, although CO was also formed. With NaCO₂H at 15 MPa and 250 to 350 °C, was found 91-97% H₂ and only 7-2% CO₂ because of the formation of NaHCO₃. We show how a range of functional groups, such as cyclic and aromatic ketones, olefins, nitriles and aldehydes react under these reducing conditions without catalyst in a continuous flow reactor. Conversions up to 80% combined with mass recoveries around 99% obtained so far show an interesting way for this kind of chemistry. The real challenge is to make the use of these solutions routine for easier, safer and greener reactions. In addition, an exciting possibility is that the same apparatus could be used either for oxidation, *via* aqueous H₂O₂, or reduction purposes, *via* HCOOH or NaCO₂H without significant change to the apparatus.

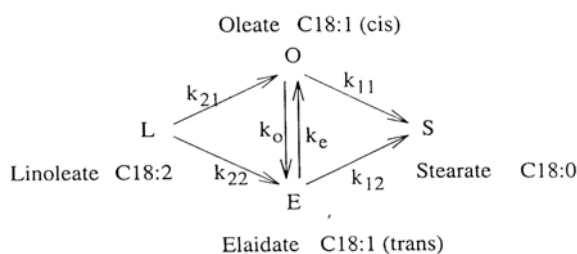
Gas-Phase Sunflower Oil Hydrogenation in High Pressure Propane: Preliminary Kinetics in an Internal-Recycle CSTR.

E. Ramírez, A. S. Oliveira, M.A. Larrayoz, F. Recasens (2003).

Proceedings of 4th European Congress of Chemical Engineering, (ECCE-4), Granada, Spain and Electronic Version on Wiley-InterScience (www.cet-journal.de).

Abstract: The kinetics for sunflower oil hydrogenation on Pd/C in a single phase using dense propane, were investigated in a gradientless fixed bed reactor operating in a well-mixed way under a wide range of temperatures (428-488 K), H₂ mol concentrations (2-10%), total weight hourly space velocities (WHSV) of $\approx 2000 \text{ h}^{-1}$ and stirrer speed (500-2500 rpm). The total system pressure, the molar oil concentration and the catalyst weight were kept constant at 200 bar, 1 % and 0.1085 g, respectively. Crushed catalyst was employed.

The proposed kinetic model for the vegetable oil was based on the general hydrogenation scheme which considers consecutive reactions of the unsaturated triglycerides together with the *cis-trans* isomerization of monoenes.



Simplified kinetic law equations for the above reaction network together with the conservation equations for a CSTR at steady state and working isothermally, were used to model the gas hydrogenation reaction for all components (linoleic, oleic, elaidic, stearic acid and hydrogen) as follows:

$$F_{j0} - F_j + Vr_j = 0$$

$$r_j = \sum_{i=1}^q r_{ij} = \sum_{i=1}^q \pm k_{ij} C_{H_2}^{1/2} C_j$$

The nonlinear system of equations for the components in the CSTR was solved with the Newton-Raphson algorithm and the kinetic constant values obtained by fitting the

reactant concentrations for each space velocity. To estimate the kinetic constants the experimental reactor outlet concentrations of each reaction component were considered for the various operating conditions.

The results suggest that k_{11} and k_{12} values are close to zero due to the low experimental conversion whereas the other constants provide a description of the experimental data in the low conversion range. Values of the kinetic constants are given.

Pd-Catalysed Hydrogenation of Sunflower Oil in SC Propane: Design of Experiments in a Well Mixed Continuous Reactor.

E. Ramírez, F. Recasens, M. Fernández, M. A. Larrayoz (2003).

Proceedings of 6th International Symposium on Supercritical Fluids, Versailles, France.

Abstract: In this paper, we report on a study of the effect of the supercritical-solvent process conditions (temperature, H₂ mol composition, liquid hourly space velocity (LHSV) and stirrer speed) on the *trans* acid content and the extension of single phase sunflower hydrogenation (expressed by the iodine value) in a CSTR reactor using a 2 % Pd/C as catalyst and SC propane as a reaction medium in order to assess them. 155-215 °C, 30-70 h⁻¹, 2-10 H₂ mol %, 500-2500 rpm were the experimental ranges of the operational variables. The observed trends shown the great influence of variable interactions (e.g. LHSV-H₂ % and T-H₂ %) on the desirable responses whereas the stirrer speed is negligible for the velocity range studied.

Sunflower Oil Hydrogenation in SCF in a Continuous Reactor: Preliminary Experimental Results.

E. Ramírez, M. A. Larrayoz (2002).

Proceedings of 4th International Symposium on High Pressure Process Technology and Chemical Engineering, Venice, Italy.

Abstract: Continuous in a single-phase hydrogenation of sunflower oil on Pd/C was carried out in a Robinson-Mahoney type, fixed bed catalyst reactor using propane as SC solvent of reaction. Different process conditions (total system pressure, temperature, H₂ partial pressure and molar feed mixture composition) were studied to evaluate their

influence on the end hydrogenation products. The phase behavior of the ternary system was theoretically determined using a Peng Robinson equation of state and phase equilibrium software (PE 2000) in order to assure one single phase of the reactant mixture at the experimental conditions. Results show that it is possible to obtain different distributions and characteristics of the final hydrogenation products only changing the operational variables.

Hydrogenation of Organics in SC Solvents: Preliminary Data on Catalytic Rates.

E. Ramírez, M.A Larrayoz, F. Recasens (2001).

Proceedings of IVth Brazilian Meeting on Supercritical Fluids, Salvador de Bahia, Brazil.

Abstract:In this paper we report on the examination of hydrogenation of organic substrates on supported Pd catalysts published during the last few years. Most often authors¹⁻⁷ have used continuous flow reactors. Under these conditions, hydrogen conversion can give an idea of the steady state rate of hydrogenation. In most publications, however, batch data are rather difficult to measure, interpret, and analyse as the rate of reaction changes with time in the vessel. In order to look at the hydrogenation rates, several authors were examined. The data of Polyakoff and co-workers² on several substrates, that of Van der Hark and Härröd⁴ and the data of Bertuccio *et al.*⁵⁻⁶, have been considered. Apparently, only the runs of Poliakoff² and Härröd⁴ were performed in the vapour phase and they seem quite consistent.

The hypothesis of the calculations were: rate is taken proportional to metal loading, well-mixed fluid, hydrogen partial pressure at reactor exit was used in kinetic considerations, and, thirdly, a slight temperature correction was allowed corresponding a small activation energy ($E = 10.000$ kcal/mole). Except in the tubular reactor of Bertuccio⁵⁻⁶, where multiphase, gas/liquid flow was present, the operating conditions of the other authors corresponded to homogeneous flow. Very recently, however, Couchi and co-workers⁹ draw attention to the fact that the liquid phase increases the rate of hydrogenation on Pd/C catalyst with CO₂ as solvent.

Our results suggest the following: 1) For most substrates, hydrogenation rates in SC CO₂ are in the order of 2-12 mol H₂/g Pd/h, for LHSV of up to 30 h⁻¹, based on catalyst volume. These values increase by about 50% in propane relative to carbon dioxide. In

both cases, the partial pressures of hydrogen are around 25 bar. The catalyst loading may vary from 1 to 5% Pd on activated carbon.

The above value for the rates represents how fast one can expect hydrogenation to proceed in SCF. In contrast, the data in low-pressure batch and continuous hydrogenations, indicate that the rates are much lower. For trickle bed operation⁷, with hydrogen-saturated liquid feed, the maximum rate on 0.75% Pd/Alumina, is 0.38 mol H₂/g Pd/h, for a LHSV of about 1000 h⁻¹. For the case of a slurry reactor⁸, assuming an average lined out productivity, the rate is somewhat higher, i.e. 1.3 mol H₂/g Pd/h. On the other hand, Tacke *et al.*, suggest that for undisclosed hydrogenation conditions (special catalyst size or hydrogen pressure) may lead to larger space time yields.

Hydrogen rates seem to be proportional to partial pressure of hydrogen so kinetic constant could be established for some of the substrates. Uncertainty on kinetics does not allow favouring a half order with respect to hydrogen as is common in hydrogenation with hydrogen adsorption with dissociation.

Hydrogenation reactions in SC solvents.

S. Zgarni, **E. Ramírez**, A. Larrayoz, F. Recasens (2001).

Proceedings of Exploratory Workshop on Supercritical Fluids as Active Media: Fundamentals and Applications, Valladolid, Spain.

Abstract: In organic syntheses SC fluids fit very well as green, sustainable solvents in clean chemical processing in general (Busch, 2001) and particularly in some industrial polymerizations (De Lissi *et al.*, 2000; Ajzenberg *et al.*, 2000) and in catalyst regeneration processes (Trabelsi *et al.*, 2000). In these processes the fluid can be cheaply and efficiently recovered from the reactor and recycled with a negligible environmental impact on and very little energy expenditure. Recently, an interesting account on the use of SCF in clean catalytic reactions has been published in a magazine (Freemantle, 2001) with several of organic processes that could benefit from SCF, including solid-catalysed hydrogenations.

Carbon dioxide is the preferred the fluid for clean chemical processing. However, it may not be the best fluid of choice. For example, the operating pressures and temperatures for CO₂ are far too high to reach the critical state of the reacting mixture.

In this regard, some workers (Pereda and co-workers, 2000, de Jong *et al.* 2001) compared CO₂ with lower alkanes for the hydrogenation of multiple double bonds in terms of multiphase equilibria.

Hitzler and coauthors report on a new method for continuous catalytic hydrogenation (in CO₂ and in propane) on supported Pd. A wide range of substrates including alkenes, alkynes, ketones and aldehydes, epoxides, phenols, nitriles, etc., was examined. An important finding is that the operating conditions (temperature, pressure, hydrogen/substrate mole ratio) can be tuned to drive reaction to the desired product distribution. The scale of operation of Hitzler *et al.* was a 5-mL reactor. In a similar way, Härröd and co-workers, studied the hydrogenation of fats and oils noting a very high rates and reduced byproduct formation that can be obtained in fixed bed reactor operating in a single gas phase. Large reaction rates were explained in terms of the higher hydrogen gradients external to the catalyst particle, as compared to the case of two-phase flow. Where faster hydrogen transfer rates could also play a role. Bertuccio *et al.* also studied hydrogenation kinetics of organics on Pd/C in a CSTR Berty-type of reactor using SC CO₂ as solvent. The system was clearly subject phase separation during operation. An increase in rate was also observed when a liquid phase appeared although the rate enhancement was less than that observed by Härröd. Devetta *et al.* also studied the hydrogenation process in a trickle-bed reactor as low pressure alternative.

More recently, Chouchi *et al.*, gave preliminary data on the results of hydrogenation of α -pinene on Pd/C in SC CO₂ in a stirred batch reactor. Again it was found that the larger rates developed whenever a two-phase system was visually observed. One-phase and two-phase systems showed very different rates.

In this work we review some of the solid catalysed hydrogenation processes with a SCF solvent. Rare values are compared with those for low-pressure slurry and trickle-bed reactors where some of the conventional hydrogenations are carried out. We want to see also if there are advantages in using SCF solvents as regards to the selectivities and the presence of multiple phases.

Journal Articles.

Sunflower Oil Hydrogenation on Commercial-Size Pd Particles in Supercritical Fluids: Solvent and Catalyst Type Effects on Kinetics and Selectivities

M. A. Larrayoz, E. Ramírez, A. Santana and F. Recasens.

JAOCS, submitted, 2005

Introduction: Supercritical fluid technology is becoming important in the lipid and food industry in a variety of fields. So far, the emphasis, however, has been on extraction processes (King and List, 1996). Reaction and catalytic applications lag well behind (Subramaniam and McHugh, 1985; Brunner, 2003). For certain industrial polymerizations (Azjenberg *et al.*, 2002), a high potential has been shown to exist. In general, the benefits of SCF in heterogeneous catalysis have been emphasized in certain isomerisation reactions involving coke deposition and for enhancing intraparticle diffusion (McHugh and Krukonis, 1994). In catalytic reactions, hydrogenation stands among the most important reactions in petroleum processes and in the food and fine chemical industries (Farrauto and Bartholomew, 1998). In this paper we examine the hydrogenation of sunflower oil in fluids, such as SC propane and SC dimethylether (DME), and on certain Pd-based catalysts using a number of supports. A main advantage of such high pressure systems is that reactions can be carried out in the vapor phase in a continuous-flow reactor (Ramírez *et al.*, 2003). For edible oil hydrogenation, this is an improvement.

The purpose of vegetable oil hydrogenation is to obtain a more stable product (no oxidation on storage), together with a suitable texture and melting-temperature range at the mouth conditions for human use as margarine and shortenings. Catalytic slurry process is customary in the vegetable oil hydrogenation industry with nickel (Raney or supported), or supported Pd as catalysts, on an otherwise well established catalysts and technology (Albright, 1961; Rase, 2000; Farrauto and Bartholomew, 1997). In contrast, the vapor phase processes were introduced in the 1990s by Härröd and Möller (1993) and Härröd *et al.* (2001) chiefly for fatty acid methyl esters (FAME) in propane (Härröd and Möller, 1994) using Engelhard Cu catalysts and by King and co-workers at ACAUR using SC carbon dioxide on supported Ni (King *et al.*, 2001) in batch stirred tank reactors. In the EU, early work of Degussa scientists (1993) showed that reaction in SC carbon dioxide using Pd is extremely fast and favorable relative to the formation of

trans C18 with triglycerides as a feed (Tacke et al.). See Ramirez *et al.*, (2002) for a review on catalytic rates in SC media.

Triglycerides exhibit *cis-trans* isomeric forms in Nature. When fatty compounds are unsaturated, the *cis* isomer is the natural one. The *trans* isomer appears during hydrogenation. If uncorrected, the *trans* content in margarines can be as large as 40 wt% in the conventional low pressure, slurry reactor hydrogenations (Rase, 1979). Although the effects on human health of *trans* isomers are not clear, they are suspect to be metabolised to the undesired (or bad) cholesterol type so affecting heart disease. So far, Denmark has been the only country in the world where the Ministry of Health has limited by law the *trans* content to less than 2% on fat components for human ingestion since May 2003. The committee of experts Codex Alimentarius of the FAO is on a debate regarding the inclusion of *trans* fatty acids content on food labels. On the other hand, the EU is favorable to include this on the label, but legal action is yet to be taken. In the US, the government (through the FDA) has put forward a campaign (announced by the Surgeon General in 2003) to label by law the % *trans* content and the % saturated fat, before 2006. The efforts of King and co-workers (2001) to develop a low *trans* process at the FDA, are in this direction.

In a previous work, we have used the methodology of the design of experiments and response surface models to achieve optimum hydrogenation conditions for Pd catalyst in SC propane in a CST reactor. By modelling the system response empirically, Ramirez *et al.*, (2004) showed that it was possible to obtain a hydrogenate fat with less than 2,5 % *trans* content in one pass through the reactor in a continuous process, with a iodine value of about 70 (starting with a value of 130). Triglyceride sunflower oil was the raw material. Furthermore, simple kinetics using standard kinetics provided the rate constants on the Pd/C catalyst.

In this work we had various purposes. First, we wanted to measure hydrogenation kinetics on Pd/C catalyst pellets of commercial size (0.55 mm), using propane and DME as SC solvents. An eggshell Pd catalyst was also examined. The other purpose was to simulate reactor operation with the kinetics so developed in order to see reactor performance and compare with experiment.

Intraparticle Diffusion Mechanisms in Supercritical Sunflower Oil Hydrogenation on Pd/C Catalyst.

E. Ramírez, M.A. Larrayoz, F. Recasens

AIChE Journal, under revision, 2005.

Abstract: We report on the Pd catalyzed hydrogenation of vegetable (soya, sunflower, palm) oil, an important process for obtaining ultra low *trans*-C18:1 and stearic C18:0 products (2.5 wt% and 19 wt%, respectively, for sunflower oil), to be used as low cholesterol precursors for margarine and shortening bases in the next few years. Further, if single vapor phase conditions are attained, a continuous operation is possible making the process quite innovative. In this work we consider the operation in supercritical propane. This is a plentiful, inexpensive, volatile solvent that can be recovered almost completely. Other SC gases are not excluded.

Reaction runs were performed on a recycle reactor at a weight hourly space velocity of 300-900 h⁻¹, based on mass of catalyst (2 %Pd on AC). Feed concentrations are 1, 4, 95 mol % (oil, H₂, C₃H₈), and reactor conditions 210°C and 275 bar. Such conditions allow a non-condensing or single vapor phase. Our interest was to decouple intrinsic kinetics from reactant diffusivities, for a rather complex network of hydrogenations and hydroisomerisations that occur simultaneously. We used the Wei (1962) concept for the differential equation vector, using however a numerical solution approach combined with nonlinear parameter fitting. First, reaction runs performed on small size of catalyst (0.4 mm) allowed to obtain kinetic constants irrespective of the diffusivity settings. Then, in a second set of runs, reactions were repeated on larger size of catalyst (up to 1mm), that is, in the diffusion-limited regime. In this second set of runs the diffusion coefficient of hydrogen and the triglycerides were evaluated by fitting the experimental diffusion fluxes. In both sets of experimental runs, the iodine value reduction was at least 44%. Only one diffusion coefficient was considered for all the triglycerides, as their mw are similar.

The results shown that while hydrogen is transported by bulk pore diffusion; the oil components seem to diffuse by surface diffusion, in view of the strong surface diffusion dependence of p and T. As regards to hydrogenation, particles of 0.1 mm are kinetically controlled, but the effectiveness factor falls to 0.3 for 1 mm particles. It is also seen that that the diffusivities for glycerides in liquid filled pores (standard slurry process at low pressure) are much lower than in the SCF, making reaction very rapid in this solvent.

Diffusivity of H₂ is about 10 times than of triglycerides, despite of the fact that the molecular weight of the latter is ~500 times that of H₂. This means that the surface migration of triglycerides is still very fast. The overall diffusivity for triglycerides is about 10⁻⁸ m²/s, and changes 3 times with an increase in pressure, and 20 times with an increase in T. Also, linoleate selectivity and isomerisation yield also improve with decreasing the diffusion path (Camps *et al.*, 2004).

Keywords: Fat hydrogenation, sunflower oil, supercritical fluids, propane, *trans*-content, kinetics, intraparticle diffusion, palladium catalyst, carbon support.

Hydrogenation of Sunflower Oil on Pd/C in Supercritical Propane: Operating Conditions in a Continuous Internal Recycle Reactor.

Ramírez, E., Recasens, F., Fernández M. and Larrayoz M. A.

AIChE Journal, 50, 6 (2004).

Abstract: Fluid-phase, continuous hydrogenations of sunflower oil on 2% Pd/C were carried out in an internal recycle, radial-flow, packed-bed microreactor (50 cm³) using propane as supercritical-fluid solvent. Temperature (428–488 K), oil liquid hourly space velocity (LHSV 30–70), H₂ mol composition (2–10%), and stirrer speed (52–262 rad/s) were changed according to a four-variable, two-level, central composite design to predict the effect of process variables on the iodine value (IV) and on *trans* fatty acid content (*trans* C18:1). Feed and product were well above the condensation conditions so that a single fluid phase was present (according to recent calculations by Pereda *et al.*). The total system pressure, the molar oil concentration and the catalyst mass were held constant at 20 MPa, 1 mol %, and 0.1085 g, respectively. An empirical quadratic-form response surface model is shown to fit the results, and shows the regions where a potential CSTR process could be operated to obtain a certain outlet iodine value and a minimum *trans* C18:1 content. For the time-on stream values used here catalyst deactivation effects were not observed. In an extension of the results, a kinetic analysis of the steady-state CSTR reaction rate data allows determination of the kinetic constants, and their temperature dependency, for the multiple reactions of hydrogenation–isomerization network involving triglyceride species. The kinetic formalism, proposed earlier for vegetable oil hydrogenations, was used.

Keywords: hydrogenation, vegetable oil, supercritical fluid solvents, phase equilibria, experimental central composite design, response-surface methodology kinetics on Pd catalyst.

Short Compilation of Published Rate Data for Catalytic Hydrogenations in Supercritical Fluids

Ramírez, E., S. Zgarni, M. A. Larrayoz, and F. Recasens.

Chem. Eng. Technol. Journal: Engineering in Life Science, 2, 9, 257 (2002).

Abstract: In this work, a short compilation is presented on heterogeneously catalyzed hydrogenations carried out in near-critical fluids. Reactions carried out in supercritical fluids, catalyzed by supported Pd, Ni or Cu, are considered as green processes in view of their negligible impact on the environment. A number of technologies are already available for clean hydrogenations, mostly performed in carbon dioxide as a dense solvent in continuous reactors. However, propane and other lower alkane solvents can perform as well as carbon dioxide but at much lower pressures. We review their behaviors in this paper in terms of observed reaction rates, space velocities, selectivities and apparent kinetic constants. In the case of vegetable oils, data are available on the effect of pressure and reaction conditions on the selectivity toward the preferred *cis*-isomer during linoleic hydrogenation.

Keywords: Hydrogenation, heterogeneous catalysts, supercritical fluid solvents, kinetics, selectivities, phase equilibria.

Patent.

Partial hydrogenation of unsaturated triglycerides in vapour-phase at high pressure in a reactor for carrying out this process.

Silvia Camps Hernán-Pérez, Mónica Fernández Garza, M^a Angels Larrayoz Iriarte, Eliana Ramírez Rangel, Francisco Recasens Baxarias & Jordi Sans Solé,

P200401793 (under revision, 2004), Spain.

Abstract: In this patent, a single vapour-phase vegetable oil hydrogenation process on supported Pd catalyst is described. The feed mixture consists of triglycerides, hydrogen and a gaseous solvent at high pressure.

The process is carried out in a mixed flow reactor consists of either a catalyst fixed bed with a radial flow or a monolith both with small particle diameter and small pressure drop. The CSTR behavior is achieved by recirculation of the reactive mixture.

By means of high turbulence into the reactor as well as small particle diameter, it is possible to obtain low *trans* C18:1 contents (less than 3.5 wt %).